

DISSERTATION

EFFORTS TOWARD THE TOTAL SYNTHESIS OF QUININE,
SYNTHESIS OF LARGAZOLE ANALOGS, AND
PROGRESS TOWARD POTENTIAL BIOSYNTHETIC INTERMEDIATES OF TAXOL

Submitted by

Jennifer Marie Bubb

Department of Chemistry

In partial fulfillment of the requirements

For the Degree of Doctor of Philosophy

Colorado State University

Fort Collins, Colorado

Summer 2012

Doctoral Committee:

Advisor: Robert M. Williams

John L. Wood
Brian R. McNaughton
Amy L. Prieto
Douglas N. Ishii

ABSTRACT

EFFORTS TOWARD THE TOTAL SYNTHESIS OF QUININE, SYNTHESIS OF LARGAZOLE ANALOGS, AND PROGRESS TOWARD POTENTIAL BIOSYNTHETIC INTERMEDIATES OF TAXOL

Herein we discuss our work involving three different projects, namely (1) efforts toward the total synthesis of quinine, (2) synthesis of largazole analogs, and (3) progress toward potential biosynthetic intermediates of taxol. Our efforts toward the synthesis of quinine have led us toward a route toward a pipercolic acid derivative that was further elaborated to a late-stage intermediate. Following an intramolecular cyclization and deoxygenation protocol, a formal synthesis of quinine could be realized.

In the second project, we have successfully synthesized and tested analogs of the known HDAC inhibitor, largazole. These analogs have demonstrated good potency towards a series of HDAC isoforms.

In the third project, efforts have been made to synthesis potential biosynthetic intermediates of taxol. Utilizing highly oxygenated intermediates isolated from the heartwood of the Japanese yew tree, we have explored the reactivities of these complex natural products in hope of devising a method to construct mono-acetylated derivatives.

ACKNOWLEDGEMENTS

First, I would like to thank my advisor, Dr. Robert M. Williams. I literally would never have made it to this point without your guidance and without you allowing me to take the time I needed to figure things out on my own terms.

I would also like to thank the Williams group, past and present, but most importantly I need to thank the lab members of B316...where do I even begin though? I could not think of a better group of people to have worked with every single day. From Mike's hilarious stories and screams, to trashcan fires and beyond, you have all made day-to-day life fun and often times, a crazy adventure.

I am forever grateful to Maria Hopkins and Punitha Vedantham, I love you ladies more than you will ever know! You are two of the best friends I have ever had. I truly cannot express how much you both have shaped who I am and how you have affected my life. You mean so much to me. Thank you for all that you have done for me, and for being two of the best friends I have ever had.

My family...I am not sure words can describe how thankful I am to all of you. My mom and dad, Deann and Bob, you have always believed in me, even when I was ready to walk away from this. Thank you so much for supporting me in EVERYTHING that I have ever done and always being there for me. My sisters, Angela and Megan, I know we are some of the most polar-opposite people on this planet, but I love you both and appreciate all you have done for me (even planning mine and Dan's wedding)! To my nieces and nephew: Jordan, Rebecca, Elizabeth, and Clayton, thank you so much

for being you! Your unconditional love and hilarious antics saved me from getting brought down in the stress of graduate school. You are beautiful people and I love and miss you every single day we are apart.

I would like to thank my mother and father-in-law, Donna and Ken Bubb. Thank you for all the support you have given me over the last couple of years and always being supportive of Dan and I. To my brother-in-law, Ken Stensrud, I am forever indebted to you. Without your suggestion to do summer research in chemistry I would never have made this leap, and most importantly, I would never have met my husband.

Last but certainly not least; I would like to thank my husband, Daniel Bubb. Meeting you over 8 years ago was the best thing that could have happened to me. Organic chemistry literally brought us together, and I could not think of a better person to share my life with. You are wonderful in everyway, and have always supported me in my decisions, without judgment. I love you, and I look forward to the future!

TABLE OF CONTENTS

ABSTRACT.....	ii
ACKNOWLEDGEMENTS.....	iii
TABLE OF CONTENTS.....	v
LIST OF TABLES.....	xi
LIST OF FIGURES.....	xii
LIST OF SCHEMES.....	xxiv
LIST OF ABBREVIATIONS.....	xxx
Chapter 1.....	1
1.1 Introduction.....	1
1.1.1 Quinine.....	1
1.1.2 Overview of Results.....	2
1.2 Largazole.....	3
1.2.1 Overview of Results.....	4
1.3 Biosynthetic Taxol Intermediates.....	4
1.3.1 Overview of Results.....	5
Chapter 2.....	7
2.1 Quinine.....	7
2.1.1 Background.....	7
2.1.2 Biological Mode of Activity.....	8
2.1.3 Mechanism of Resistance.....	10
2.2 Previous Synthetic Studies.....	11

2.2.1	Rabé-Kindler Synthesis of Quinine.....	11
2.2.2	Woodward-Doering Synthesis of Quinine.....	12
2.2.3	Uskokovics Routes to Quinine.....	13
2.2.4	Stork's Asymmetric Synthesis of Quinine.....	16
2.2.5	Jacobsen's Synthesis of Quinine.....	17
2.2.6	Kobayashi's Route to Quinine.....	19
2.2.7	Krische's Formal Synthesis of Quinine.....	20
2.2.8	Aggarwal's Sulfur-Ylide Method Toward Quinine.....	22
2.2.9	Sarkar's Asymmetric Synthesis of Quinine.....	23
2.2.10	Friestads Mn-Mediated Radical Method Toward Quinine.....	24
2.3	Previous William's Group Studies.....	26
2.3.1	Dr. Deidre John's Method Toward 7-Hydroxy-Quinine.....	26
2.3.2	Dr. Aaron Smith's Method Toward 7-Hydroxyquinine.....	27
2.4	Concluding Remarks.....	28
Chapter 3	29
3.1	Studies Toward the Total Synthesis of Quinine.....	29
3.1.1	First Generation Strategy.....	29
3.2	Second Generation Approach.....	35
3.2.1	Towards C2-Functionalized Piperidines.....	35
3.2.2	Utilization of Smith's Enamine.....	35
3.2.3	Serine Metathesis Route.....	36
3.2.4	Dibenzyl Serine Route.....	38

3.3	Review of Initial Williams' Group Findings.....	40
3.3.1	Dr. Deidre John's Findings.....	40
3.3.2	Dr. Aaron Smith's Findings.....	41
3.4	3 rd Generation Approach.....	42
3.4.1	3 rd Generation Retrosynthetic Analysis.....	42
3.4.2	Sulfoxonium Ylide Method.....	43
3.4.3	Avery's Ring Expansion Method.....	45
3.4.4	Kiesel's Mn(OAc) ₂ Approach.....	46
3.4.5	Allylglycine & Cyclohydrocarbonylation Approach.....	47
3.4.6	Halo-Quinoline Fragment.....	50
3.4.7	Coupling Attempts.....	50
3.5	Late Stage Intermediates.....	53
3.5.1	Late Stage Silyl Intermediate.....	53
3.5.2	Advanced Quinine Intermediate.....	53
3.6	Conclusion.....	54
Chapter 4	56
4.1	Histone Deacetylase Inhibitors: Introduction.....	56
4.1.1	HDAC Enzyme Function.....	57
4.2	HDAC Inhibitors.....	56
4.2.1	Acyclic HDAC Inhibitors.....	57
4.2.2	Macrocyclic HDAC Inhibitors.....	60
4.2.3	Sulfur-Containing HDAC Inhibitors.....	61

4.3	Largazole.....	62
4.3.1	Luesch Isolation.....	62
4.4	Previous Syntheses.....	63
4.4.1	Luesch Synthesis.....	63
4.4.2	Phillips and Cramer Syntheses.....	65
4.4.3	Williams' Synthesis.....	66
4.4.4	Ghosh's Synthesis.....	67
4.4.5	Ye's Synthesis.....	68
4.4.6	Doi's Synthesis.....	69
4.4.7	Forsythe Synthesis.....	70
4.5	Williams' Pursuit of Potent Analogs.....	71
4.6	Conclusion.....	74
Chapter 5.....		76
5.1	Synthesis of Thiazoline-Oxazole Containing Analogs.....	76
5.1.1	Retrosynthetic Analysis of Thiazoline-Oxazole Analogs.....	76
5.1.2	Synthesis Thiazoline-Oxazole Analogs.....	77
5.1.3	Oxazoline-Thiazole Retrosynthetic Analysis.....	80
5.1.4	Progress Toward Oxazoline-Thiazole Analog.....	81
5.2	Biological Activity.....	82
5.3	Conclusion.....	83
Chapter 6.....		85
6.1	Progress Toward the Biosynthesis of Taxol.....	85

6.1.1	Efforts Toward Elucidating the Biosynthetic Path of Taxol.....	85
6.2	Early Stages of Taxol Biosynthesis.....	87
6.2.1	Taxadiene Synthase.....	87
6.2.2	Mechanism of Taxadiene Synthase.....	90
6.2.3	Over Production of Taxadiene.....	92
6.3	Efforts Toward Biosynthetic Intermediates to Probe the 5 α -Hydroxylase Pathway.....	94
6.3.1	Taxa-4(5)-11,12-diene and Taxa-4(20),11(12)-diene.....	94
6.3.2	Synthesis of Taxa-4(20),11(12)-diene-5 α -ol.....	96
6.3.3	Elucidation of the Mechanism of Taxadiene Hydroxylase.....	99
6.3.4	Over-Production of Taxa-4(20),11(12)-diene-5 α -ol.....	102
6.4	Syntheses of Lightly Functionalized Taxoids.....	102
6.4.1	Synthesis of Taxa-4(20),11(12)-diene-2 α ,5 α -diol.....	102
6.4.2	Compounds from Japanese Yew-derived Taxadien-tetraol.....	104
6.4.3	Deoxygenation of Taxusin.....	108
6.4.4	Attempt to Deoxygenate Taxusin at C-13.....	109
6.5	Subsequent Biosynthetic Transformations of the 5-Hydroxytaxadiene Core....	112
6.5.1	10 β - and 13 α -Hydroxylase.....	112
6.5.2	2 α - and 7 β -Hydroxylase.....	113
6.5.3	Uncharacterized Hydroxylases.....	115
6.5.4	Conversion to the 5,14-diol: A Case of Aberrant Metabolism.....	115
6.6	Studies on the Formation of the Oxetane Ring.....	117

6.7 C13 Acylation: Final Step in the Biosynthesis of Taxol.....	119
6.8 Conclusion.....	120
Chapter 7.....	121
7.1 Synthetic Progress Toward the Synthesis of Potential Biosynthetic Intermediates of Taxol.....	121
7.1.1 Biosynthetic Intermediates from Taxusin.....	121
7.1.2 Deoxygenated Taxoids.....	126
7.2 Conclusion.....	128
References.....	129
Chapter 8.....	136
Table of Experimental Procedures and Relevant Spectra.....	136
8.1 General Considerations.....	137
8.2 Experimental Procedures.....	138
Appendix 1: Publications.....	360

LIST OF TABLES

Chapter 4

Table 4.1. Biological Activity of Largazole Analogs.....	65
Table 4.2. Biological Activity of Williams Group Analogs.....	72
Table 4.3 Biological Data Comparing Largazole and its Amide Isostere (IC ₅₀ nM).....	73

Chapter 5

Table 5.1. HDAC Activity of Largazole Analogs.....	83
--	----

LIST OF FIGURES

Chapter 1

Figure 1.1. Failed Deoxygenation of Quinine.....	2
Figure 1.2. Hypothetical Deoxygenation of Quinuclidine.....	2
Figure 1.3. Possible Route to Quinuclidine Core.....	3
Figure 1.4. Allylglycine Route to Quinuclidine Core.....	3
Figure 1.5. Core for Largazole Analogs.....	4
Figure 1.6. Biosynthetic Route Towards Taxol.....	5
Figure 1.7. Analogs from Natural Products.....	6

Chapter 2

Figure 2.1. Quinine.....	7
Figure 2.2. Quinoline Containing Anti-Malarial Drugs.....	8
Figure 2.3. Events in the Parasite Food Vacuole.....	9

Chapter 4

Figure 4.1. Acyclic HDAC Inhibitors.....	58
Figure 4.2. Tentative Catalytic Mechanism for HDAC.....	59
Figure 4.3. Pharmacophore of HDAC Enzymes.....	60
Figure 4.4. Selected Macrocyclic HDAC Inhibitors.....	60
Figure 4.5. Sulfur-Containing HDAC Inhibitors.....	61
Figure 4.6. Leusch Analogs of Largazole.....	65
Figure 4.7. Williams Group Analogs.....	72
Figure 4.8 Largazole Thiol and Largazole Amide Isosteres.....	73

Figure 4.9. Largazole and Amide Isostere Conformations.....	74
---	----

Chapter 6

Figure 6.1. The structure of Taxol (6.1) and Taxotere (6.2).....	86
--	----

Figure 6.2. Small sculpture made from Japanese Yew by Hida Ichii Ittoubori Kyoudou Kumiai of The Engraving Craftsman Association, Japan.....	105
---	-----

Chapter 8

Figure 8.1. <i>N</i> -(4-methoxyphenyl)-3-oxobutanamide (3.16).....	138
---	-----

Figure 8.2. ¹ H NMR of <i>N</i> -(4-methoxyphenyl)-3-oxobutanamide (3.16).....	139
---	-----

Figure 8.3. 6-methoxy-4-methylquinolin-2-ol (3.17).....	140
---	-----

Figure 8.4. ¹ H NMR of 6-methoxy-4-methylquinolin-2-ol (3.17).....	141
---	-----

Figure 8.5. 2-chloro-6-methoxy-4-methylquinoline (3.18a).....	142
---	-----

Figure 8.6. ¹ H NMR of 2-chloro-6-methoxy-4-methylquinoline (3.18a).....	143
---	-----

Figure 8.7. 6-methoxy-4-methylquinoline (3.18).....	144
---	-----

Figure 8.8. ¹ H NMR of 6-methoxy-4-methylquinoline (3.18).....	145
---	-----

Figure 8.9. 6-methoxyquinoline-4-carbaldehyde (3.10).....	146
---	-----

Figure 8.10. ¹ H NMR of 6-methoxyquinoline-4-carbaldehyde (3.10).....	147
--	-----

Figure 8.11. (6-methoxyquinolin-4-yl)methanol (3.19).....	148
---	-----

Figure 8.12. ¹ H NMR of (6-methoxyquinolin-4-yl)methanol (3.19).....	149
---	-----

Figure 8.13. 4-(chloromethyl)-6-methoxyquinoline (3.11).....	150
--	-----

Figure 8.14. ¹ H NMR of 4-(chloromethyl)-6-methoxyquinoline (3.11).....	151
--	-----

Figure 8.15. Quinuclidin-3-yl-4-methylbenzenesulfonate (3.31).....	152
--	-----

Figure 8.16. ¹ H NMR of Quinuclidin-3-yl-4-methylbenzenesulfonate (3.31).....	153
--	-----

Figure 8.17. 3-(tosyloxy)quinuclidin-1-ium-1-yl)trihydroborate (3.32).....	154
Figure 8.18. ¹ H NMR of 3-(tosyloxy)quinuclidin-1-ium-1-yl)trihydroborate (3.32).....	155
Figure 8.19. 1-azabicyclo[2.2.2]oct-2-en-1-ium-1-yltrihydroborate (3.1).....	156
Figure 8.20. ¹ H NMR of 1-azabicyclo[2.2.2]oct-2-en-1-ium-1-yltrihydroborate (3.1)....	157
Figure 8.21. (1 <i>S</i> ,3 <i>S</i> ,4 <i>S</i>)-3-(tosyloxy)quinuclidine 1-oxide (3.35).....	158
Figure 8.22. ¹ H NMR of (1 <i>S</i> ,3 <i>S</i> ,4 <i>S</i>)-3-(tosyloxy)quinuclidine 1-oxide (3.35).....	159
Figure 8.23. 1-azabicyclo[2.2.2]oct-2-ene 1-oxide (3.4).....	160
Figure 8.24. ¹ H NMR of 1-azabicyclo[2.2.2]oct-2-ene 1-oxide (3.4).....	161
Figure 8.25. tert-butyl 3-hydroxypiperidine-1-carboxylate (3.43a).....	162
Figure 8.26. ¹ H NMR of tert-butyl 3-hydroxypiperidine-1-carboxylate (3.43a).....	163
Figure 8.27. tert-butyl 3-oxopiperidine-1-carboxylate (3.44).....	164
Figure 8.28. ¹ H NMR of tert-butyl 3-oxopiperidine-1-carboxylate (3.44).....	165
Figure 8.29. methyl 3-(benzyloxy)-2-((<i>tert</i> -butoxycarbonyl)amino)propanoate (3.48)..	166
Figure 8.30. ¹ H NMR of methyl 3-(benzyloxy)-2-((<i>t</i> Boc)amino)propanoate (3.48).....	167
Figure 8.31. <i>tert</i> -butyl (1-(benzyloxy)-3-((TBSO)propan-2-yl)carbamate (3.49).....	168
Figure 8.32. ¹ H NMR of propan-2-yl-carbamate (3.49).....	169
Figure 8.33. <i>t</i> -Bu-allyl(1-(benzyloxy)-3-((TBS)oxy)propan-2-yl)carbamate (3.50).....	170
Figure 8.34. ¹ H NMR of <i>t</i> -Bu-allyl(1-(BnO)-3-((TBS)oxy)propanyl)carbamate (3.50)...	171
Figure 8.35. <i>t</i> -Bu-allyl(1-(BnO)-3-hydroxypropanyl)carbamate (3.50a).....	172
Figure 8.36. ¹ H NMR of <i>t</i> -Bu-allyl(1-(BnO)-3-hydroxypropan-2-yl)carbamate (3.50a)..	173
Figure 8.37. <i>t</i> -Bu-allyl(1-(BnO)-3-oxopropan-2-yl)carbamate (3.51).....	174
Figure 8.38. ¹ H NMR of <i>t</i> -Bu-allyl(1-(BnO)-3-oxopropan-2-yl)carbamate (3.51).....	175

Figure 8.39. <i>t</i> -Bu-allyl(1-(BnO)-3-hydroxypent-4-en-2-yl)carbamate (3.52).....	176
Figure 8.40. ¹ H NMR of <i>t</i> -Bu-allyl(1-(BnO)-3-hydroxypentenyl)carbamate (3.52).....	177
Figure 8.41. <i>t</i> -Bu-6-((BnO)methyl)dihydropyridine carboxylate (3.53).....	178
Figure 8.42. ¹ H NMR of <i>t</i> -Bu-6-((BnO)methyl)dihydropyridine carboxylate (3.53).....	179
Figure 8.43. (S)-methyl 2-(dibenzylamino)-3-hydroxypropanoate (3.57).....	180
Figure 8.44. ¹ H NMR of (S)-methyl 2-(dibenzylamino)-3-hydroxypropanoate (3.57)....	181
Figure 8.45. (S)-methyl 3-((TBSO)-2-(dibenzylamino)propanoate (3.58).....	182
Figure 8.46. ¹ H NMR of (S)-methyl 3-((TBSO)-2-(dibenzylamino)propanoate (3.58)...	183
Figure 8.47. (R)-3-((TBSO)-2-(dibenzylamino)propan-1-ol (3.59).....	184
Figure 8.48. ¹ H NMR of (S)-methyl 3-((TBSO)-2-(dibenzylamino)propanoate (3.58)...	185
Figure 8.49. (S)-3-((TBSO)-2-(dibenzylamino)propanal (3.60).....	186
Figure 8.50. ¹ H NMR of (S)-3-((TBSO)-2-(dibenzylamino)propanal (3.60).....	187
Figure 8.51. (2S,3R)-1-((TBSO)-2-(dibenzylamino)hept-6-en-3-ol (3.61).....	188
Figure 8.52. ¹ H NMR of (2S,3R)-1-((TBSO)-2-(dibenzylamino)hept-6-en-3-ol (3.61)...	189
Figure 8.53. (2S)-1-((TBSO)-2-(dibenzylamino)hept-6-en-3-yl acetate (3.62).....	190
Figure 8.54. ¹ H NMR of (2S)-1-(TBSO)-2-(dibenzylamino)heptenyl acetate (3.62)....	191
Figure 8.55. (2S,3R)-1-(TBSO)-2-(dibenzylamino)-6-oxohexan-3-yl acetate (3.63)...	192
Figure 8.56. ¹ H NMR of (TBSO)-2-(dibenzylamino)oxohexanyl acetate (3.63).....	193
Figure 8.57. (S)-5-(hydroxymethyl)pyrrolidin-2-one (3.87).....	194
Figure 8.58. ¹ H NMR of (S)-5-(hydroxymethyl)pyrrolidin-2-one (3.87).....	195
Figure 8.59. ¹³ C NMR of (S)-5-(hydroxymethyl)pyrrolidin-2-one (3.87).....	196
Figure 8.60. (S)-5-((TBSO)methyl)pyrrolidin-2-one (3.88).....	197

Figure 8.61. ^{13}C NMR of (<i>S</i>)-5-(TBSO)methylpyrrolidin-2-one (3.88).....	198
Figure 8.62. ^{13}C NMR of (<i>S</i>)-5-(TBSO)methylpyrrolidin-2-one (3.88).....	199
Figure 8.63. Tert-butyldimethylsilylether-sulfoxonium ylide (3.89).....	200
Figure 8.64. ^1H NMR of Tert-butyldimethylsilylether-sulfoxonium ylide (3.89).....	201
Figure 8.65. ^{13}C NMR of Tert-butyldimethylsilylether-sulfoxonium ylide (3.89).....	202
Figure 8.66. (<i>S</i>)- <i>tert</i> -butyl 2-(TBSO)methyl-5-oxopiperidine-1-carboxylate (3.90)....	203
Figure 8.67. ^1H NMR of (<i>S</i>)- <i>t</i> -Bu 2-(TBSO)methyl-oxopiperidinecarboxylate (3.90)...	204
Figure 8.68. (<i>S</i>)-1- <i>tert</i> -butyl 2-methyl 5-oxopyrrolidine-1,2-dicarboxylate (3.91).....	205
Figure 8.69. ^1H NMR (<i>S</i>)- <i>tert</i> -butyl methyl oxopyrrolidine-1,2-dicarboxylate (3.91)....	206
Figure 8.70. ^{13}C NMR (<i>S</i>)- <i>tert</i> -butyl methyl oxopyrrolidine-1,2-dicarboxylate (3.91)...	207
Figure 8.71. Methylester Sulfoxonium Ylide (3.92).....	208
Figure 8.72. ^1H NMR of Methylester Sulfoxonium Ylide (3.92).....	209
Figure 8.73. ^{13}C NMR of Methylester Sulfoxonium Ylide (3.92).....	210
Figure 8.74. 1-((benzyloxy)carbonyl)-4-hydroxypyrrolidine-2-carboxylic acid (3.95)....	211
Figure 8.75. ^1H NMR of 1-((BnO)carbonyl)hydroxypyrrolidinecarboxylic acid (3.95)...	212
Figure 8.76. ^{13}C NMR of 1-((BnO)carbonyl)hydroxypyrrolidinecarboxylic acid (3.95)..	213
Figure 8.77. (<i>S</i>)-1-benzyl 2- <i>tert</i> -butyl 4-oxopyrrolidine-1,2-dicarboxylate (3.96).....	214
Figure 8.78. ^1H NMR of (<i>S</i>)-1-benzyl <i>tert</i> -butyl oxopyrrolidine dicarboxylate (3.96)....	215
Figure 8.79. ^{13}C NMR of (<i>S</i>)-1-benzyl <i>tert</i> -butyl oxopyrrolidine dicarboxylate (3.96)...	216
Figure 8.80. (<i>S</i>)-1-benzyl 2- <i>tert</i> -butyl oxopyrrolidinedicarboxylate (3.97).....	217
Figure 8.81. ^1H NMR of (<i>S</i>)-1-benzyl <i>tert</i> -butyl oxopyrrolidine dicarboxylate (3.97)....	218
Figure 8.82. (6 <i>S</i>)- tricarboxylate (3.98) & (2 <i>S</i>)- tricarboxylate (3.99).....	219

Figure 8.83. ^1H NMR of (6S)- tricarboxylate (3.98) & (2S)- tricarboxylate (3.99).....	220
Figure 8.84. ^{13}C NMR of (6S)- tricarboxylate (3.98) & (2S)- tricarboxylate (3.99).....	221
Figure 8.85. (S)-2,6-bis((tert-butoxycarbonyl)amino)hexanoic acid (3.101).....	222
Figure 8.86. ^1H NMR of (S)-2,6-bis((Boc)amino)hexanoic acid (3.101).....	223
Figure 8.87. ^{13}C NMR of (S)-2,6-bis((Boc)amino)hexanoic acid (3.101).....	224
Figure 8.88. (S)-methyl 2,6-bis((Boc)amino)hexanoate (3.102).....	225
Figure 8.89. ^1H NMR of (S)-methyl 2,6-bis((Boc)amino)hexanoate (3.102).....	226
Figure 8.90. Dicarboxylate (3.103).....	227
Figure 8.91. ^1H NMR of Dicarboxylate (3.103).....	228
Figure 8.92. ^{13}C NMR of Dicarboxylate (3.103).....	229
Figure 8.93. Diethyl-2-((Boc)amino)malonate (3.107).....	230
Figure 8.94. ^1H NMR of Diethyl-2-((Boc)amino)malonate (3.107).....	231
Figure 8.95. Diethyl 2-allyl-2-((Boc)amino)malonate (3.108).....	232
Figure 8.96. ^1H NMR of Diethyl 2-allyl-2-((Boc)amino)malonate (3.108).....	233
Figure 8.97. Ethyl 2-((tert-butoxycarbonyl)amino)pent-4-enoate (3.109).....	234
Figure 8.98. ^1H NMR of Ethyl 2-((tert-butoxycarbonyl)amino)pent-4-enoate (3.109)...	235
Figure 8.99. (S)-2-((<i>tert</i> -butoxycarbonyl)amino)pent-4-enoic acid (3.110).....	236
Figure 8.100. ^1H NMR of (S)-2-((Boc)amino)pent-4-enoic acid (3.110).....	237
Figure 8.101. (S)-methyl 2-pent-4-enoate (3.111).....	238
Figure 8.102. ^1H NMR of (S)-methyl 2-pent-4-enoate (3.111).....	239
Figure 8.103. ^{13}C NMR of (S)-methyl 2-pent-4-enoate (3.111).....	240
Figure 8.104. 3,3'-di- <i>t</i> -Bu-5,5'-dimethoxy-[1,1'-biphenyl]-2,2'-diol (3.114).....	241

Figure 8.105. ^1H NMR of 3,3'-di- <i>t</i> -Bu-5,5'-dimethoxy-[1,1'-biphenyl]-2,2'-diol (3.114).....	242
Figure 8.106. ^{13}C NMR of 3,3'-di- <i>t</i> -Bu-5,5'-dimethoxy-[1,1'-biphenyl]-2,2'-diol (3.114).....	243
Figure 8.107. 6-chlorodibenzo[d,f][1,3,2]dioxaphosphepine (3.116).....	244
Figure 8.108. BIPHENPHOS Ligand (3.117).....	245
Figure 8.109. ^1H NMR of BIPHENPHOS Ligand (3.117).....	246
Figure 8.110. (S)-1- <i>t</i> Bu 2-methyl 3,4-dihydropyridine dicarboxylate (3.104).....	247
Figure 8.111. ^1H NMR of (S)-1- <i>t</i> Bu 2-methyl dihydropyridine dicarboxylate (3.104)....	248
Figure 8.112. (2S)- hydroxypiperidine dicarboxylate (3.105).....	249
Figure 8.113. ^1H NMR of (2S)- hydroxypiperidine dicarboxylate (3.105).....	250
Figure 8.114. ^{13}C NMR of (2S)- hydroxypiperidine dicarboxylate (3.105).....	251
Figure 8.115. Methyl 3-((4-methoxyphenyl)amino)acrylate (3.118).....	252
Figure 8.116. ^1H NMR of Methyl 3-((4-methoxyphenyl)amino)acrylate (3.118).....	253
Figure 8.117. 6-methoxyquinolin-4(1H)-one (3.119).....	254
Figure 8.118. ^1H NMR of 6-methoxyquinolin-4(1H)-one (3.119).....	255
Figure 8.119. 4-bromo-6-methoxyquinoline (3.81).....	256
Figure 8.120. ^1H NMR of 4-bromo-6-methoxyquinoline (3.81).....	257
Figure 8.121. (2S) 5-((TBSO)piperidine dicarboxylate (3.120).....	258
Figure 8.122. ^1H NMR of (2S)-5-((TBSO)piperidine dicarboxylate (3.120).....	259
Figure 8.123. ^{13}C NMR of (2S)-5-((TBSO)piperidine dicarboxylate (3.120).....	260
Figure 8.124. (2S)-((TBSO)-2-(hydroxymethyl)piperidine-1-carboxylate (3.121).....	261
Figure 8.125. ^1H NMR of (2S)- ((TBSO)-2-piperidine-1-carboxylate (3.121).....	262
Figure 8.126. (8S)- tetrahydro-1 <i>H</i> -oxazolo[3,4- <i>a</i>]pyridin-3(5 <i>H</i>)-one (3.123).....	263

Figure 8.127. ^1H NMR of (8 <i>S</i>)- tetrahydro-1 <i>H</i> -oxazolopyridin-3(5 <i>H</i>)-one (3.123).....	264
Figure 8.128. ^{13}C NMR of (8 <i>S</i>)- tetrahydro-1 <i>H</i> -oxazolopyridin-3(5 <i>H</i>)-one (3.123).....	265
Figure 8.129. 1-hydroxypent-4-en-2-yl-carbamate (3.129a).....	266
Figure 8.130. ^1H NMR of 1-hydroxypent-4-en-2-yl-carbamate (3.129a).....	267
Figure 8.131. ^{13}C NMR of 1-hydroxypent-4-en-2-yl-carbamate (3.129a).....	268
Figure 8.132. Pent-4-en-2-yl-carbamate (3.129).....	269
Figure 8.133. ^1H NMR of Pent-4-en-2-yl-carbamate (3.129).....	270
Figure 8.134. 3,4-dihydropyridine-1(2 <i>H</i>)-carboxylate (3.130).....	271
Figure 8.135. ^1H NMR of 3,4-dihydropyridine-1(2 <i>H</i>)-carboxylate (3.130).....	272
Figure 8.136. 5-hydroxypiperidine-1-carboxylate (3.131).....	273
Figure 8.137. ^1H NMR of 5-hydroxypiperidine-1-carboxylate (3.131).....	274
Figure 8.138. ^{13}C NMR of 5-hydroxypiperidine-1-carboxylate (3.131).....	275
Figure 8.139. 5-((TMS)oxy)piperidine (3.131a).....	276
Figure 8.140. ^1H NMR of 5-((TMS)oxy)piperidine (3.131a).....	277
Figure 8.141. ^{13}C NMR of 5-((TMS)oxy)piperidine (3.131a).....	278
Figure 8.142. 5-((TMS)oxy)piperidin-1-yl)but-2-en-1-yl benzoate (3.133).....	279
Figure 8.143. ^1H NMR of 5-((TMS)oxy)piperidin-1-yl)but-2-en-1-yl benzoate (3.133).....	280
Figure 8.144. ^{13}C NMR of 5-((TMS)oxy)piperidin-1-yl)but-2-en-1-yl benzoate (3.133).....	281
Figure 8.145. 5-hydroxypiperidin-1-yl)but-2-en-1-yl benzoate (3.134).....	282
Figure 8.146. ^1H NMR of 5-hydroxypiperidin-1-yl)but-2-en-1-yl benzoate (3.134).....	283
Figure 8.147. ^{13}C NMR of 5-hydroxypiperidin-1-yl)but-2-en-1-yl benzoate (3.134).....	284
Figure 8.148. Piperidine-2-carboxylate (3.135).....	285

Figure 8.149. ¹ H NMR of Piperidine-2-carboxylate (3.135).....	286
Figure 8.150. ¹³ C NMR of Piperidine-2-carboxylate (3.135).....	287
Figure 8.151. 5-((trimethylsilyl)oxy)piperidine-2-carboxylate (3.136).....	288
Figure 8.152. ¹ H NMR of 5-((trimethylsilyl)oxy)piperidine-2-carboxylate (3.136).....	289
Figure 8.153. ¹³ C NMR of 5-((trimethylsilyl)oxy)piperidine-2-carboxylate (3.136).....	290
Figure 8.154. 5-hydroxypiperidine-2-carboxylate (3.136a).....	291
Figure 8.155. ¹ H NMR of 5-hydroxypiperidine-2-carboxylate (3.136a).....	292
Figure 8.156. ¹³ C NMR of 5-hydroxypiperidine-2-carboxylate (3.136a).....	293
Figure 8.157. 5-oxopiperidine-2-carboxylate (3.137).....	294
Figure 8.158. ¹ H NMR of 5-oxopiperidine-2-carboxylate (3.137).....	295
Figure 8.159. ¹³ C NMR of 5-oxopiperidine-2-carboxylate (3.137).....	296
Figure 8.160. 1,2,3,6-tetrahydropyridine-2-carboxylate (3.138).....	297
Figure 8.161. ¹ H NMR of 1,2,3,6-tetrahydropyridine-2-carboxylate (3.138).....	298
Figure 8.162. (<i>E</i>)-5-(tritylthio)pent-2-enal (5.11).....	299
Figure 8.163. ¹ H NMR of (<i>E</i>)-5-(tritylthio)pent-2-enal (5.11).....	300
Figure 8.164. 3-hydroxy-7-(tritylthio)hept-4-en-1-one (5.13).....	301
Figure 8.165. ¹ H NMR of 3-hydroxy-7-(tritylthio)hept-4-en-1-one (5.13).....	302
Figure 8.166. 3-hydroxy-7-(tritylthio)hept-4-enoate (5.5).....	303
Figure 8.167. ¹ H NMR of 3-hydroxy-7-(tritylthio)hept-4-enoate (5.5).....	304
Figure 8.168. N-Fmoc-Val-7-(tritylthio)hept-4-enoate (5.14).....	305
Figure 8.169. ¹ H NMR of N-Fmoc-Val-7-(tritylthio)hept-4-enoate (5.14).....	306
Figure 8.170. Oxazole (5.7).....	307

Figure 8.171. ^1H NMR of Oxazole (5.7).....	308
Figure 8.172. Thiazoline-Oxazole Acid (5.4).....	309
Figure 8.173. ^1H NMR of Thiazoline-Oxazole Acid (5.4).....	310
Figure 8.174. ^{13}C NMR of Thiazoline-Oxazole Acid (5.4).....	311
Figure 8.175. Thiazoline-Oxazole Acycle Analog (5.3).....	312
Figure 8.176. ^1H NMR of Thiazoline-Oxazole Acycle Analog (5.3).....	314
Figure 8.177. ^{13}C NMR of Thiazoline-Oxazole Acycle Analog (5.3).....	315
Figure 8.178. Thiazoline-Oxazole Macrocyclic Analog (5.2).....	316
Figure 8.179. ^1H NMR of Thiazoline-Oxazole Macrocyclic Analog (5.2).....	318
Figure 8.180. ^{13}C NMR of Thiazoline-Oxazole Macrocyclic Analog (5.2).....	319
Figure 8.181. Thiazoline-Oxazole Dimer (5.15).....	320
Figure 8.182. ^1H NMR of Thiazoline-Oxazole Dimer (5.15).....	321
Figure 8.183. ^{13}C NMR of Thiazoline-Oxazole Dimer (5.15).....	322
Figure 8.184. Thiazoline-Oxazole Thiol Analog (5.16).....	323
Figure 8.185. ^1H NMR of Thiazoline-Oxazole Thiol Analog (5.16).....	324
Figure 8.186. ^{13}C NMR of Thiazoline-Oxazole Thiol Analog (5.16).....	325
Figure 8.187. Thiazoline-Oxazole Thioester Analog (5.1).....	326
Figure 8.188. ^1H NMR of Thiazoline-Oxazole Thioester Analog (5.1).....	328
Figure 8.189. ^{13}C NMR of Thiazoline-Oxazole Thioester Analog (5.1).....	329
Figure 8.190. Thiazole-peptide (5.23).....	330
Figure 8.191. ^1H NMR of Thiazole-peptide (5.23).....	331
Figure 8.192. ^{13}C NMR of Thiazole-peptide (5.23).....	332

Figure 8.193. N-Fmoc-thiazole peptide (5.24).....	333
Figure 8.194. ^1H NMR of N-Fmoc-thiazole peptide (5.24).....	334
Figure 8.195. ^{13}C NMR of N-Fmoc-thiazole peptide (5.24).....	335
Figure 8.196. Oxazoline-thiazole-peptide (5.26).....	336
Figure 8.197. ^1H NMR of Oxazoline-thiazole-peptide (5.26).....	337
Figure 8.198. ^{13}C NMR of Oxazoline-thiazole-peptide (5.26).....	338
Figure 8.199. Oxazoline-Thiazole Acycle (5.19).....	339
Figure 8.200. ^1H NMR of Oxazoline-Thiazole Acycle (5.19).....	340
Figure 8.201. ^{13}C NMR of Oxazoline-Thiazole Acycle (5.19).....	341
Figure 8.202. Taxoid 7.8.....	342
Figure 8.203. ^1H NMR of Taxoid 7.8.....	343
Figure 8.204. Taxoid 7.6.....	344
Figure 8.205. ^1H NMR of Taxoid 7.6.....	345
Figure 8.206. Taxoid 7.10.....	346
Figure 8.207. ^1H NMR of Taxoid 7.10.....	347
Figure 8.208. Taxoid 7.7.....	348
Figure 8.209. ^1H NMR of Taxoid 7.7.....	349
Figure 8.210. Taxoid 7.14.....	350
Figure 8.211. ^1H NMR of Taxoid 7.14.....	351
Figure 8.212. Taxoid 7.11.....	352
Figure 8.213. ^1H NMR of Taxoid 7.11.....	353
Figure 8.214. Taxoid 7.15.....	354

Figure 8.215. ^1H NMR of Taxoid 7.15.....	355
Figure 8.216. Taxoid 7.13.....	356
Figure 8.217. ^1H NMR of Taxoid 7.13.....	357
Figure 8.218. Taxoid 7.16.....	358
Figure 8.219. ^1H NMR of Taxoid 7.16.....	359

LIST OF SCHEMES

Chapter 2

Scheme 2.1. Rabé-Kindler Partial Synthesis of Quinine.....	11
Scheme 2.2. Woodward-Doering Formal Total Synthesis of Quinine.....	12
Scheme 2.3. Uskokovic 1973 Route to Quinine.....	13
Scheme 2.4. Uskokovic 1978 Route to Quinine.....	14
Scheme 2.5. Uskokovic's Convergent Route to Quinine.....	15
Scheme 2.6. Stork Asymmetric Total Synthesis of Quinine.....	16
Scheme 2.7. Jacobsen Total Synthesis of Quinine.....	18
Scheme 2.8. Kobayashi's Total Synthesis of Quinine.....	20
Scheme 2.9. Krische's Formal Total Synthesis of Quinine.....	21
Scheme 2.10. Arshad's Sulfur-Ylide Route to Quinine.....	22
Scheme 2.11 Sarkars Total Synthesis of Quinine.....	23
Scheme 2.12. Friestad Formal Synthesis of Quinine.....	25
Scheme 2.13. William's Route to 7-hydroxyquinine.....	26
Scheme 2.14. Smith's route to 7-Hydroxy-9-Deoxy-Quinine.....	27

Chapter 3

Scheme 3.1. O'Neils α -Proton Activation Chemistry.....	29
Scheme 3.2. First Generation Route Towards Quinine.....	30
Scheme 3.3. Synthesis of Quinoline Fragments.....	31
Scheme 3.4 Strategy for Formation of the Quinuclidine Intermediate.....	32
Scheme 3.5. Coupling of Quinoline and Quinuclidine Fragments.....	32

Scheme 3.6. Amine-Borane Complex.....	33
Scheme 3.7. Model System with N-Oxide.....	34
Scheme 3.8 2 nd Generation Retrosynthetic Analysis.....	35
Scheme 3.9 Smith's Route Toward Enamine 3.45.....	36
Scheme 3.10. Attempted C2 Alkylations.....	36
Scheme 3.11 Serine Metathesis Route.....	37
Scheme 3.12. Oxidation Conditions.....	38
Scheme 3.13 Dibenzyl Serine Route.....	39
Scheme 3.14 Oxidation Conditions.....	39
Scheme 3.15. Intramolecular Cyclization.....	40
Scheme 3.16. Previous Williams' Cyclization Result.....	40
Scheme 3.17. Possible Mechanistic Explanation of Pd-Cyclization.....	41
Scheme 3.18. Smith's Unpublished Results.....	42
Scheme 3.19 3 rd Generation Retrosynthetic Analysis.....	43
Scheme 3.20. Mangion's Route to Substituted Pipecolic Acid Derivatives.....	43
Scheme 3.21. Synthesis of Sulfoxonium Ylide (3.89).....	44
Scheme 3.22. Synthesis of Sulfoxonium Ylide (3.92).....	44
Scheme 3.23. Avery's Ring Expansion Method.....	45
Scheme 3.24. Kiesel's Manganese Acetate Approach.....	46
Scheme 3.25. Hydroboration/Oxidation of Enamine 3.104.....	47
Scheme 3.26. Synthesis of Allylglycine.....	48
Scheme 3.27 Ojima's Cyclohydrocarbonylation Reaction.....	48

Scheme 3.28. Synthesis of BIPHENPHOS Ligand.....	49
Scheme 3.29 Synthesis of Pipecolic Acid Derivative.....	49
Scheme 3.30. Synthesis of 4-bromo-6-methoxy-quinoline.....	50
Scheme 3.31. Unexpected Intramolecular Cyclization.....	51
Scheme 3.32. Precedent for Intramolecular Cyclization.....	51
Scheme 3.33. Initial Coupling Attempts.....	52
Scheme 3.34. Late Stage Silyl Intermediate.....	53
Scheme 3.35. Late Stage Quinine Intermediate.....	54
Scheme 3.36. Possible Interception of Uskokovic's Intermediate.....	55

Chapter 4

Scheme 4.1. Largazole Activation.....	63
Scheme 4.2. General Strategy Towards Largazole.....	63
Scheme 4.3. Luesch's Route to Largazole.....	64
Scheme 4.4. Phillips and Cramer Routes to Largazole.....	66
Scheme 4.5. Williams' Route to Largazole.....	67
Scheme 4.6. Ghosh's Route Towards Largazole.....	68
Scheme 4.7. Ye's Route to Largazole.....	69
Scheme 4.8. Doi's Route to Largazole.....	70
Scheme 4.9. Forsyth's Route to Largazole.....	71

Chapter 5

Scheme 5.1. Thiazoline-Oxazole Analog Retrosynthetic Analysis.....	77
Scheme 5.2. Synthesis of Thiazoline-Oxazole Fragment.....	77

Scheme 5.3. Heptenoic Acid Synthesis.....	78
Scheme 5.4. Formation of Analog Acycle.....	78
Scheme 5.5. Macrocyclization and Formation of Homo-Dimer.....	79
Scheme 5.6. Deprotection and Acetylation.....	79
Scheme 5.7. Oxazoline-Thiazole Analog Retrosynthetic Analysis.....	80
Scheme 5.8. Oxazoline-Thiazole Synthesis and Coupling.....	81
Scheme 5.9. Acycle Formation.....	82

Chapter 6

Scheme 6.1. Early Biosynthetic Proposal from ggPP to Taxol.....	87
Scheme 6.2. Products of Recombinant Taxadiene Synthase.....	88
Scheme 6.3. Mechanism of Taxadiene Synthase.....	90
Scheme 6.4. Total Synthesis of Taxa-4(5),11(12)-diene (6.5) and Taxa-4(20),11(12)-diene (6.4).....	95
Scheme 6.5. Early Hydroxylation and Acetylation Steps.....	96
Scheme 6.6. Synthesis of Taxadiene 5 α - and 5 β -ols (6.26 and 6.28)	98
Scheme 6.7. Mechanism of Taxadiene Hydroxylase.....	101
Scheme 6.8. Production of Novel Taxane, OCT.....	102
Scheme 6.9. Synthesis of Taxa-4(20),11(12)-dien-2 α ,5 α -diol (6.39)	104
Scheme 6.10. Synthesis of tritiated taxa-4(20) 11(12)-dien-5 α -yl-acetate-10 β -ol (6.47)	106

Scheme 6.11. Synthesis of taxa-4(20), 11(12)-dien-5 α -yl-acetate-2 α ,10 β -diol (6.49)	107
Scheme 6.12. Synthesis of the 5,10,14-triol; the 2,5,10-triol and the 5,10-diol.....	108
Scheme 6.13. Alternative route to taxa-4(20),11(12)-diene-5 α -acetate	108
Scheme 6.14. Synthesis of the 5,9,13-triol and the 5,10,13-triol by deoxygenation of taxusin.....	110
Scheme 6.15. Synthesis of taxa-4(20),11(12)-dien-5 α ,13 α -diol.....	111
Scheme 6.16. Alternative syntheses of the 5,9,13-triol and the 5,10,13-triol by deoxygenation of taxusin.....	112
Scheme 6.17. 13 α - and 10 β -hydroxylase.....	113
Scheme 6.18. 2 α - and 7 β -Hydroxylase Activity.....	114
Scheme 6.19. Biosynthetic formation of the 5 α ,14 β -diol (6.75)	116
Scheme 6.20. 14 β -hydroxylase Activity.....	117
Scheme 6.21. Original Theory of Oxetane Ring Formation.....	118
Scheme 6.22. Acylation of C4 in Advanced Taxanes.....	118
Scheme 6.23. C13 Side-chain Construction and Implementation.....	119

Chapter 7

Scheme 7.1. Compounds Derived from Taxusin.....	121
Scheme 7.2. Synthesis of Ketone 7.8.....	122
Scheme 7.3. Reduction Conditions.....	122
Scheme 7.4. Attempted Reduction of 7.10.....	123
Scheme 7.5. Mono-TBS Protection.....	123

Scheme 7.6. Deprotection of C13 TBS.....	124
Scheme 7.7. Failed Acetonide Removal.....	124
Scheme 7.8. Conditions for Removal of Acetonide.....	125
Scheme 7.9. HF•Pyridine Removal of Silyl Ether 7.13.....	125
Scheme 7.10. Desired Potential Biosynthetic Intermediates.....	126
Scheme 7.11. Removal of C5 and C13 Acetates.....	126
Scheme 7.12. Formation of Separable Taxoids.....	127
Scheme 7.13. Xanthate Ester Formation.....	127
Scheme 7.14. Attempted Deoxygenation.....	128

LIST OF ABBREVIATIONS

Ac ₂ O	Acetic anhydride
Bn	Benzyl
BnBr	Benzyl bromide
Boc	<i>tert</i> -Butoxycarbonyl
Boc ₂ O	di- <i>tert</i> -Butyldicarbonate
BOMCl	Benzyloxymethyl chloride
BOP	(Benzotriazol-1-yloxy)tris(dimethylamino) phosphonium hexafluorophosphate
BuLi	Butyllithium
DBU	1,8-Diazabicyclo[5.4.0]undec-7-ene
DCC	<i>N,N'</i> -Dicyclohexylcarbodiimide
DCM	Dichloromethane
Dess-Martin Periodinane	Triacetoxy <i>o</i> -iodoxybenzoic acid
DIBAL-H	Diisobutylaluminum hydride
DIPEA	Diisopropylethylamine
DMAP	4-(Dimethylamino)pyridine
DME	Dimethoxyethane
DMF	Dimethylformamide
DMSO	Dimethylsulfoxide
EDCI (or EDC)	<i>N</i> -(3-dimethylaminopropyl)- <i>N'</i> -ethylcarbodiimide

EtOAc	Ethyl acetate
Et ₂ O	Diethyl ether
Fmoc	Fluorenylmethyloxycarbonyl
FmocOSu	9-Fluorenylmethyl <i>N</i> -succinimidyl carbonate, <i>N</i> -(9-Fluorenylmethoxycarbonyloxy)succinimide
HATU	<i>O</i> -(7-Azabenzotriazol-1-yl)- <i>N,N,N',N'</i> -tetramethyluronium hexafluorophosphate
HOAt	1-Hydroxy-7-azabenzotriazole
HOBt	1-Hydroxybenzotriazole
imid.	Imidazole
KHMDS	Sodium (bis)trimethylsilyl amide
LDA	Lithium <i>N,N</i> -diisopropylamide)
LHMDS (or LiHMDS)	Lithium (bis)trimethylsilyl amide
<i>m</i> CPBA	<i>m</i> -Chloroperbenzoic acid
MeI	Iodomethane
MeOH	Methanol
MsCl	Methanesulfonyl chloride
Mukaiyama reagent	2-Chloro-1-methylpyridinium iodide
NHMDS (or NaHMDS)	Sodium (bis)trimethylsilyl amide
PCC	Pyridinium chlorochromate
Pd(OAc) ₂	Palladium (II) acetate
Pd ₂ (dba) ₃	Tris(dibenzylideneacetone)dipalladium

PPTS	Pyridinium-toluenesulfonate
<i>p</i> TSA	<i>p</i> -Toluenesulfonic acid
Py. or Pyr.	Pyridine
PyAOP	(7-Azabenzotriazol-1-yloxy) tripyrrolidinophosphonium- hexafluorophosphate
PyBOP	Benzotriazol-1-yl- oxytripyrrolidinophosphonium hexafluorophosphate
Red-Al	Sodium bis(2-methoxyethoxy)aluminum
TBAF	Tetrabutylammonium fluoride
TBAI	Tetrabutylammonium iodide
TBDPS	<i>tert</i> -Butyldiphenylsilyl
TBSCI	<i>tert</i> -Butyldimethylsilyl chloride
<i>t</i> -BuOK	Potassium <i>tert</i> -butoxide
TEMPO	2,2,6,6-Tetramethyl-1-piperidinyloxy
TESOTf	Triethylsilyl trifluoromethanesulfonate
TFA	Trifluoroacetic acid
THF	Tetrahydrofuran
TMEDA	<i>N,N,N',N'</i> -Tetramethylethylenediamine
TMS	Trimethylsilyl
TMSCI	Trimethylsilyl chloride

TPAP	Tetrapropylammonium perruthenate
TrocCl	Trichloroethyl chloroformate
TrSH (or TrtSH)	Triphenylmethanethiol
TsCl	<i>p</i> -Toluenesulfonyl chloride
TSE	2-Trimethylsilyl ethyl
TsOH	<i>p</i> -Toluenesulfonic acid

Chapter 1: Introduction and Overview

1.1 Introduction

Here in we discuss three separate projects in the area of natural product synthesis: (1) efforts toward the total synthesis of quinine, (2) synthesis of largazole analogs, and (3) efforts towards potential biosynthetic intermediates of taxol. The synthesis of bioactive natural products is of extreme interest to the Williams group, and the first two projects widely encompass this passion. Additionally, the biosynthetic construction of complex natural products is also an ongoing research project in our group. The development of potential biosynthetic intermediates of taxol would allow for a better understanding of how nature makes this complex, and highly sought after anti-cancer drug.

1.1.1 Quinine

Efforts towards the total synthesis of quinine have been an ongoing project in the Williams group. Initial efforts were employed toward utilizing a unique C3-C4 Pd- π -allyl ring closure that has never been utilized in any other synthesis of quinine (a complete history of the previous routes toward quinine can be seen in chapter 2). Early efforts arrived at advanced intermediates, oxygenated at the C7 position.¹ Unfortunately, an

abundance of evidence has demonstrated that removal of a C7 hydroxyl is impossible and it is thought to be due to the sterics of the complex quinoline-quinuclidine system.²

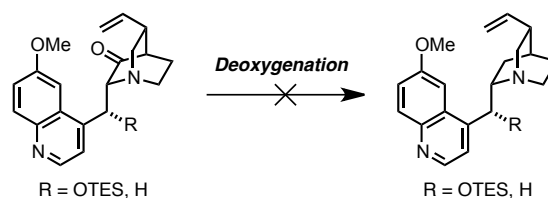


Figure 1.1. Failed Deoxygenation of Quinine.

With this in mind potential route towards an advanced intermediate has been developed that, while still requiring the deoxygenation of a late stage intermediate, would provide an intermediate with the requisite hydroxyl moiety at the C5 position, hopefully eliminating the aforementioned troubles with deoxygenation (see chapter 3).



Figure 1.2. Hypothetical Deoxygenation of Quinuclidine.

1.1.2 Overview of Results

The first generation route towards our late stage, advanced intermediate was based off the development of a C2-functionalized piperidine system. Unfortunately, the development of this type of intermediate proved to be cumbersome and after exhausting several routes, another approach was embarked upon.

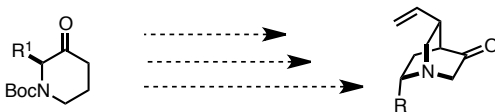


Figure 1.3. Possible Route to Quinuclidine Core.

The second generation route was geared towards the development of a pipecolic acid derivative. Several published routes towards our desired fragment were investigated, with the most viable route being realized from allylglycine.³ Further elaboration of allylglycine provided us with an advanced intermediate set up for the Willams' group C3-C4 cyclization reaction. Although an attempt was made at this late-stage cyclization, a lack of material as well as advancing on towards another project prevented further work with this system.

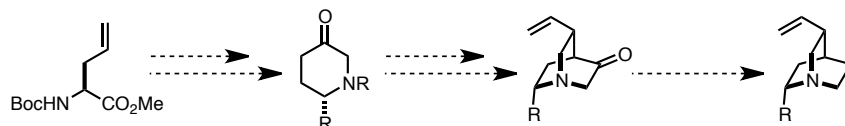


Figure 1.4. Allylglycine Route to Quinuclidine Core.

1.2 Largazole Analogs

In 2008 the macrocyclic peptide, largazole, was published (see chapter 4 for the history of largazole).⁴ The Williams group completed the synthesis of largazole and as part of an ongoing collaboration in our group with researchers at Harvard University,

SAR studies have been done and work towards the development of more potent HDAC inhibitors of the largazole variety have been synthesized and tested.

1.2.1 Overview of Results

Current efforts utilizing a route similar to that of the Williams' group synthesis of largazole⁵ have led to the synthesis of three new analogs (see chapter 5), which have been tested against HDACs 1-9, by our collaborators at Harvard.

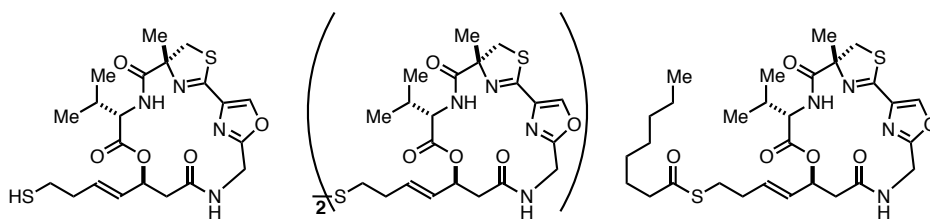


Figure 1.5. Core for Largazole Analogs.

1.3 Biosynthetic Intermediates of Taxol

Another collaborative project in our group is the study of the biosynthesis of taxol. Efforts with the Croteau group have led to the understanding of early pathway metabolites as well as the initial sequence of events towards potent anti-cancer natural product (see chapter 6 for a full account of the collaboration to date). Elucidation of the biosynthetic pathway, and subsequent bioengineering could provide a route to taxol

production that would provide this highly sought after anti-cancer drug in mass quantities.

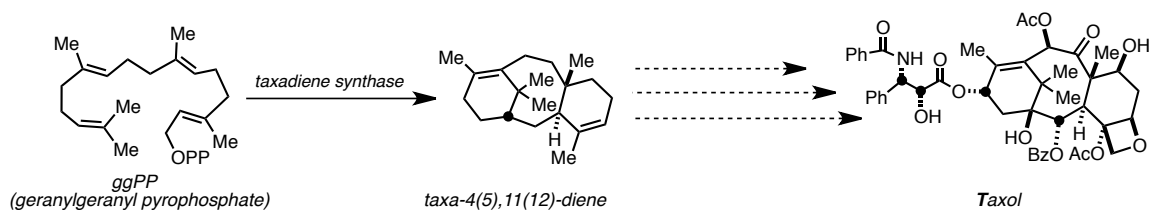


Figure 1.6. Biosynthetic Route Towards Taxol.

Recent work in the Williams group has been directed toward the synthesis of C5-acetate derivatives of highly oxygenated taxoids. The synthesis of these mono-acylated derivatives would allow for a greater understanding of the sequence of events that occur and would help in answering the question surrounding the removal and reintroduction of the C5-acetate.

1.3.1 Overview of Results

Work has been directed toward the synthesis of a series of compounds that could be developed from advanced intermediates isolated from the heartwood of the Japanese yew tree.

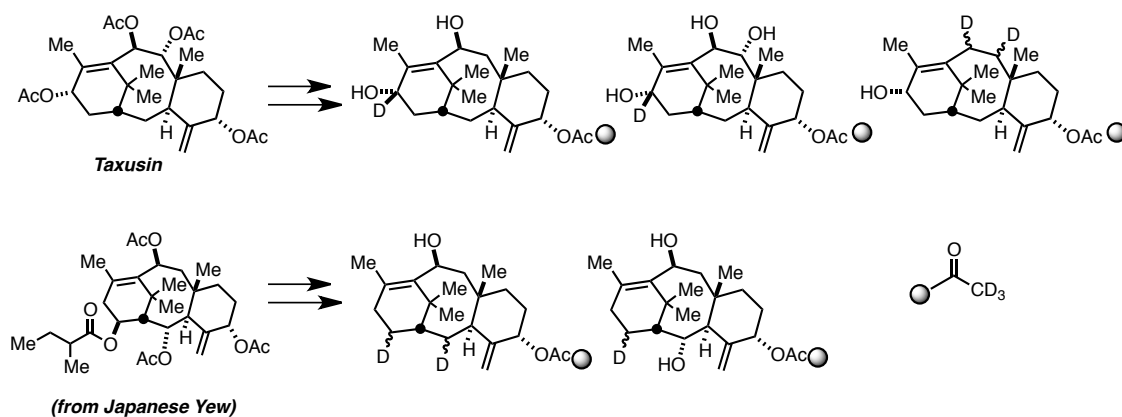


Figure 1.7. Analogs from Natural Products.

Efforts have been made at developing late stage intermediates, with the mono-acetate derivatives having yet to be realized

Chapter 2: Quinine

2.1 Introduction

2.1.1 Isolation and Background

Quinine (**2.1**, Figure 2.1), an extract from the bark of the cinchona tree located in the rain forests of the eastern Andes Mountains, was the first chronicled treatment for malaria. In 1820, French chemist Joseph Bienaimé Caventou isolated quinine from the cinchona tree, and thirty-four years later, German chemist Adolf Strecker and French chemist Pierre Joseph Pelletier determined its molecular formula.⁶ In 1907 Paul Rabé correctly proposed the structure.⁷

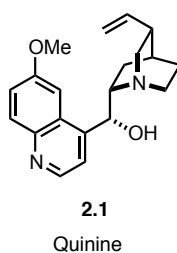


Figure 2.1. Quinine

2.1.2 Biological Mode of Action

Malaria is a disease caused by a parasite called *Plasmodium*, which is transmitted from the bites of infected mosquitoes. Left untreated, malaria becomes a life-threatening disease due to its ability to disrupt the blood supply to vital organs.⁸ Each year, malaria is responsible for infecting over 200 million people and is responsible for the deaths of nearly 1 million.⁸ Current treatments target different stages of the malaria cycle, with the majority of them acting on the intra-erythrocytic phases of the development of the malaria parasite.^{9,10} Quinoline-containing drugs fall into two categories, type-1 drugs: 4-aminoquinolines such as chloroquine (2.2), amodiaquine (2.3), and pyronaridine (2.4), and type-2-drugs: aryl-amino alcohols such as quinine (2.1), mefloquine (2.5), quinidine (2.6), and halofantrine (2.7) (Figure 2.2).⁹

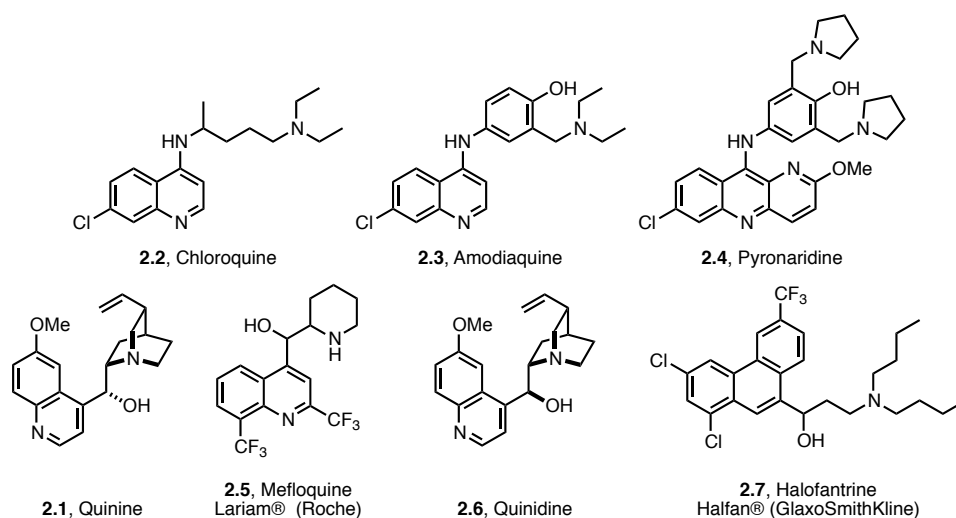


Figure 2.2. Quinoline Containing Anti-Malarial Drugs

The type-1 drugs are weak bases and are di-protonated and hydrophilic at neutral pH, whereas quinoline-type-2 drugs are weak bases and very lipid-soluble at neutral pH. The mechanism of action and mode of resistance to quinoline drugs is still being investigated. The commonly accepted hypothesis for the emergence of resistance acquired against quinoline-containing drugs revolves around heme disposal, a process in which intra-erythrocytic-stage malaria parasites detoxify heme in the food vacuole (Figure 2.3).¹⁰

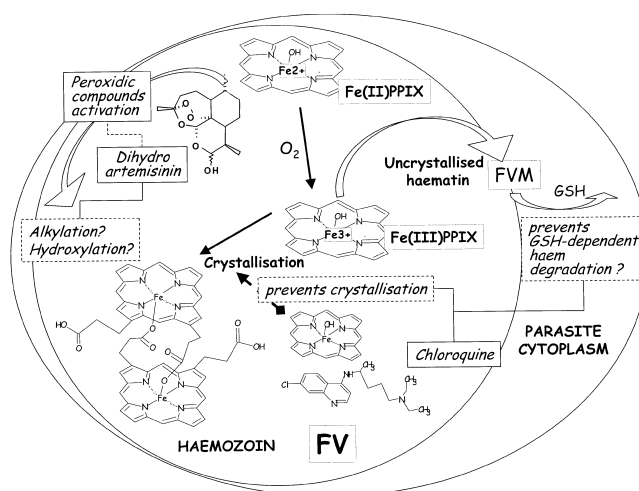


Figure 2.3. Events in the Parasite Food Vacuole¹⁰

The proposed mode of action of chloroquine is that it first increases the pH of the food vacuole, and that increase in pH could inhibit hemoglobin degradation by either vacuolar proteinases or hemeazoin formation. Next, heme likely reacts with peroxide displaying catalase and peroxidase activities that may contribute to heme degradation that are prevented by chloroquine. The peroxide buildup effectively causes peroxidative damage to lipids or proteins. Chloroquine appears to act by forming a quinoline-heme

complex that terminates hemozoin chain extension. By inhibiting chain extension, toxic heme or heme-drug complexes are in abundance, and the parasite can no longer break down heme and is effectively poisoned.^{9,10}

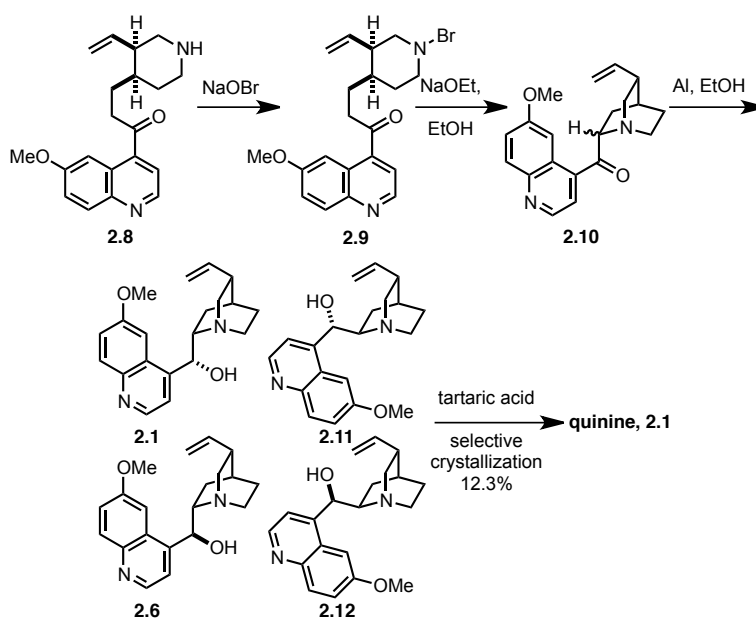
2.1.3 Mechanism of Resistance

It is generally accepted that resistance to quinolines is the result of multiple gene mutations. One theory is that the resistance to quinoline-containing anti-malarials may be linked to an accelerated drug efflux that would occur at the food vacuole membrane and would be mediated by an enhanced expression of an ATP-dependent pump, termed P-glycoprotein.¹¹ This pump can be classified as an ATP-binding cassette transporter, which has been linked to the mediation of multidrug resistance.⁹ Another hypothesis of resistance includes an altered proton flux or transporter at the food vacuole membrane. Because quinolines are weak bases, these molecules would be sensitive to pH changes. A decrease in pH gradient between the parasitic cytoplasm and the food vacuole would effectively reduce the concentration of the quinolines in the food vacuoles, allowing the parasite to survive.⁹

2.2. Previous Synthetic Studies

2.2.1 Rabé-Kindler Synthesis of Quinine

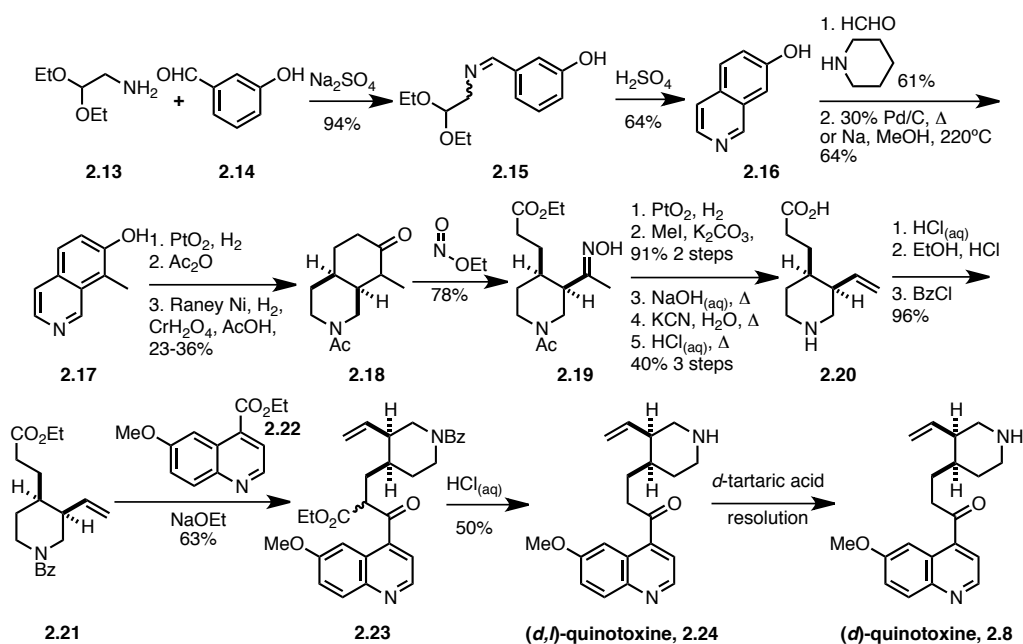
To date, there are more than 12 reported syntheses of quinine (**2.1**). The first semi-synthesis of quinine was reported by Rabé and Kindler in 1918, starting from (*d*)-quinotoxine (**2.8**), which underwent *N*-bromination, followed by base-mediated ring closure and subsequent reduction with aluminum to give four diastereomers of quinine (**2.1**, **2.6**, **2.11**, **2.12**, Scheme 2.1).¹² The final step in isolating quinine, a tartaric acid resolution, delivered quinine (**2.1**) in 12.3% yield.



Scheme 2.1. Rabé-Kindler Partial Synthesis of Quinine

2.2.2 Woodward-Doering Synthesis of Quinine

The next formal synthesis was carried out by Woodward and Doering in 1945.^{13,14} Woodward intercepted Rabé's (*d*)-quinotoxine intermediate (**2.8**, Scheme 2.2)¹² in 19 steps starting from aminoacetaldehyde diethyl acetal (**2.13**) and generating the Schiff base (**2.15**). In the presence of sulfuric acid, 7-hydroxyquinoline (**2.16**) was isolated in 64% yield.



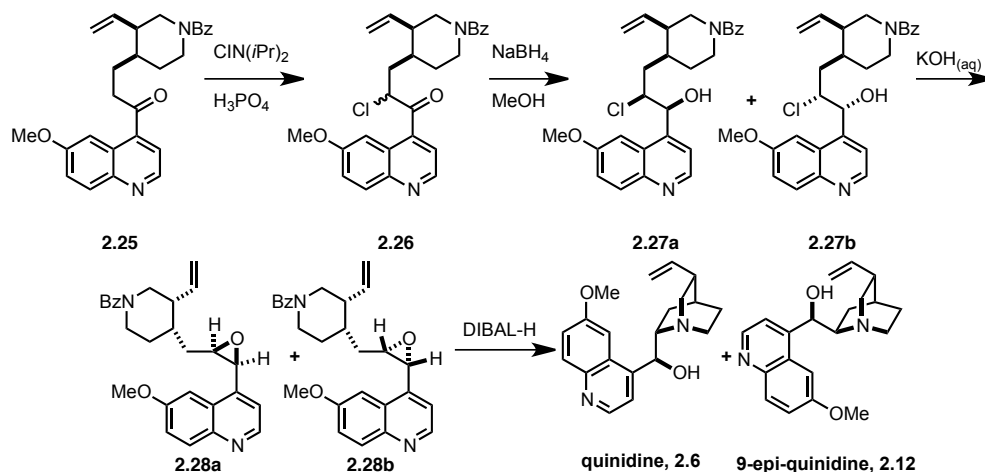
Scheme 2.2. Woodward-Doering Formal Total Synthesis of Quinine

Heating **2.16** in sodium methoxide gave **2.17**, which was then reduced in the presence of platinum oxide and hydrogen, protected, and further reduced with Raney nickel (**2.18**). Hydroxyimine formation and further reduction and deprotection gave **2.20**. Carboxylic acid **2.20** was then esterified and *N*-protected to give benzoyl protected-

piperidine **2.21**. In the presence of sodium ethoxide, the quinoline fragment (**2.22**) was coupled with **2.21**, delivering **2.23**, which was then deprotected and decarboxylated to give (*d,l*)-quinotoxine (**2.24**). Racemic quinotoxine underwent a tartaric acid resolution to intercept Rabé's late state intermediate, (*d*)-quinotoxine (**2.8**).

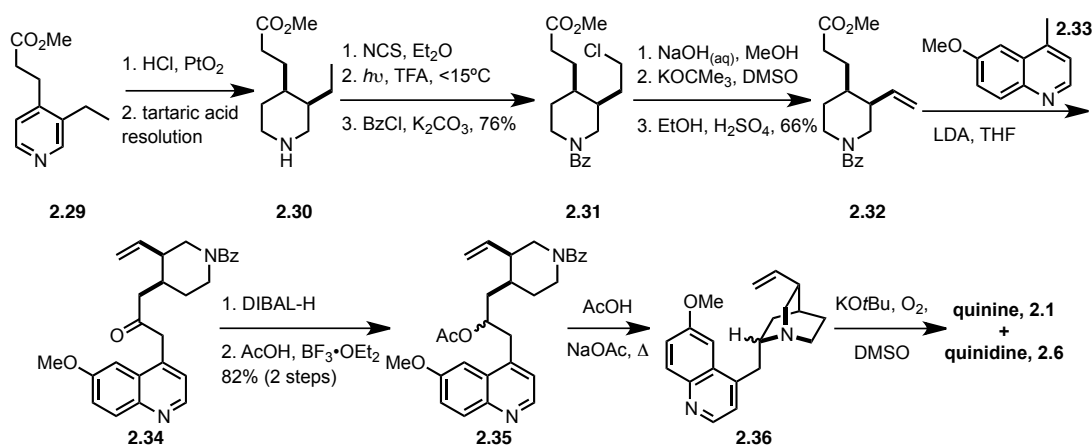
2.2.3 Uskokovic's Routes to Quinine

In 1973, Uskokovic¹⁵ published a route starting from *N*-protected-(*d*)-quinotoxine (**2.25**, Scheme 2.3). Reacting **2.25** with *N*-chlorodiisopropylamine and phosphoric acid gave **2.26**, and further reduction of the chloroketone (**2.26**) with sodium borohydride lead to a mixture of **2.27a** and **2.27b**, which, after rearrangement in the presence of base and reduction with DIBAL-H, afforded quinidine (**2.6**) and 9-*epi*-quinidine (**2.12**).



Scheme 2.3. Uskokovic 1973 Route to Quinine

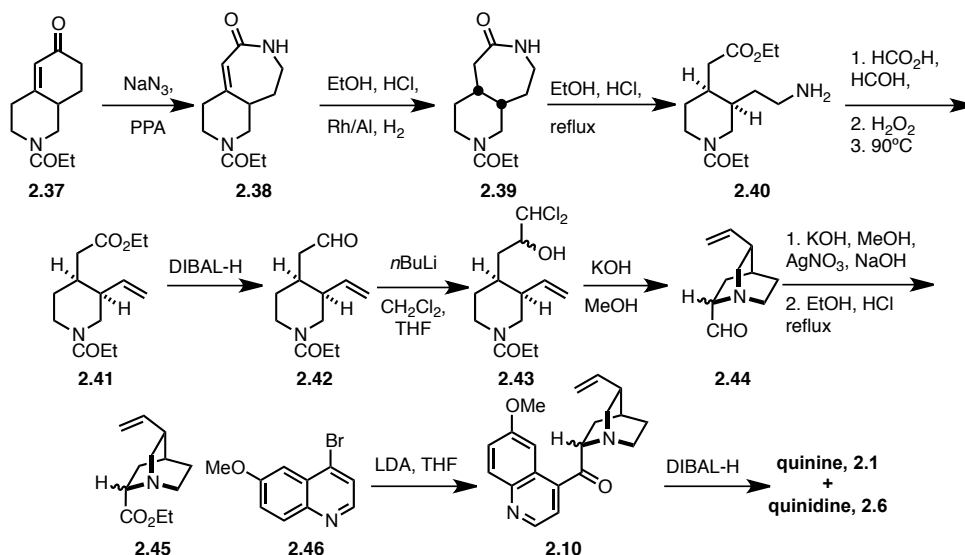
In 1978 Uskokovic published another route to quinine utilizing the Rabe' C8-N1 disconnect (Scheme 2.4).¹⁶⁻¹⁹ Uskokovic's route started with catalytic hydrogenation of disubstituted pyridine **2.29**, followed by a tartaric acid resolution yielding **2.30**. *N*-Chlorination followed by a Hoffman-Löffler-Freytag reaction and protection of the amine afforded **2.31**. After subsequent saponification, dehydrochlorination and esterification, **2.32** was obtained. Addition of the lithiate anion of **2.33** followed by reduction and deprotection with DIBAL-H and subsequent chemoselective acetylation of the alcohol using glacial acetic acid activated by $\text{BF}_3 \cdot \text{OEt}_2$ provided **2.34**. Cyclization of **2.34** in the presence of buffered acetic acid (**2.35**) and a final oxygenation at C9 afforded quinine (**2.1**) and quinidine (**2.6**).



Scheme 2.4. Uskokovic 1978 Route to Quinine

Uskokovic also published a third, convergent route to quinine and quinidine in 1978.^{15,20-22} Starting from α,β -unsaturated isoquinoline **2.37**, a Schmidt rearrangement with sodium azide and polyphosphoric acid provided **2.38** (Scheme 2.5). Reduction of

2.38 with Rh/Al and opening of the lactam with ethanolic HCl delivered **2.40**, which was then pushed through a Cope elimination sequence to afford **2.41**. Reduction provided the aldehyde (**2.42**) and reaction with *n*BuLi and CH₂Cl₂ provided alcohol **2.43**. Deprotection of the nitrogen and cyclization afforded the quinuclidine core and final oxidation delivered ethyl ester **2.45**.

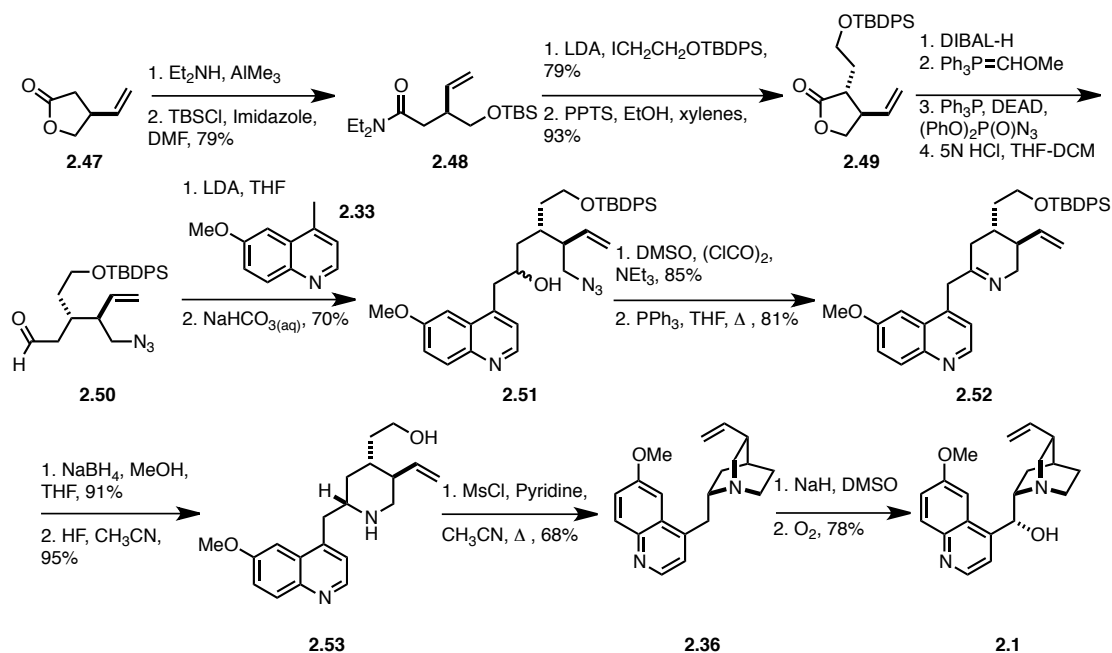


Scheme 2.5. Uskokovic's Convergent Route to Quinine

With the quinuclidine core in hand, Uskokovic then added in lithiated quinoline **2.46** and a final reduction provided quinine (**2.1**) and quinidine (**2.6**). Additionally, quinine was also synthesized by Gates and Taylor in 1970 and 1972, respectively using routes similar to that of Uskokovic.^{23,24}

2.2.4 Stork's Asymmetric Synthesis of Quinine

The first asymmetric total synthesis of quinine was reported by Stork in 2001 (Scheme 2.6).^{25,26} Opening of lactone **2.47** and subsequent protection of the primary alcohol gave amide **2.48** in good yield. Alkylation of **2.48** with TBDPS-protected iodoethanol, and subsequent deprotection afforded lactone **2.49** in >20:1 selectivity.



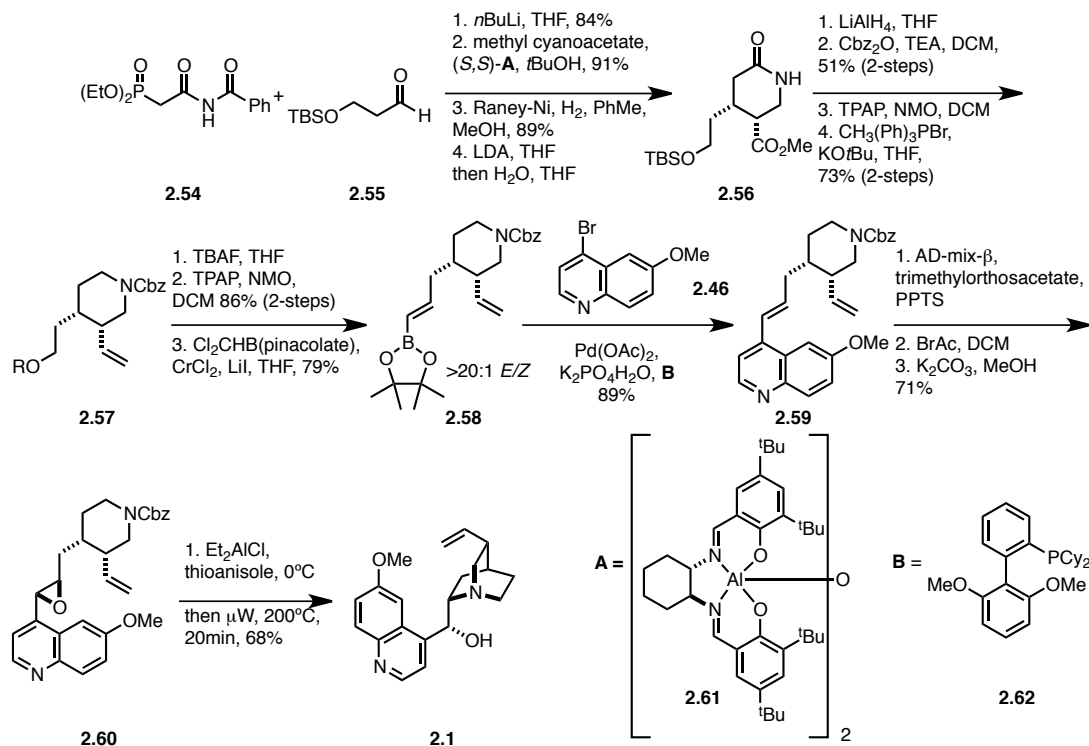
Scheme 2.6. Stork Asymmetric Total Synthesis of Quinine

Disubstituted lactone **2.49** was then reduced with DIBAL-H to give the corresponding lactol, which was then subjected to Wittig conditions and further converted to the azide which, following aqueous hydrolysis conditions, afforded azidoaldehyde **2.50**. Azide **2.51** was formed in 70% yield by treating **2.50** with the lithium salt of quinoline fragment **2.33**. The mixture of alcohol epimers (**2.51**) was then subjected to

a Swern oxidation and underwent an intramolecular Staudinger reaction to afford **2.52**. Addition of NaBH₄ and removal of the silyl group gave piperidine **2.53**, which was then treated with mesyl chloride in the presence of pyridine and refluxed to give 9-deoxyquinine (**2.36**) in 68% yield. Deoxyquinine (**2.36**) was oxidized to quinine with oxygen and sodium hydride in DMSO (Stork oxidation) to give quinine (**2.1**) in greater than 14:1 diastereoselectivity.

2.2.5 Jacobsen's Synthesis of Quinine

Jacobsen delivered the next synthesis of quinine in 2004.²⁷ Starting from known phosphonate imide **2.54**, lactam **2.65** was formed via a Horner-Wadsworth-Emmons olefination of aldehyde **2.55** (Scheme 2.7). Conjugate addition of methyl cyanoacetate in the presence of a (salen)-Al complex (**2.61**) in 92% *ee*, followed by Raney nickel hydrogenation and further protecting group manipulations gave selective formation of **2.56** in a 3:1 *cis/trans* ratio. Reduction of the ester and the amide of **2.56** with LiAlH₄ followed by protection of the amine with benzyloxycarbonyl anhydride, and subsequent oxidation and Wittig olefination delivered **2.57**. Removal of the TBS protecting group followed by oxidation of the aldehyde and subsequent alkylation under modified Takai conditions gave (*E*)-vinyl pinacolatoboronic ester (**2.58**) in greater than 20:1 *E/Z* ratio.

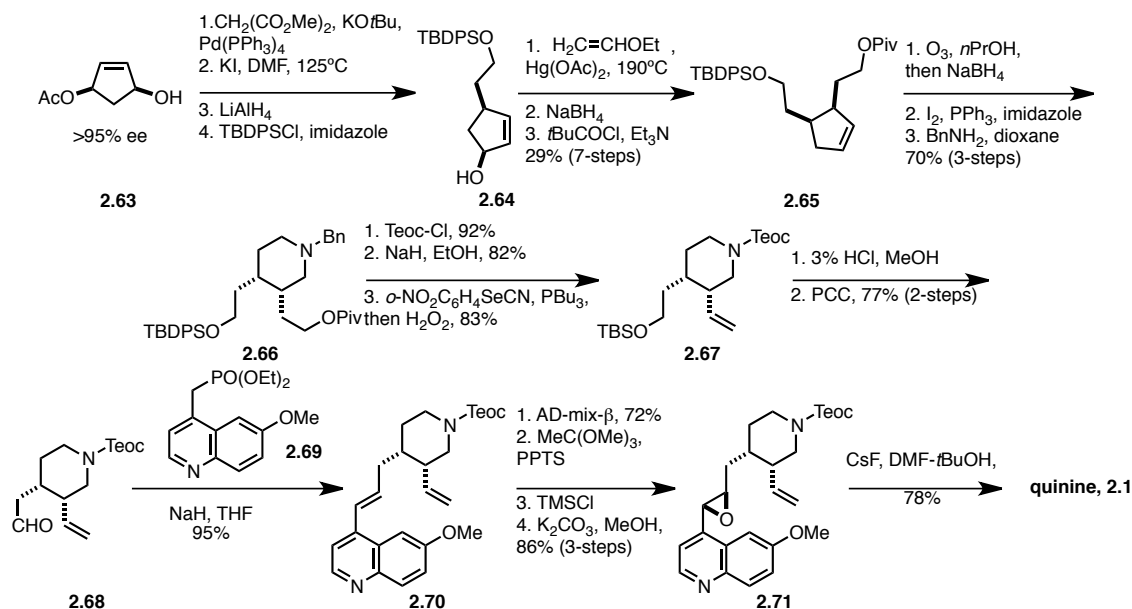


Scheme 2.7. Jacobsen Total Synthesis of Quinine

Using modified Buchwald conditions, **2.59** was generated in the presence of $\text{Pd}(\text{OAc})_2$ ²⁷. Diene **2.59** was then subjected to Sharpless dihydroxylation conditions, giving the corresponding diol in greater than 96:4 dr, with only trace amounts of the tetra-ol present. Subsequent treatment of the diol with trimethylorthoacetate, acetyl bromide, and potassium carbonate provided epoxide **2.60**. Finally, removal of the benzyl carbamate protecting group and heating at 200°C gave quinine (**2.1**).

2.2.6 Kobayashi's Route to Quinine

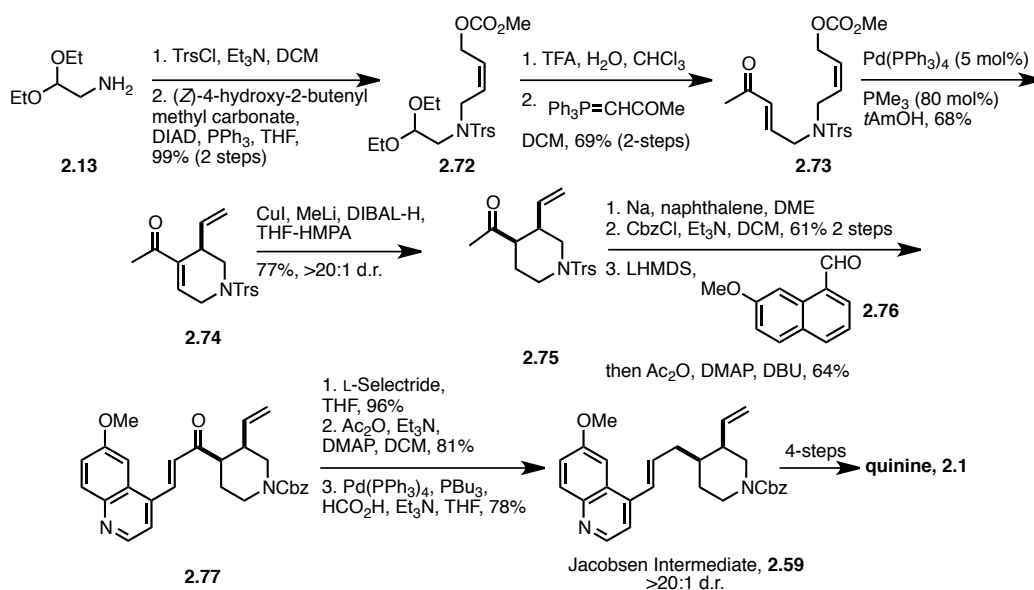
Kobayashi was able to take acetate **2.63**, and in a series of 21 steps, make quinine (**2.1**) in 4.5% overall yield (Scheme 2.8).²⁸ Monoacetate **2.63** was converted to the corresponding methyl ester followed by reduction and selective protection of the primary alcohol to give **2.64**. Next, a Claisen rearrangement with vinyl ether and $\text{Hg}(\text{OAc})_2$ afforded the aldehyde, which was then reduced and protected as pivaloyl ester (**2.65**). Ozonolysis of **2.65** followed by a reductive work up and subsequent conversion to the diiodide, and amino cyclization with benzylamine provided piperidine **2.66**. Conversion to the 2-(trimethylsilyl)ethoxycarbonylamine and elimination of the pivaloyl ester gave alkene **2.67**. Deprotection of **2.67** and subsequent PCC oxidation gave aldehyde **2.68**. Wittig olefination with the quinoline-phosphonate (**2.69**) afforded **2.70** in 95% yield. The remaining steps in the synthesis are similar to Jacobsen's, in that the internal double bond is dihydroxylated and converted to epoxide **2.71**. Upon deprotection of the amine, cyclization occurred in the presence of cesium fluoride, affording quinine (**2.1**).



Scheme 2.8. Kobayashi's Total Synthesis of Quinine

2.2.7 Krische's Formal Synthesis of Quinine

In 2008, Krische devised a route towards quinine (**2.1**) that intercepted Jacobsen's intermediate (**2.59**, Scheme 2.9).^{2,27} Jacobsen's intermediate²⁷ (**2.59**) was made utilizing a strategy that was two steps shorter, and the selectivity at the C-3 position was increased from 1.7:1 in Jacobsen's work (over 2 steps)²⁷ to 3:1 (1 step) in Krische's synthesis. Starting from commercially available **2.13**, the amine was converted to the sulfonamide, and under Mitsunobu conditions, was coupled with (*Z*)-4-hydroxy-2-butenyl methyl carbonate to give carbonate **2.72**.

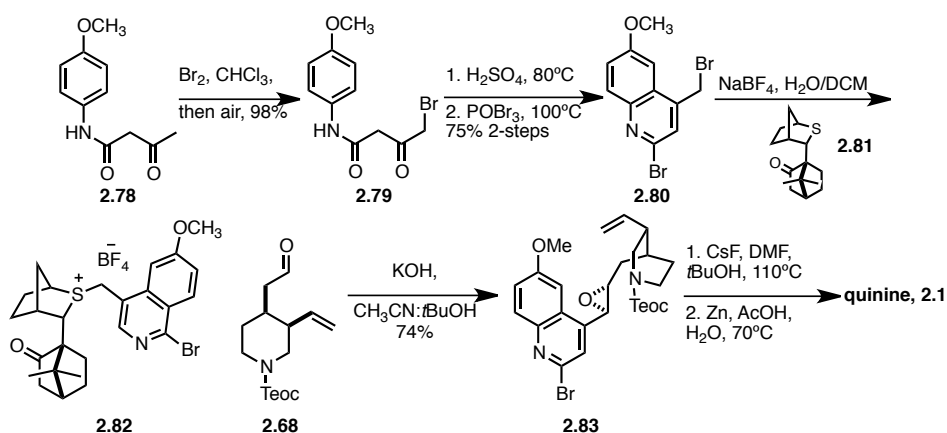


Scheme 2.9. Krische's Formal Total Synthesis of Quinine

Hydrolysis with TFA, followed by Wittig olefination of the aldehyde gave α,β -unsaturated ketone **2.73**. Cyclization with Morita-Baylis-Hillman-Tsuji-Trost conditions gave protected piperidine **2.74** in 68% yield. Subsequent 1,4-reduction via a modified Tsuda and Saegusa method gave **2.75** as a single diastereomer.²⁹ The sulfonyl moiety was then cleaved with naphthalene, and the amine was reprotected and transformed into **2.77** via an aldol coupling-dehydration reaction. Selective 1,2-reduction gave the secondary alcohol, which was then converted to the acetate and reduced with palladium to afford **2.59**. Having arrived at **2.59** (Jacobsen intermediate), quinine could be synthesized in 4 more steps.

2.2.8 Aggarwal's Sulfur-Ylide Method to Quinine

In 2010, Aggarwal and coworkers published a synthesis of quinine and quinidine using sulfur ylide-mediated asymmetric epoxidation (Scheme 2.10).³⁰ Aggarwal first synthesized the required sulfonium salts for the key reaction in their sequence by reacting **2.78** with bromine and then refluxing the system in sulfuric acid, followed by bromination to deliver **2.80**. Reaction of the dibromide (**2.80**) with sulfide **2.81** delivered **2.82**.

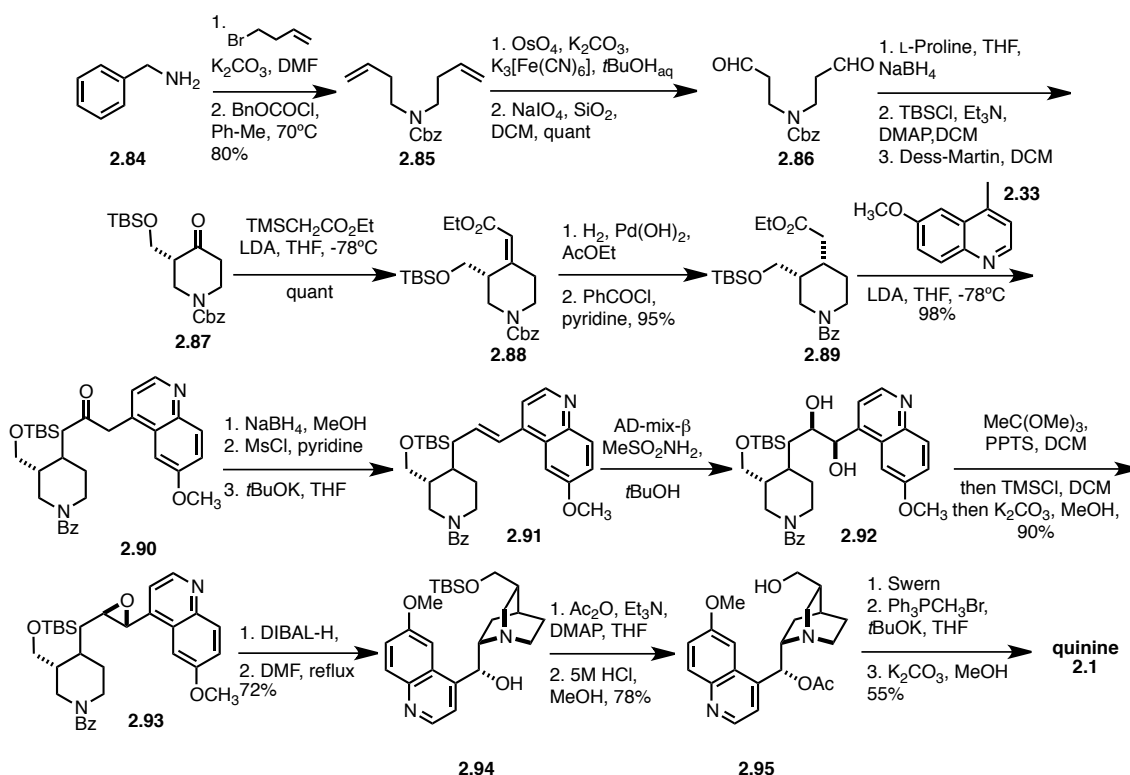


Scheme 2.10. Arshad's Sulfur-Ylide Route to Quinine

Addition of **2.82** to Kobayashi's intermediate (**2.68**)²⁸ in the presence of KOH delivered the corresponding epoxide (**2.83**) and removal of the Teoc protecting group mediated a cyclization onto the epoxide and final removal of the bromine with Zn delivered quinine (**2.1**) in excellent yield. Quinidine (**2.3**) could also be realized with the use of the enantiomer of sulfide **2.81**.

2.2.9 Sarkar's Asymmetric Synthesis of Quinine

In early 2011, Sarkar and Hatakeyama published their asymmetric total synthesis of quinine and quinidine (Scheme 2.11).³¹ Starting from benzylamine (**2.84**), alkylation and a protecting group manipulation afforded alkylamine **2.85**. Oxidation and cleavage provided dialdehyde **2.86**, which was subjected to a proline-catalyzed asymmetric cycloaldolization (96% *ee*) and further manipulated to ketone **2.87**. A Peterson olefination and another protecting group manipulation afforded **2.89**, which was reacted with lithiated quinoline **2.32**, to deliver **2.90**.



Scheme 2.11 Sarkars Total Synthesis of Quinine

Reduction and elimination installed the trans double bond (**2.91**), which was then asymmetrically dihydroxylated and converted to the epoxide (**2.93**). Deprotection of the amine and refluxing **2.93** in DMF provided the core of quinine (**2.94**). Swapping out the protecting groups and homologating **2.95** delivered quinine (**2.1**).

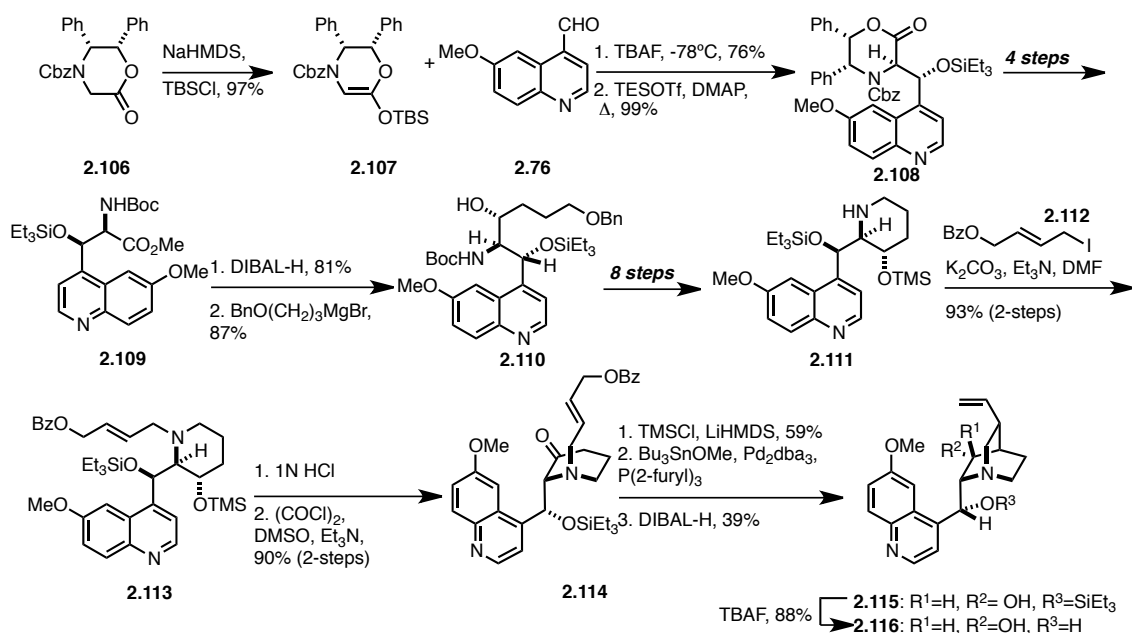
2.2.10 Friestads Mn-Mediated Radical Method Toward Quinine

Most recently, Friestad and coworkers completed a formal synthesis of quinine and quinidine by intercepting Uskokovic's quinuclidine intermediate (**2.45**)²² via a stereocontrolled Mn-mediated radical addition of an alkyl iodide to chiral *N*-acylhydrazone (Scheme 2.12).^{32,33} Starting from **2.96** and elaborating in several steps they were able to arrive at alkyl iodide **2.97**. Mn-mediated radical addition of **2.98** gave **2.99**, and the chiral auxiliary was removed and a cyclization with Mitsunobu conditions afforded piperidine **2.100**.

2.3 Previous Williams Group Studies

2.3.1 Dr. Deidre John's Method Toward 7-Hydroxy-Quinine

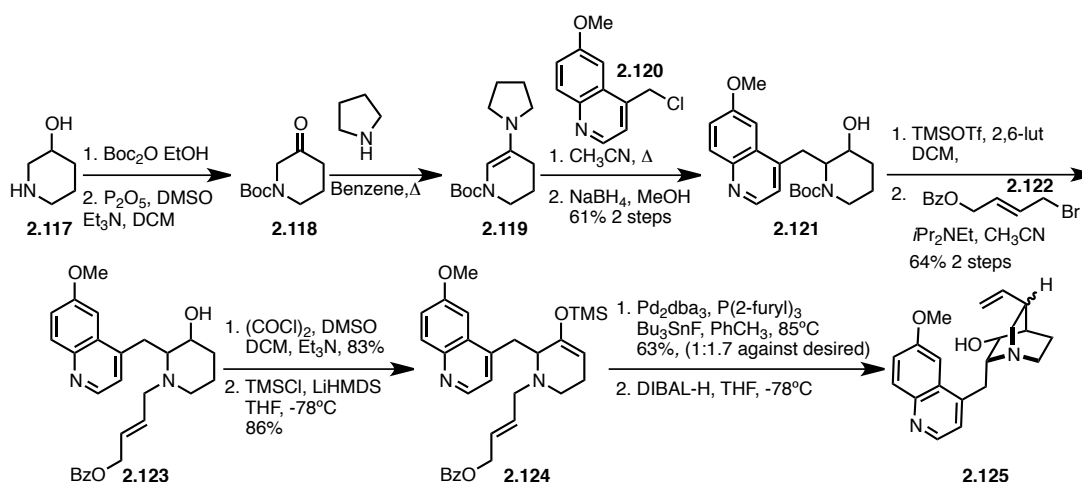
Dr. Deidre John's route (Scheme 2.13) started with Williams' lactone (**2.106**), which was converted to the TBS enolate and coupled with quinoline **2.76**, affording **2.108** with greater than 30:1 dr.¹ Carbamate **2.108** was elaborated to the α -amino- β -silyloxy-ester (**2.109**), then reduced and alkylated through a Grignard reaction to afford **2.110**. Further elaboration and alkylation delivered **2.113**, which was deprotected and oxidized to **2.114**. Subsequent enolate formation and cyclization followed by deprotection gave 7-hydroxyquinine (**2.116**). Substrate **2.115** was subjected to various deoxygenation conditions, but quinine (**2.1**) was never obtained.



Scheme 2.13. William's Route to 7-hydroxyquinine

2.3.2 Dr. Aaron Smith's Method Toward 7-Hydroxyquinine.

In an attempt to shorten Dr. John's synthesis and focus on the deoxygenation, Dr. Aaron Smith developed a simplified route towards 7-hydroxy-9-deoxyquinine (**2.115**, Scheme 2.14).³⁴ Starting from commercially available 3-hydroxypiperidine (**2.117**), Smith formed the *N*-Boc carbamate and oxidized the alcohol to arrive at **2.118**. Enamine formation (**2.119**), addition into **2.120** and reduction provided **2.121**. Removal of the *t*-butylcarbamate with Ohfuné's conditions³⁵ and subsequent alkylation of the amine with **2.122**, oxidation of the secondary alcohol and conversion to the TMS-enol ether provided **2.124**. Enol ether **2.124** was then cyclized with John's conditions, although this time providing a mixture of stereoisomers at C3 (1:1.7 against desired isomer). The cyclized product was then readily reduced with DIBAL-H to give **2.125**.



Scheme 2.14. Smith's route to 7-Hydroxy-9-Deoxy-Quinine

The major problem with these two routes was the interception of 7-hydroxyquinine and 7-hydroxy-9-deoxyquinine intermediates (**2.125**, **2.115**). Numerous attempts were made to deoxygenate at the C7 position, but none proved fruitful. A similar intermediate was also intercepted in Krische's initial synthesis² wherein 7-hydroxyquinine (**2.125**) was made, and the final deoxygenation was never achieved.

2.4 Conclusion

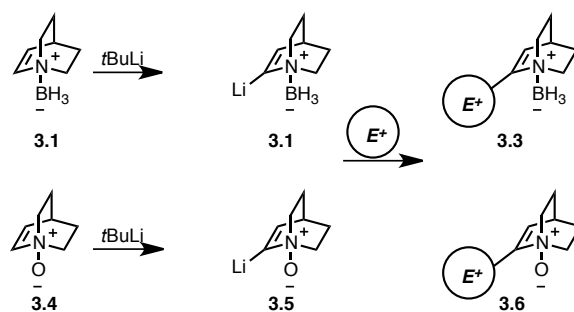
Overall, quinine has been the object of much interest for almost a century. Newer anti-malarial drugs, exhibiting less resistance than quinine, have begun to make the demand for this amazing molecule decline, but its structural complexity still lends itself to the production of new and interesting methodologies in organic chemistry.

Additionally, within the Williams' group, further investigation into the synthesis of quinine utilizing the group's unique C3-C4 cyclization is still being explored, *vide infra*.

3.1 Studies Toward the Total Synthesis of Quinine

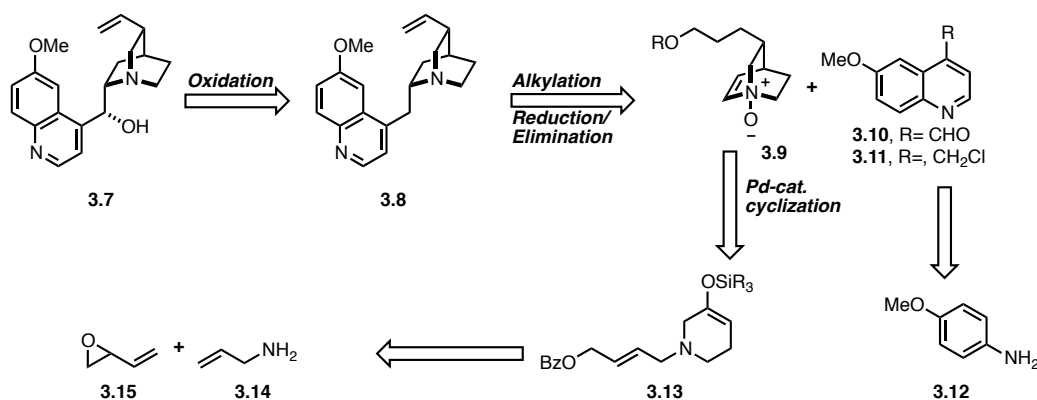
3.1.1 First Generation Strategy

With vast amounts of data suggesting the inability to remove the C7-hydroxyl, we decided to move toward a more convergent approach to the synthesis of quinine. Based off of work by O'Neil and coworkers (Scheme 3.1), which utilizes the activation of the α -proton of the quinuclidine fragment and the entrapment of electrophiles, we explored a convergent route toward quinine.^{36,37}



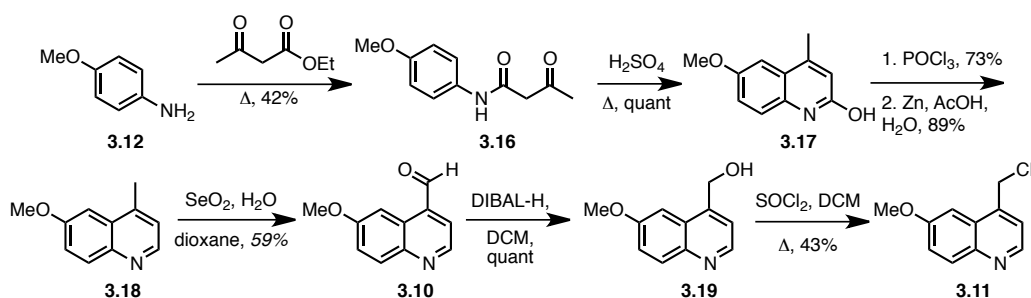
Scheme 3.1. O'Neil's α -Proton Activation Chemistry

We envisioned that quinine could be accessed through a benzylic oxidation of **3.8** (Scheme 3.2) and a coupling of activated enamine **3.9** with either quinoline **3.10** or **3.11**. Ion **3.9** could be achieved by a palladium-catalyzed cyclization of silyl enol ether **3.13**, which could be made starting from commercially available vinyl epoxide (**3.15**) and allylamine (**3.14**).



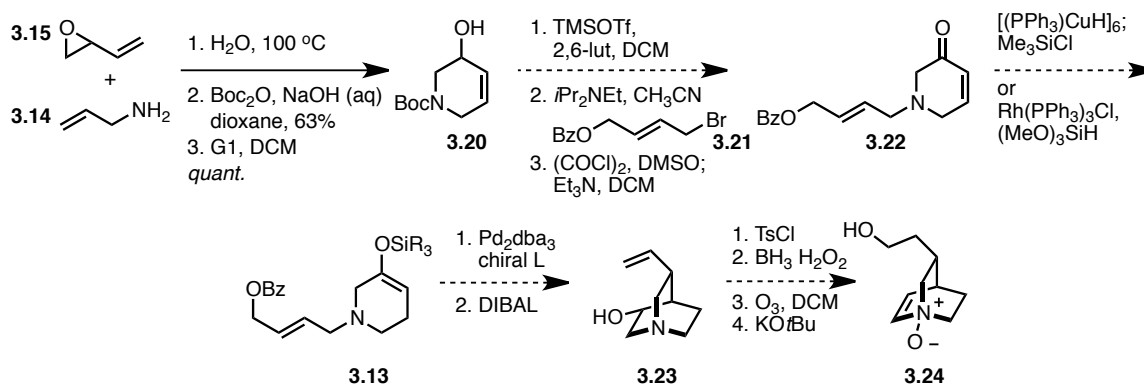
Scheme 3.2. First Generation Route Towards Quinine

Work initially began with the synthesis of the desired quinoline fragments **3.10** and **3.11** (Scheme 3.3). Following a protocol by Campbell,³⁸ *p*-anisidine (**3.12**) was condensed onto ethylacetoacetate and then cyclized in refluxing sulfuric acid to give **3.17**. Conversion of the alcohol to the chloride and hydrogenolysis delivered 6-methoxy-4-methyl-quinoline (**3.18**). Oxidation provided the desired aldehyde (**3.10**), which was further elaborated to chlorine **3.11**.



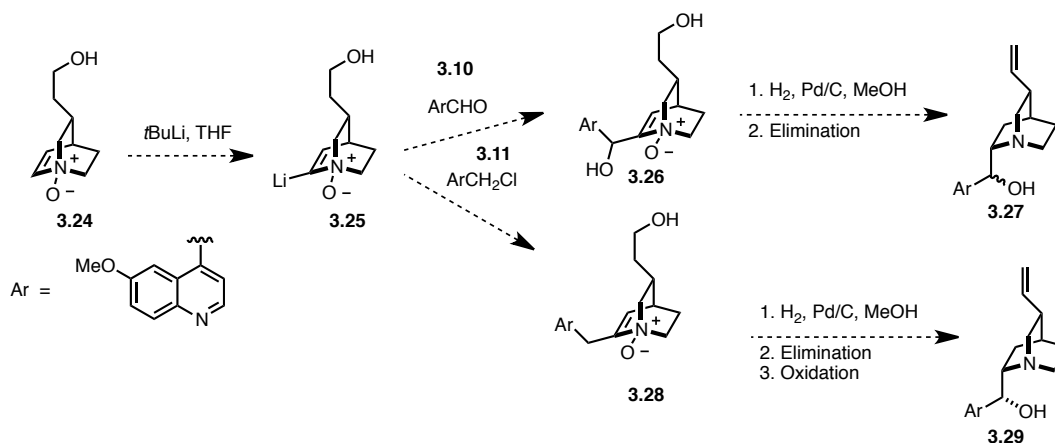
Scheme 3.3. Synthesis of Quinoline Fragments

With the desired quinolines in hand, we outlined a possible route towards **3.24** (Scheme 3.4). *N*-Boc-3-hydroxypiperidine (**3.20**) has been synthesized in three steps by Ouchi and co-workers from commercially available starting materials (**3.13**, **3.15**).³⁹ From Boc-hydroxypiperidine (**3.20**), we envisioned that a deprotection with Ohfuné conditions³⁵ would lead to the TMS-protected alcohol as an intermediate, which could then undergo alkylation with allylbromide **3.21** to provide the corresponding alcohol and then oxidation to provide ketone **3.22**. From **3.22**, a TMS-enolate could be realized by 1,4-hydride addition with Strykers reagent, followed by cyclization using Pd₂dba₃ and subsequent DIBAL-H reduction to afford 3-hydroxyquinuclidine (**3.23**). Elaboration to the primary alcohol and formation of the activated enamine would give **3.24**.



Scheme 3.4 Strategy for Formation of the Quinuclidine Intermediate

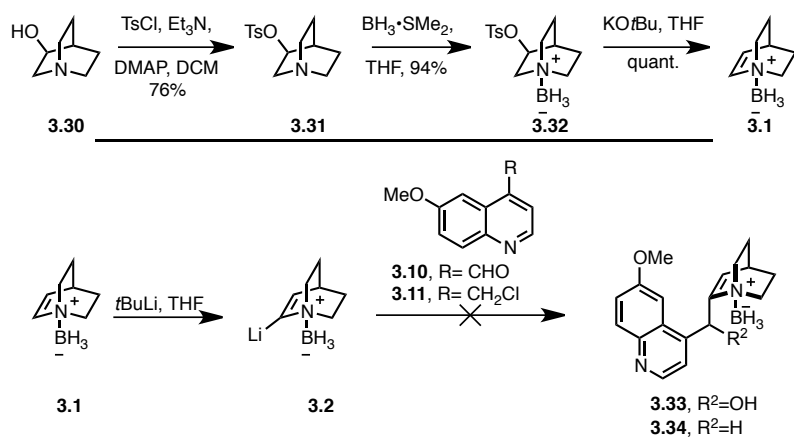
With **3.24** in hand Scheme 3.5 shows the outlined plan for coupling **3.24** with either quinoline **3.10** or **3.11** by lithiate formation of **3.24** to deliver **3.25** and further elaborating to either **3.26** or **3.28**.



Scheme 3.5. Coupling of Quinoline and Quinuclidine Fragments

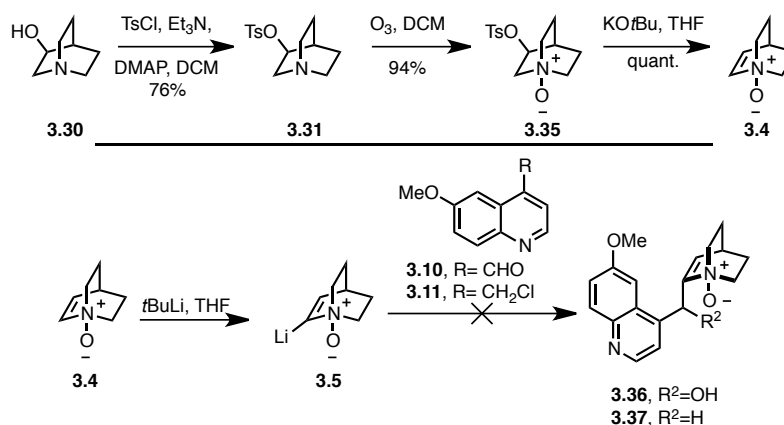
Before working towards our advanced quinuclidine intermediate, we first decided to test O'Neils chemistry through a model system, which proved to be quite challenging. Initially, an amine-borane species (**3.1**, Scheme 3.6) was being used, and was made through the protection of **3.30** and formation of the *N*-Borane species (**3.32**). Elimination

provided **3.1**, which was subjected to *t*BuLi (**3.2**), but any attempt at the coupling sequence did not deliver desired product, even when using benzaldehyde as the electrophile.³⁷



Scheme 3.6. Amine-Borane Complex

After contacting O'Neil regarding a more complete experimental procedure for this methodology, it was suggested that the *N*-oxide quinuclidine be used, due to the instability of the amine-borane species. The *N*-Oxide (**3.4**) intermediate was developed in the same manner as the N-Borane species, with the exception that **3.31** was reacted with ozone to provide **3.35** (Scheme 3.7).



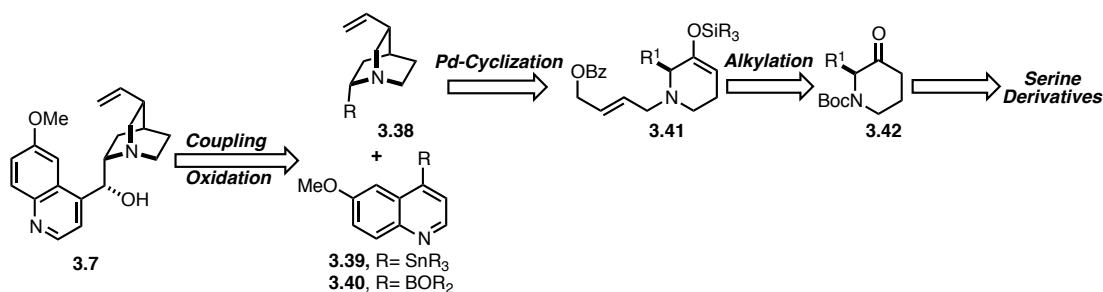
Scheme 3.7. Model System with N-Oxide

Reacting **3.4** with *t*BuLi at -78°C for 30 minutes followed by addition of benzaldehyde delivered a small amount of the addition product, but use of the **3.10** or **3.11** as the electrophile failed to provide any desired products. As a test reaction, the lithiated quinoline (**3.5**) was quenched with CD₃OD, but the isolated product failed to show any deuterium incorporation, demonstrating the likelihood that the lithium ion was not being generated in this reaction sequence. Insight into why this reaction sequence was problematic could be due to the difficulty in transferring the N-oxide substrate. The gel-like substance was extremely viscous and only slightly soluble in methanol. The presence of trace methanol in the substrate could have been the cause of the problems seen. Because of the problems with employing O'Neils chemistry, another route towards quinine was explored.

3.2 Second Generation Strategy

3.2.1 Towards C2-Functionalized Piperidines

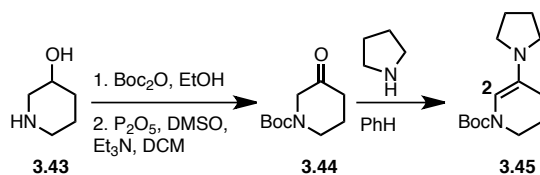
The second-generation synthesis of quinine utilized a similar route that required the coupling of a substituted quinuclidine (**3.38**) system to a quinoline moiety (**3.39** or **3.40**, Scheme 3.8).



Scheme 3.8 2nd Generation Retrosynthetic Analysis

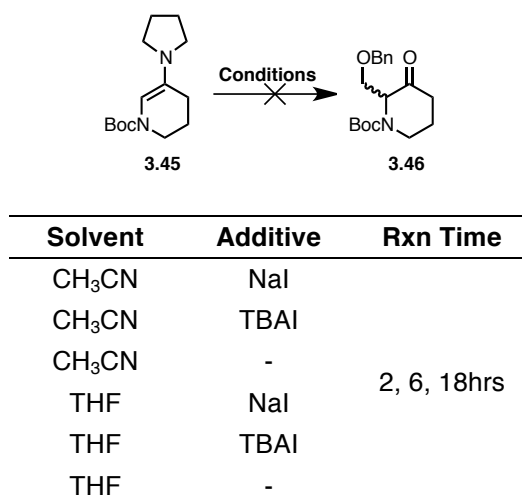
3.2.2 Utilization of Smith's Enamine

Work on this method began by utilizing chemistry from Dr. Smith's sequence to 7-hydroxyquinine (Scheme 3.9).³⁴ 3-hydroxypiperidine (**3.43**) was first protected as the *t*-Butylcarbamate and then oxidized to the ketone (**3.44**) and elaborated to enamine **3.45**.



Scheme 3.9 Smith's Route Toward Enamine 3.45

From enamine **3.45**, the goal was to α -alkylate at C2 with BOMCl (**3.46**, Scheme 3.10). Unfortunately, the desired addition product was never observed even when changing the solvent or through the use of additives.

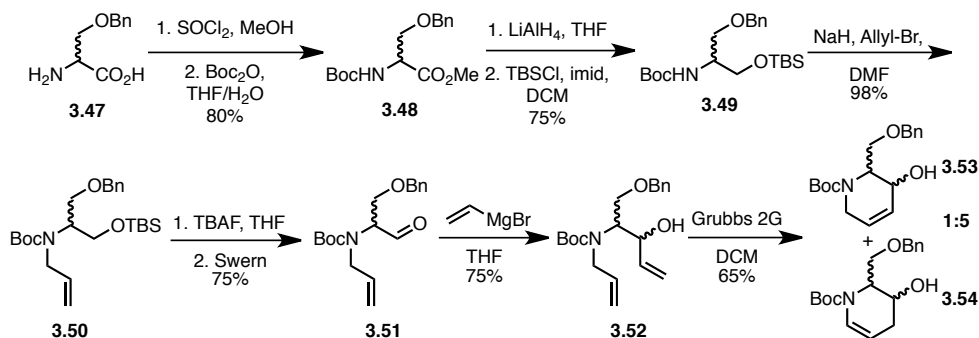


Scheme 3.10. Attempted C2 Alkylations

3.2.3 Serine Metathesis Route

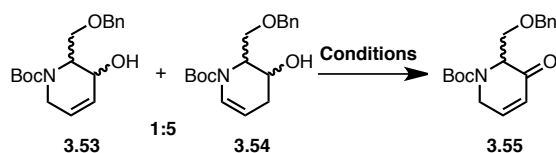
The next route towards a C2 functionalized piperidine was based off of work by Helmchen⁴⁰ and began with *O*-Bn-Ser-OH (**3.47**, Scheme 3.11), which was first converted to the methyl ester and then Boc protected to give **3.48**. Reduction with

LiAlH₄ and protection of the primary alcohol as the TBS-ether delivered **3.49**. The secondary amine was then alkylated with sodium hydride and allylbromide (**3.50**) and the TBS-ether was deprotected and oxidized to the aldehyde (**3.51**) with standard Swern oxidizing conditions.



Scheme 3.11 Serine Metathesis Route

Commercially available vinyl Grignard was then added into the aldehyde giving **3.52** and a ring closing metathesis reaction with Grubbs 2nd generation catalyst was performed giving a mixture of **3.53** and **3.54**. From **3.53** and **3.54**, the next task was to push both products forward to the desired α,β -unsaturated ketone. Oxidation of the alcohol (**3.60**) using various conditions delivered the desired ketone, but in very poor, unusable yields (Scheme 3.12).



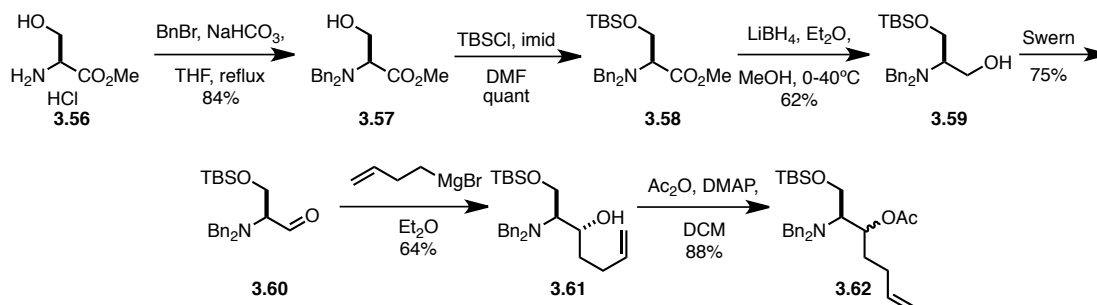
Oxidation Conditions	Result
PCC, DCM reflux	4%
MnO ₂ , DCM, reflux	Decomposition
RuCl ₂ (PPh ₃) ₃ , TEMPO, O ₂ , 100°C, PhMe	Decomposition

Scheme 3.12. Oxidation Conditions

While other oxidation conditions could have been employed, due to the challenges faced with the oxidation, and the subsequent need for gram-scale amounts of the desired piperidine, another method was explored.

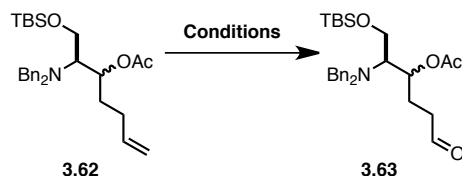
3.2.4 Dibenzyl Serine Route

Utilizing a route by Andres,⁴¹ we moved forward in our pursuit of our 2-substituted-piperidine ring (Scheme 3.13). Starting from L-Ser-OMe•HCl (**3.56**), the nitrogen was doubly protected with benzyl bromide, affording **3.57**. Protection of the primary alcohol as the TBS-ether (**3.58**), reduction of the ester (**3.59**), and a Swern oxidation provided **3.60**. A Grignard reaction, this time with homo-allylbromide, gave the desired addition product (**3.61**) in moderate yield.



Scheme 3.13 Dibenzy serine Route

The alcohol was then protected as the acetate (**3.62**) and a series of oxidation conditions were evaluated to convert the alkene to the aldehyde (**3.63**, Scheme 3.14).

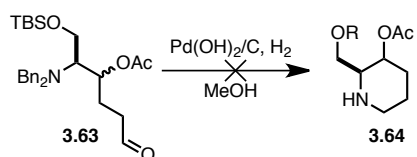


Conditions	Results
O ₃ , DCM	Decomposition
RuCl ₃ , NaIO ₄ , CH ₃ CN/H ₂ O	Decomposition
OsO ₄ , NMO, Acetone, H ₂ O, DCM then NaIO ₄ , SiO ₂ , DCM	60%

Scheme 3.14 Oxidation Conditions

It was realized that NMO and OsO₄ followed by SiO₂ and NaIO₄ were the best reaction conditions, delivering the desired aldehyde in 60% yield.⁴² From aldehyde **3.63**, the next step was to deprotect the amine and induce an intramolecular cyclization onto the aldehyde, followed by reduction of the subsequent imine to afford **3.64** (Scheme 3.15). Unfortunately, any attempts at completing this sequence were

unfruitful, and further exploration of cyclization conditions were not explore (*vide infra*).



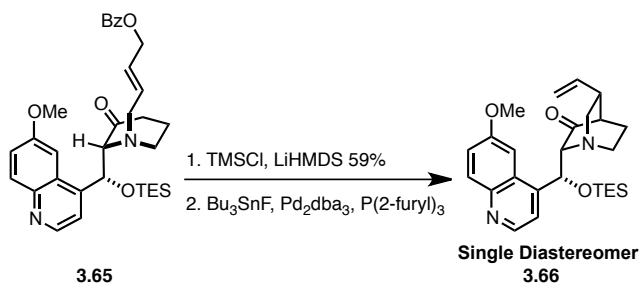
Scheme 3.15. Intramolecular Cyclization

It was at this stage that because of the difficulties in obtaining the desired C2 functionalized piperidine, and the potential for elimination of the installed functionality at C2, that another route was embarked upon towards the synthesis of quinine.

3.3 Review of Initial Group Findings

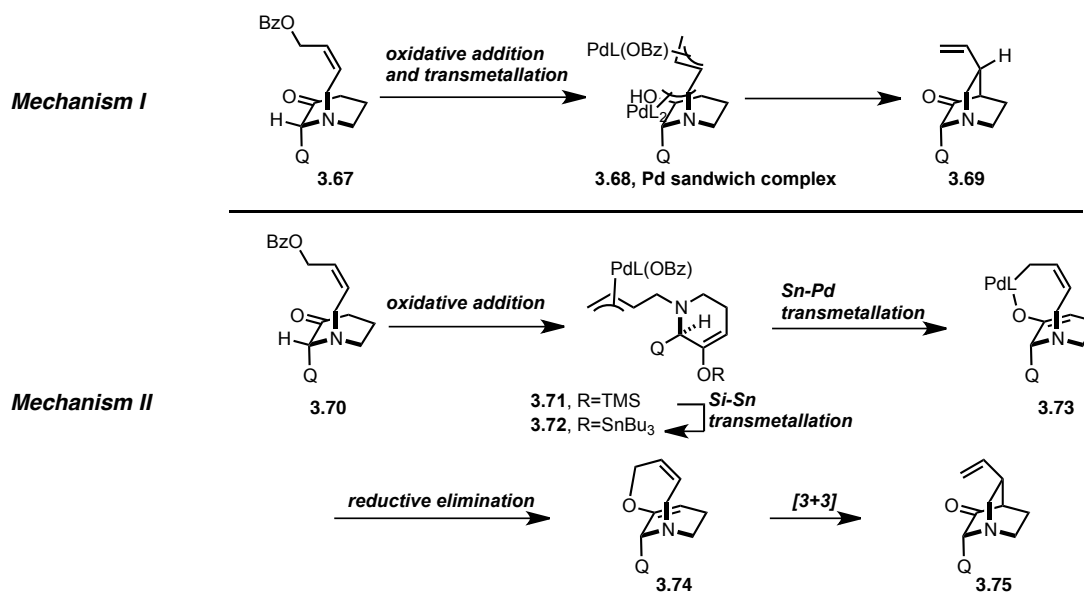
3.3.1 Dr. Deidre John's Findings

Studies by Dr. John's showed that the Pd-mediated cyclization delivered a single diastereomer as the product (**3.66**, Scheme 3.16).¹



Scheme 3.16. Previous Williams' Cyclization Result

The stereochemical outcome of this reaction was perceived to go through one of two mechanisms (Scheme 3.17). The first predicted mechanism was that the advanced intermediate would first go through an oxidative addition and transmetalation to afford a Pd sandwich complex (**3.68**) involving an η^3 Pd-enolate and a π -allyl Pd species undergoing allylic alkylation (**3.69**). The second proposed mechanism speculated that the system could undergo a Pd-mediated etherification (**3.74**), followed by a Claisen rearrangement (**3.75**).

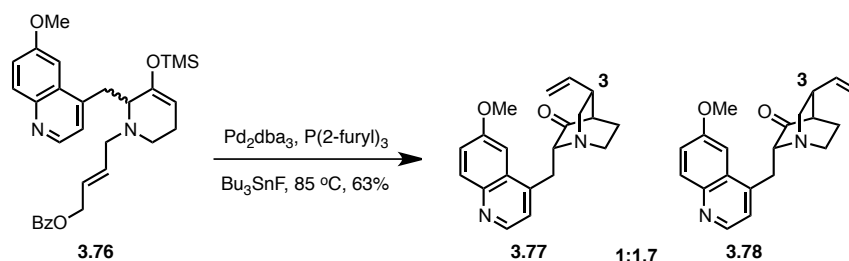


Scheme 3.17. Possible Mechanistic Explanation of Pd-Cyclization

3.3.2 Dr. Aaron Smith's Findings

What was interesting was that in Dr. Smith's hands, the use of racemic material lacking the requisite C9-hydroxyl (**3.76**), showed a 1:1.7 mixture of diastereomers

against the desired configuration at the C3 position (**3.77** + **3.78**, Scheme 3.18).



Scheme 3.18. Smith's Unpublished Results

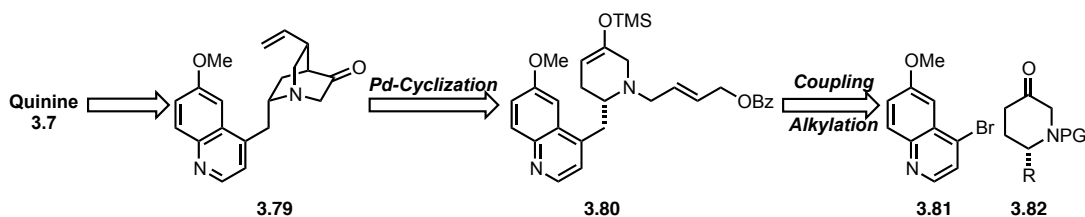
Smith's results suggest that the mechanistic possibilities previously deduced might be correct in determining the stereochemical outcome of the Pd-cyclization. The question still exists of exactly how this reaction works. With the mechanistic behavior of this reaction in question, and deoxygenation at C7 at late stages impossible,^{2,34} we decided to pursue a pipercolic acid derivative and a route towards quinine that would utilize the same C3-C4 disconnect, but this time cyclizing on the other side of the piperidine ring to afford the resulting ketone at the C5 position, rather than the C7 position.

3.4 3rd Generation Approach

3.4.1 3rd Generation Retrosynthetic Analysis

The 3rd generation approach towards quinine was developed so that the key C3-C4 disconnect and Pd-mediated cyclization would be used, but instead of the requisite

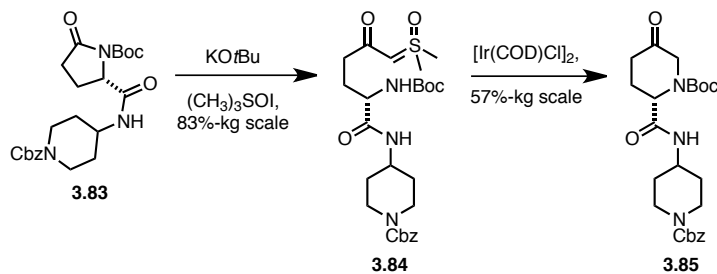
ketone at C7, it would be done in such a way to afford **3.79** from elaborated pipecolic acid **3.80** (Scheme 3.19). This elaborated system could be envisioned to come from a coupling of quinoline **3.81**, with pipecolic acid derivative **3.82**.



Scheme 3.19 3rd Generation Retrosynthetic Analysis

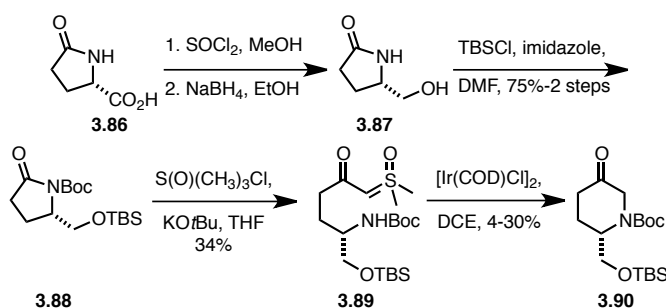
3.4.2 Sulfoxonium Ylide Method

Efforts toward the desired pipecolic acid derivative began with a method published by Mangion^{43,44} using sulfoxonium ylides as an intermediate towards substituted pipecolic acid derivatives (Scheme 3.20). Mangion showed that starting with lactam **3.83**, conversion to the sulfoxonium ylide (**3.84**), and then cyclization with Ir catalyst provided **3.85**.



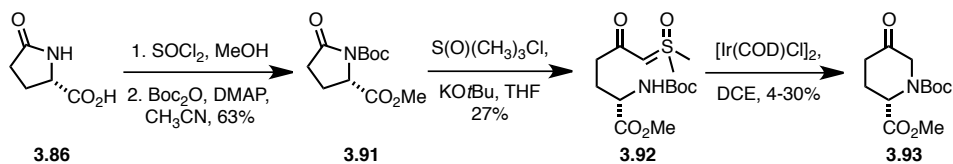
Scheme 3.20. Mangion's Route to Substituted Pipecolic Acid Derivatives

Based off of this example, we first started with pyroglutamic acid (**3.86**), and elaborated it to the primary alcohol (**3.87**) (Scheme 3.21). Protection as the silyl ether (**3.88**) and opening of the lactam with $(\text{CH}_3)_3\text{SOCl}$ and KO^tBu afforded sulfoxonium ylide **3.89** in very modest yields.



Scheme 3.21. Synthesis of Sulfoxonium Ylide (3.89)

Unfortunately, any attempts at the cyclization with iridium catalysts only produced the desired product (**3.90**) in poor yield, and purification proved to be tedious. In an effort to make a simpler system, the ester variant (**3.91**) was developed (Scheme 3.22). Again starting from pyroglutamic acid (**3.86**), the *N*-protected-methyl ester (**3.91**) was realized in good yields over 2 steps.

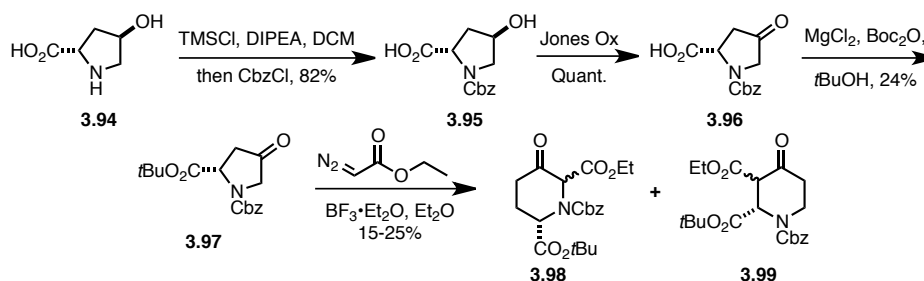


Scheme 3.22. Synthesis of Sulfoxonium Ylide (3.92)

Opening of the lactam to the sulfoxonium ylide (**3.92**) proceeded in 27% yield and, as seen before, the cyclization (**3.93**) did not prove fruitful. Further optimization of this method was not attempted, and another method was pursued.

3.4.3 Avery's Ring Expansion Method

The next method explored was Avery's ring expansion method (Scheme 3.23).⁴⁵ Starting from 3-hydroxy-L-proline (**3.94**), the nitrogen was protected and a Jones oxidation provided the desired ketone (**3.96**) in quantitative yields. Esterification followed by an ethyldiazoacetate/ $\text{BF}_3 \cdot \text{Et}_2\text{O}$ mediated ring expansion provided a regioisomeric mixture of products (**3.98**, **3.99**) in 3.6% yield over two steps.

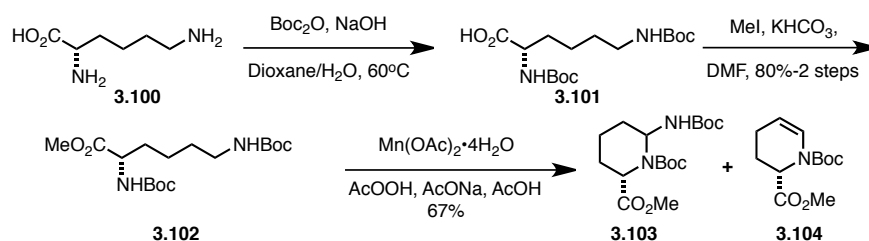


Scheme 3.23. Avery's Ring Expansion Method

Avery published this method using multi-gram quantities of materials, but any attempt at recreating the published results, even through distillation of reagents, were not productive.

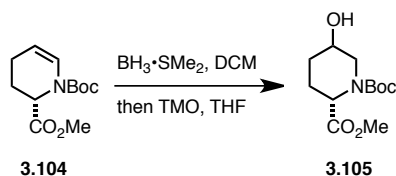
3.4.4 Kiesel's $\text{Mn}(\text{OAc})_2$ Approach

In 2004 Kiesel and coworkers published a route towards enamine X (Scheme 3.24).⁴⁶ Starting from L-Lysine (**3.100**), the nitrogens were both protected as the *t*-Buylcarbamates (**3.101**) and the acid was esterified in the presence of MeI and KHCO_3 (**3.102**). In Kiesel's studies they first tried a variety of oxidation conditions that were met with failure. It was then that they decided to "follow up Nature's suggestion" by using $\text{Mn}(\text{OAc})_2$ with a buffered NaOAc/peracetic acid solution. In doing so, they were able to deliver a mixture of **3.103** and **3.104** in moderate yield.



Scheme 3.24. Kiesel's Manganese Acetate Approach

It should be noted that while the two products (**3.103**, **3.104**) were separable, the reaction could be further driven to completion with longer reaction times or by reacting the mixture of products with AcOH at room temperature overnight. Reproducing Kiesel's results proceeded without issue and a subsequent hydroboration/oxidation with $\text{BH}_3 \cdot \text{SMe}_2$ and trimethylamine-*N*-oxide (TMO) delivered the desired alcohol (**3.105**) in a 9:1 (anti:syn) ratio (Scheme 3.25).⁴⁷

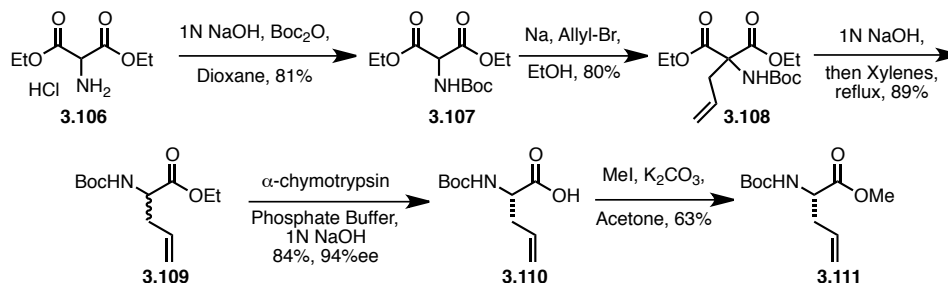


Scheme 3.25. Hydroboration/Oxidation of Enamine 3.104

The stereochemistry of the oxidation was not of concern to us since the alcohol would be oxidized to the ketone at a later stage in the synthesis. Although this route seemed quite promising, the use of commercially available peracetic acid from Sigma Aldrich was required, and became because of the product being continually on backorder. For these reasons, another route was explored.

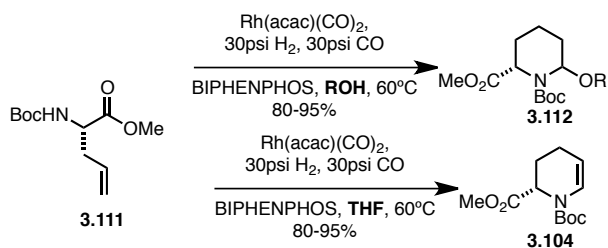
3.4.5 Allylglycine & Cyclohydrocarbonylation Approach

Further examination of the literature led to a route towards our desired pipecolic acid fragment that started from allylglycine.³ Due to the high cost of this unnatural amino acid, we began by synthesizing it, starting from diethylaminomalonate•HCl (**3.106**, Scheme 3.26).⁴⁸ From **3.106**, the amine was free-based and protected with Boc₂O (**3.107**). Alkylation with allylbromide in the presence of sodium ethoxide and subsequent saponification and decarboxylation provided racemic allylglycine **3.109**.



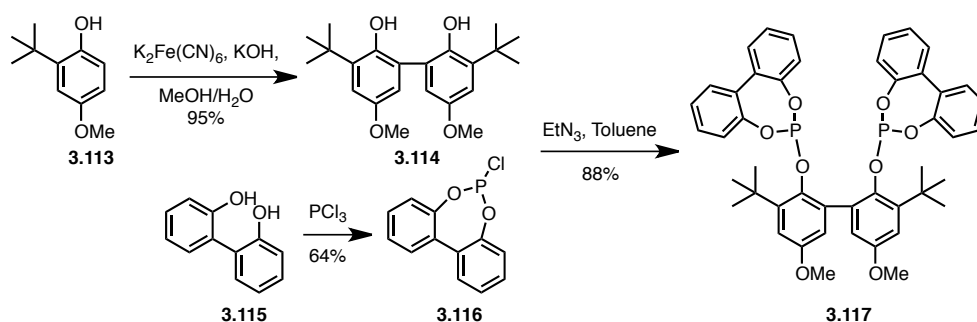
Scheme 3.26. Synthesis of Allylglycine

An enzymatic resolution with α -chymotrypsin in a phosphate buffer provided the desired enantiomer (**3.110**) in 84% yield and 94%*ee*, which was subsequently esterified, providing **3.111**. From here the next step in our sequence was to move this material forward through a sequence published by Ojima, wherein he showed that a cyclohydrocarbonylation on allylglycine could be achieved to afford desired enamine **3.104** (Scheme 3.27).³ Additionally, Ojima showed that in the presence of a BIPHENPHOS ligand and THF as the solvent, that the desired enamine (**3.104**) would be delivered over the oxygenated (**3.112**) product that was produced with the use of alcoholic solvents.³



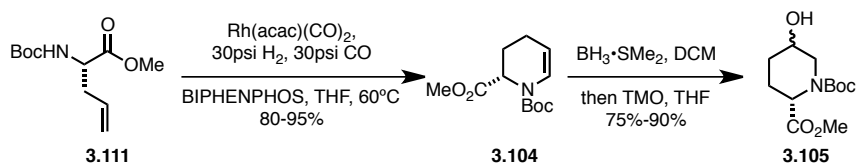
Scheme 3.27 Ojima's Cyclohydrocarbonylation Reaction

The desired ligand was synthesized by first performing an auto-oxidation reaction of **3.113**, to deliver **3.114** (Scheme 3.28).⁴⁹ Conversion of **3.115** with PCl_3 afforded **3.116**, which was immediately reacted with **3.114** to deliver the desired BIPHENPHOS ligand (**3.117**) in excellent yields.⁴⁹



Scheme 3.28. Synthesis of BIPHENPHOS Ligand

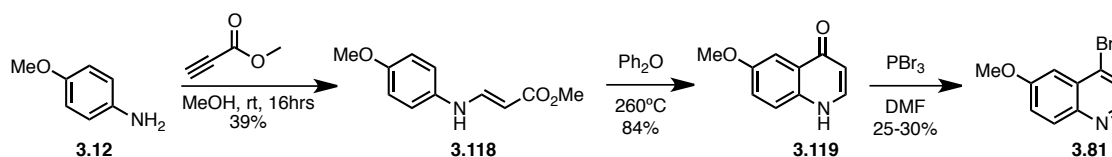
With the BIPHENPHOS ligand in hand, the cyclohydrocarbonylation reaction was performed, delivering the desired enamine (**3.104**) in consistent and excellent yields (Scheme 3.29). Hydroboration/oxidation with Le Corre's aforementioned conditions provided the desired alcohol (**3.105**) in upwards of 90% yield.⁴⁷



Scheme 3.29 Synthesis of Pipecolic Acid Derivative

3.4.6 Halo-Quinoline Fragment

With the functionalized pipecolic acid fragment in hand, our work shifted toward obtaining the needed 4-bromo-6-methoxy-quinoline (**3.81**, Scheme 3.30). Starting from *p*-anisidine (**3.12**), **3.118** was afforded in moderate yields. Jacobsen reported using DowthermA® as the solvent for cyclizing the quinoline ring (**3.119**), but it was realized that in our hands, following Banwell's method of using diphenyl ether as the solvent was a better choice.⁵⁰ Aromatization and conversion of the ketone to the bromine in the presence of PBr₃ delivered the desired quinoline (**3.81**) in modest yields.⁵⁰

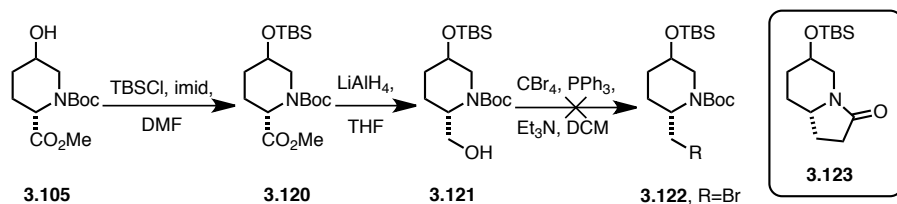


Scheme 3.30. Synthesis of 4-bromo-6-methoxy-quinoline

3.4.7 Coupling Attempts

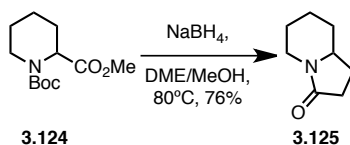
With the two desired fragments in hand, work focused on the coupling of our fragments. Alcohol **3.105** was first TBS-protected and then the ester was reduced to the primary alcohol (**3.121**, Scheme 3.31). From alcohol **3.121**, it was desired to halogenate the alcohol (**3.122**) to ready this fragment for either a Stille or Suzuki reaction. Unfortunately, any attempts at making the desired halide were thwarted by an intramolecular cyclization reaction, wherein the only product was lactam **3.123**, in

quantitative yield.



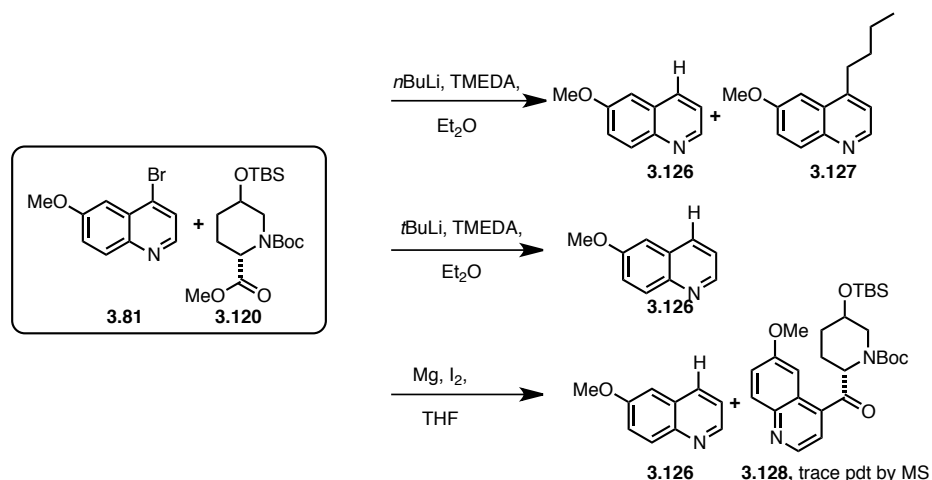
Scheme 3.31. Unexpected Intramolecular Cyclization

Further screening of the literature showed that even simpler systems had succumbed to this same fate (Scheme 3.32).⁴⁷



Scheme 3.32. Precedent for Intramolecular Cyclization

With evidence suggesting that obtaining the desired halide would be challenging with the *N*-carbamate, direct addition into the ester was pursued (Scheme 3.33). Lithiation of the brominated quinoline (**3.81**) and addition into the ester did not prove fruitful, with initial attempts using *n*BuLi as the lithiating reagent, delivering either the reduced quinoline (**3.126**) or the alkylated quinoline (**3.127**).



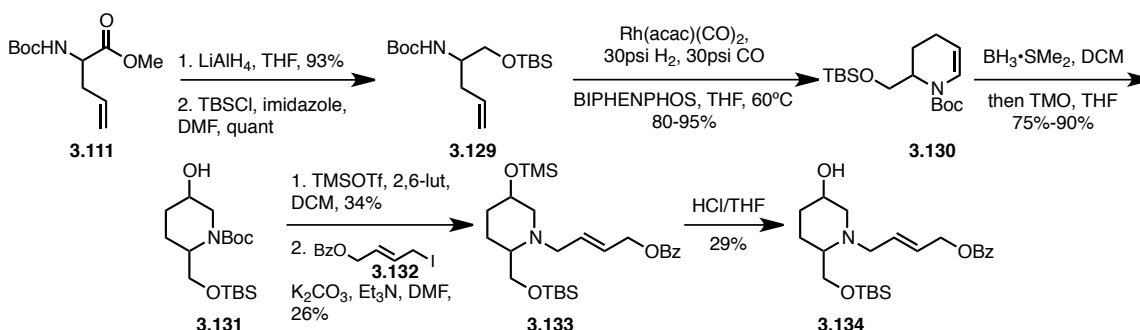
Scheme 3.33. Initial Coupling Attempts

Changing the base to $t\text{BuLi}$ remedied the alkylation problems, but again, the only product was **3.126**. Uskokovic reported that formation of lithiated quinolines was tedious and at temperatures $>50^\circ\text{C}$, would decompose, and this could have led to the problems that were being seen with the lithiation reactions.^{15,20-22} Attempts at converting **3.81** to a Grignard were also challenging, with only trace amounts of product (**3.128**) being observed by mass spectral analysis. It was at this stage that we decided to push forward and devise a method towards the quinuclidine fragment and that coupling could be revisited at a later stage.

3.5 Late Stage Quinine Intermediates

3.5.1 Late Stage Silyl Intermediate

Initially, racemic allylglycine was used and first reduced and protected as the TBS-ether (**3.129**, Scheme 3.34). Cyclohydrocarbonylation with Ojima's conditions and the BIPHENPHOS ligand provided the desired enamine (**3.130**) in good yield. Le Corre's hydroboration/oxidation sequence provided **3.131**, which was then deprotected with Ohfuné's conditions,³⁵ and alkylation with **3.132** provided *N*-alkylated **3.133**. Removal of the TMS group provided the desired alcohol (**3.134**) in modest yield.

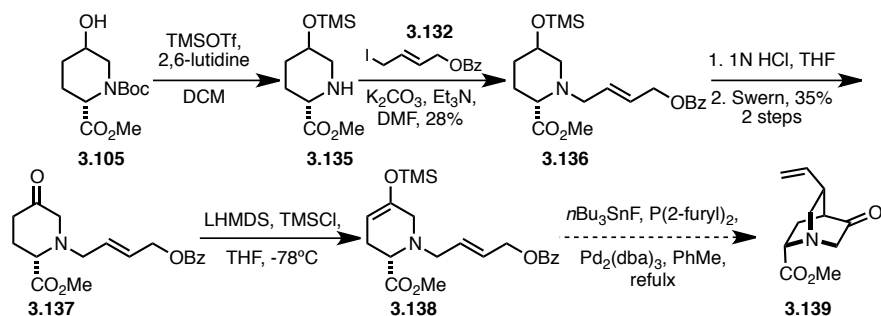


Scheme 3.34. Late Stage Silyl Intermediate

3.5.2 Advanced Quinine Intermediate

The low yields of the aforementioned reaction sequence were problematic, and it was thought that the bulk of the TBS group could be influencing the reactivities of the system. Because of this, the reaction sequence was performed on chiral, non-racemic

3.105 (Scheme 3.35). Ohfuné's deprotection conditions³⁵ and alkylation with **3.132** afforded **3.136**, and deprotection of the alcohol and oxidation via Swern conditions provided the desired ketone (**3.137**).



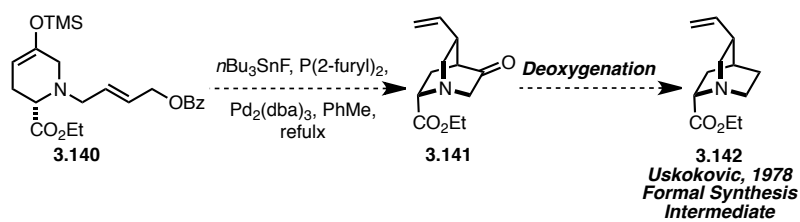
Scheme 3.35. Late Stage Quinine Intermediate

Conversion of ketone **3.137** to the TMS-enol ether provided **3.138**, which was immediately taken on to the cyclization reaction. Cyclization using John's conditions¹ were employed, and by crude NMR there appeared to be a terminal double bond, but due to the inherently low yield of this reaction, and the fact that this was performed on ~60mg, there was not enough material for purification and quinuclidine **3.139** was never realized.

3.6 Conclusion

It was through tedious work that a route toward our desired pipecolic acid fragment was realized and further development of the late-stage quinine intermediate **3.138** was achieved. From this point in the synthesis, the cyclization conditions and the

deoxygenation would still need to be explored, and completion of these studies could actually lead to a quinuclidine intermediate that, as the ethyl ester, would afford a formal synthesis of quinine, intercepting one of Uskokovic's intermediates (**3.142**, Scheme 3.36).



Scheme 3.36. Possible Interception of Uskokovic's Intermediate

Chapter 4: Histone Deacetylase Inhibitors

4.1 Introduction

4.1.1 HDAC Enzyme Functions

An extensive amount of work has gone in to the publication of review on the structure and function of HDAC inhibitors. Dr. Teneya Newkirk, a former member of the Williams' group, published an extensive review in 2009, which will be touched up on in this chapter. For a more extensive review of early HDAC inhibitors and their influence on HDAC related research, please refer to the review published in Natural Product Reports.⁵¹

In eukaryotic cells, DNA packaging influences transcription.^{52,53} DNA is packaged into chromatin, which is a nucleosome composed of an octamer of four core histones with a 146 bp strand of DNA wrapped around it. The interaction holding the DNA around the octamer is through positively charged lysine residues on histone proteins, which are able to attract the negatively charged DNA backbone.⁵⁴ During transcription, DNA is made available to DNA binding proteins through a modification of the nucleosome.^{52,55} Histone acetylation occurs at the ϵ amino groups of a conserved lysine residue located at the N-termini, effectively removing the charged interaction and allowing the DNA to unwrap from around the histone.^{54,56} At the completion of

replication, HDAC enzymes remove the *N*-acetyl moiety, allowing for the charge to be restored and for DNA to wrap around the histone, returning to its inactive state.

Malfunction of HDAC enzymes has been linked to numerous maladies ranging from cancer to heart disease, as well as autoimmune conditions such as rheumatoid arthritis.⁵⁷⁻⁵⁹ HDAC enzymes can be grouped into three different categories, based on structure and phylogenetic class. Class I HDACs (1, 2, 3, & 8), class II HDACs (4-7, 9-10) and class IV HDAC (11) are all Zn²⁺ dependent.⁶⁰⁻⁶³

Class I and II HDACs differ in both size and catalytic domain, with class I being 49-55 kDa and class II being 80-131 kDa in size.⁶⁴ The catalytic domain of class I resides at the N-terminus, whereas the class II domain is at the C-terminus. Class I isoforms are expressed and confined to the nucleus, and class II isoforms are tissue-selective and tend to move between the nucleus and cytoplasm.⁶⁴

4.2 HDAC Inhibitors

4.2.1 Acyclic HDAC Inhibitors

HDAC inhibitors have been found to disrupt the level of histone acetylation, leading to a state of hyperacetylation of very specific chromatin regions and thus deregulated transcription of a subset of genes, resulting in the transcriptional activation of some genes and repression of others. Generally, the result is a cell cycle arrest in G1 or G2/M, differentiation, and apoptosis in cancer cells.⁶⁵

Early HDAC inhibitors were acyclic small molecules (Figure 4.1). Additionally, the first FDA approved HDAC inhibitor, SAHA (**4.2** Zolinza, Merck Pharmaceuticals), is an acyclic, synthetic small molecule. Other acyclic small molecules that have paved the way in HDAC inhibitor research (Figure 4.1) include trichostatin A (TSA) (**4.1**), MS-275 (**4.3**), and Depucelin (**4.5**).^{51,66-69}

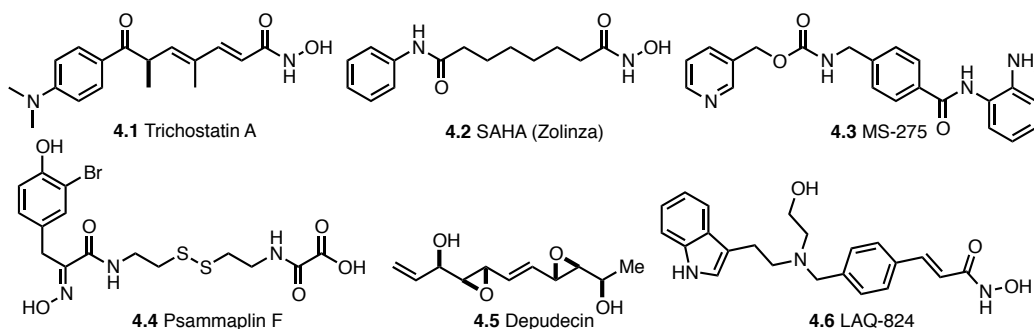


Figure 4.1. Acyclic HDAC Inhibitors

TSA (**4.1**), isolated in 1976 by Yoshida in 1995, initially paved the way for HDACi research.^{68,69} Crystallographic studies were able to show a tapered channel (~11Å) narrowing to ~7.5Å in the active site. At the bottom of this channel exists a Zn^{2+} cation coordinated to aspartic acid residues, a histidine residue, and a water molecule (Figure 4.2). Furthermore, a crystal structure with TSA (**4.1**) bound, allowed for further explanation of the function of the enzyme.^{70,71}

It has been proposed that an acetylated lysine residue coordinates with the Zn^{2+} cation and that the attack of water forms a tetrahedral intermediate, which then collapses to furnish the lysine residue (Figure 4.2).⁷¹

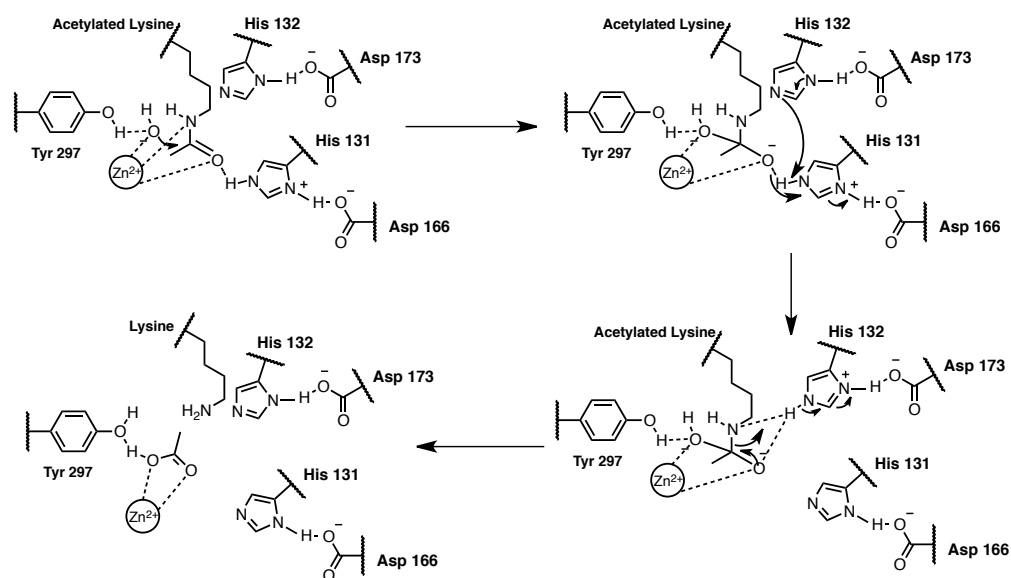


Figure 4.2. Tentative Catalytic Mechanism for HDAC

From studies with TSA, it can be seen that various regions of HDAC inhibitors interact with the enzyme in specific ways. Namely, that the cap region affects interactions with amino acid residues around the rim of the channel to the active site, whereas the linker region lowers a zinc-binding arm through the hydrophobic channel, and the zinc-binding region displaces the water molecule to facilitate coordination to the cation. Figure 4.3 shows the HDAC pharmacophore with respect to various HDAC inhibitors.

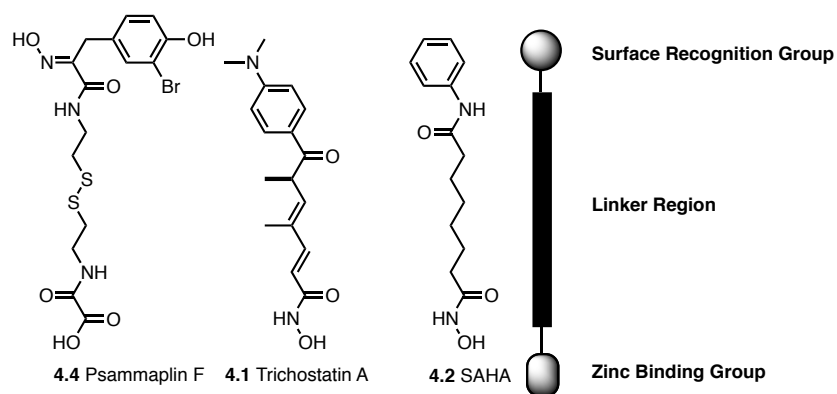


Figure 4.3. Pharmacophore of HDAC Enzymes

4.2.2 Macrocyclic HDAC Inhibitors

Another class of HDAC inhibitors that has been under extensive study are macrocyclic HDAC inhibitors (Figure 4.4).

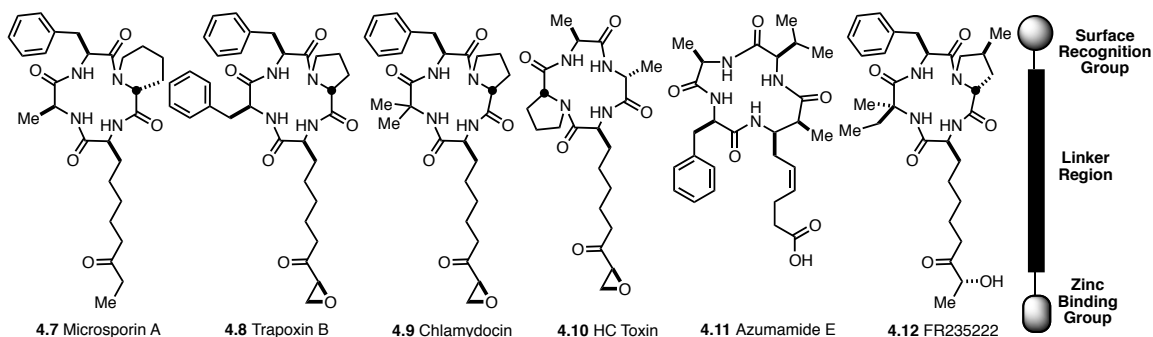


Figure 4.4. Selected Macrocyclic HDAC Inhibitors

The large macrocyclic core (cap region) has been shown to increase biological activity over the acyclic HDAC inhibitors.^{63,72} HC-Toxin (**4.10**) was the first tetrapeptide to be isolated (*Helminthosporium carbonium*) and contains an α -epoxy ketone as its

zinc-binding moiety.^{72,73} As seen with Trapoxin B (**4.8**) and Chlamydocin (**4.9**), the α -epoxy ketone is a common functional group of the tetrapeptide HDAC inhibitors.^{63,67} The Microsporins (**4.7**), which lack the epoxy moiety of the trapoxins and HC toxin (**4.10**), have been found to retain the nanomolar activity seen in the tetrapeptides.⁵¹

4.2.3 Sulfur-Containing HDAC Inhibitors

HDAC inhibitors displaying a novel zing-binding motif have been isolated (Figure 4.5).^{51,72} This group of molecules contain a unique (3*S*,4*E*)-3-hydroxy-7-mercapto-4-heptenoic acid side chain. Included in this sub-family of natural products are the spiruchostatins (**4.13**), FR901375 (**4.14**), FK228 (**4.15**), and largazole (**4.16**).

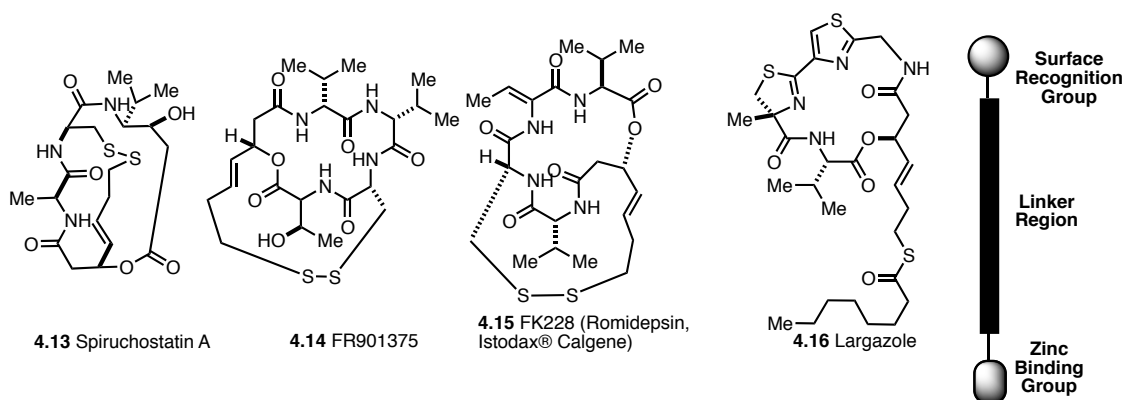


Figure 4.5. Sulfur-Containing HDAC Inhibitors

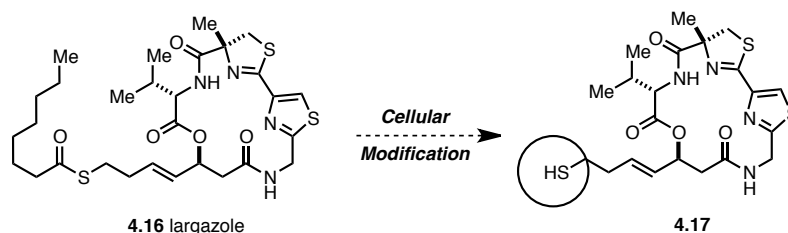
These molecules have been the targets of several total syntheses and numerous biological studies, with the spiruchostatins showing micromolar inhibitory activity.^{51,74}

FK228 (**4.15**), also known as romidepsin and Istodax®, was the first sulfur-containing HDAC inhibitor discovered and was approved for use against peripheral and cutaneous T-cell lymphoma in 2009. FK228 has been studied extensively⁷⁵ to identify its specific protein targets,⁷⁶ revealing at least 27 proteins involved in an array of cellular processes. Much of what is known about these types of HDAC inhibitors was discovered from studies with FK228.⁵¹

4.3 Largazole

4.3.1 Luesch Isolation

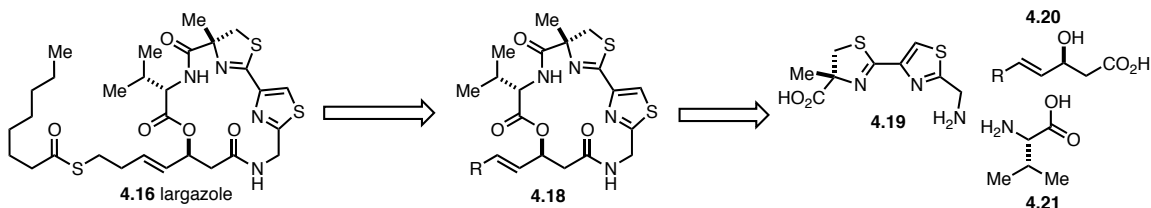
In early 2008, Luesch and coworkers isolated a potent HDAC inhibitor, largazole, from the Floridian marine cyanobacterium *Symploca* sp.⁷⁷ Largazole has one structural similarity to FK228, in that it possesses the same 3-hydroxy-7-mercaptohept-4-enoic acid moiety.⁷⁷ Additionally, in place of the disulfide linkage found in FK228, largazole displays an octanoyl thioester as a capping group for the thiol. Based on the similarities to FK228, it was suggested that largazole, like FK228, may be a prodrug, and that the realization of the thiol would reveal the zinc-binding motif of the molecule (Scheme 4.1), supported by the biological tests that show largazole to be nearly inactive, and the free-thiol (**4.17**) showing increased activity.⁵



Scheme 4.1. Largazole Activation

4.4 Previous Syntheses

Since largazole's isolation in 2008, there have been more than eight total syntheses. The general approach towards the molecule's construction is shown in Scheme 4.2.⁵¹

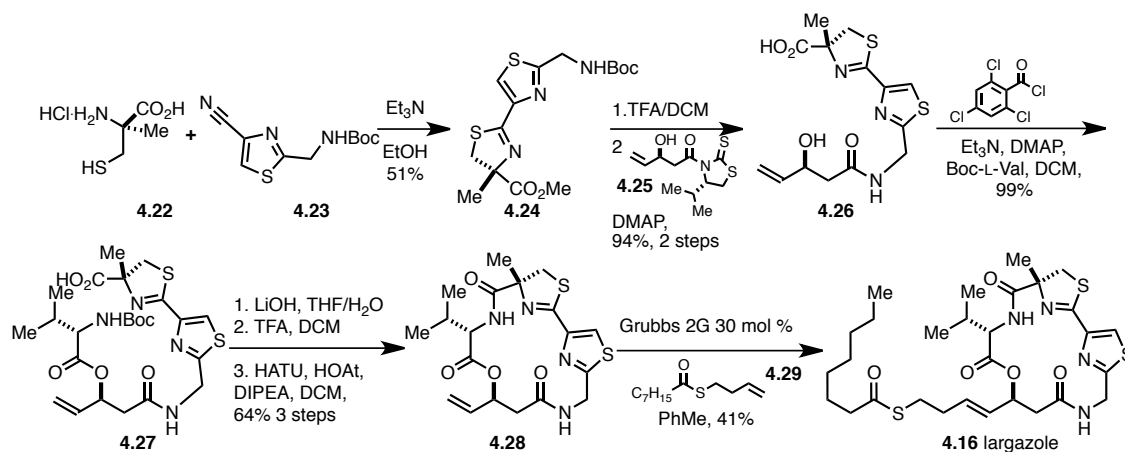


Scheme 4.2. General Strategy Towards Largazole

4.4.1 Luesch Synthesis

The first total synthesis of largazole was published by Luesch and coworkers in 2008.⁴ By condensing α -Me-Cys-OH·HCl (**4.22** Scheme 4.3) onto thiazole **4.23**, the corresponding thiazoline-thiazole moiety was realized. Deprotection and displacement of the chiral auxiliary (**4.25**) provided peptide **4.26**, which was then coupled to *N*-Boc-Val

to afford **4.27**. Conversion to the free acid and free amine, followed by subsequent macrocyclization, then delivered the vinylogous macrocycle (**4.28**) in modest yields, with a final metathesis reaction installing the requisite side chain to realize largazole (**4.16**).



Scheme 4.3. Luesch's Route to Largazole

Luesch also synthesized several analogs of largazole to probe the linker length and stereochemistry at the depsipeptide C17 region.⁷⁸ Structure-activity relationships suggested that the four-atom linker between the macrocycle and the octanoyl group in the side chain, as well as the *S*-configuration at C17, are both critical to HDAC inhibition (Figure 4.6, Table 4.1).⁷⁸

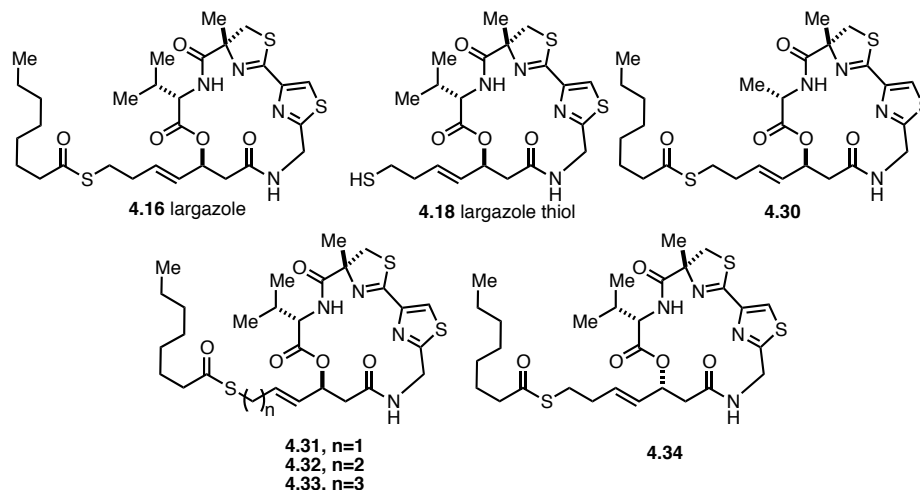


Figure 4.6. Leusch Analogs of Largazole

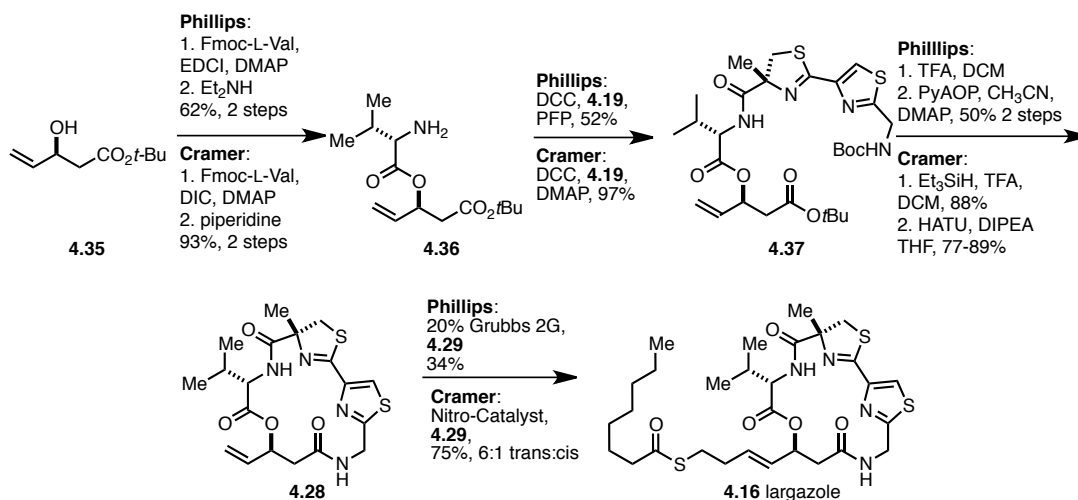
Table 4.1. Biological Activity of Largazole Analogs

Compound	HDAC1 (nM)	HDAC6 (nM)
Largazole (4.16)	7.6	1,800
4.18	0.77	570
4.31	Not Tested	Not Tested
4.32	690	>10,000
4.33	1,900	>10,000
4.30	44	3,300
4.34	Not Tested	Not Tested

4.4.2 Phillips and Cramer Syntheses

Phillips and Cramer published very similar routes to Largazole on July 11th and July 16th of 2008, respectively (Scheme 4.4).^{79,80} Starting from alcohol **4.35**, peptide coupling provided them with **4.36**, and a subsequent coupling with the aforementioned thiazoline-thiazole moiety (**4.19**) then delivered dipeptide **4.37**. Deprotection and macrocyclization with either PyBOP (Phillips' synthesis) or a HATU coupling (Cramer's

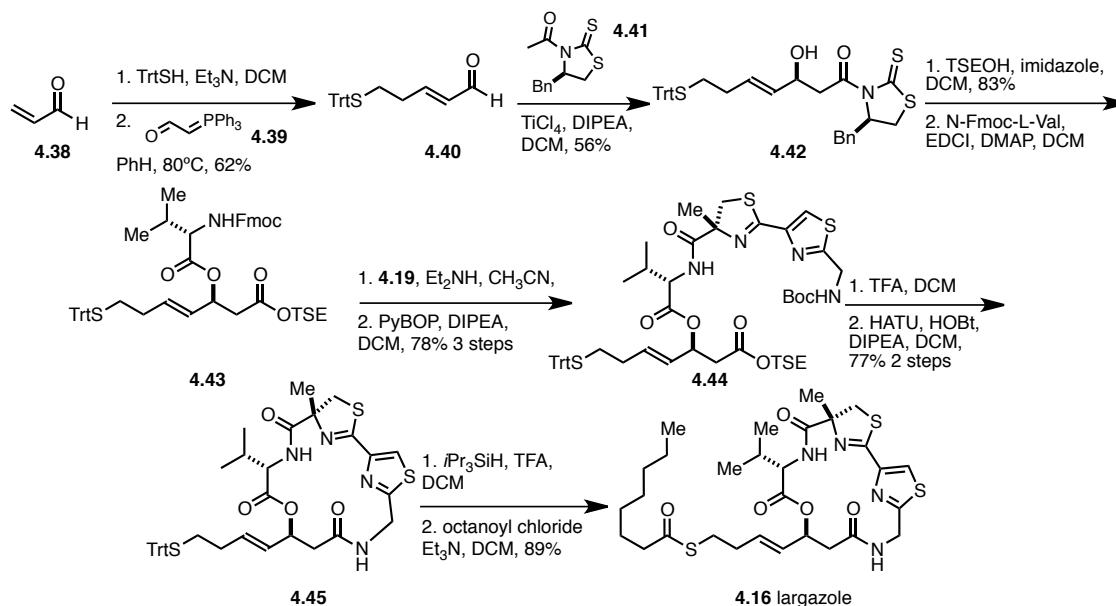
route) delivered macrocycle **4.28**. Olefin metathesis was again used to install the side chain and deliver the final target (**4.16**).



Scheme 4.4. Phillips and Cramer Routes to Largazole

4.4.3 Williams' Synthesis

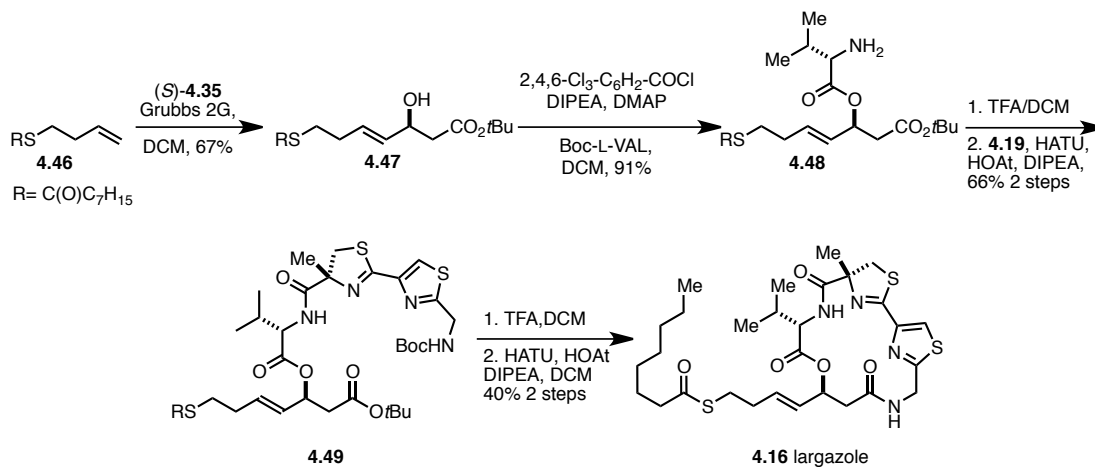
On July 19th, 2008 the Williams group published their route toward largazole (Scheme 4.5).⁵ The chiral auxiliary on alcohol **4.42** was first displaced to form the TMS-ethanolic-ester, and coupling with *N*-Fmoc-L-Val then provided dipeptide **4.43**. Installation of the thiazoline-thiazole moiety (**4.19**) with PyBOP provided the desired acycle (**4.44**). Deprotection and subsequent cyclization with HATU/HOBt formed the macrocycle (**4.45**), which was then deprotected and converted to largazole (**4.16**) by converting the free thiol to the thioester.



Scheme 4.5. Williams' Route to Largazole

4.4.4 Ghosh's Synthesis

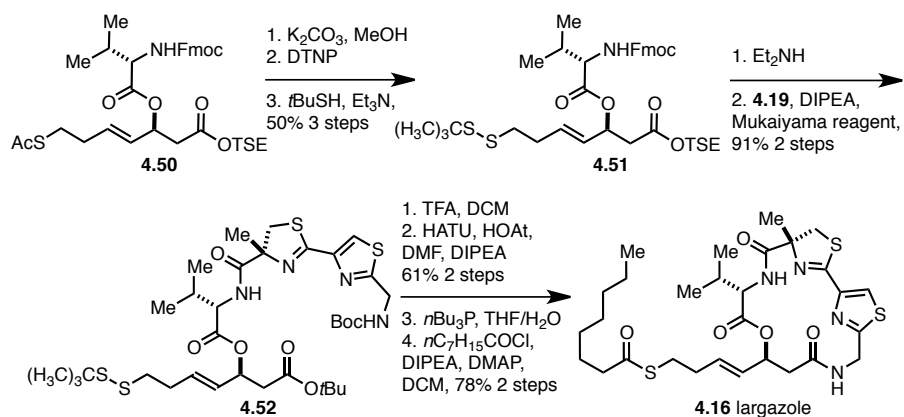
A mere 10 days after Williams' publication, Ghosh's route towards largazole was released (Scheme 4.6).⁸¹ From **4.46**, Ghosh first performed the metathesis reaction to fully form the side chain (**4.47**). Coupling of *N*-Boc-L-Val and thiazoline-thiazole **4.19** then delivered acycle **4.49**, with a final deprotection and HATU macrolactamization unveiling the final target (**4.16**).



Scheme 4.6. Ghosh's Route Towards Largazole

4.4.5 Ye's Synthesis

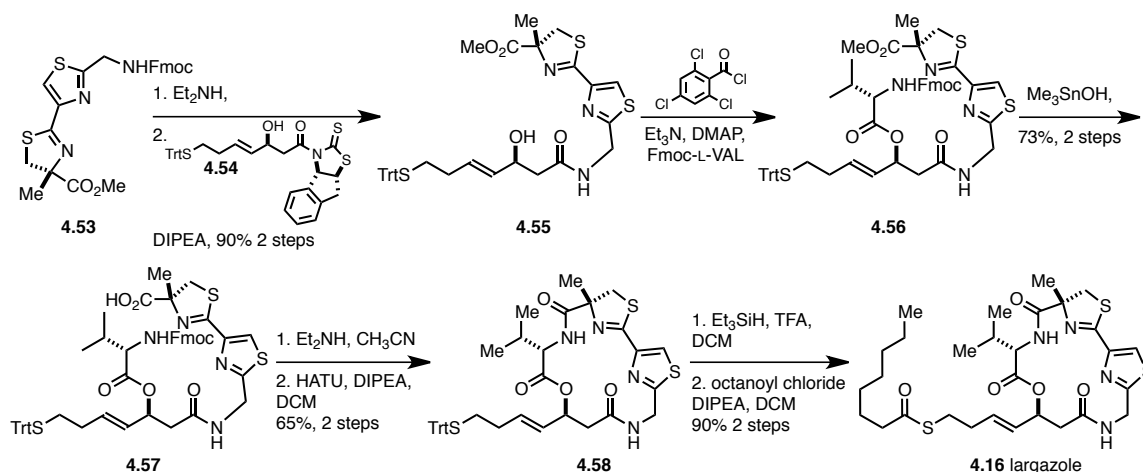
Ye published his route towards largazole in August of 2008 (Scheme 4.7).⁸² From peptide **4.50**, the thioester was first converted to the asymmetric disulfide (**4.51**). Coupling of the thiazoline-thiazole moiety (**4.19**) delivered the desired acycle (**4.52**). Deprotection and macrocyclization followed by reduction of the disulfide and esterification with octanoyl chloride then delivered largazole (**4.16**).



Scheme 4.7. Ye's Route to Largazole

4.4.6 Doi's Synthesis

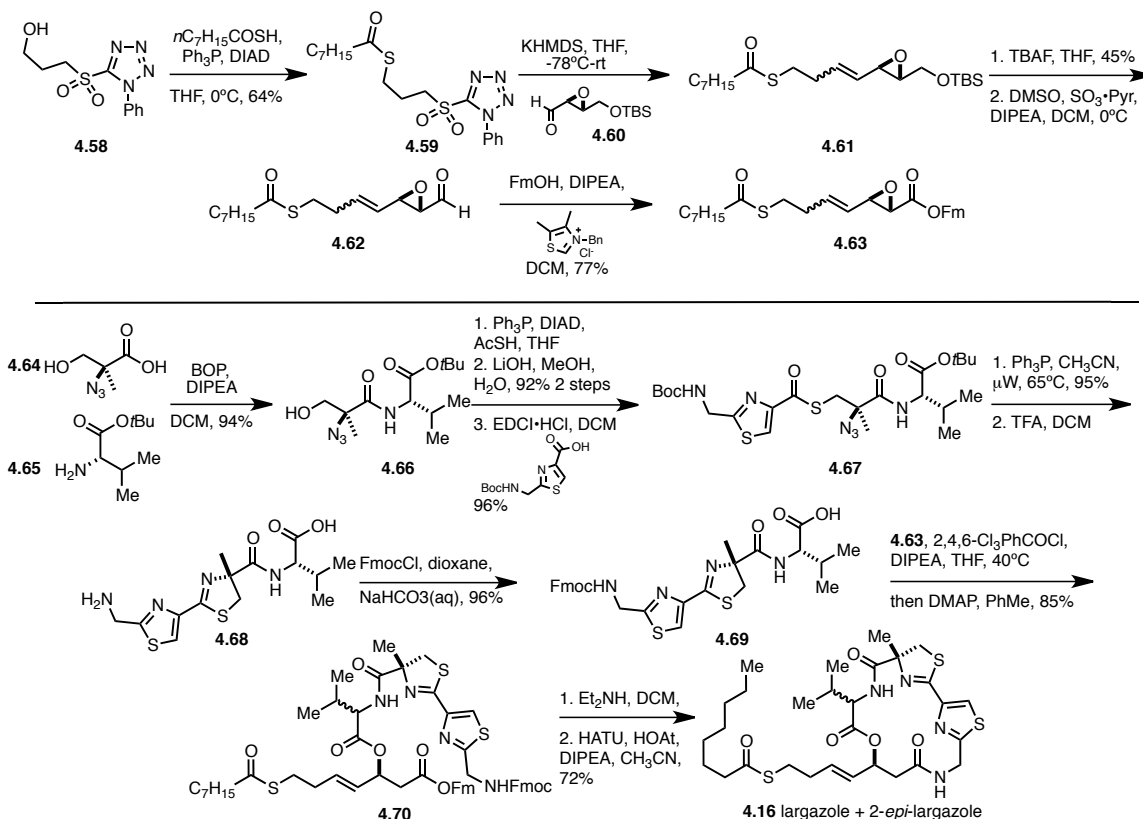
Doi published his route to largazole (Scheme 4.8) a few weeks after Ye, again displacing the chiral auxiliary on **4.54** with the thiazoline-thiazole fragment (**4.53**) to deliver **4.55**.⁸³ Coupling to *N*-Fmoc-L-Valine delivered **4.56**, from which the acid and free amine were released and cyclized to furnish **4.57**. Removal of the trityl group and conversion to the thioester then delivered largazole (**4.16**).



Scheme 4.8. Doi's Route to Largazole

4.4.7 Forsythe Synthesis

Nearly a year after the first route to largazole was disclosed, Forsyth published his own strategy towards the ever-popular HDAC inhibitor (Scheme 4.9).⁸⁴ Thus, thiazoline-thiazole-Valine peptide **4.69** was coupled with vinylogous epoxide **4.63**. Following removal of the requisite Fmoc-protecting groups and macrolactamization, largazole was realized (**4.16**) along with 2-*epi*-largazole.



Scheme 4.9. Forsyth's Route to Largazole

Since the first wave of largazole syntheses were released, a number of additional routes have also been disclosed, based primarily upon the original routes published in 2008.

4.5 Williams Pursuit of Potent Analogs

In addition to the synthesis of largazole, the William's group has also synthesized numerous analogs to probe structural differences in the cap region, linker length, the depsipeptide, and the zinc-binding motif.⁸⁵ Figure 4.7 shows a selection of analogs that

have been synthesized, as well as the resulting outcome of the biological studies on these compounds.⁸⁶

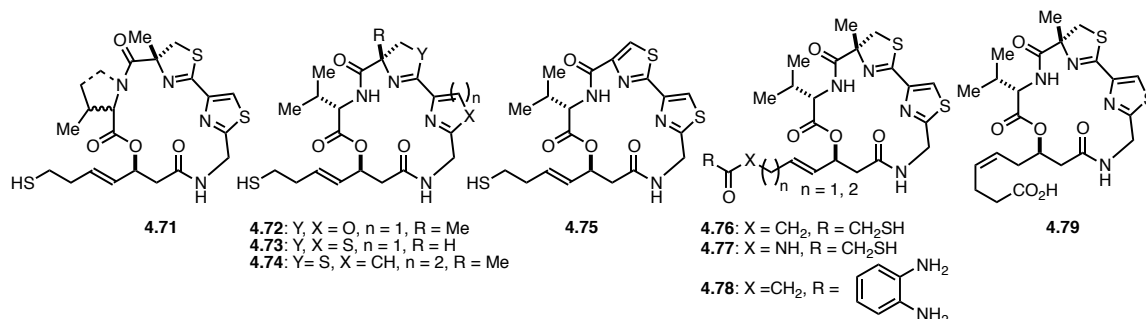


Figure 4.7. Williams Group Analogs

Table 4.2. Biological Activity of Williams Group Analogs

Compound	HDAC1 (μM)	HDAC2 (μM)	HDAC3 (μM)	HDAC6 (μM)
largazole thiol (4.76)	0.0012	0.0035	0.0034	0.049
proline substitution (4.71)	0.11	0.8	0.58	13
larg.-azumamide 4.79	>30	>30	>30	>30
benzamide (4.78)	0.27	4.1	4.1	>30
Thioamide (4.77)	0.67	1.6	0.96	0.7
cysteine substitution (4.73)	0.0019	0.0048	0.0038	0.13
thiazole-thiazole (4.75)	0.077	0.12	0.085	>30
thiazole-pyridine (4.74)	0.00032	0.00086	0.0011	0.029
oxazoline-oxazole (4.72)	0.00069	0.0017	0.0015	0.045
SAHA	0.01	0.026	0.017	0.013
MS-275	0.045	0.13	0.17	>30

To date, the most potent analog synthesized has been the thiazoline-pyridine-containing species **4.74**, which exhibits sub-nanomolar inhibitory activity (Figure 4.7, Table 4.2).⁸⁵ Additionally, the half-life of largazole is very short lived, and as such, conversion of the depsipeptide to that of the amide isostere as been explored (Figure 4.8, Table 4.3). The hope would be that the more rigid amide bond would increase the

existence of the molecule in the cell before the drug was destroyed. Testing of amide isostere **4.81** as well as the corresponding thiol (**4.80**) showed a decrease in biological activity.⁸⁶

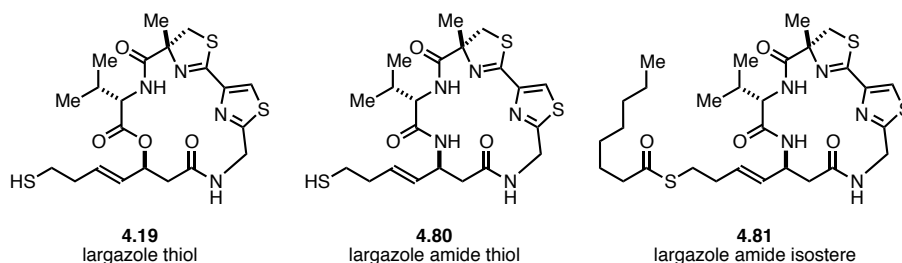


Figure 4.8 Largazole Thiol and Largazole Amide Isosteres

Table 4.3. Biological Data Comparing Largazole and its Amide Isostere (IC₅₀ nM)

Compound	HDAC1 nM	HDAC2 nM	HDAC3 nM	HDAC6 nM
largazole thiol 4.19	0.1	0.8	1	40
amide isostere thiol 4.80	0.9	4	4	1500
amide isostere 4.81	>3000	>3000	>3000	>3000
SAHA	10	40	30	30

The loss of biological activity was investigated with computational studies performed by Dr. Olaf Wiest, as shown below in Figure 4.9.⁸⁶

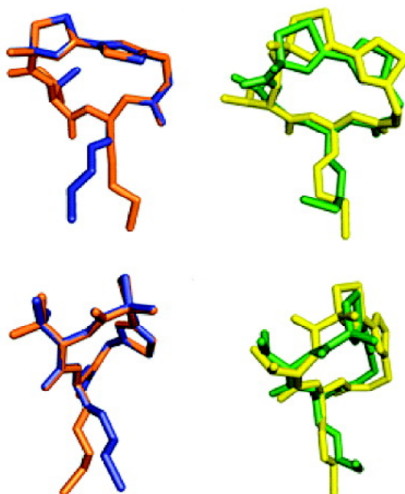


Figure 4.9. Largazole and Amide Isostere Conformations

The orange representation of largazole is the lowest energy binding conformation, superimposed by the average lowest energy conformation in blue. In yellow, the lowest energy binding conformation of the amide isostere is superimposed by its average lowest energy conformation in green. This shows some distortion of the cap region of the amide isostere, possibly explaining the decrease in biological activity.⁸⁶

4.6 Conclusion

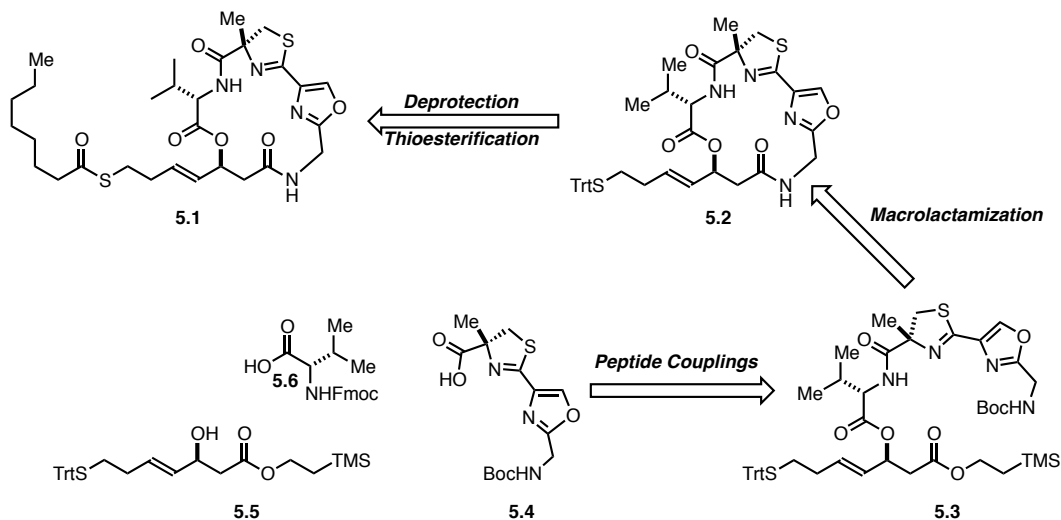
Early studies of acyclic HDAC inhibitors as well as the later studies on sulfur-containing HDAC inhibitor FK228 have paved the way for novel HDAC inhibitors. The emergence of largazole has led to an explosion of work in the field of HDAC inhibition, one that our group has taken a strong interest in.

Our studies on largazole and analogs of it have led us to increasingly more potent and selective compounds. Furthermore, work is still being performed in our group making analogs that are further exploring the cap region, the Zn-binding motif, as well as altering the depsipeptides and constructing the amide isostere of all analogs to determine if this will aid in delivering a more drug-like series of compounds.

5.1 Synthesis of Thiazoline-Oxazole Containing Analogs

5.1.1 Retrosynthetic Analysis of Thiazoline-Oxazole Analogs

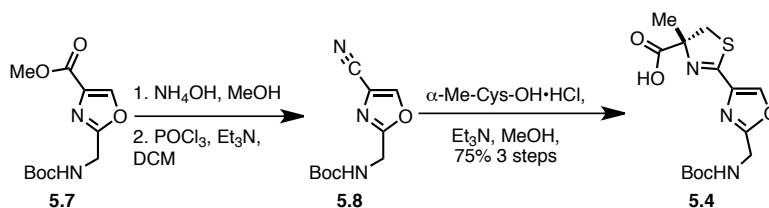
Work towards analogs of largazole is on going in the Williams' group.⁵ In an effort to see how changing the heteroatoms on the thiazoline-thiazole fragment of largazole would affect its biological activity, we pursued a thiazoline-oxazole species, as well as the oxazoline-thiazole analog. Based on the synthesis of largazole, reported by our group, we decided to utilize a similar route towards thiazoline-oxazole containing analogs, which could be delivered through the deprotection and esterification of **5.2**, which could be made through a macrolactamization of acycle **5.3**. Coupling of the allylic alcohol (**5.5**), L-Valine, and the thiazoline-oxazole moiety (**5.4**) would deliver the requisite acycle (**5.3**) (Scheme 5.1).



Scheme 5.1. Thiazoline-Oxazole Analog Retrosynthetic Analysis

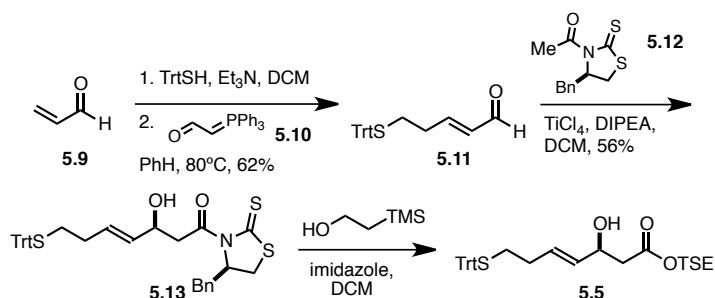
5.1.2 Synthesis of Thiazoline-Oxazole Analogs

The synthetic approach to this analog is based off of the synthetic sequence previously used by our group in generating numerous other largazole analogs. The thiazoline-oxazole fragment (**5.4**) was constructed starting from known oxazole **5.7**.⁸⁵ From **5.7**, conversion to the nitrile (**5.8**) proceeded via a two-pot procedure wherein **5.7** was first treated with NH_4OH in MeOH, then POCl_3 with Et_3N in DCM. The crude nitrile (**5.8**) was then condensed onto α -methyl-cysteine made in 5 steps from cysteine) to provide the thiazoline-oxazole fragment (**5.4**) in 75% yield over 3 steps.



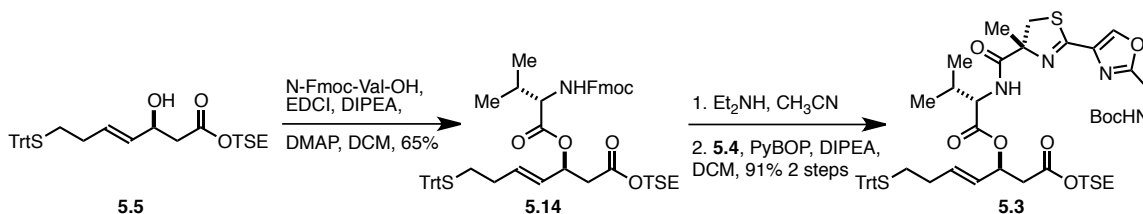
Scheme 5.2. Synthesis of Thiazoline-Oxazole Fragment

The synthesis of heptenoic acid fragment **5.5**, starting from acrolein, began with a Michael addition, followed by a Wittig reaction with commercially available (Formylmethylene)triphenylphosphorane (**5.10**), which delivered α,β -unsaturated aldehyde **5.11**.⁵ An aldol reaction utilizing a Crimmins-type auxiliary (**5.12**) provided the β -hydroxy acid **5.13** and the chiral auxiliary was then displaced with trimethylsilyl ethanol to give the requisite coupling fragment (**5.5**).⁵



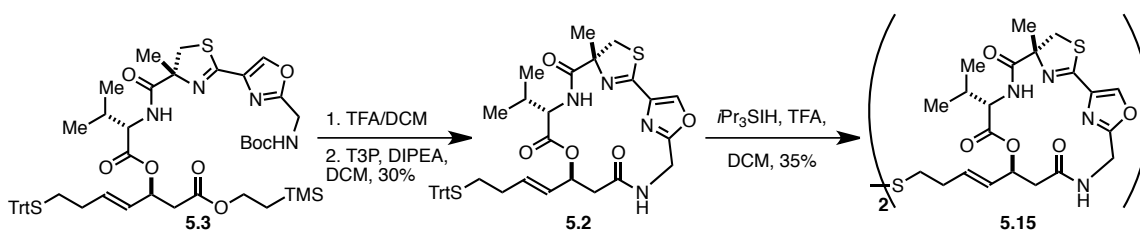
Scheme 5.3. Heptenoic Acid Synthesis

Construction of the macrocycle began by coupling β -hydroxy acid **5.5** to *N*-Fmoc-Val-OH with EDCI and Hunig's base, giving peptide **5.14**.⁵ Deprotection followed by coupling of thiazoline-oxazole **5.4** with PyBOP and Hünig's base gave the desired acycle (**5.3**) in 91% yield over 2 steps.⁸⁵



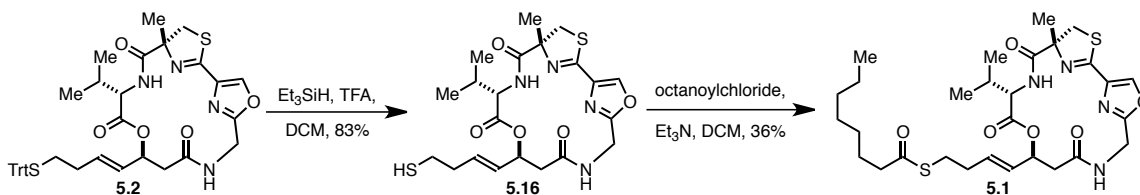
Scheme 5.4. Formation of Analog Acycle

Previously, macrocyclizations in our group utilized HATU/HOBt coupling protocols.^{5,85} Initial efforts towards **5.2** were carried out using this standard protocol, however, due to vast amounts of the common HATU byproduct, tetramethylurea, an alternative approach was investigated to ease the purification of the macrocycle. Following a one-pot double-deprotection of the acycle, the desired macrocycle (**5.2**) was obtained in 30% yield using T3P and Hünig's base in a new coupling protocol. Deprotection of macrocycle **5.2** with TFA and *i*Pr₃SiH in degassed DCM to give the requisite thiol, instead, delivered homo-dimer **5.15** in 35% yield.



Scheme 5.5. Macrocyclization and Formation of Homo-Dimer

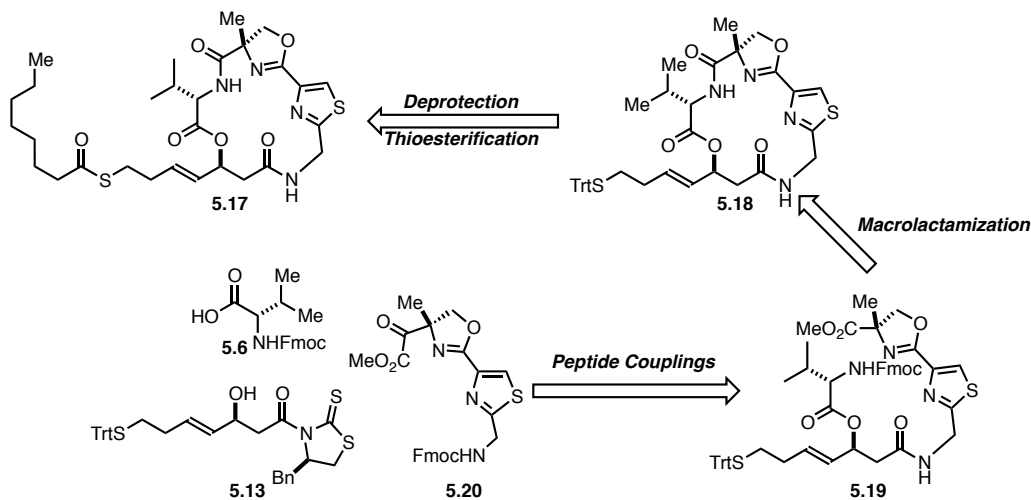
Interestingly, it was found that deprotection of trityl thiol **5.2** with Et₃SiH instead of *i*Pr₃SiH in degassed DCM gave the desired thiol (**5.16**), which was immediately acylated affording octanoyl thioester **5.1**.



Scheme 5.6. Deprotection and Acetylation

5.1.3 Oxazoline-Thiazole Retrosynthetic Analysis

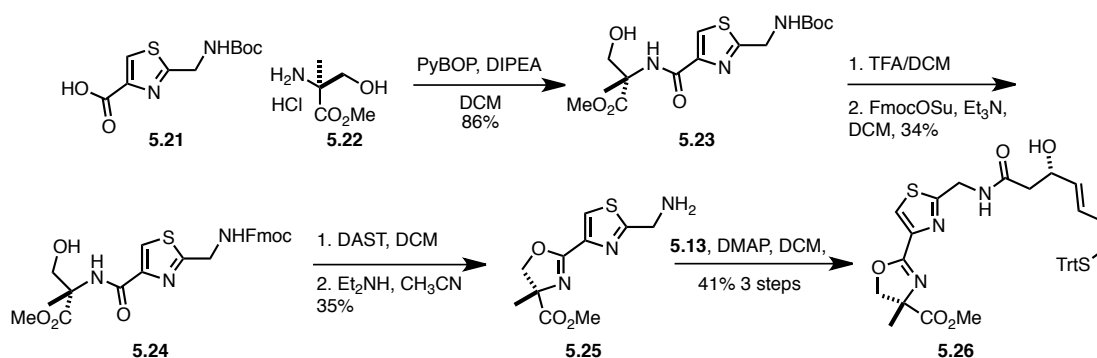
In addition to the thiazoline-oxazole analog, the oxazoline-thiazole analog was pursued. Due to the instability of oxazoline moieties to strongly acidic conditions, the synthesis of macrocycle **5.18** was altered (Scheme 5.7).⁸⁵ Macrocycle **5.18** could be made through a macrolactamization, this time between the valine nitrogen and the carboxylic acid moiety on the oxazoline-thiazole fragment (**5.19**). Acycle **5.19** could come from a coupling of the oxazoline-thiazole fragment (**5.20**) to β -hydroxy acid **5.13** and a subsequent peptide coupling to *N*-Fmoc-L-Valine (**5.6**).



Scheme 5.7. Oxazoline-Thiazole Analog Retrosynthetic Analysis

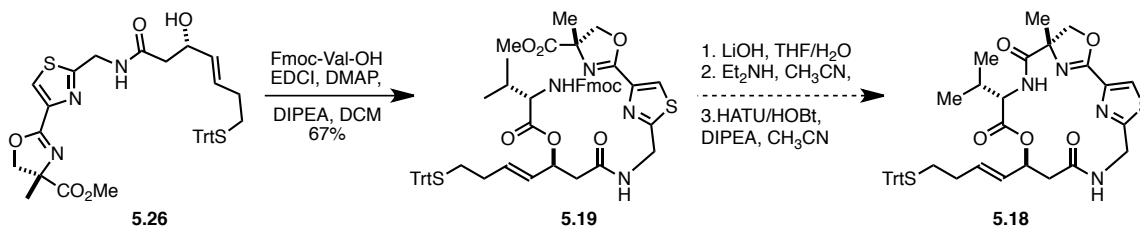
5.1.4 Progress Toward Oxazoline-Thiazole Analog

From known thiazole **5.21**, α -Me-Ser-OH•HCl (**5.22**, generously provided to us from Ajinomoto Co., Japan) was coupled with PyBOP and Hünig's base to give peptide **5.23**. A protecting group manipulation of **5.23** delivered *N*-Fmoc protected **5.24**, although in very modest yields. Cyclization of the oxazoline ring with DAST and removal of the *N*-Fmoc protecting group delivered primary amine **5.25**, which was reacted with β -hydroxy acid **5.13** to displace the chiral auxiliary, providing **5.26**.



Scheme 5.8. Oxazoline-Thiazole Synthesis and Coupling

From alcohol **5.26**, a coupling with Fmoc-L-Val-OH using EDCI provided acycle **5.19**. Saponification and removal of the *N*-Fmoc moiety readied the peptide for cyclization. Standard HATU/HOBt conditions⁸⁵ were used and after numerous purifications, sufficient material did could not be obtained to characterize and confirm **5.18**. Unfortunately, more material has yet to be brought forward to complete the oxazoline-thiazole macrocycle.



Scheme 5.9. Acycle Formation

5.2 Biological Activity of Largazole Analogs

Compounds **5.1**, **5.15**, and **5.16** were tested against HDAC1-9 and the activity was determined with an optimized homogenous assay performed in a 384-well plate. Reactions were performed in assay buffer (50 mM HEPES, 100 mM KCl, 0.001% Tween-20, 0.05% BSA and pH 7.4. Additional 200 μ M TCEP was added for HDAC6) and followed by fluorogenic release of 7-amino-4-methylcoumarin from substrate upon deacetylase and trypsin enzymatic activity. Fluorescence measurements were obtained every five minutes using a multilabel plate reader and plate-stacker (Envision; Perkin-Elmer). Each plate was analyzed by plate repeat, and the first derivative within the linear range was imported into analytical software (Spotfire DecisionSite). Replicate experimental data from incubations with inhibitor were normalized to DMSO controls ([DMSO] < 0.5%). IC_{50} is determined by logistic regression with unconstrained maximum and minimum values. The recombinant, full-length HDAC protein (BPS Biosciences) was incubated with fluorophore conjugates substrate, MAZ1600 and MAZ1675 at K_m =[substrate] with the following results listed in Table 5.1.

Table 5.1. HDAC Activity of Largazole Analogs

HDAC isoform	HDAC Activity IC ₅₀ (μM)								
	1	2	3	4	5	6	7	8	9
Dimer (5.15)	0.15	1.3	0.55	--	--	0.05	--	--	--
Thiol (5.16)	0.0044	0.02	0.0072	--	--	0.098	--	--	--
Thioester (5.1)	0.9	2.1	1.9	--	--	1	--	--	--

While the data for the dimer (**5.15**) shows it to be a potent HDAC inhibitor with some selectivity for HDAC 6, the free thiol (**5.16**) is highly active for both HDAC's 1-3 as well as for HDAC 6. Insight into why these analogs appear to be more active for HDAC 6 is currently being explored and will be published at a later date.

5.3 Conclusion

Overall the syntheses of three new largazole analogs containing a thiazoline-oxazole cap region moiety have been completed. While the biological data of homo-dimer (**5.15**) is promising, we are still awaiting the data for the thiol (**5.16**) as well as the thioester (**5.1**). It is interesting to note that the homo-dimer does display some selectivity for HDAC 6, and class II isoform, and this has rarely been seen among the compounds tested (see Figure 4.7). To date, the most potent compound analog synthesized by our group is the thiazoline-pyridine complex (**4.103**).

Further work on this project, with regards to these two series of analogs, will be to complete the synthesis of the oxazoline-thiazole containing compounds and to submit that series of analogs for biological testing as well as to synthesize the amide isostere version of all of these compounds.

Chapter 6: Progress Toward the Biosynthesis of Taxol

6.1 Introduction

6.1.1 Efforts Toward Elucidating the Biosynthetic Path of Taxol

Our group has been interested in elucidating the biosynthetic path towards Taxol. Here, an overview of our synthetic and biological efforts, along with our collaborators is presented (excerpted from our review on this topic).⁸⁷

Chemists and biologists alike have been drawn to taxol⁸⁸ (**1**, paclitaxel) and its semi-synthetic congener taxotere (**2**) due to their promising spectrum of antineoplastic activity, unique mechanism of action, and the synthetic challenge that the complex, and densely functionalized ring system poses.⁸⁹⁻⁹⁶ Taxol was first isolated from the bark of the Pacific yew, *Taxus brevifolia* Nutt.⁹⁷ Unfortunately, the yew is slow growing and is primarily found in environmentally sensitive areas of the Pacific Northwest, and stripping the tree of its bark kills the yew. It takes three trees to obtain ~10 Kg of bark from which 1 gm of taxol can be isolated.⁹⁴ FDA approval of taxol for the treatment of advanced ovarian cancer⁸⁹ has created a severe supply and demand problem. Collection of renewable *Taxus* sp. needles and clippings has attenuated this problem somewhat, but as the drug becomes more widely adopted, particularly for use earlier in the course of cancer intervention and for new therapeutic applications, pressure on the yew

population is likely to increase worldwide. Alternative means of taxol production are being vigorously pursued since cost and availability will continue to be significant issues.

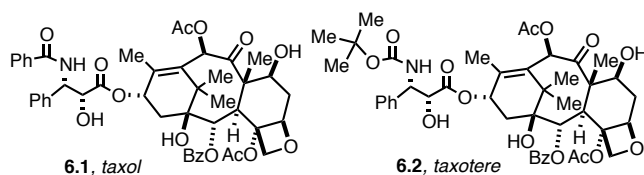


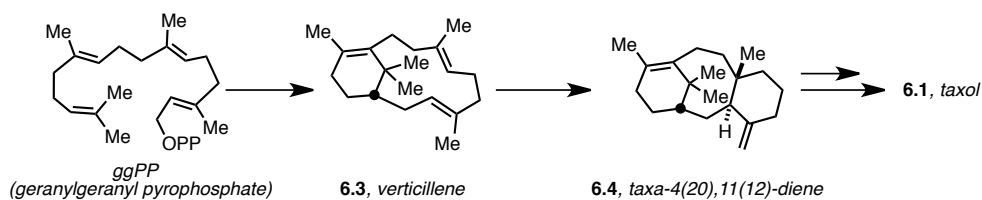
Figure 6.1. The Structure of Taxol (6.1) and Taxotere (6.2)

To date, totally synthetic methods have fallen short as an alternative source for taxol production,⁹⁸⁻¹¹² due to the complex structure of taxol that mandates lengthy and expensive synthetic routes. A method that has proven viable is the semi-synthesis of taxol from 10-deacetylbaccatin III, a renewable, which is isolated from the needles of yew species.^{90,94} The commercial supply of taxol and semi-synthetic precursors will have to increasingly rely on biological methods of production. This can be reasonably achieved by: (1) extraction from intact *Taxus* plants, (2) *Taxus* cell culture,¹¹³ or (3) microbial systems.¹¹⁴⁻¹²² In order to produce large quantities of taxol or a pharmacophoric equivalent by semi-synthetic approaches, or perhaps by genetically engineered biosynthetic methods, it is essential to gain a better understanding of the detailed biosynthetic pathways¹¹³⁻¹²⁴ in *Taxus sp.*

6.2 Early Stages of Taxol Biosynthesis

6.2.1 Taxadiene Synthase

In 1966, Lythgoe and coworkers proposed a biosynthetic pathway in which the tricyclic carbon framework of the taxoids was envisioned to arise by the sequential intramolecular cyclizations of the double bonds of geranylgeranyl pyrophosphate (ggPP) to 1(*S*)-verticillene (**6.3**) and then to taxa-4(20),11(12)-diene (**6.4**, Scheme 6.1).^{125,126}

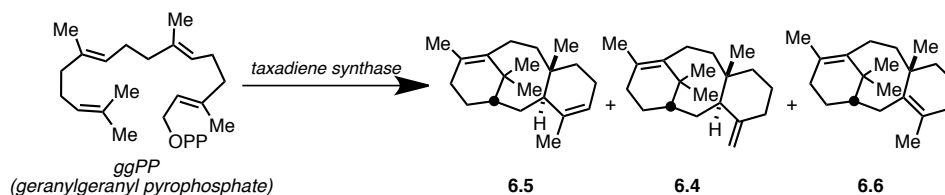


Scheme 6.1. Early Biosynthetic Proposal from ggPP to Taxol

Our highly collaborative program has been aimed at manipulating taxoid biosynthesis at the genetic level in cell culture; as such, the slow steps in the biosynthetic pathway need to be elucidated. Since ggPP serves as a starting material for many other biosynthetic pathways,¹²⁷⁻¹³¹ any number of the steps may be rate-limiting in the secondary metabolic flux to taxol. As a first step toward targeting the slow steps in the biosynthesis of taxol, we deployed several parallel strategies involving: (1) the biosynthetic production of lightly oxygenated taxoids using synthetic, tritium-labeled substrates; (2) total synthesis and isotopic labeling of pathway metabolites; (3) isolation

and structure determination of pathway intermediates; (4) identification, cloning and functional expression of the biosynthetic genes; (6) incorporation of candidate pathway metabolites into taxol *in vivo* and; (7) mechanistic studies on the individual pathway enzymes.

We discovered that the “Lythgoe taxadiene” (**6.4**) is not the first committed intermediate on the taxoid biosynthetic pathway, but rather that taxa-4(5),11(12)-diene (**6.5**, Scheme 6.2) is the major metabolite.¹³²⁻¹³⁹ This was demonstrated by a total synthesis^{138,139} of both **6.4** and **6.5** and administration of synthetic ¹³C-labeled taxa-4(20),11(12)-diene (**6.4**) to microsomes of *Taxus Canadensis*.¹³⁴ Cross-over experiments and the lack of detectable biotransformation of the Lythgoe diene (**6.4**) in *Taxus* microsomes had initially cast considerable doubt on the intermediacy of this substance in taxoid biosynthesis.¹³⁷ On the other hand, using ggPP as a substrate, taxa-4(5),11(12)-diene (**6.5**) has been shown to be the primary product of taxadiene synthase, an enzyme recently characterized, and the corresponding gene cloned and functionally expressed.¹³²⁻¹³⁵ However, recent results from our laboratories have revealed that recombinant taxadiene synthase indeed produces ~5% of the Lythgoe diene (**6.4**) plus <1% percent of the 3,4-diene isomer (**6.6**).¹³⁷

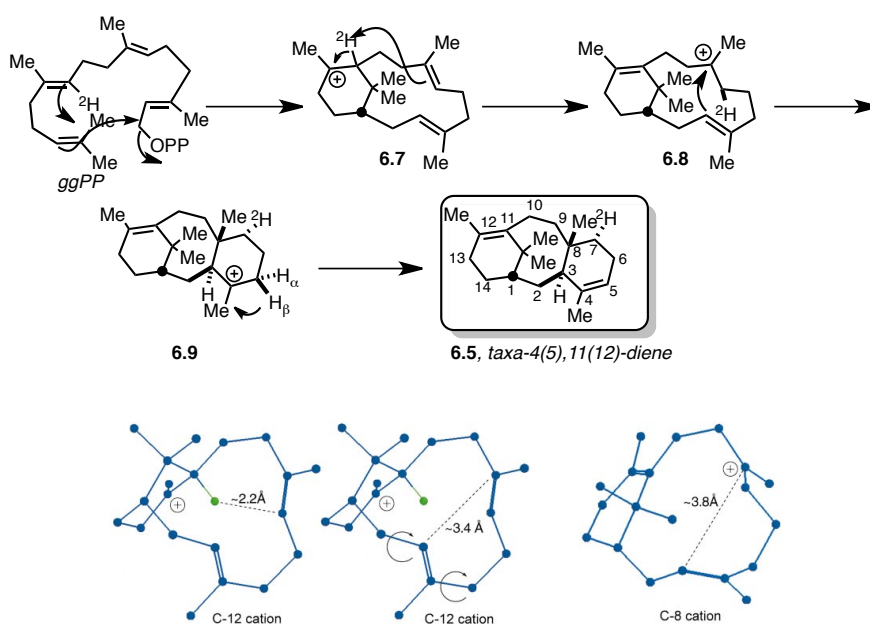


Scheme 6.2. Products of Recombinant Taxadiene Synthase

Taxadiene synthase from *Taxus* species catalyzes the first committed step in the biosynthesis of taxol and related taxoids by the cyclization of the universal diterpenoid precursor (*E,E,E*)-geranylgeranyl diphosphate (ggPP) to the parent hydrocarbon taxa-4(5),11(12)-diene (**6.5**). Following the remarkable one-step construction of taxadiene, an extended and complex series of oxygenation and acylation reactions ensue, culminating in the production of taxol.^{132,140} Taxadiene synthase, which has been isolated from both yew saplings¹³³ and cell cultures,¹⁴¹ catalyzes a slow, but apparently not rate limiting step in the taxol biosynthetic pathway.¹⁴¹ A cDNA encoding the taxadiene synthase from *T. brevifolia* has been obtained by a homology-based PCR cloning method.¹³⁵ A truncated version of the enzyme, in which the plastidial targeting peptide of the preprotein has been deleted, has been functionally expressed in *Escherichia coli* and shown to resemble the native enzyme in kinetic properties.¹⁴² Native taxadiene synthase is constituted of 862 amino acids with a molecular weight of 98.3 kD. The recombinant enzyme (after deletion of the plastid-targeting sequence) is constituted of 783 amino acids and has a molecular weight of ~80 kD. Overexpression of the truncated, recombinant synthase has been successfully accomplished in *E. coli*. This significant milestone has made available sufficient amounts of the enzyme, and the enzyme products, to permit a more detailed study of the electrophilic cyclization reaction cascade. Recently, the X-ray crystal structure of a truncated variant of taxadiene synthase was reported by Koksai and coworkers.¹⁴³

6.2.2 Mechanism of Taxadiene Synthase

In collaboration with the Croteau laboratory, the Coates laboratory (University of Illinois) and the Floss laboratory (University of Washington), we have determined the fascinating mechanism of the “one-step” cyclization of ggPP to taxa-4(5),11(12)-diene (**6.5**) as shown in Scheme 6.3.¹³⁷



Scheme 6.3. Mechanism of Taxadiene Synthase¹³⁷

The Coates lab focused on the stereochemistry of the A-ring formation¹⁴⁴ and demonstrated that, as expected, the pyrophosphate-bearing carbon atom undergoes a clean Walden inversion, and that the attack of the C11/C12 p-system on the incipient cation to form the A-ring quaternary center is an antarafacial reaction. Our group has

focused on the stereochemistry and mechanistic implications of the unprecedented migration of the C11 hydrogen atom to C7.¹³⁷ The Floss lab synthesized the requisite deuterated ggPP substrate (shown in Scheme 6.3) and this substrate was converted into taxadiene *via* soluble recombinant synthase from *Taxus cuspidata*. We observed >90% retention of deuterium at C7 in taxadiene (**6.5**). Our laboratory elucidated the stereochemistry of the deuterium migration by 2D NMR and 1D TOCSY and has unambiguously established that the deuterium atom migrates to the α -face of C-7. The observation that the deuterium transfer from C11 to C7 occurs with such a high degree of isotopic retention, coupled with the exclusive transfer to the α -face of C7, suggests that the mechanism for the transfer of the deuterium from C11 to C7 occurs *intramolecularly*. Such an intramolecular proton transfer during an olefin-cation cyclization reaction is highly unusual.¹³⁷

Of further interest, is the facial bias of the final C8/C3 olefin-cation cyclization. Considering the known relative stereochemistry of the taxoid B/C ring juncture, the C3/C4 p-system *must* attack the putative C8 cation (**6.8**) formed immediately following the C11/C7 proton migration, from the *same face* to which the newly installed proton at C7 migrated. Molecular modeling of this process, which formally involves a criss-cross of bond formation across the C7/C8 p-system, proved quite insightful. The molecular model of the C8 cation suggests that, upon pyramidalization at C7 and fashioning of the C11/C12 olefin, the conformation of the 12-membered ring twists, relative to that of the C12 cation, rocking the C3/C4 p-system into the correct facial orientation for capture of the C8 cation establishing the *trans*-fused B/C ring juncture.

Taxadiene synthase is therefore a remarkable terpene cyclase that appears to function by non-covalent binding and ionization of the substrate ggPP and mediates an enantio- and face-selective polyolefin-cation cascade, involving the formation of three carbon-carbon bonds, three stereogenic centers, and the loss of a hydrogen atom in "a single step". The apparently unassisted C-11/C-7 intramolecular proton transfer mechanism of taxadiene synthase is seemingly rare in this regard, and suggests that this enzyme type is capable of mediating complex olefin-cation cyclizations, *with absolute stereochemical fidelity, by conformational control alone*. These provocative experimental results have provided important insight into the molecular architecture of the first dedicated step of taxol biosynthesis that creates the taxane carbon skeleton. We further note that these observations have broad relevance and implications for the general mechanistic capability of the large family of terpenoid cyclization enzymes that catalyze related electrophilic reaction cascades.

6.2.3 Overproduction of Taxadiene

With the production of large scale advanced intermediates enroute to taxol being quite limited, work towards developing routes aimed at overproduction of metabolites have been explored. Developments in metabolic engineering, as well as synthetic biology, have enabled new avenues for the overproduction of complex natural products through the optimization of microbial hosts.^{145,146} Using a partitioned metabolic pathway utilizing the upstream methylerythritol-phosphate (MEP) forming IPP and the

heterologous downstream terpenoid forming pathway, Ajikumar, *et al* reported that they were successfully able to develop a multivariate-modular approach towards metabolic-pathway engineering and were able to increase titers of taxadiene to a $\sim 1\text{g/L}$, essentially a 15,000-fold increase in an *E. coli* strain.¹⁴⁷ Additionally, Boghigian, *et al*, have compared the heterologous production of taxadiene in two lineages of *E. coli*, K and B.¹⁴⁸ Boghigian was able to show that the K-derivative outperformed the B-derivative and probed this finding by applying global transcript profiling to the two strains, thus revealing notable differences in pyruvate metabolism and central metabolism. Further studies demonstrated that temperature had a significant effect on taxadiene production and that indole inhibited the growth of both strains, which was consistent with their earlier observations.¹⁴⁸

Metabolic engineering has also been applied in the realm of overexpressing natural product metabolites to help foster a more amenable route toward taxadiene production.¹⁴⁹ Boghigian identified targets both within and outside of the isoprenoid precursor pathway and then tested them for over-expression in a heterologous *E. coli* host.¹⁴⁹ The use of an algorithm for identifying over-expression targets is unique, since most metabolic engineering efforts have used computational methods to model cellular metabolism.

Collectively, the use of both heterologous hosts and metabolic engineering are paving the way for the over-expression of taxadiene synthase and future endeavors of developing routes toward the overexpression of downstream taxol pathway genes.

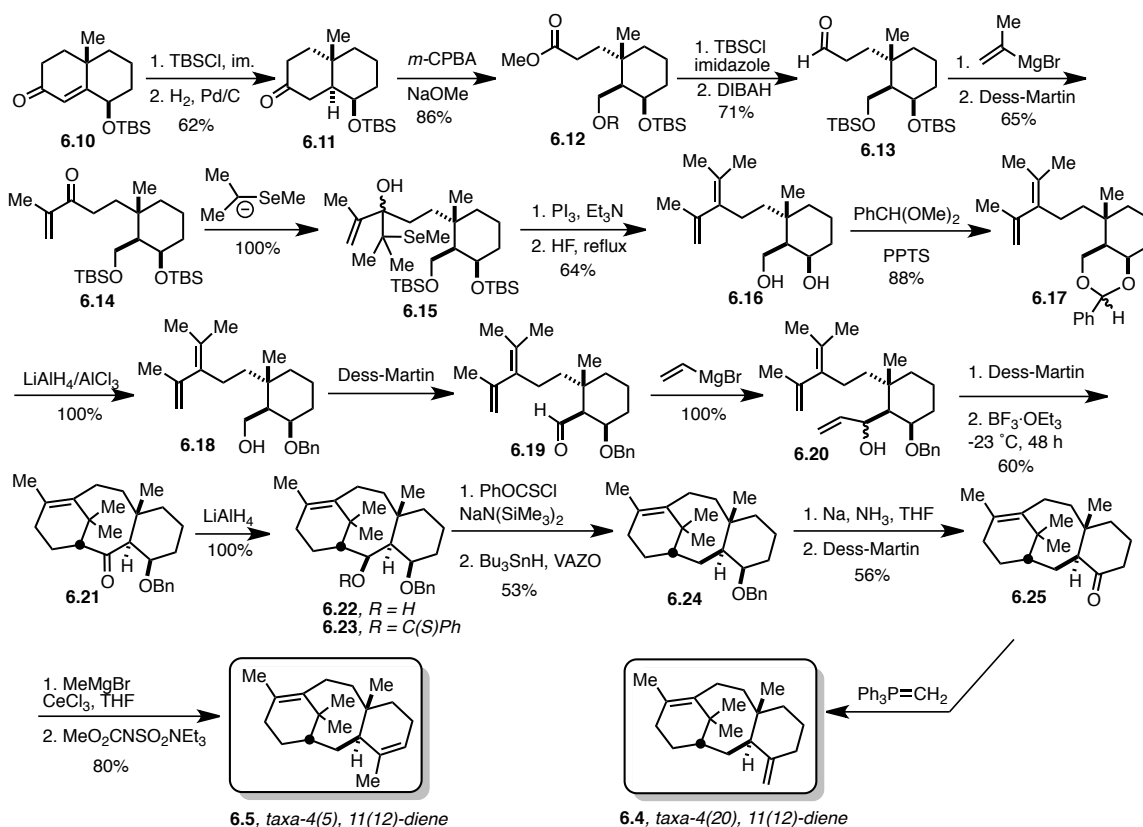
6.3 Efforts Toward Biosynthetic Intermediates to Probe the 5 α -Hydroxylase Pathway

6.3.1 Synthesis of Taxa-4(5),11(12)-diene and Taxa-4(20), 11(12)-diene

The total syntheses of taxa-4(20),11(12)-diene (**6.4**) and taxa-4(5),11(12)-diene (**6.5**) are outlined in Scheme 4. Synthetic access to these substrates (albeit in racemic form) has proven to be critical in penetrating the early stages of taxol biosynthesis. After evaluating several alternatives, we decided to adapt a route originally devised by Shea and Davis,^{150,151} that relied on the use of an intramolecular Diels-Alder (IMDA) cyclization reaction forming the A-B-ring system with an aromatic C-ring. This strategy was also explored by Jenkins and coworkers¹⁵²⁻¹⁵⁴ to access a model A-B/(saturated) C-ring system containing the C-19 methyl group with the correct relative stereochemistry, but devoid of functionality in the C-ring. This IMDA approach for the synthesis of the taxadienes (**6.4** and **6.5**) was easily employed by installing a functional group at C-4 in the C-ring for the ultimate installation of the C-20 carbon atom and the 4(20)- or 4(5)-double bonds. The synthesis illustrated in Scheme 6.4 closely parallels the Jenkins synthesis with the important difference being the early introduction of a hydroxyl group in the C-ring precursor, which ultimately became the functionalized C-4 carbon of the taxadienes.

The key intermediate in this synthesis proved to be ketone **6.25**, which could be elaborated into the “Lythgoe diene” (**6.4**) by a simple Wittig reaction or, alternatively, to

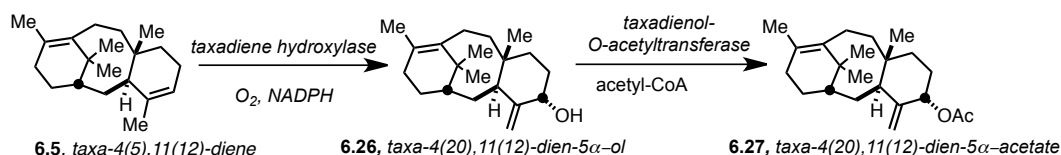
taxa-4(5),11(12)-diene (**6.5**) by a Grignard-dehydration sequence (this procedure also gives **6.4**). The late-stage installation of the C-20 carbon atom by either approach turned out to be very significant, in that we were readily able to introduce tritium, deuterium and/or ^{13}C at C-20 by the appropriate choice of relatively inexpensive, commercially available, isotopically labeled versions of methyl iodide.



Scheme 6.4. Total Synthesis of Taxa-4(5),11(12)-diene (6.5**) and Taxa-4(20),11(12)-diene (**6.4**)**

6.3.2 Synthesis of Taxa-4(20),11(12)-dien-5 α -ol

We have further established that the first hydroxylation product in the taxol pathway is taxa-4(20),11(12)-dien-5 α -ol (**6.26**, Scheme 6.5) through total synthesis and bioconversion of this substance into taxol, 10-deacetylbaccatin III and cephalomannine *in vivo* in *Taxus brevifolia*.¹⁵⁵ Furthermore, a synthetic sample of taxa-4(20),11(12)-dien-5 α -acetate (**6.27**) has been used to establish that, following hydroxylation of **6.5** to **6.26**, the next step in the pathway appears to be acetylation of **6.26** to acetate **6.27**.¹⁵⁶ The Croteau lab has cloned and expressed taxa-4(20),11(12)-dien-5 α -ol-*O*-acetyl transferase from *Taxus canadensis* in *E. coli*.¹⁵⁶

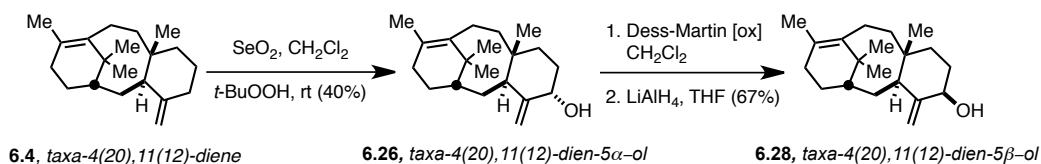


Scheme 6.5. Early Hydroxylation and Acetylation Steps

Due to the very low yield of natural taxadiene obtainable from biological sources (an extract from 750 kg of *Taxus brevifolia* bark powder yielded¹³² ~1 mg of 85% pure **6.5**) and the remaining uncertainty as to the sequence of hydroxylation reactions to taxoids,^{132-135,157-160} synthetic access to these isotopically labeled tricyclic diterpenes has become essential for several reasons: (1) synthesis provides radio-labeled substrates from which pathway metabolites can be made by enzymatic biotransformation and; (2) the synthetic metabolites facilitate the identification, isolation and structure elucidation of new pathway

metabolites that are produced biosynthetically in very tiny amounts. The second point was amply demonstrated by our synthesis of taxa-4(20),11(12)-dien-5 α -ol (**6.26**) which *preceded* the identification and isolation of this substance from *Taxus brevifolia*.¹⁵⁸⁻¹⁶⁰ Indeed, the identification of this substance as a biosynthetic intermediate would have proven far more difficult if the synthetic reference sample were not available. The first point has also been amply demonstrated, since synthetic, tritium-labeled **6.26** and the corresponding acetate **6.27** have served as key substrates from which numerous intermediate hydroxylation products (diol, triol, tetraol and pentaol) have been produced biosynthetically. It should also be noted that taxol has now been identified in several strains of microorganisms,¹¹⁴⁻¹²² and our laboratory has provided samples of stable- and radio-isotopically labeled taxadienes to numerous other laboratories interested in identifying pathway intermediates to taxoids produced in other biological systems.

The synthesis of taxa-4(20),11(12)-dien-5 α -ol (**6.26**) is illustrated in Scheme 6.6 and proceeds *via* selenium dioxide oxidation of the synthetic Lythgoe diene (**6.4**). We observed exclusive formation of the naturally configured 5 α -alcohol (**6.26**) from this reaction whose stereochemistry was confirmed by extensive 2D NMR analysis (¹H, nOe, DQF-COSY, HMQC, HMBC). To interrogate the possible intermediacy of the corresponding β -alcohol diastereomer **6.28**, synthetic **6.26** was oxidized to the corresponding C-5 ketone with Dess-Martin periodinane and stereoselectively reduced with lithium aluminum hydride to deliver **6.28**. This authentic, synthetic sample made it possible to interrogate taxadiene hydroxylase for the possible production of trace amounts of this diastereomer, which was not observed.



Scheme 6.6. Synthesis of Taxadiene 5 α - and 5 β -ols (6.26 and 6.28)

Preparative incubations of synthetic C20-[^3H]-taxadiene (**6.5**) with *Taxus* microsomes were next carried out to accumulate sufficient biosynthetic product (~ 3 nmol) for full spectrum GC-MS analysis. Comparison of GC retention time and mass spectral fragmentation pattern of the TLC-purified biosynthetic product to those of authentic *taxa*-4(20),11(12)-dien-5 α -ol (**6.26**) indicated that the two compounds were identical. Final experimental corroboration was secured through the conversion of the purified, tritium-labeled biosynthetic product (42.8 nCi) to the corresponding 3,5-dinitrobenzoate ester (90% yield), which was diluted with authentic (\pm)-*taxa*-5(20),11(12)-dien-5 α -yl dinitrobenzoate, and recrystallized to constant specific activity and melting point (4.67 ± 0.09 nCi/ μmol , m.p. 171°C , dec.). These analyses, including quantitative evaluation of the radiochemical crystallization studies, revealed that a minimum of 87% of the oxygenation product of *taxa*-4(5),11(12)-diene (**6.5**) is *taxa*-4(20),11(12)-dien-5 α -ol (**6.26**).

We were also able to detect low levels of **6.26** as a natural metabolite in *Taxus* sp. bark extract. Thus, radiochemically-guided fractionation of a *T. brevifolia* bark extract (0.25 μCi of (\pm)-[20- ^3H]*taxa*-4(20),11(12)-dien-5 α -ol diluted into an extract of 250 kg dry bark) utilizing argentation TLC, and reverse-phase chromatography, before and after

alkaline hydrolysis of half of the extract, followed by GC-MS analysis of the partially purified product, demonstrated the alcohol to be present in the 5-10 $\mu\text{g/kg}$ range and ester(s) of **6.26** to be present in the 25-50 $\mu\text{g/kg}$ range.

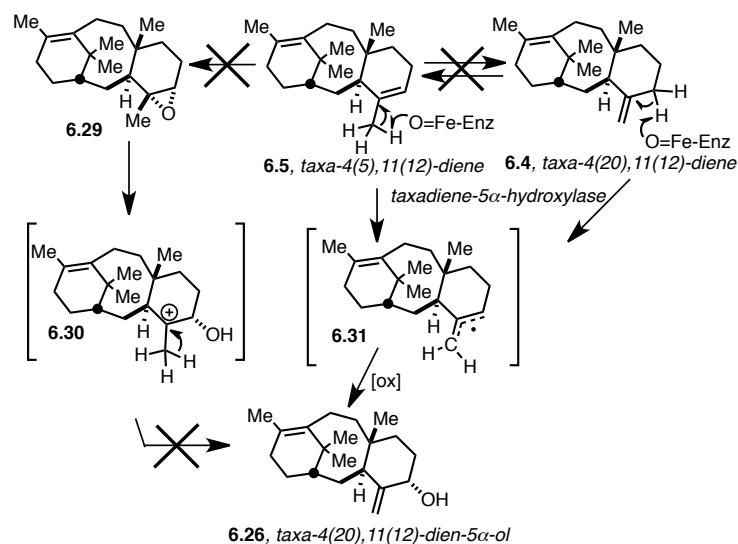
6.3.3 Elucidation of the Mechanism of Taxadiene Hydroxylase

We have examined the interesting mechanistic question regarding the cytochrome P450 mediated conversion of taxa-4(5),11(12)-diene (**6.5**) into taxa-4(20),11(12)-dien-5 α -ol (**6.26**) with a contrathermodynamic allylic transposition.¹⁵⁵ We designed an experiment to discern if the cytochrome P450 hydroxylation of taxa-4(5),11(12)-diene (**6.5**) to taxa-4(20),11(12)-dien-5 α -ol (**6.26**) proceeds through an epoxide intermediate or an allylic radical species. No isomerization of taxa-4(5),11(12)-diene (**6.5**) to the 4(20),11(12)-diene isomer (**6.4**) (or *vice versa*) was observed in *Taxus* sp. microsomes (or *Spodoptera* microsomes enriched in the recombinant 5 α -Hydroxylase)¹⁵⁵ under standard assay conditions but in the absence of NADPH or in the absence of O₂, or in the presence of CO, 100 μM miconazole, or 100 μM clotrimazole (all conditions under which hydroxylation activity is negligible), nor was isomerization observed in boiled controls containing all cofactors and reactants. Similarly, no interconversion of either positional isomer was observed in the presence of Mg⁺², NAD⁺, NADH, NADP⁺, or flavin cofactors, at pH values from 4~10. From these studies, we concluded that taxa-4(5),11(12)-diene (**6.5**) is not appreciably isomerized to taxa-4(20),11(12)-diene (**6.4**) under physiological conditions, and that the migration of the

double bond from the 4(5)- to the 4(20)-position in the process of taxadienol formation is an inherent feature of the cytochrome P450 oxygenase reaction with taxa-4(5),11(12)-diene (**6.5**) as substrate. It is of further interest to note that taxa-4(20),11(12)-diene (**6.4**) is but a minor natural product of *Taxus* sp. formed by taxadiene synthase that is an adventitious, yet efficient, substrate for the 5 α -hydroxylase.

Previous efforts to evaluate the 5 α -hydroxylation reaction by the native enzyme, by search for an epoxide intermediate and through the use of [20-²H₃]taxa-4(5),11(12)-diene to examine a kinetic isotope effect (KIE) on the deprotonation step, failed to distinguish between two reasonable mechanistic possibilities.¹⁵⁸

The two mechanistic manifolds that were considered involve: (1) preliminary conversion of the 4(5)-double bond of taxa-4(5),11(12)-diene (**6.5**) to the corresponding 4(5)-epoxide (**6.29**), followed by ring-opening to carbenium ion species **6.30** and b-proton elimination from the C20 methyl group to yield the allylic alcohol product (**6.26**) or, (2) an alternate route involving cytochrome P450-mediated abstraction of hydrogen radical from the C20 methyl of the substrate (**6.5**) to yield the allylic radical (**6.31**) to which oxygen is added at C5 yielding **6.26** (Scheme 6.7).

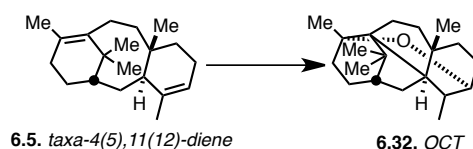


Scheme 6.7. Mechanism of Taxadiene Hydroxylase¹⁵⁵

The utilization of the isomeric taxa-4(20),11(12)-diene (**6.4**) by the hydroxylase, with efficiency comparable to that of the natural substrate, would appear to rule out an intermediate epoxide (**6.29**) in the reaction cycle. *These results instead suggest a mechanism involving abstraction of a hydrogen radical from C20 for 6.5 (or from C5 in the case of the 4(20)-isomer 6.4), leading to the common intermediate, allylic radical 6.31, followed by oxygen insertion selectively from the 5 α -face of this radical intermediate to accomplish the net oxidative rearrangement.* It also appears that the somewhat tighter binding of the 4(20)-isomer substrate (**6.4**) may be a reflection that this isomer more closely mimics the allylic radical intermediate.¹⁵⁵

6.3.4 Over-Production of Taxa-4(20),11(12)-dien-5 α -ol

As with the studies on the overproduction of taxadiene, Ajikumar and coworkers have also engineered a P450-based oxidation to convert taxadiene to taxa-4(20),11(12)-dien-5 α -ol.¹⁴⁷ The engineered strain of *E. coli* improved the production of taxa-4(20),11(12)-dien-5 α -ol some 2400-fold over Dejong's yeast alternative.¹⁶¹ Interestingly, work towards the metabolic engineering of taxa-4(20),11(12)-dien-5 α -ol formation in tobacco demonstrated that a novel taxane was also being produced as a by product (Scheme 6.8, **6.32**).¹⁶²



Scheme 6.8. Production of Novel Taxane, OCT

Rontein and coworkers reported that the rearrangement of taxadiene to OCT is mediated by CYP725A4 and does not rely on additional enzymes or factors.¹⁶² Furthermore, it was also demonstrated by Ajikumar and coworkers that the production of OCT (**6.32**) is likely due to the functional plasticity of the 5 α -hydroxylase with its chimeric CYP450 enzymes.¹⁴⁷

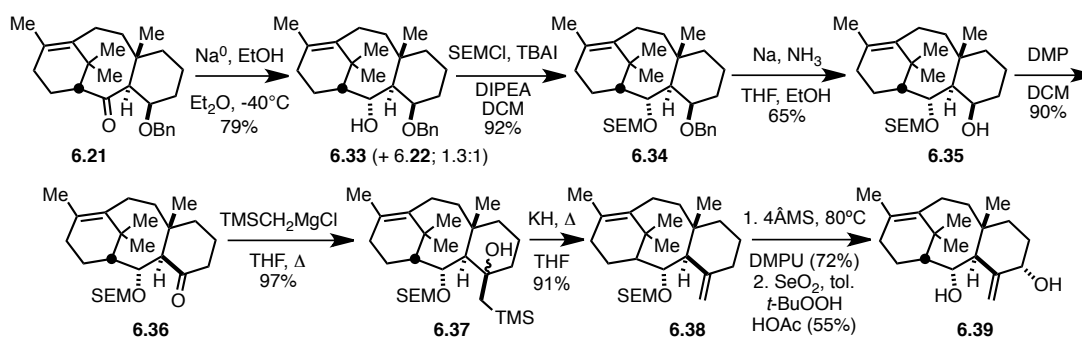
6.4 Syntheses of Lightly Functionalized Taxoids

To approach subsequent biosynthetic steps considered to involve hydroxylation and acylation of the taxane core,¹⁶³ lightly oxygenated taxoids bearing the C5-hydroxyl group were prepared to evaluate them as bioconversion intermediates in *Taxus* cell feeding studies and as substrates for both native and recombinant enzymes from *Taxus*.

6.4.1 Synthesis of Taxa-4(20),11(12)-dien-2 α ,5 α -diol

We have completed a synthesis of the 2 α ,5 α -diol (**6.39**) as shown in Scheme 9 utilizing the Shea-Jenkins type II IMDA construction¹⁶⁴ that was developed and refined in the course of our first total synthesis of taxa-4(5),11(12)-diene (**6.5**).^{138,139,150-154} The key issue came down to devising a means to reduce the ketone moiety of **6.21** to the 2 α -alcohol. During the course of synthetic studies on taxol, Wender⁹⁹ reported the dissolving metal reduction of a substrate structurally related to **6.21** affording a mixture of α - and β -epimeric alcohols. Indeed, reduction of ketone **6.21** (Na⁰/EtOH/Et₂O) resulted in a 1.3:1 separable mixture (flash column silica gel chromatography) of **6.22** and **6.33** respectively in 58% yield, along with unreacted starting material (13%). We found that when the reduction of **6.21** is conducted at -40°C the ratio **6.22**:**6.33** can be reversed to 1:1.3 and the yield increased to 79% (Scheme 6.9). This synthesis provided the first authentic specimen of this material and proved invaluable in identifying this

material as a component of *Taxus* tissue extracts,¹⁶⁴ but its role as a biosynthetic pathway intermediate is presently uncertain and may be verified by radio labeling and incorporation experiments.



Scheme 6.9. Synthesis of Taxa-4(20),11(12)-dien-2 α ,5 α -diol (6.39)

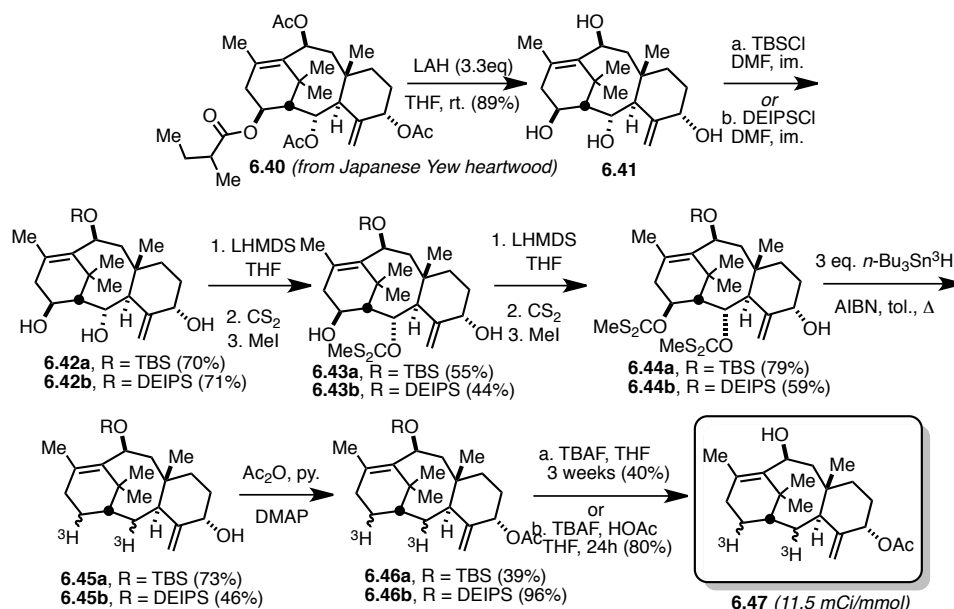
6.4.2 Compounds from a Japanese Yew-derived Taxadien-tetraol

Extensive effort was expended on devising totally synthetic approaches to lightly oxygenated taxoids bearing oxygen atoms at C5 and also at either C9 and/or C10 but without success.¹⁶⁵ We then turned to semi-synthetic approaches using naturally occurring taxoid shunt metabolites that accumulate in *Taxus* sp. heartwood. We acquired over 100 kg of Japanese yew heartwood from a wood sculptor in Japan (Hida Ichii Ittoubori Kyoudou Kumiai of The Engraving Craftsman Association, Japan; see Figure 6.2) and have extracted more than 3.5 grams of 2 α ,5 α ,10 β -triacetoxy-14 β -(2-methyl)-butyryloxytaxa-4(20),11-diene (**6.40**) as a raw material for the preparation of a host of lightly oxygenated taxoids. We have completed the semi-synthesis of taxa-4(20),11(12)-dien-5 α -yl-acetate-10 β -ol (**6.47**)¹⁶⁶ and taxa-4(20),11(12)-dien-5 α -yl-

acetate-2 α ,10 β -diol (**6.49**)¹⁶⁷ as shown in Schemes 10 and 11. Thus, selective manipulation of the hydroxyl groups of this substrate has led to the synthesis taxa-4(20)-11(12)-diene-5 α -yl-acetate-10 β -ol (**6.47**, Scheme 6.10) in tritium-labeled form in preparatively useful amounts. This has provided a key substrate that the Croteau laboratory has utilized for characterization of downstream hydroxylases. In a first pass, we prepared 32 mgs of tritium-labeled **6.46** with a specific activity of 11.5 Ci/mol. The Barton deoxygenation protocol permitted the facile tritium labeling of these materials through the purchase of commercially available Bu₃Sn³H of high specific activity.



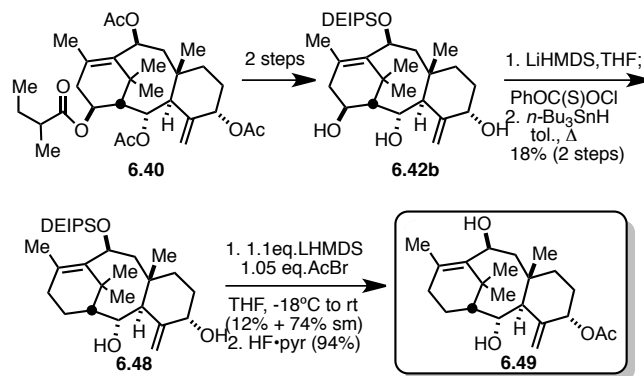
Figure 6.2. Small sculpture made from Japanese Yew by Hida Ichii Ittoubori Kyoudou Kumiai of The Engraving Craftsman Association, Japan.



Scheme 6.10. Synthesis of tritiated taxa-4(20),11(12)-dien-5 α -yl-acetate-10 β -ol (6.47)¹⁶⁶

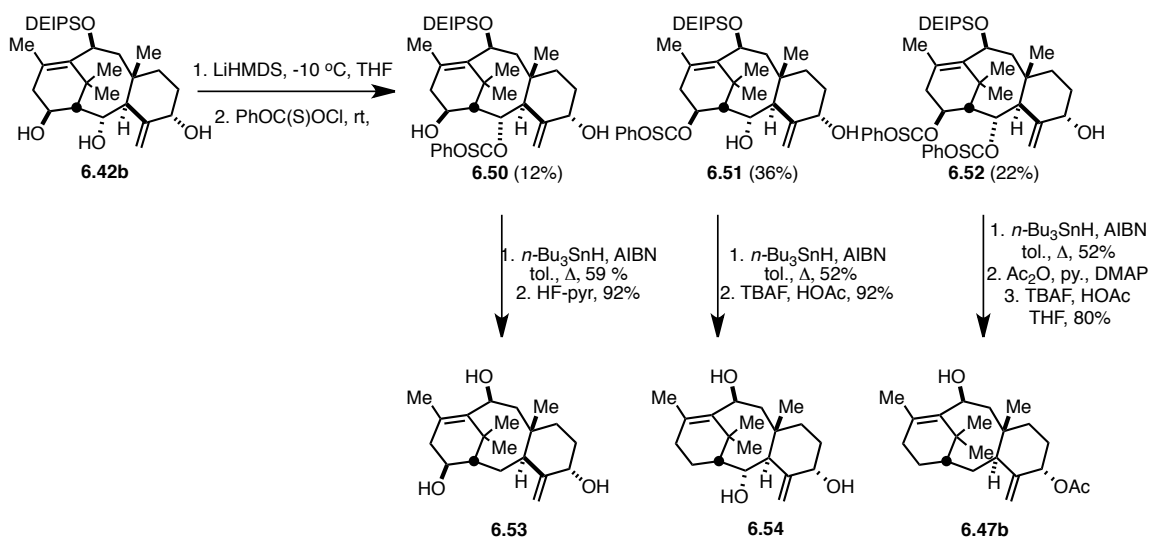
Using the same approach, we prepared taxa-4(20),11(12)-dien-5 α -yl-acetate-2 α ,10 β -diol (6.49).¹⁶⁷ Substrates bearing the 5 α -acetate residue have proven particularly important and, in some cases, difficult to selectively prepare.

For example, diol 6.49, prepared by the radical deoxygenation of 6.42b (Scheme 6.11), was subjected to a variety of acetylation conditions. After extensive work, it was found that treatment of 6.48 with LHMDS at -18 $^{\circ}$ C and careful addition of acetyl bromide, cleanly afforded the C-5 mono-acetate, although only in 12% isolated yield. Fortunately, unreacted 6.48 could be readily recovered in 74% yield. Removal of the silyl residue with HF \cdot pyridine gave taxa-4(20),11(12)-dien-5 α -yl-acetate-2 α ,10 β -diol- (6.49, Scheme 6.11).



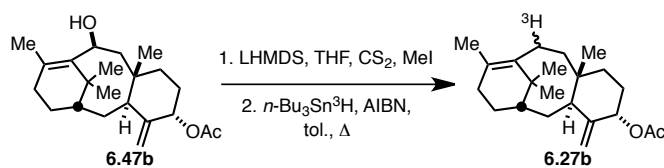
Scheme 6.11. Synthesis of Taxa-4(20),11(12)-dien-5 α -yl-acetate-2 α ,10 β -diol (6.49)¹⁶⁷

Substrate **6.42b** turned out to be a very useful species for the preparation of several triols as well as constituting an alternate source of the 5,10-diol-mono-acetate (**6.47**) as shown in Scheme 6.12. The acylation of **6.42b** with phenylthionochloroformate, was non-regioselective giving a separable mixture of **6.50**, **6.51** and **6.52**. Tin hydride-based deoxygenation of each species provided the first authentic specimens of taxa-4(20),11(12)-dien-5 α , 10 β ,14 β -triol (**6.53**) and taxa-4(20),11(12)-dien-2 α ,5 α ,10 β -triol (**6.54**). Substitution of $\text{Bu}_3\text{Sn}^2\text{H}$ or $\text{Bu}_3\text{Sn}^3\text{H}$ provided the corresponding isotopomers.



Scheme 6.12. Synthesis of the 5,10,14-triol; the 2,5,10-triol and the 5,10-diol

Compound **6.47b** has also constituted an alternative and expedient source for the synthesis of tritiated C5-mono-acetate **6.27b** (Scheme 6.13). This has proven significant since the totally synthetic route initially devised to prepare **6.47** described above, requires extensive time and effort to repeat.¹⁶⁶



Scheme 6.13. Alternative Route to Taxa-4(20),11(12)-diene-5α-acetate

6.4.3 Deoxygenation of Taxusin

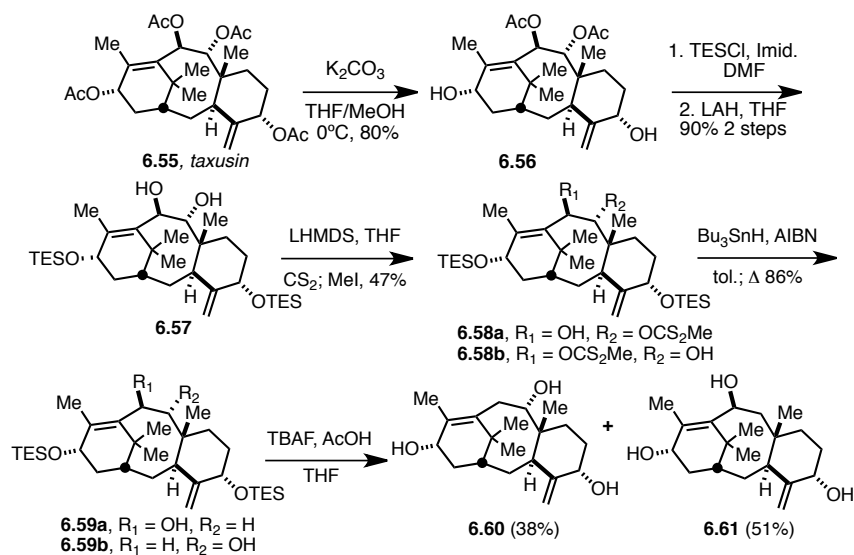
Taxusin is an abundantly available taxoid that makes up a significant weight% of *Taxus* sp. heart wood. We obtained 5 kg of *Taxus brevifolia* heartwood chips from Prof.

Croteau from which we extracted and purified 4.5 grams of taxusin and developed a tetraol protection strategy.

6.4.4 Attempt to Deoxygenate Taxusin at C-13

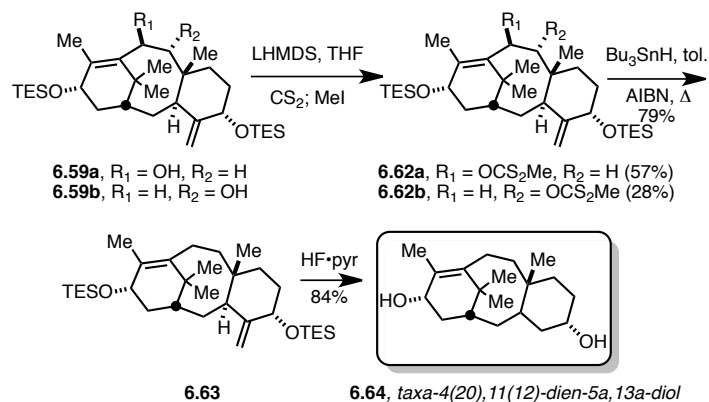
Despite considerable effort, we were unable to effect the deoxygenation of taxusin at C13 without concomitant migration of the 11(12)-bridgehead alkene. This would have provided convenient access to the 5,9-diol, 5,10-diol and 5,9,10-triol that are potential candidates as pathway metabolites. This approach has been abandoned in favor of the successful deoxygenation of a taxadien-tetraol obtained from Japanese yew heartwood described above.

Despite the failure to utilize taxusin to prepare C13-deoxytaxoids, we have developed deoxygenation strategies for the other hydroxyl residues at C9 and C10.¹⁶⁸ Thus, treatment of taxusin with potassium carbonate in methanol, selectively removes the C5 and C13 acetate residues (**6.56**, Scheme 6.14). Protection of the C5 and C13 hydroxyl groups as the triethylsilyl (TES) ethers and LAH removal of the acetates furnished **6.57**. Xanthate formation gave a mixture of **6.58a** and **6.58b** which could be subjected to radical deoxygenation and fluoride-based desilylation to produce taxa-4(20),11(12)-dien-5 α ,9 α ,13 α -triol (**6.60**) and taxa-4(20),11(12)-dien-5 α ,10 β ,13 α -triol (**6.61**).¹⁶⁸



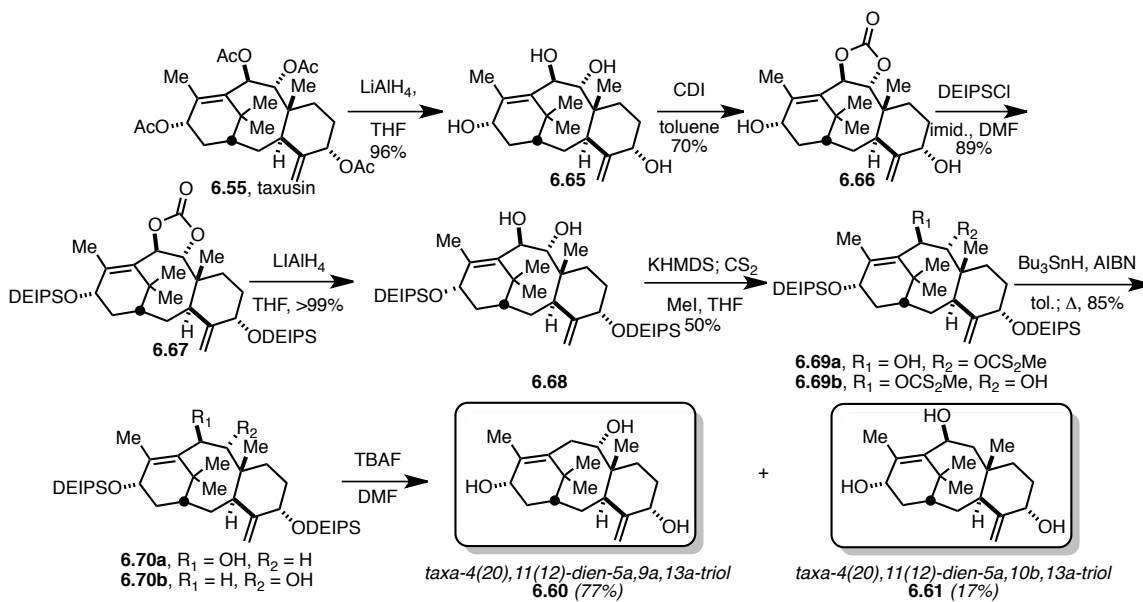
Scheme 6.14. Synthesis of the 5,9,13-triol and the 5,10,13-triol by Deoxygenation of Taxusin

The mixture of **6.59a/b**, also provided an opportunity for the synthesis of the corresponding taxa-4(20),11(12)-diene-5 α ,13 α -diol (**6.64**). As shown in Scheme 6.15, **6.59a/b** was treated with LHMDS, carbon disulfide and methyl iodide to give a mixture of the xanthates **6.62a/b**, which could be separated on column but was used as a mixture in the following step. Barton deoxygenation of **6.62a/b** furnished the protected diol **6.63** in 79% yield. Final treatment of **6.63** with HF•pyridine complex afforded taxa-4(20),11(12)-diene-5 α ,13 α -diol (**6.64**).¹⁶⁸



Scheme 6.15. Synthesis of Taxa-4(20),11(12)-dien-5 α ,13 α -diol

While this route provided the first authentic specimens of **6.60** and **6.64**, it proved to be capricious due to the lability of the *O*-TES ethers. As such, a more robust, second-generation synthesis was devised as shown in Scheme 6.16 where *O*-diethyl-*iso*-propylsilyl ethers (ODEIPS) were employed. In addition, we found that conversion of taxusin into the corresponding tetraol, followed by protection of the 9,10-diol unit as its cyclic carbonate proved advantageous and reproducible.¹⁶⁹

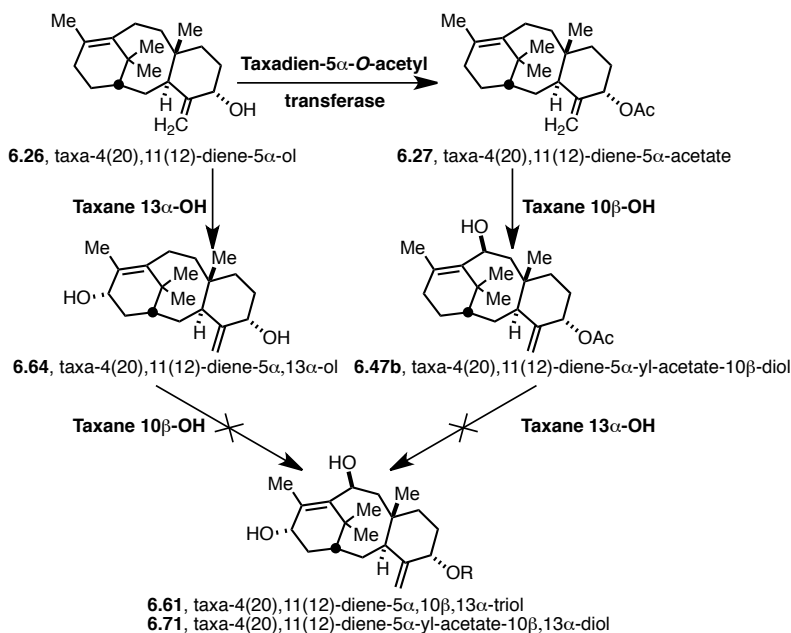


Scheme 6.16. Alternative Syntheses of the 5,9,13-triol and the 5,10,13-triol by Deoxygenation of Taxusin

6.5 Subsequent Biosynthetic Transformations of the 5-Hydroxytaxadiene Core

6.5.1 10 β - and 13 α -hydroxylase

The predicted second and third hydroxylation steps in the pathway are the 13 α - and 10 β -hydroxylations. The responsible microsomal enzymes have been fully characterized, and the respective cytochrome P450 genes have been cloned.^{170,171} The enzymes, originally obtained from *T. cuspidata*,¹⁷⁰ show conversion of taxa-4(20),11(12)-diene-5 α -ol (**6.26**) (as well as its C20 tritium labeled isotope), to the subsequent diols, but 10 β -hydroxylase prefers taxa-4(20),11(12)-diene-5 α -acetate (**6.27**) (as well as its C20 tritium labeled isotope) as substrate and 13 α -hydroxylase prefers taxa-4(20),11(12)-diene-5 α -ol (**6.26**) (Scheme 6.17).



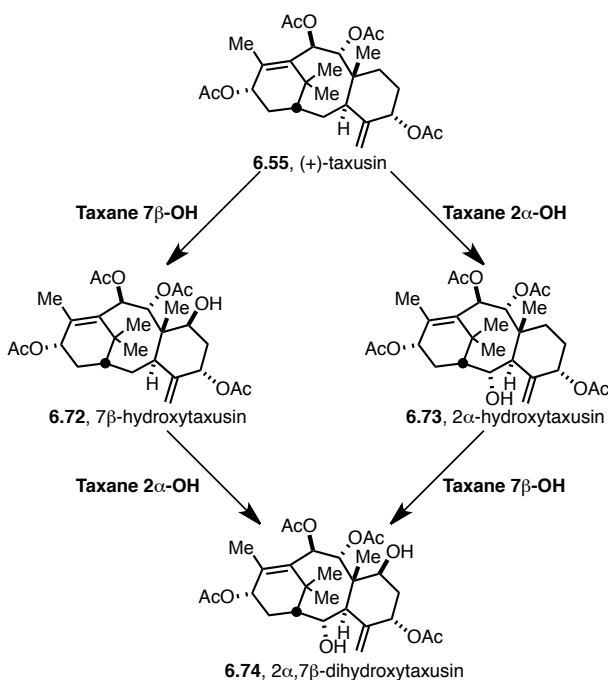
Scheme 6.17. 13 α - and 10 β -hydroxylase

13 α -Hydroxylase was characterized as a member of the CYP725A gene family, whereas the 10 β -hydroxylase was determined to be of the CYP725A1 gene line. Subsequent attempts at hydroxylation of either the 10 β /13 α -diols to deliver the corresponding triol were unsuccessful with either of the 10 β /13 α -hydroxylases.¹⁷⁰

6.5.2 2 α - and 7 β -hydroxylase

Work towards the identification and characterization of the 2 α - and 7 β -hydroxylases utilized what is a presumed dead-end metabolite from yew heartwood, (+)-taxusin (6.55). This metabolite actually proved to be a useful surrogate to examine the oxygenations on route to taxol (6.1). Studies using (+)-taxusin (6.55) showed that it

could be hydroxylated to give either 2 α -hydroxytaxusin (**6.73**) or 7 β -hydroxytaxusin (**6.72**) via their corresponding hydroxylases and that these two intermediates could be further elaborated with the opposing enzyme to give 2 α ,7 β -dihydroxytaxusin (**6.74**) (Scheme 6.18). Unfortunately, no structurally simpler taxoids could be utilized by these hydroxylases suggesting that they function later in the biosynthesis of taxol.^{171,172}



Scheme 6.18. 2 α - and 7 β -hydroxylase Activity

Furthermore, the 2 α - and 7 β -hydroxylases genes have been cloned from *Taxus* species and are very similar to those of the CYP725A gene family. Studies show that both of these enzymes operate sequentially with 7 β -hydroxylation occurring first, and 2 α -hydroxylation occurring second.¹⁷² Through catalytic as well as binding studies¹⁷³, it was found that 7 β -hydroxylase was not able to convert less functionalized taxadienes or

highly substituted taxoids, which further supported the concept that 7 β -hydroxylation is an intermediate step in the biosynthetic pathway.

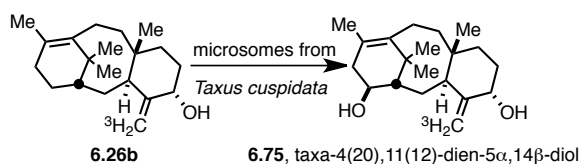
6.5.3 Uncharacterized Hydroxylases

Oxygenation at C-9 is assumed to happen early in the biosynthetic pathway.⁹¹ A cDNA clone for 9 α -hydroxylase was tentatively identified using taxa-4(20),11(12)-diene-5 α -ol (**6.26**) as a substrate by in vivo feeding of yeast that were transformed with P450 sequences, but subsequent identification of the product has not been performed due to a lack of material, and the enzyme has not been characterized¹⁷⁴. Two additional oxidation steps, at C1 and in the side-chain, remain uncharacterized.¹⁷¹

6.5.4 Conversion to the 5,14-diol: A Case of Aberrant Metabolism

Additional work has been done surrounding the biosynthetic conversion to 14-hydroxylated taxoids. We synthesized a large (150 mg) quantity of tritium-labeled taxa-4(20),11(12)-dien-5 α -ol^{139,158-160} (**6.26b**) and have used this as a substrate (~1 mg aliquots, the current maximum scale based on microsomal preps) for biosynthetic conversion to more polar products in *Taxus* microsomes. This substrate actually gives three products with a molecular mass of 304 (diol) and three products with a molecular mass of 320 (triol). We obtained 200 mg of the major diol (a heroic, maxi-prep experiment) and have purified this substance by HPLC. Detailed ¹H NMR analysis

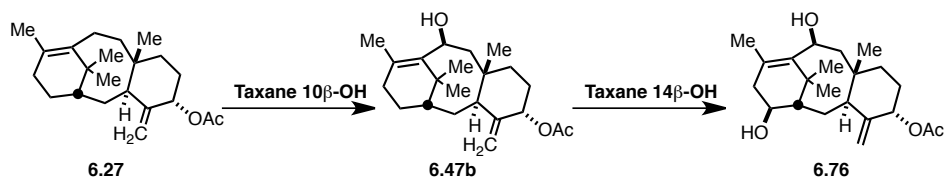
(principally 1D TOCSY) revealed that the structure was that of a 5 α ,14 β -diol (**6.75**, Scheme 6.19).^{156,175}



Scheme 6.19. Biosynthetic Formation of the 5 α ,14 β -diol (6.75**)**

Since it is quite unlikely that such a metabolite is on the pathway to taxol, this substance presumably arose *via* a C-14-specific P450 hydroxylase that converts a more highly oxygenated taxoid into the C-14 β -alcohol and accepted **6.26b** as an adventitious substrate. Due to the low yield and difficulty in separating the other two minor diols, we are focusing on the conversion of taxa-4(20),11(12)-dien-5 α -acetate (**6.27**) into the diol mono-acetates *via* the relevant recombinant P450 hydroxylases.

A clone for the 14 β -hydroxylase was discovered by *in vivo* screening of transformed yeast cells bearing candidate P450's genes,¹⁶³ and the corresponding recombinant enzyme was characterized.^{163,175-177} Further studies determined that the 14 β -hydroxylase is able to convert taxa-4(20),11(12)-diene-5 α -yl-acetate,10 β -diol (**6.47b**) to taxa-4(20),11(12)-diene-5 α -yl-acetate,10 β ,14 β -triol, **6.76** (Scheme 6.20).

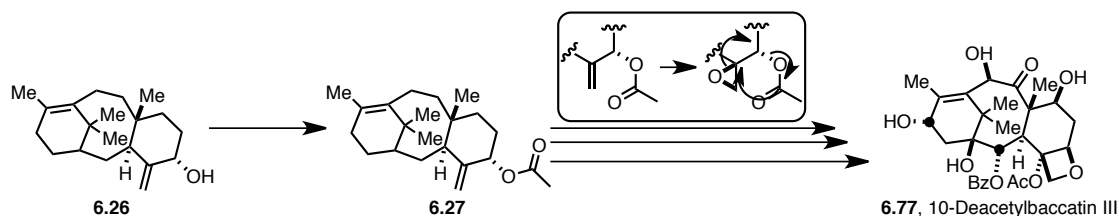


Scheme 6.20. 14 β -hydroxylase Activity

In the case of taxol, hydroxylation at the C-14 position does not occur, but the accumulation of metabolites that are hydroxylated at C-14 is quite significant. The availability of the cDNA encoding for the 14b-hydroxylase suggests a possible strategy to suppress this gene thereby permitting redirection of the pathway flux toward taxol. Further examination of the 14 β -hydroxylase revealed that it contained several of the typical characteristics of cytochrome P450 enzymes, namely, the oxygen binding motif, a heme-binding motif with the PFG element, and a conserved cysteine at position 444. Alternately, the enzyme contained an additional number of residues at the N-terminus.¹⁷⁵

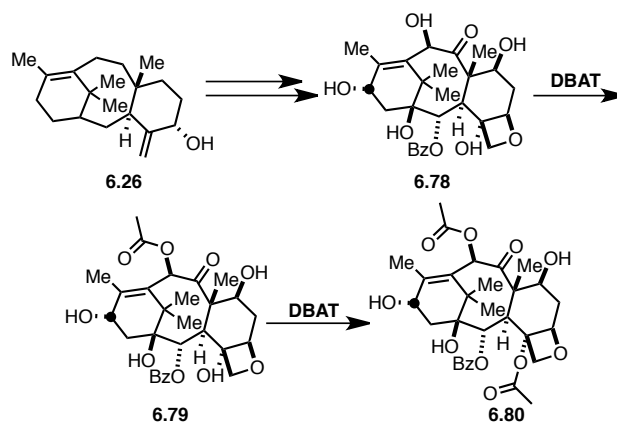
6.6 Studies on the Formation of the Oxetane Ring

The biosynthetic pathway to taxol also includes five acyltransferase-catalyzed steps. Each transacylase delivers an acyl group from acyl CoA to a pathway intermediate.¹⁷⁸⁻¹⁸⁰ Previous theories indicate that the ene-acetoxy functional group of taxa-4(20),11(12)-diene-5 α -yl-acetate (**6.26**) transforms into the 5-acetoxy-4(20)-epoxy moiety with subsequent rearrangement to the oxetane (**6.77**) (Scheme 6.21).¹⁸¹



Scheme 6.21. Original Theory of Oxetane Ring Formation

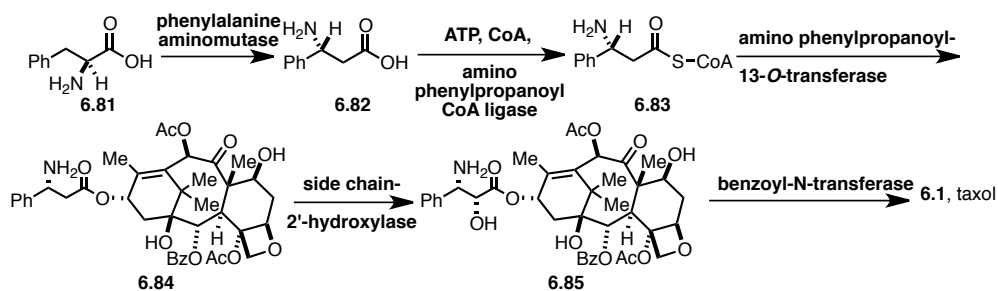
Alternatively, studies by Ondari and Walker now suggest another possibility. Ondari showed that when using advanced taxanes deacetylated at C4, a regioselective acetylation with a recombinantly expressed *Taxus* 10-Deacetylbaccatin 10 β -O-acetyltransferase (**DBAT**) catalyzes transfer to the tertiary C4 position on the oxetane ring, in this case, on 4-DAB (**6.79**).¹⁸² This new evidence adds another possibility to the sequence of events in the biosynthesis of taxol.



Scheme 6.22. Acylation of C4 in Advanced Taxanes

6.7 C13 Acylation: Final Step in the Biosynthesis of Taxol

Extensive work has been done decoding the final steps towards the production of taxol, namely, the acylation at C13. Early *in vivo* studies showed that the intact side chain⁹¹ was not incorporated into taxol, whereas b-phenylalanine and a-phenylalanine and phenylisoserine were incorporated. These findings suggested that b-phenylalanine is attached to baccatin III, and that this side chain is subsequently hydroxylated and then N-benzoylated to complete the biosynthesis of taxol.¹⁸³ Walker and coworkers discovered a cDNA clone encoding a taxoid C13 O-phenylpropanoyltransferase which yielded a recombinant enzyme that selectively catalyzed the selective 13-O-acylation of baccatin III with b-phenylalaninoyl CoA (**6.83**) as the acyl donor, forming N-debenzoyl-2'-deoxytaxol (**6.84**).^{178,179} Interestingly, 2*S*- α -phenylalanine (**6.81**) is converted to 3*R*- β -phenylalanine (**6.82**) by phenylalanine aminomutase (PAM).¹⁸⁴ The stereochemical mechanism of PAM actually involves the removal and interchange of the pro-3*S* hydrogen and the amino group, which subsequently rebonds at C3 with retention of configuration (Scheme 6.23).¹⁸⁴



Scheme 6.23. C13 Side-chain Construction and Implementation

Furthermore, the crystal structure as well as additional mechanistic insight into the phenylalanine aminomutase has been recently reported.¹⁸⁵

6.8 Conclusion

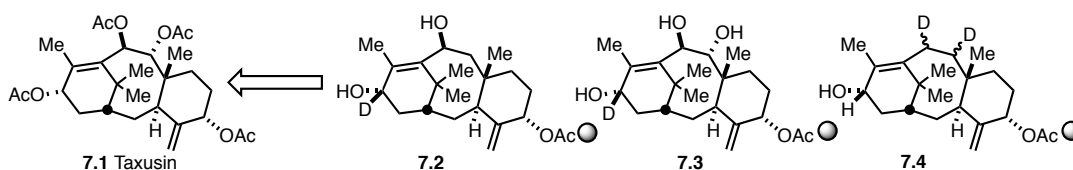
Overall, a combination of total synthesis and semi-synthesis has been used to prepare taxoids as putative substrates for interrogating the substrate specificity of the cytochrome P450 enzymes involved in hydroxylations of the tricyclic hydrocarbon core of taxol. Both stable-isotope and radio-isotope labeling have been employed, with the former being utilized more dominantly at the present time. Furthermore a greater understanding of the biosynthetic pathway is being gained and is helping to piece together the puzzle of the biosynthesis of taxol. Additionally, advances in bioengineering and overexpression of recombinant enzymes are leading the way in pushing the biosynthetic pathway towards a functional synthesis of taxol.

Chapter 7: Progress Toward the Synthesis of Potential Biosynthetic Intermediates of Taxol

7.1 Synthetic Progress

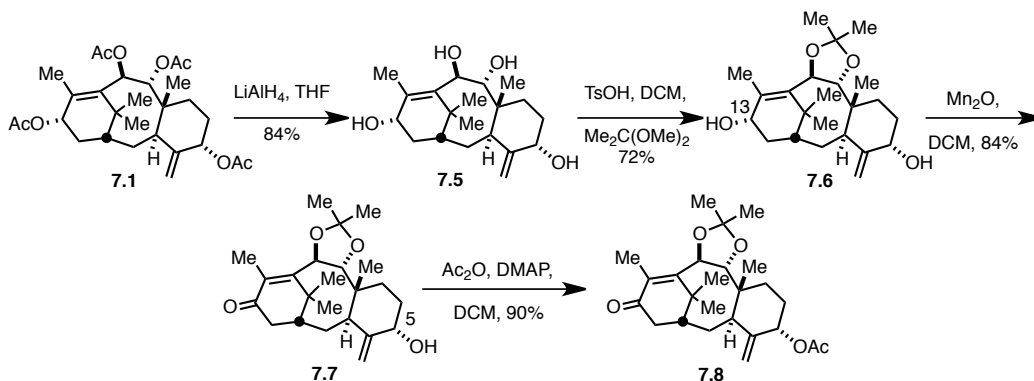
7.1.1 Biosynthetic Intermediates From Taxusin

Our first goal with this project was to develop a strategy for the synthesis of deuterium and C13-labeled **7.2-7.4**, which could be envisioned to start from taxusin (**7.1**, Scheme 7.1). Due to the extreme cost of using C13-labeled acetic anhydride, initial efforts were explored using unlabeled materials.



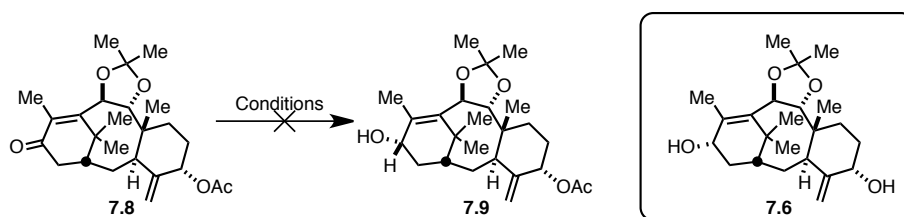
Scheme 7.1. Compounds Derived from Taxusin

Initially we set out to make taxoid **7.3**. Starting from taxusin (**7.1**, isolated from the bark of the Japanese yew in our lab) we first performed a global deprotection to afford tetra-ol **7.5**, in good yield. Protection of the 1,2-diol as the acetonide (**7.6**) and allylic oxidation of the C13 alcohol provided **7.7** and a final protection of the C5 alcohol resulted in **7.8**.



Scheme 7.2. Synthesis of Ketone 7.8

The next step in our sequence was the reduction of the ketone at C13 (**7.8**) to the secondary alcohol. Unfortunately, reduction of this system was problematic, and in the event that a taxoid could be isolated from the reaction mixture, it was always the resulting 5,13-diol (**7.6**) and not the desired mono-ol (**7.9**).

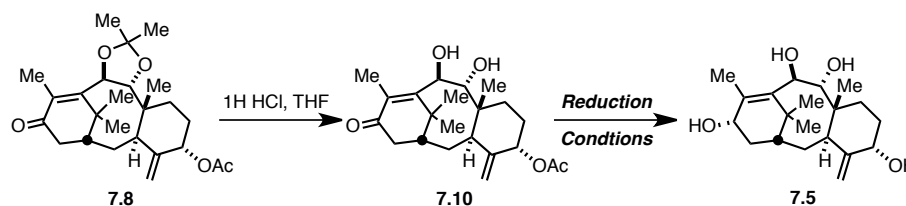


Conditions	Result
NaBH ₄ , MeOH, 0°C	5,13-diol (7.6)
NaBH ₄ , Dioxane, RT, 3 days	Decomposition
NaBH ₄ , Dioxane, 0°C, 3 days	Decomposition
DIBAL-H, Toluene, 0°C	Decomposition
NaBH ₄ , CeCl ₃	5,13-diol (7.6)

Scheme 7.3. Reduction Conditions

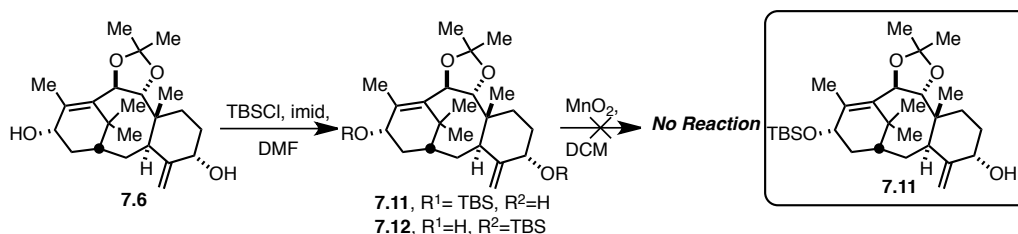
Because of this unforeseen reactivity, we decided to rearrange the steps in this sequence. Starting from **7.8**, we first removed the acetonide to reform the 1,2-diol

(7.10). From here the goal was to again reduce the C13 ketone in the presence of the C5 acetate moiety. As with the previous route, the only product was the bis-reduction product, which resulted in tetra-ol **7.5**.



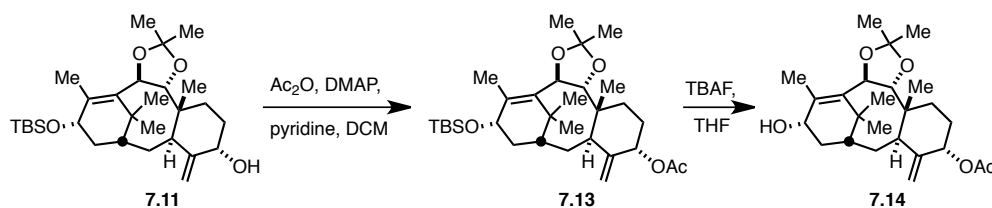
Scheme 7.4. Attempted Reduction of 7.10

Knowing that we were able to selectively oxidize the C13-alcohol in the presence of the C5-OH (Scheme 7.2), we decided to do some experiments to gauge the reactivity of the taxoid system. The goal was to attempt to mono-protect the C13-OH in the presence of the C5-OH. From the 5,13-diol (**7.6**) we reacted the system with TBSCl and imidazole to afford, by NMR, a single silyl-protected product (**7.11** or **7.12**). Due to the complexity of the taxoid NMR's, we then decided to attempt to oxidize the C13 position, and as suspected, no reaction took place, confirming the isolation of the C13-TBS-protected taxoid (**7.11**, Scheme 7.5).



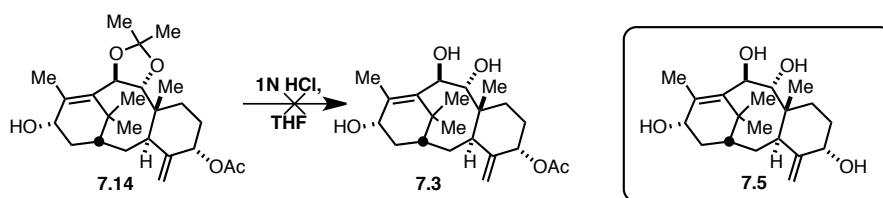
Scheme 7.5. Mono-TBS Protection

Subsequent protection of the C5-hydroxyl as the acetate and removal of the silyl group in the presence of TBAF delivered **7.14**.



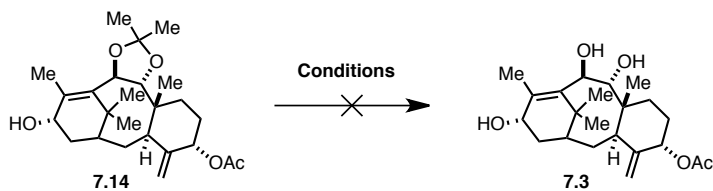
Scheme 7.6. Deprotection of C13 TBS

The last remaining step in this sequence was the removal of the acetonide. Reaction of the acetonide (**7.14**) with conditions previous employed resulted in the formation of the tetra-ol (**7.5**), not the expected tri-ol (**7.3**).



Scheme 7.7. Failed Acetonide Removal

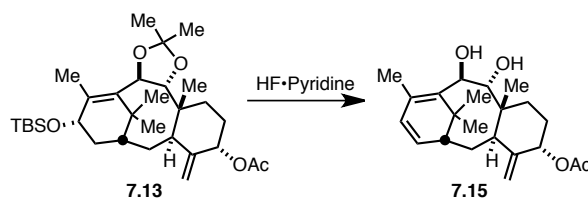
Various conditions for the removal of the acetonide were explored (Scheme 7.8), but the result was either decomposition of starting material, or formation of the tetra-ol (**7.5**).



Conditions		
Dowex	Rt	SM
	Reflux	Decomposition
Strongly Acidic Amberlite	RT or Reflux	Decomposition
Weakly Acidic Amberlite	RT or Reflux	Decomposition
Neopentyl glycol, CSA	RT	Decomposition

Scheme 7.8. Conditions for Removal of Acetonide

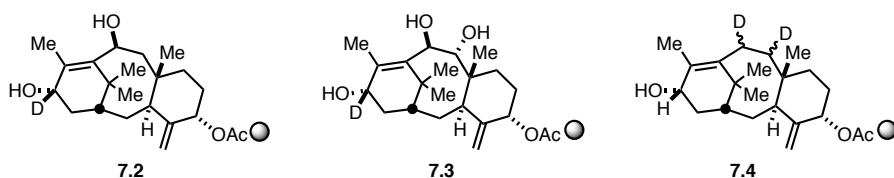
From fully protected taxoid **7.13**, HF•Pyridine was employed, in hopes of providing a method of removing the silyl group, and also clipping the acetonide in a one-pot procedure (Scheme 7.9). Unfortunately, although the silyl group and the acetonide were removed, the resulting product was the elimination product (**7.15**).



Scheme 7.9. HF•Pyridine Removal of Silyl Ether 7.13

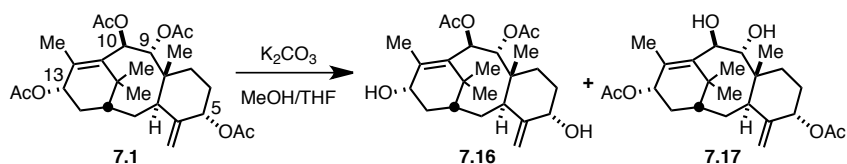
7.1.2 Deoxygenated Taxoids

From here we decided to switch the target molecule from **7.3** to **7.2** and **7.4**, again utilizing a synthetic sequence starting from taxusin (**7.1**, Scheme 7.10).



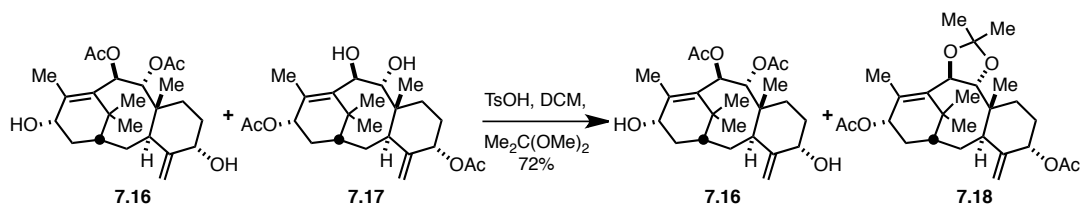
Scheme 7.10. Desired Potential Biosynthetic Intermediates

Starting from taxusin (**7.1**) we first attempted to deprotect the C5 and C13 acetates in the presence of the C9 and C10 acetates, which had been previously reported.¹⁶⁸ Interestingly, the only products ever obtained from this reaction were a mixture of what appears to be the two diol compounds (**7.16**, **7.17**) by NMR (Scheme 7.11).



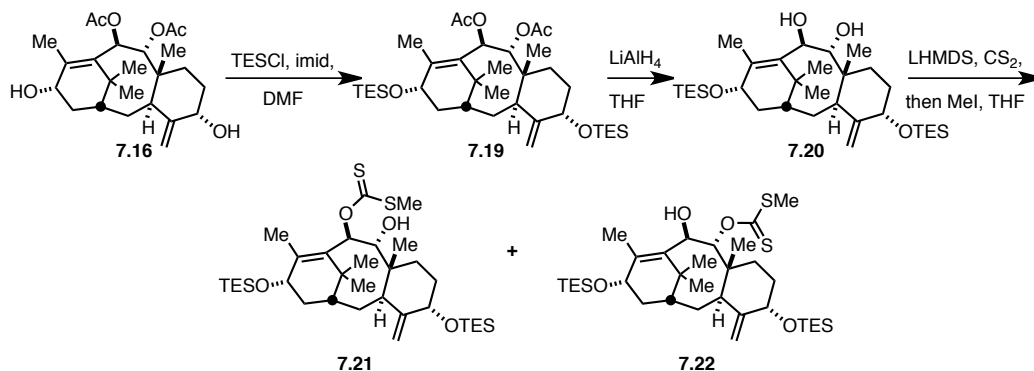
Scheme 7.11. Removal of C5 and C13 Acetates

In order to circumvent this problem, we decided to move the reaction mixture forward and protect the undesired diol (**7.17**) as the acetonide (**7.18**), which resulted in a separable mixture of products (Scheme 7.12).



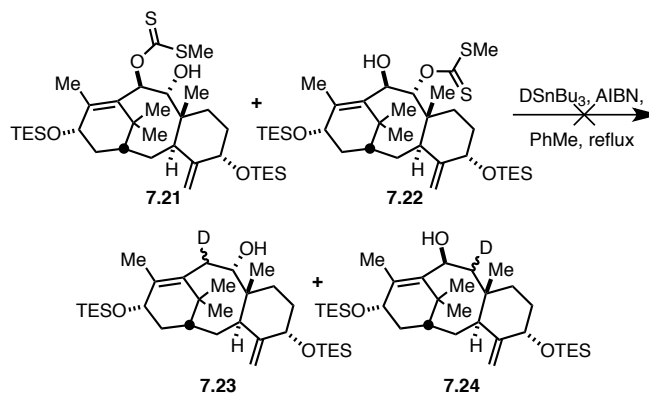
Scheme 7.12. Formation of Separable Taxoids

From **7.16**, the diol was doubly-protected as the triethylsilyl ether (**7.19**) and the acetates were removed in the presence of LiAlH_4 (**7.20**, Scheme 7.14).¹⁶⁸ The diol was subjected to xanthate formation conditions, resulting in what appeared to be a mixture of xanthates **7.21** and **7.22** by crude NMR.



Scheme 7.13. Xanthate Ester Formation

With only ~8mg of the xanthate mixture available, deoxygenation was attempted (Scheme 7.14), but the desired products (**7.23** and **7.24**) were never isolated.



Scheme 7.14. Attempted Deoxygenation

7.2 Conclusion

From the aforementioned sequence of work, we have learned about the unique and unexpected reactivity of the taxane system. The information obtained from this work will be used in the future endeavor towards the synthesis of these C5-acetate analogs.

REFERENCES

1. Johns, D. M., Mori, M.; Williams, R. M., *Org. Lett.* **2006**, *8*, 4051.
2. Webber, P.; Krische, M., *J. Org. Chem.* **2008**, *73*, 9379.
3. Ojima, I., Tzamarioudaki, M.; Eguchi, M., *J. Org. Chem.* **1995**, *60*, 7078.
4. Ying, Y. C., Taori, K., Kim, H., Hong, J. Y.; Luesch, H., *J. Am. Chem. Soc.* **2008**, *130*, 8455.
5. Bowers, A., West, N., Taunton, J., Schreiber, S. L., Bradner, J. E.; Williams, R. M., *J. Am. Chem. Soc.* **2008**, *130*, 11219.
6. Nicolaou, K. C.; Montagnon, T., *Molecules that changed the world: a brief history of the art and science and synthesis and its impact on society*. Wiley-VCH: Weinheim, 2008.
7. Rabe, P., Ackerman, E.; Schneider, W., *Berichte Der Deutschen Chemischen Gesellschaft* **1907**, *40*, 3655.
8. Report, W. M.
9. Oliaro, P., *Pharmacol. Ther.* **2001**, *89*, 207.
10. Mungthin, M., Bray, P. G., Ridley, R. G.; Ward, S. A., *Antimicrob. Agents Chemother.* **1998**, *37*, 1108.
11. Riordan, J. R., Deuchars, K., Kartner, N., Alon, N., Trent, J.; Ling, V., *Nature* **1985**, *316*, 817.
12. Rabe, P.; Kindler, K., *Berichte Der Deutschen Chemischen Gesellschaft* **1918**, *51*, 466.
13. Woodward, R. B.; Doering, W. E., *J. Am. Chem. Soc.* **1945**, *67*, 860.
14. Woodward, R. B.; Doering, W. E., *J. Am. Chem. Soc.* **1944**, *66*, 849.
15. Gutzwiller, J.; Uskokovic, M. R., *J. Am. Chem. Soc.* **1978**, *100*, 576.
16. Grethe, G., Gutzwill, J., Uskokovi, M.; Lee, H. L., *Helv. Chim. Acta* **1972**, *55*, 1044.
17. Gutzwill, J.; Uskokovi, M., *J. Am. Chem. Soc.* **1970**, *92*, 204.
18. Gutzwill, J.; Uskokovi, M., *Helv. Chim. Acta* **1973**, *56*, 1494.
19. Uskokovi, M., Gutzwill, J.; Henderso, T., *J. Am. Chem. Soc.* **1970**, *92*, 203.
20. Uskokovic, M. R., Henderson, T., Reese, C., Lee, H. L., Grethe, G.; Gutzwiller, J., *J. Am. Chem. Soc.* **1978**, *100*, 571.
21. Grethe, G., Lee, H. L., Mitt, T.; Uskokovic, M. R., *J. Am. Chem. Soc.* **1978**, *100*, 589.
22. Grethe, G., Lee, H. L., Mitt, T.; Uskokovic, M. R., *J. Am. Chem. Soc.* **1978**, *100*, 581.
23. Gates, M., Sugavana, B.; Schreibe, W., *J. Am. Chem. Soc.* **1970**, *92*, 205.
24. Taylor, E. C.; Martin, S. F., *J. Am. Chem. Soc.* **1972**, *94*, 6218.
25. Stork, G., Niu, D., Fujimoto, A., Koft, E. R., Balkovec, J. M., Tata, J. R.; Dake, G. R., *J. Am. Chem. Soc.* **2001**, *123*, 3239.
26. Stork, G., Niu, D. Q., Fujimoto, R. A., Koft, E. R., Balkovec, J. M., Tata, J. R.; Dake, G. R., *J. Am. Chem. Soc.* **2001**, *123*, 8644.
27. Raheem, I. T., Goodman, S. N.; Jacobsen, E. N., *J. Am. Chem. Soc.* **2004**, *126*, 706.
28. Igarashi, J., Katsukawa, M., Wang, Y. G., Acharya, H. P.; Kobayashi, Y., *Tetrahedron Lett.* **2004**, *45*, 3783.
29. Tsuda, T., Hayashi, T., Satomi, H., Kawamoto, T.; Saegusa, T., *J. Org. Chem.* **1986**, *51*, 537.
30. Arshad, M., Fernandez, M. A., McGarrigle, E. M.; Aggarwal, V. K., *Tetrahedron-Asymmetry* **2010**, *21*, 1771.
31. Sarkar, S. M., Taira, Y., Nakano, A., Takahashi, K., Ishihara, J.; Hatakeyama, S., *Tetrahedron Lett.* **2011**, *52*, 923.
32. Friestad, G. K., Ji, A., Korapala, C. S.; Qin, J., *Org. Biomol. Chem.* **2011**, *9*, 4039.

33. Friestad, G. K., Ji, A., Baltrusaitis, J., Korapala, C. S.; Qin, J., *J. Org. Chem.* **2012**, ASAP.
34. Smith, A. C., *Unpublished Work*.
35. Sakaitani, M.; Ohfune, Y., *J. Org. Chem.* **1990**, 55, 870.
36. O'neil, I. A., Hitchin, J., Bhamra, I., Chorlton, A. P.; Tapoluay, D. J., *Tetrahedron Lett.* **2008**, 49, 7416.
37. O'neil, I. A., Wynn, D.; Lai, J. Y. Q., *Tetrahedron Lett.* **2000**, 41, 271.
38. Campbell, K. N., Tipson, R. S., Elderfield, R. C., Campbell, B. K., Clapp, M. A., Gensler, W. J., Morrison, D.; Moran, W. J., *J. Org. Chem.* **1946**, 11, 803.
39. Ouchi, H., Mihara, Y.; Takahata, H., *J. Org. Chem.* **2005**, 70, 5207.
40. Schleich, S.; Helmchen, G., *Eur. J. Org. Chem.* **1999**, 2515.
41. Andres, J. M., Pedrosa, R.; Perez-Encabo, A., *Eur. J. Org. Chem.* **2007**, 1803.
42. Mena, M.; Bonjoch, J., *Tetrahedron* **2005**, 61, 8264.
43. Mangion, I. K., Nwamba, I. K., Shevlin, M.; Huffman, M. A., *Org. Lett.* **2009**, 11, 3566.
44. Blizzard, T., Chen, H., Gude, C., Hermes, J., Imbriglio, J.; Kim, S. 2009.
45. Jung, J. C.; Avery, M. A., *Tetrahedron-Asymmetry* **2006**, 17, 2479.
46. Rossen, K., Kolarovic, A., Baskakov, D.; Kiesel, M., *Tetrahedron Lett.* **2004**, 45, 3023.
47. Le Corre, L., Kizirian, J. C., Levraud, C., Boucher, J. L., Bonnet, V.; Dhimane, H., *Org. Biomol. Chem.* **2008**, 6, 3388.
48. Schneider, H., Sigmund, G., Schricker, B., Thirring, K.; Berner, H., *J. Org. Chem.* **1993**, 58, 683.
49. Jana, R.; Tunge, J. A., *Org. Lett.* **2009**, 11, 971.
50. Bissember, A.; Banwell, M., *Org. Prep. Proc. Int.* **2008**, 40, 557.
51. Newkirk, T. L., Bowers, A. A.; Williams, R. M., *Nat. Prod. Rep.* **2009**, 26, 1293.
52. Johnstone, R. W., *Nat Rev Drug Discov* **2002**, 1, 287.
53. De Ruijter, A., Caron, H., Kemp, S., Van Kuilenberg, A.; Van Gennip, A., *Biochem. J.* **2003**, 370, 737.
54. Meinke, P. T.; Liberator, P., *Curr. Med. Chem.* **2001**, 8, 211.
55. Linares, G. E. G., Ravaschino, E. L.; Rodriguez, J. B., *Curr. Med. Chem.* **2006**, 13, 335.
56. Khan, N., Jeffers, M., Kumar, S., Hackett, C., Boldog, F., Khramtsov, N., Qian, X. Z., Mills, E., Berghs, S. C., Carey, N., Finn, P. W., Collins, L. S., Tumber, A., Ritchie, J. W., Jensen, P. B., Lichenstein, H. S.; Sehested, M., *Biochem. J.* **2008**, 409, 581.
57. Lin, H. S., Hu, C. Y., Chan, H. Y., Liew, Y. Y., Huang, H. P., Lepescheux, L., Bastianelli, E., Baron, R., Rawadi, G.; Clement-Lacroix, P., *Br. J. Pharmacol.* **2007**, 150, 862.
58. Dai, Y. S., Xu, J.; Molkentin, J. D., *Mol. Cell. Biol.* **2005**, 25, 9936.
59. Avila, A. M., Burnett, B. G., Taye, A. A., Gabanella, F., Knight, M. A., Hartenstein, P., Cizman, Z., Di Prospero, N. A., Pellizzoni, L., Fischbeck, K. H.; Sumner, C. J., *J. Clin. Invest.* **2007**, 117, 659.
60. Glozak, M. A.; Seto, E., *Oncogene* **2007**, 26, 5420.
61. Xu, W. S., Parmigiani, R. B.; Marks, P. A., *Oncogene* **2007**, 26, 5541.
62. Gray, S. G.; Ekstrom, T. J., *Exp. Cell Res.* **2001**, 262, 75.
63. Furumai, R., Komatsu, Y., Nishino, N., Khochbin, S., Yoshida, M.; Horinouchi, S., *Proc. Natl. Acad. Sci. USA* **2001**, 98, 87.
64. Grozinger, C. M., Hassig, C. A.; Schreiber, S. L., *Proc. Natl. Acad. Sci. U. S. A.* **1999**, 96, 4868.
65. Papeleu, P., TVanhaecke, T., Elaut, G., Vinken, M., Henkens, T., Snykers, S.; Rogiers, V., *Critical Reviews in Toxicology* **2005**, 35, 363.

66. Marks, P. A.; Breslow, R., *Nat. Biotechnol.* **2007**, *25*, 84.
67. Taunton, J., Hassig, C. A.; Schreiber, S. L., *Science* **1996**, *272*, 408.
68. Tsuji, N., Kobayashi, M., Nagashima, K., Wakisaka, Y.; Koizumi, K., *J Antibiot (Tokyo)* **1976**, *29*, 1.
69. Yoshida, M., Horinouchi, S.; Beppu, T., *BioEssays* **1995**, *17*, 423.
70. Miller, T. A., Witter, D. J.; Belvedere, S., *J. Med. Chem.* **2003**, *46*, 5097.
71. Finnin, M. S., Donigian, J. R., Cohen, A., Richon, V. M., Rifkind, R. A., Marks, P. A., Breslow, R.; Pavletich, N. P., *Nature* **1999**, *401*, 188.
72. Crabb, S. J., Howell, M., Rogers, H., Ishfaq, M., Yurek-George, A., Carey, K., Pickering, B. M., East, P., Mitter, R., Maeda, S., Johnson, P. W. M., Townsend, P., Shin-Ya, K., Yoshida, M., Ganesan, A.; Packham, G., *Biochem. Pharmacol.* **2008**, *76*, 463.
73. Pringle, R. B., *Plant Physiol.* **1970**, *46*, 45.
74. Chen, Y. P., Gambs, C., Abe, Y., Wentworth, P.; Janda, K. D., *J. Org. Chem.* **2003**, *68*, 8902.
75. VanderMolen, K. M., McCulloch, W., Pearce, C. J.; Oberlies, N. H., *J Antibiot (Tokyo)* **2011**, *64*, 525.
76. Chang, Y.-Q., Yang, M.; Matter, A., *Applied Environmental Microbiology* **2007**, *73*, 3460.
77. Taori, K., Paul, V. J.; Luesch, H., *J. Am. Chem. Soc.* **2008**, *130*, 1806.
78. Ying, Y. C., Liu, Y. X., Byeon, S. R., Kim, H., Luesch, H.; Hong, J. Y., *Org. Lett.* **2008**, *10*, 4021.
79. Nasveschuk, C. G., Ungermannova, D., Liu, X. D.; Phillips, A. J., *Org. Lett.* **2008**, *10*, 3595.
80. Seiser, T., Kamena, F.; Cramer, N., *Angew. Chem., Int. Ed.* **2008**, *47*, 6483.
81. Ghosh, A. K.; Kulkarni, S., *Org. Lett.* **2008**, *10*, 3907.
82. Ren, Q., Dai, L., Zhang, H., Tan, W. F., Xu, Z. S.; Ye, T., *Synlett* **2008**, 2379.
83. Numajiri, Y., Takahashi, T., Takagi, M., Shin-Ya, K.; Doi, T., *Synlett* **2008**, 2483.
84. Wang, B.; Forsyth, C. J., *Synthesis* **2009**, 2873.
85. Bowers, A. A., West, N., Newkirk, T. L., Troutman-Youngman, A. E., Schreiber, S. L., Wiest, O., Bradner, J. E.; Williams, R. M., *Org. Lett.* **2009**, *11*, 1301.
86. Bowers, A. A., Greshock, T. J., West, N., Estiu, G., Schreiber, S. L., Wiest, O., Williams, R. M.; Bradner, J. E., *J. Am. Chem. Soc.* **2009**, *131*, 2900.
87. Guerra-Bubb, J., Croteau, R.; Williams, R. M., *Nat. Prod. Rep.* **2012**, *29*, 683.
88. Wan, Y. S. S., Chau, J. L. H., Yeung, K. L.; Gavrilidis, A., *J. Catal.* **2004**, *223*, 241.
89. Georg, G., Ali, S., Zygmunt, J.; Jayasinghe, L., *Exp. Op. Ther. Pat.* **1994**, *4*, 109.
90. Boa, A. N., Jenkins, P.R., Lawrence, M.J., *Contemp. Org. Synth.* **1994**, 47.
91. Floss, H. G., Moeck, U., Biosynthesis of Taxol. In *Taxol: Science and Applications*, CRC Press: Boca Raton, 1995.
92. Guenard, D., Guerittevoegelein, F.; Potier, P., *Acc. Chem. Res.* **1993**, *26*, 160.
93. Kingston, D. G. I., *Pharmacol. Ther.* **1991**, *52*, 1.
94. Nicolaou, K. C., Dai, W. M.; Guy, R. K., *Angew. Chem. Int. Ed. Eng* **1994**, *33*, 15.
95. Rohr, J., *Angew. Chem. Int. Ed. Eng* **1997**, *36*, 2190.
96. Swindell, C. S., *Org. Prep. Proced. Int.* **1991**, *23*, 465.
97. Wani, M. C., Taylor, H. L., Wall, M. E., Coggon, P.; McPhail, A. T., *J. Am. Chem. Soc.* **1971**, *93*, 2325.

98. Holton, R. A., Juo, R. R., Kim, H. B., Williams, A. D., Harusawa, S., Lowenthal, R. E.; Yogai, S., *J. Am. Chem. Soc.* **1988**, *110*, 6558.
99. Wender, P. A.; Mucciario, T. P., *J. Am. Chem. Soc.* **1992**, *114*, 5878.
100. Nicolaou, K. C., Yang, Z., Liu, J. J., Ueno, H., Nantermet, P. G., Guy, R. K., Claiborne, C. F., Renaud, J., Couladouros, E. A., Paulvannan, K.; et al., *Nature* **1994**, *367*, 630.
101. Nicolaou, K. C., Nantermet, P. G., Ueno, H., Guy, R. K., Couladouros, E. A.; Sorensen, E. J., *J. Am. Chem. Soc.* **1995**, *117*, 624.
102. Nicolaou, K. C., Liu, J. J., Yang, Z., Ueno, H., Sorensen, E. J., Claiborne, C. F., Guy, R. K., Hwang, C. K., Nakada, M.; Nantermet, P. G., *J. Am. Chem. Soc.* **1995**, *117*, 634.
103. Nicolaou, K. C., Yang, Z., Liu, J. J., Nantermet, P. G., Claiborne, C. F., Renaud, J., Guy, R. K.; Shibayama, K., *J. Am. Chem. Soc.* **1995**, *117*, 645.
104. Nicolaou, K. C., Ueno, H., Liu, J. J., Nantermet, P. G., Yang, Z., Renaud, J., Paulvannan, K.; Chadha, R., *J. Am. Chem. Soc.* **1995**, *117*, 653.
105. Holton, R. A., Somoza, C., Kim, H. B., Liang, F., Biediger, R. J., Boatman, P. D., Shindo, M., Smith, C. C., Kim, S. C., Nadizadeh, H., Suzuki, Y., Tao, C. L., Vu, P., Tang, S. H., Zhang, P. S., Murthi, K. K., Gentile, L. N.; Liu, J. H., *J. Am. Chem. Soc.* **1994**, *116*, 1597.
106. Holton, R. A., Kim, H. B., Somoza, C., Liang, F., Biediger, R. J., Boatman, P. D., Shindo, M., Smith, C. C., Kim, S. C., Nadizadeh, H., Suzuki, Y., Tao, C. L., Vu, P., Tang, S. H., Zhang, P. S., Murthi, K. K., Gentile, L. N.; Liu, J. H., *J. Am. Chem. Soc.* **1994**, *116*, 1599.
107. Masters, J. J., Link, J. T., Snyder, L. B., Young, W. B.; Danishefsky, S. J., *Angew. Chem., Int. Ed.* **1995**, *34*, 1723.
108. Wender, P. A., Badham, N. F., Conway, S. P., Floreancig, P. E., Glass, T. E., Granicher, C., Houze, J. B., Janichen, J., Lee, D. S., Marquess, D. G., McGrane, P. L., Meng, W., Mucciario, T. P., Muhlebach, M., Natchus, M. G., Paulsen, H., Rawlins, D. B., Satkofsky, J., Shuker, A. J., Sutton, J. C., Taylor, R. E.; Tomooka, K., *J. Am. Chem. Soc.* **1997**, *119*, 2755.
109. Wender, P. A., Badham, N. F., Conway, S. P., Floreancig, P. E., Glass, T. E., Houze, J. B., Krauss, N. E., Lee, D. S., Marquess, D. G., McGrane, P. L., Meng, W., Natchus, M. G., Shuker, A. J., Sutton, J. C.; Taylor, R. E., *J. Am. Chem. Soc.* **1997**, *119*, 2757.
110. Morigiwa, K., Hara, R., Kawahara, S., Nishimori, T., Nakamura, N., Kusama, H.; Kuwajima, I., *J. Am. Chem. Soc.* **1998**, *120*, 12980.
111. Paquette, L. A., Wang, H. L., Su, Z.; Zhao, M. Z., *J. Am. Chem. Soc.* **1998**, *120*, 5213.
112. Mukaiyama, T., Shiina, I., Iwadare, H., Saitoh, M., Nishimura, T., Ohkawa, N., Sakoh, H., Nishimura, K., Tani, Y., Hasegawa, M., Yamada, K.; Saitoh, K., *Chem.-Eur. J.* **1999**, *5*, 121.
113. Han, K. H., Fleming, P., Walker, K., Loper, M., Chilton, W. S., Mocek, U., Gordon, M. P.; Floss, H. G., *Plant Science* **1994**, *95*, 187.
114. Stierle, A., Strobel, G.; Stierle, D., *Science* **1993**, *260*, 214.
115. Strobel, G., Yang, X. S., Sears, J., Kramer, R., Sidhu, R. S.; Hess, W. M., *Microbiology-Uk* **1996**, *142*, 435.
116. Strobel, G. A., Hess, W.M., Ford, E., Sidhu, R., Yang, X., *J. Ind. Microbiol.* **1996**, *17*, 417.
117. Strobel, G. A., Hess, W. M., Li, J. Y., Ford, E., Sears, J., Sidhu, R. S.; Summerell, B., *Australian Journal of Botany* **1997**, *45*, 1073.
118. Hoffman, A. K., W.; Waroapng, J.; Strobel, G.; Griffin, D., Arbogast, B.; Barofsky, D.; Boone, R.B.; Ning, L.; Zheng, P.; Daley, L., *Spectroscopy* **1999**, *13*, 22.

119. Stierle, A., Stierle, D., Strobel, G., Bignami, G., Grothaus, P., Bioactive Metabolites of the Endophytic Fungi of Pacific Yew, *Taxus brevifolia*. In *Taxane Anticancer Agents*, American Chemical Society: 1995; pp 82.
120. Shrestha, K., Strobel, G. A., Shrivastava, S. P.; Gewali, M. B., *Planta Med.* **2001**, 67, 374.
121. Li, J. Y., Sidhu, R.S., Ford, E.J., Long, D.M., Strobel, G.A., *J. Ind. Microbiol. Biotech.* **1998**, 20, 259.
122. Metz, A. M., Haddad, A., Worapong, J., Long, D. M., Ford, E. J., Hess, W. M.; Strobel, G. A., *Microbiology* **2000**, 146, 2079.
123. Fleming, P. E., Knaggs, A. R., He, X. G., Mocek, U.; Floss, H. G., *J. Am. Chem. Soc.* **1994**, 116, 4137.
124. Fleming, P. E., Mocek, U.; Floss, H. G., *J. Am. Chem. Soc.* **1993**, 115, 805.
125. Harrison, J. W. S., R.M.; Lythgoe, B., *J. Chem. Soc. (C)*. **1966**, 1933.
126. Gueritte-Voegelein, F., Guenard, D.; Potier, P., *J. Nat. Prod.* **1987**, 50, 9.
127. Herbert, B. A., *The Biosynthesis of Secondary Metabolites*. Chapman and Hall: London, 1981.
128. Nakanishi, K., Goto, T., Ito, S., Nozoe, S., *Natural Products Chemistry*. Kodansha, Ltd: Tokyo, 1974; Vol. 1.
129. Towers, G. H., Biochemistry of the Mevalonic Acid Pathway to Terpenoids. In *Recent Advances in Phytochemistry*, Stafford, H. A., Ed. Plenum Press: New York, 1990; Vol. 24.
130. Luckner, M., *Secondary Metabolism in Microorganisms, Plants and Animals*. Springer-Verlag: Berlin, 1990.
131. Eisenrich, W. M., B.; Hylands, P.J.; Zenk, M.H.; Bacher, A, *Proc. Natl. Acad. Sci. U. S. A.* **1996**, 93, 6431.
132. Koeppe, A. E., Hezari, M., Zajicek, J., Vogel, B. S., LaFever, R. E., Lewis, N. G.; Croteau, R., *J. Biol. Chem.* **1995**, 270, 8686.
133. Hezari, M., Lewis, N. G.; Croteau, R., *Arch. Biochem. Biophys.* **1995**, 322, 437.
134. Lin, X., Hezari, M., Koeppe, A. E., Floss, H. G.; Croteau, R., *Biochemistry* **1996**, 35, 2968.
135. Wildung, M. R.; Croteau, R., *J. Biol. Chem.* **1996**, 271, 9201.
136. Hezari, M.; Croteau, R., *Planta Med.* **1997**, 63, 291.
137. Williams, D. C., Carroll, B. J., Jin, Q., Rithner, C. D., Lenger, S. R., Floss, H. G., Coates, R. M., Williams, R. M.; Croteau, R., *Chem. Biol.* **2000**, 7, 969.
138. Rubenstein, S. M.; Williams, R. M., *J. Org. Chem.* **1995**, 60, 7215.
139. Rubenstein, S. M., *Dissertation: Elucidating the Biosynthetic Pathway to Taxol*, Colorado State University **1996**.
140. Walker, K. C., R., *Rec. Adv. Phytochem.* **1999**, 33, 31.
141. Hezari, M., Ketchum, R. E. B., Gibson, D. M.; Croteau, R., *Arch. Biochem. Biophys.* **1997**, 337, 185.
142. Williams, D. C., Wildung, M. R., Jin, A. Q. W., Dalal, D., Oliver, J. S., Coates, R. M.; Croteau, R., *Arch. Biochem. Biophys.* **2000**, 379, 137.
143. Koksai, M., Jin, Y., Coates, R.M., Croteau, R., Christianson, D.W., *Nature* **2011**, 469, 116.
144. Jin, Q., Williams, D. C., Hezari, M., Croteau, R.; Coates, R. M., *J. Org. Chem.* **2005**, 70, 4667.
145. Tyo, K. E., Alper, H. S.; Stephanopoulos, G. N., *Trends Biotechnol.* **2007**, 25, 132.
146. Ajikumar, P. K., Tyo, K., Carlsen, S., Mucha, O., Phon, T. H.; Stephanopoulos, G., *Mol. Pharm.* **2008**, 5, 167.

147. Ajikumar, P. K., Xiao, W. H., Tyo, K. E. J., Wang, Y., Simeon, F., Leonard, E., Mucha, O., Phon, T. H., Pfeifer, B.; Stephanopoulos, G., *Science* **2010**, 330, 70.
148. Boghigian, B. A., Salas, D., Ajikumar, P. K., Stephanopoulos, G.; Pfeifer, B. A., *Appl. Microbiol. Biotechnol.* **2012**, 93, 1651.
149. Boghigian, B. A., Armando, J., Salas, D.; Pfeifer, B. A., *Appl. Microbiol. Biotechnol.*
150. Shea, K. J., Davis, P.D., *Angew. Chem. Int. Ed. Eng* **1983**, 22, 419.
151. Shea, K. J., Davis, P.D., *Angew. Chem. Int. Ed. Eng* **1983**, 22, 546.
152. Bonnert, R. V., Jenkins, P.R., *J. Chem. Soc. Perkin Trans. 1* **1989**, 413.
153. Brown, P. A., Jenkins, P.R., *J. Chem. Soc. Perkin Trans. 1* **1986**, 1303.
154. Brown, P. A., Jenkins, P.R., Fawcett, J., Russell, D.R., *J. Chem. Soc. Perkin Trans. 1* **1984**, 253.
155. Jennewein, S., Long, R. M., Williams, R. M.; Croteau, R., *Chem. Biol.* **2004**, 11, 379.
156. Wheeler, A. L., Long, R.M., Ketchum, R.E., Rithner, C.D., Williams, R.M., Croteau, R., *Arch. Biochem. Biophys.* **2001**, 390, 265.
157. Hezari, M.; Croteau, R., *Planta Med.* **1997**, 63, 291.
158. Hefner, J., Rubenstein, S. M., Ketchum, R. E., Gibson, D. M., Williams, R. M.; Croteau, R., *Chem. Biol.* **1996**, 3, 479.
159. Borman, S., *Chem. Eng. News* **1996**, 74, 27.
160. Rubenstein, S. M., Vazquez, A., Sanz-Cervera, J. F.; Williams, R. M., *J. Labelled Compd. Radiopharm.* **2000**, 43, 481.
161. DeJong, J. M., Liu, Y. L., Bollon, A. P., Long, R. M., Jennewein, S., Williams, D.; Croteau, R. B., *Biotechnol. Bioeng.* **2006**, 93, 212.
162. Rontein, D., Onillon, S., Herbette, G., Lesot, A., Werck-Reichhart, D., Sallaud, C.; Tissier, A., *J. Biol. Chem.* **2008**, 283, 6067.
163. Croteau, R., Ketchum, R. E., Long, R. M., Kaspera, R.; Wildung, M. R., *Phytochem. Rev.* **2006**, 5, 75.
164. Vazquez, A.; Williams, R. M., *J. Org. Chem.* **2000**, 65, 7865.
165. Lenger, S. R., *Dissertation: Studies on the Total Synthesis of Putative Intermediates in the Biosynthesis of Taxol* **2003**.
166. Horiguchi, T., Rithner, C. D., Croteau, R.; Williams, R. M., *J. Labelled Compd. Radiopharm.* **2008**, 51, 325.
167. Horiguchi, T. R., C.D.; Croteau, R.; Williams, R.M., *J. Org. Chem.* **2002**, 67, 4901.
168. Li, H., Horiguchi, T., Croteau, R.; Williams, R. M., *Tetrahedron* **2008**, 64, 6561.
169. Horiguchi, T. R., C.D.; Croteau, R.; Williams, R.M., *Tetrahedron* **2003**, 59, 267.
170. Jennewein, S., Rithner, C. D., Williams, R. M.; Croteau, R. B., *Proc. Natl. Acad. Sci. U. S. A.* **2001**, 98, 13595.
171. Kaspera, R.; Croteau, R., *Phytochem. Rev.* **2006**, 5, 433.
172. Chau, M.; Croteau, R., *Arch. Biochem. Biophys.* **2004**, 427, 48.
173. Chau, M., Jennewein, S., Walker, K.; Croteau, R., *Chem. Biol.* **2004**, 11, 663.
174. Walker, K., Fujisaki, S., Long, R.; Croteau, R., *Proc. Natl. Acad. Sci. U. S. A.* **2002**, 99, 12715.
175. Jennewein, S., Rithner, C. D., Williams, R. M.; Croteau, R., *Arch. Biochem. Biophys.* **2003**, 413, 262.
176. Ketchum, R. E., Rithner, C. D., Qiu, D., Kim, Y. S., Williams, R. M.; Croteau, R. B., *Phytochemistry* **2003**, 62, 901.
177. Ketchum, R. E. G., D.M.; Croteau, R.; Shuler, M.L, *Biotechnol. Bioeng.* **1999**, 62, 97.

178. Walker, K., Long, R.; Croteau, R., *Proc. Natl. Acad. Sci. U. S. A.* **2002**, 99, 9166.
179. Walker, K., Fujisaki, S., Long, R.; Croteau, R., *Proc. Natl. Acad. Sci. U. S. A.* **2002**, 99, 12715.
180. Walker, K.; Croteau, R., *Phytochemistry* **2001**, 58, 1.
181. Gueritte-Voegelein, F., Guenard, D.; Potier, P., *J. Nat. Prod.* **1987**, 50, 9.
182. Ondari, M. E.; Walker, K. D., *J. Am. Chem. Soc.* **2008**, 130, 17187.
183. Long, R. M.; Croteau, R., *Biochem. Biophys. Res. Commun.* **2005**, 338, 410.
184. Walker, K. D., Klettke, K., Akiyama, T.; Croteau, R., *J. Biol. Chem.* **2004**, 279, 53947.
185. Feng, L., Wanninayake, U., Strom, S., Geiger, J.; Walker, K. D., *Biochemistry* **2011**, 50, 2919.
186. Laib, T., Chastanet, J.; Zhu, J. P., *J. Org. Chem.* **1998**, 63, 1709.
187. Fiaux, H., Kuntz, D. A., Hoffman, D., Janzer, R. C., Gerber-Lemaire, S., Rose, D. R.; Juillerat-Jeanneret, L., *Bioorg. Med. Chem.* **2008**, 16, 7337.
188. Bartoli, G., Bosco, M., Carlone, A., Dalpozzo, R., Marcantoni, E., Melchiorre, P.; Sambri, L., *Synthesis* **2007**, 3489.
189. Cuny, G. D.; Buchwald, S. L., *J. Am. Chem. Soc.* **1993**, 115, 2066.

Chapter 8: Experimental Section

Table of Procedures and Spectra

Quinine Experimentals	142
Largazole Analog Exerimentals	280
Thiazoline-Oxazole Macrocycle (5.2)	296
Thiazoline-Oxazole Dimer (5.15)	299
Thiazoline-Oxazole Thiol (5.16)	301
Thiazoline-Oxazole Thioester (5.1)	303
Oxazoline-Thiazole Acycle (5.19)	313
Taxoid Experimentals	315

8.1 General Considerations

Unless otherwise noted, all reactions were run under an argon atmosphere in flame or oven dried glassware. Reaction products were purified via column chromatography using silica gel 60 (230 X 400 mesh) was purchased from Sorbent Technologies. Dichloromethane, tetrahydrofuran, triethylamine, acetonitrile, DMF, toluene, diethyl ether, were passed through a solvent purification system (J.C. Meyer of Glass Contour) using argon pressure and in some cases additionally distilled (see individual preps). Reagents were purchased from either Aldrich or VWR and generally used as received, without additional purification, unless otherwise noted in the experimental preparations. ^1H NMR and ^{13}C NMR spectra were recorded on Varian 300, 400 MHz NMR spectrometers with chemical shifts reported in ppm relative to CHCl_3 or the solvent being used (see individual spectra data). Mass spectra were obtained on Fisions VG Autospec. Optical rotations were collected at 589 nm on a Rudolph Research Automatic Polarimeter Autopol III. IR spectra were obtained on a Bruker Tensor 27 IR spectrometer on NaCl plates.

8.2 Experimental Data

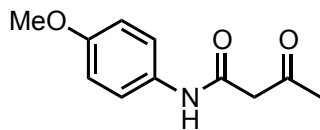


Figure 8.1. *N*-(4-methoxyphenyl)-3-oxobutanamide (**3.16**)³⁸

Ethylacetoacetate (205mL, 1624.036mmol) was heated to 160°C and *p*-anisidine (**3.12**) (50g, 406.009mmol) was then added over 45 minutes in portions. The reaction was then allowed to stir at 160°C for 30 minutes. The reaction was then cooled to room temperature and placed in the freezer overnight to facilitate precipitation. The following morning the reaction was then warmed to room temperature and filtered and then washed with *n*-pentane. The solid was then placed in the oven at 60°C until the solid was dry (42%)

[JMG-1-129]

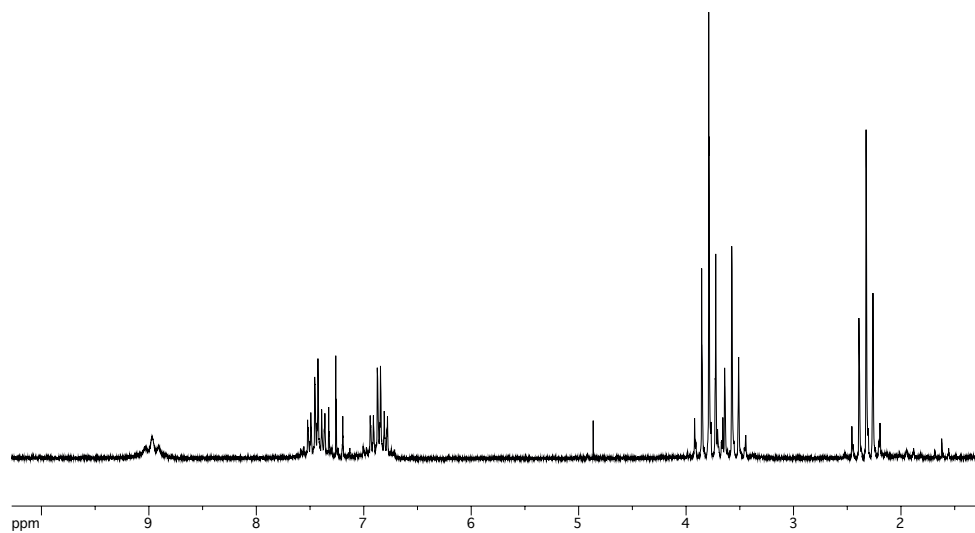


Figure 8.2. ^1H NMR of *N*-(4-methoxyphenyl)-3-oxobutanamide (3.16)

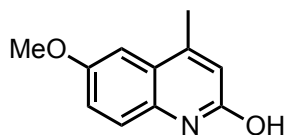


Figure 8.3. 6-methoxy-4-methylquinolin-2-ol (3.17)³⁸

To **3.16** (15g, 72.383mmol) was added concentrated sulfuric acid (8mL). The reaction as heated until the internal temperature was 100°C, slowly, over 2 hours. The reaction was the cooled to ~95°C and was kept heating for 2 additional hours. The reaction was then cooled to room temperature and filtered. The solids were then washed with water and the solid was placed in the over at 60°C for several days to dry (**3.17**, quant).

[JMG-1-142]

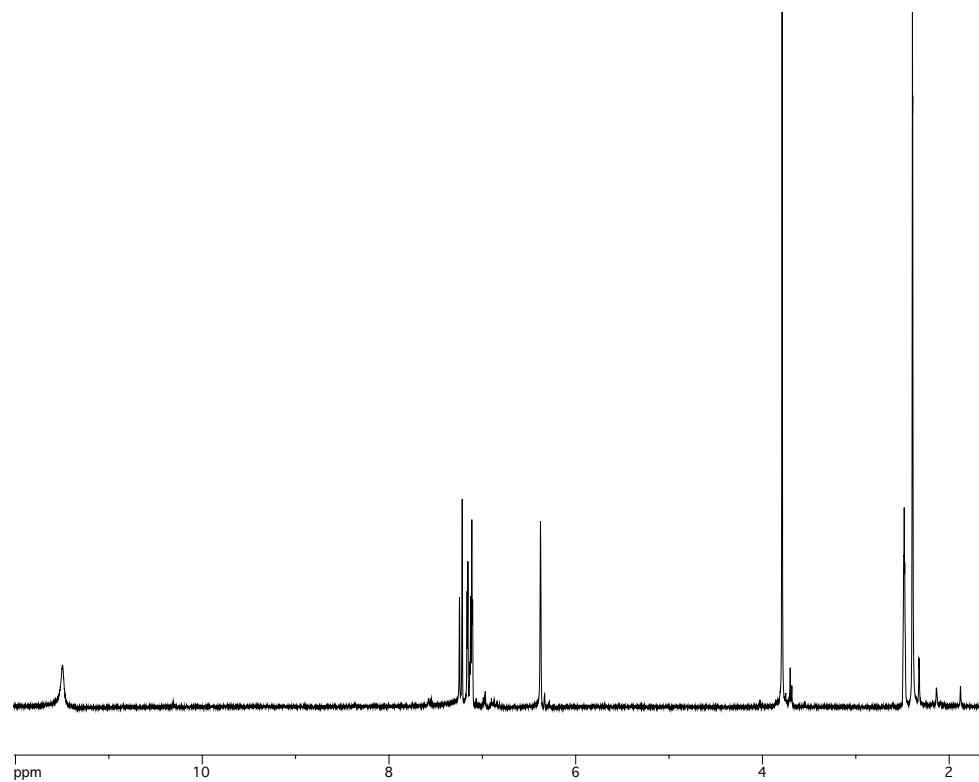


Figure 8.4. ^1H NMR of 6-methoxy-4-methylquinolin-2-ol (3.17)

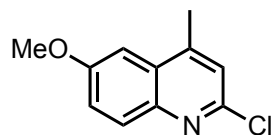


Figure 8.5. 2-chloro-6-methoxy-4-methylquinoline (3.18a)³⁸

3.17 (8.87g, 46.879mmol) was placed into a round bottom flask and fitted with a reflux condenser and a drying tube. POCl₃ (35mL, 375.033mmol) was then added and the reaction was heated to 90°C over 30 minutes. The bath temp was raised to 108°C over 20 minutes and then the reaction was kept at 108°C for an additional 10 minutes. The bath was then raised to 120°C over 30 minutes and the reaction was then allowed to cool to room temperature. The reaction was then concentrated taken up in water and the excess POCl₃ was quenched by slow addition of bicarbonate. The solid was filtered and the reaction was allowed to dry at room temperature overnight and then was placed in the oven for additional drying at 60°C for several days (**3.18a**, 73%).

[JMG-1-144]

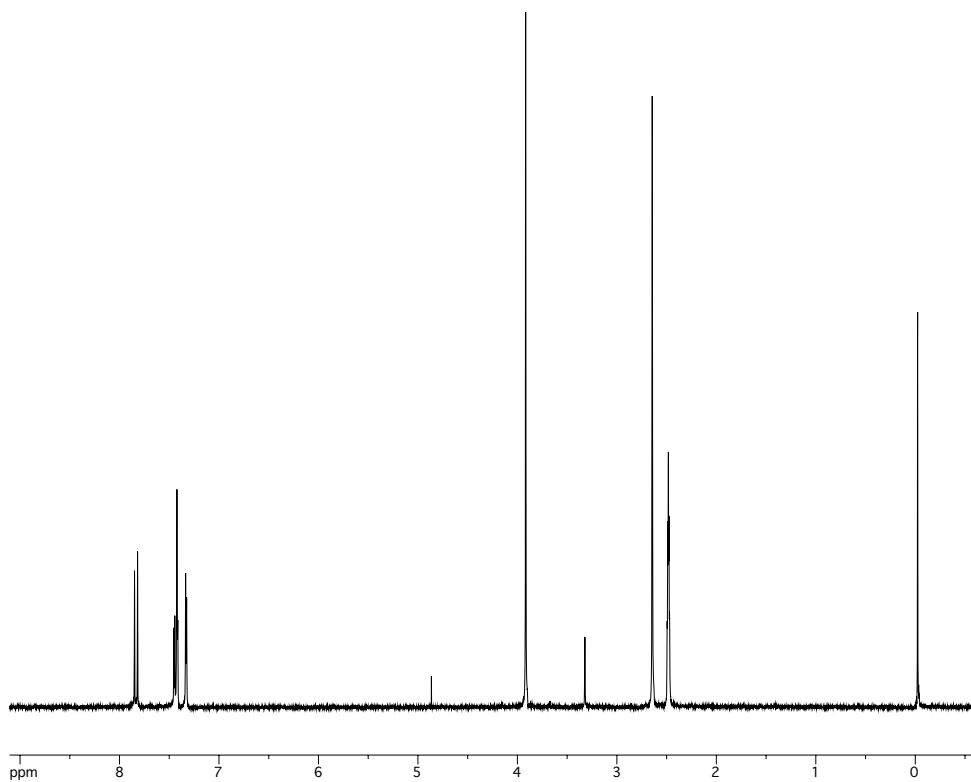


Figure 8.6. ^1H NMR of 2-chloro-6-methoxy-4-methylquinoline (3.18a)³⁸

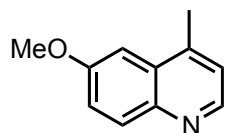


Figure 8.7. 6-methoxy-4-methylquinoline (3.18)³⁸

3.18a (17.72g, 85.330mmol) was dissolved in AcOH (120mL) and H₂O (15mL) and then heated to reflux (70°C) and Zn granules (8.4g, 127.998mmol) was added in one portion. The reaction was allowed to reflux for an additional 6 hours. The hot solution as then filtered and the remaining solids were washed with water. The filtrate was then concentrated down and washed with 1M NaOH (2 X 200mL) to get rid of the remaining AcOH and extracted in CHCl₃. The organic layer was dried over Na₂SO₄ and concentrated down. (**3.18**, 89%)

[JMG-1-158]

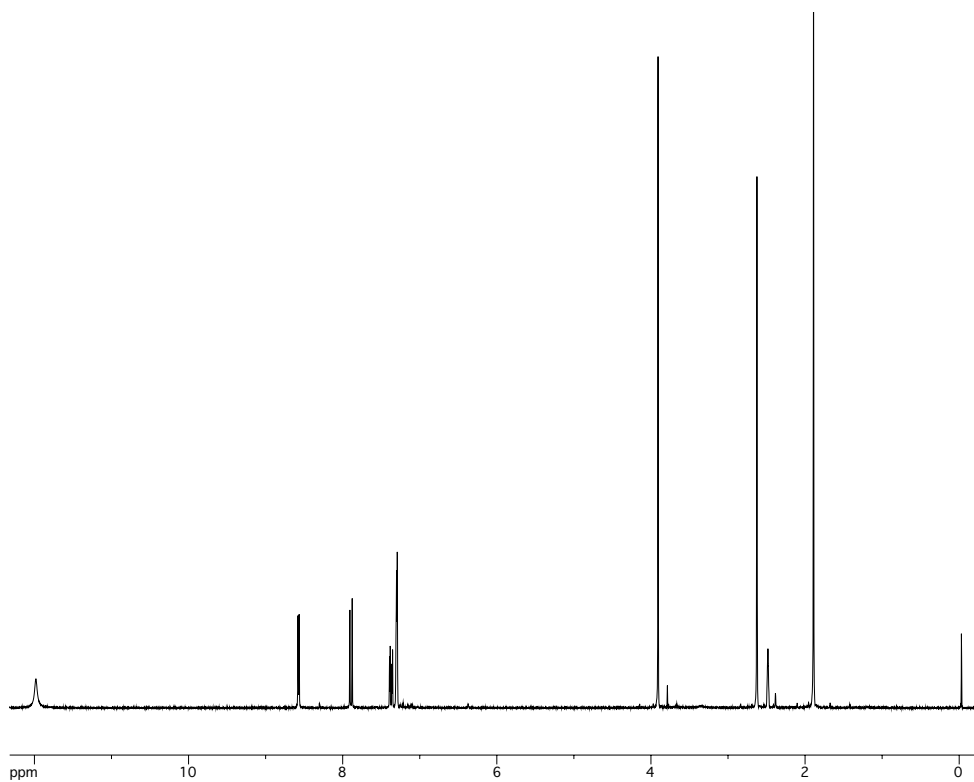


Figure 8.8. ^1H NMR of 6-methoxy-4-methylquinoline (3.18)³⁸

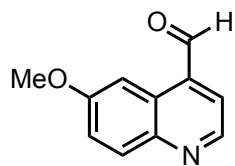


Figure 8.9. 6-methoxyquinoline-4-carbaldehyde (3.10)³⁸

3.18 (5.31g, 30.656mmol) was dissolved in dioxane (20mL) and heated to 80°C. SeO₂ (5.1g, 45.985mmol) was then added to dioxane (20mL) and H₂O (10mL) and placed in an addition funnel. The SeO₂ solution was added dropwise to the starting material at 80°C, over 30 minutes. The reaction was heated to 90°C and left stirring overnight. The following morning the reaction was filtered. The solids were dissolved in hot MeOH and then filtered. The filtrate was concentrated down. (**3.10**, quant)

[JMG-1-149-1]

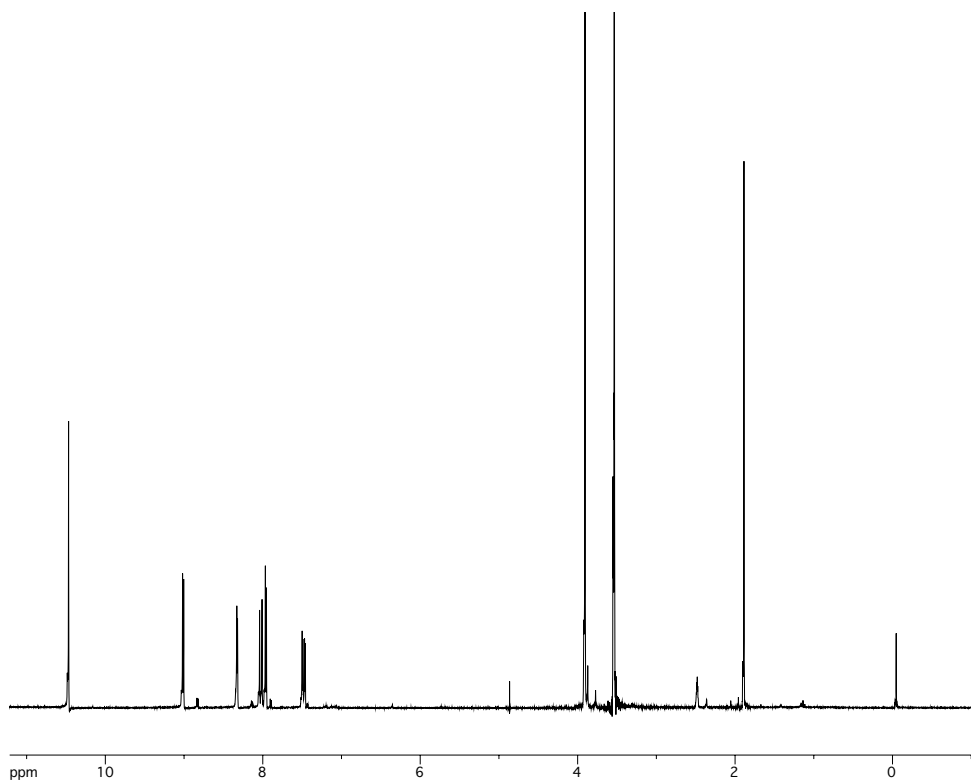


Figure 8.10. ^1H NMR of 6-methoxyquinoline-4-carbaldehyde (3.10)³⁸

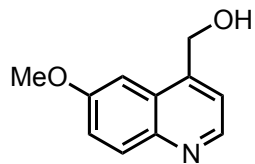


Figure 8.11. (6-methoxyquinolin-4-yl)methanol (**3.19**)³⁸

3.10 (2g, 10.692mmol) was dissolved in DCM (107mL) and cooled to 0°C. DIBAL-H (1M soln' 25mL, 21.384mmol) was then added over 1 hour. The reaction as then allowed to stir at 0°C for an additional hour and was then warmed to room temperature and quenched with Rochelle's salt and allowed to stir over night. The following morning the solution was extracted with DCM and dried over Na₂SO₄ and concentrated. (**3.19**, quant).

[JMG-1-169]

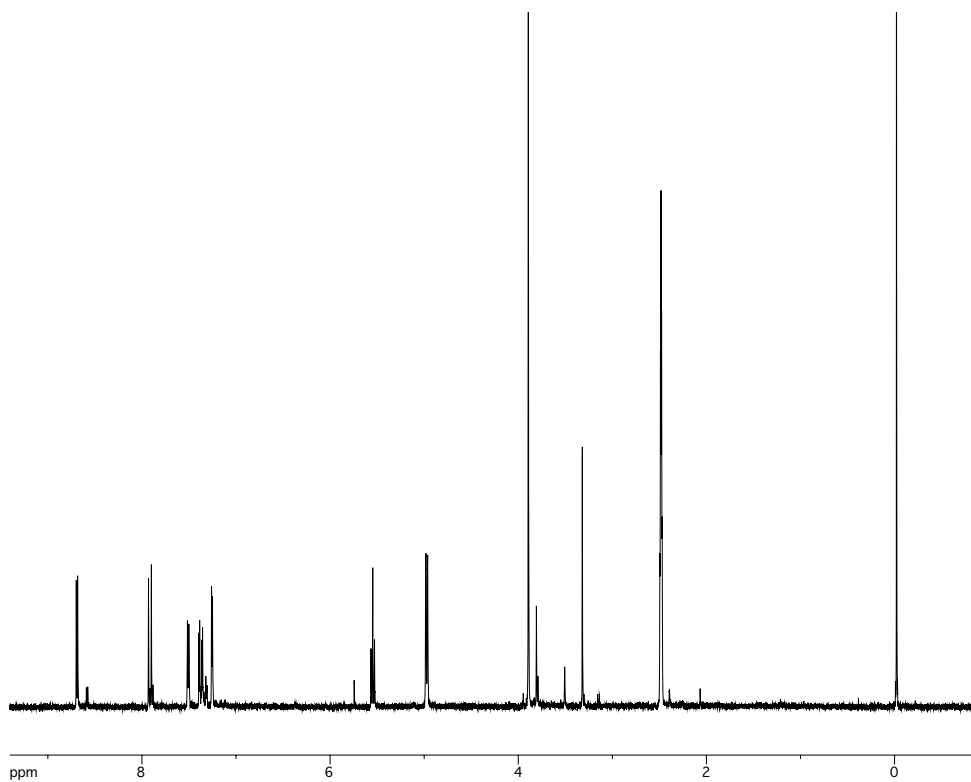


Figure 8.12. ^1H NMR of (6-methoxyquinolin-4-yl)methanol (3.19)³⁸

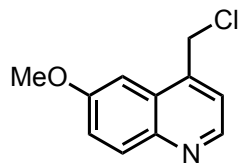


Figure 8.13. 4-(chloromethyl)-6-methoxyquinoline (**3.11**)³⁸

3.19 (8.05g, 42.545mmol) was dissolved in DCM (220mL) and cooled to 0°C. SOCl₂ (31mL, 425.543mmol) was then added via addition funnel and the reaction was heated to reflux for 1 hour and then cooled to room temperature and concentrated and put on under high vacuum over night. (**3.11**, 43%)

[JMG-1-171]

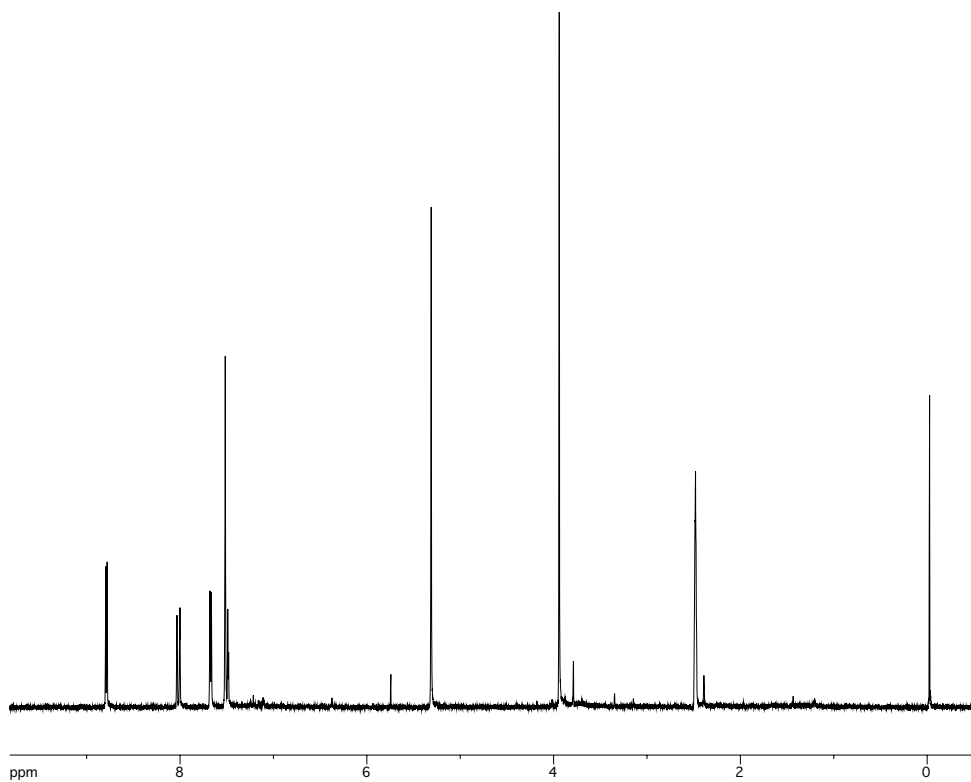


Figure 8.14. ^1H NMR of 4-(chloromethyl)-6-methoxyquinoline (3.11)³⁸

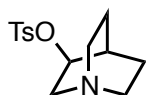


Figure 8.15. Quinuclidin-3-yl-4-methylbenzenesulfonate (3.31)^{36,37}

3.30 (3g, 23.585mmol) was added to DCM (120mL) followed by TsCl (6.5g, 34.085mmol) and DMAP (cat.), Et₃N (6.6mL, 47.170mmol) and the reaction was stirred at room temperature for 4 hours. The reaction was then extracted with brine and dried over Na₂SO₄ and purified via column chromatography. (**3.31**, 76%)

[JMG-1-205-2]

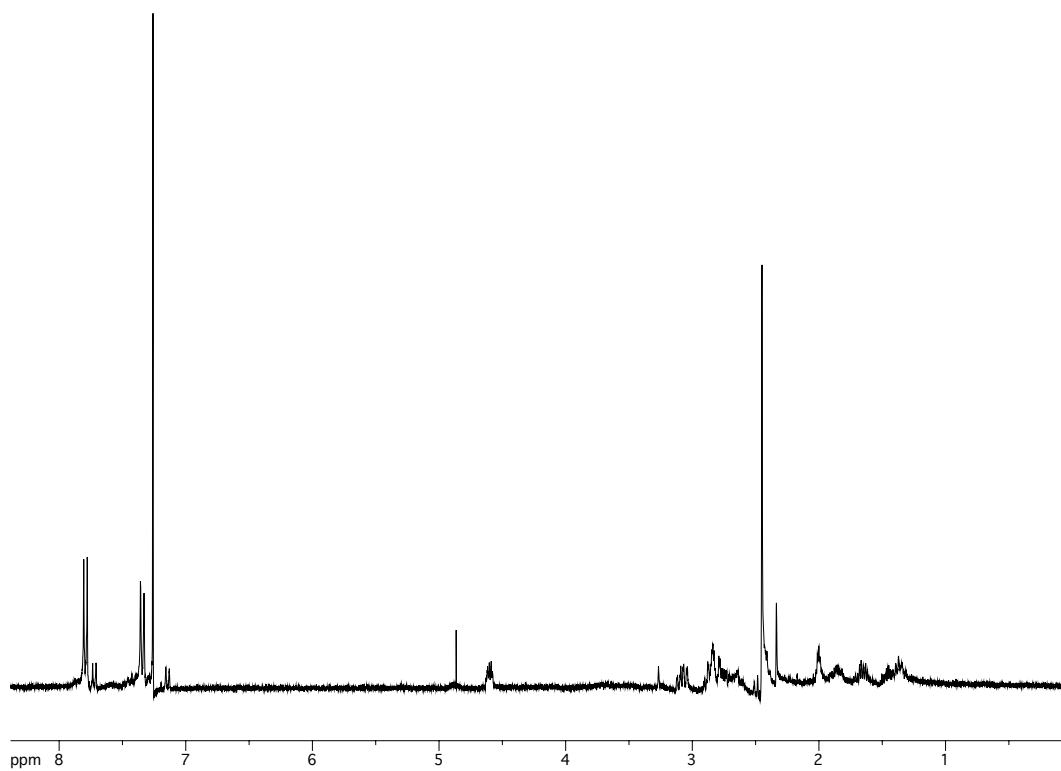


Figure 8.16. ^1H NMR of Quinuclidin-3-yl-4-methylbenzenesulfonate (3.31)^{36,37}

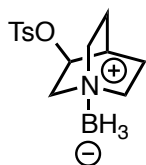


Figure 8.17. 3-(tosyloxy)quinuclidin-1-ium-1-yl)trihydroborate (3.32)^{36,37}

3.31 (3.54g, 12.581mmol) was dissolved in THF (125mL) and cooled to 0°C. $\text{BH}_3 \cdot \text{SMe}_2$ (1.5mL, 15.098mmol) was then added dropwise. The reaction was allowed to warm to room temperature and was monitored by TLC for disappearance of starting material. The reaction was then concentrated down and CHCl_3 was then added and the solution was washed with water and then brine. The reaction was then concentrated and dried over MgSO_4 . (**3.32**, 79%)

[JMG-1-200]

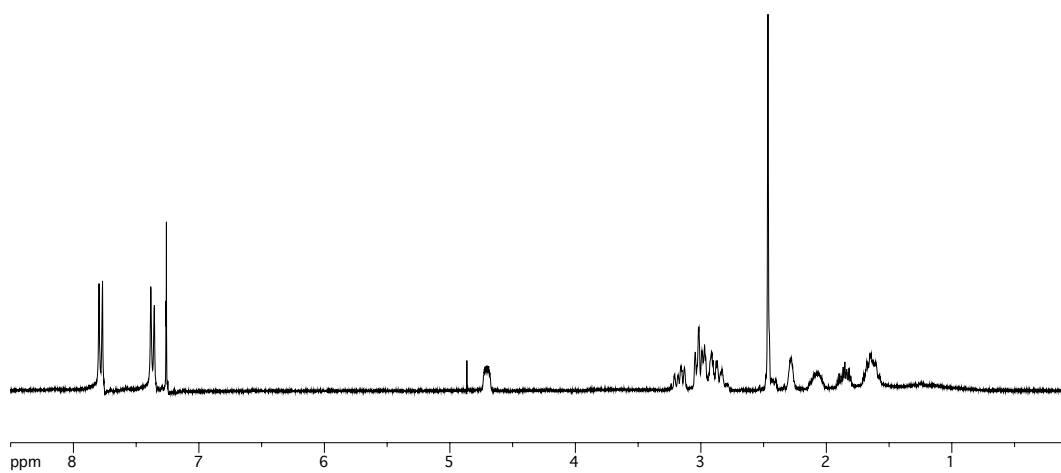


Figure 8.18. ^1H NMR of 3-(tosyloxy)quinuclidin-1-ium-1-yl)trihydroborate (3.32)^{36,37}

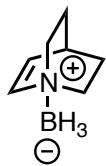


Figure 8.19. 1-azabicyclo[2.2.2]oct-2-en-1-ium-1-yltrihydroborate (**3.1**)^{36,37}

3.32 (619mg, 2.097mmol) was dissolved in THF (25mL) and cooled to -78°C. KOtBu (551mg, 4.914mmol) was then added and the reaction was stirred for 10 minutes. The reaction as allowed warmed to room temperature over 1 hour when it was concentrated and diluted with DCM and washed with bicarbonate and brine and dried over MgSO₄.

(3.1, 82%)

[JMG-1-195-2]

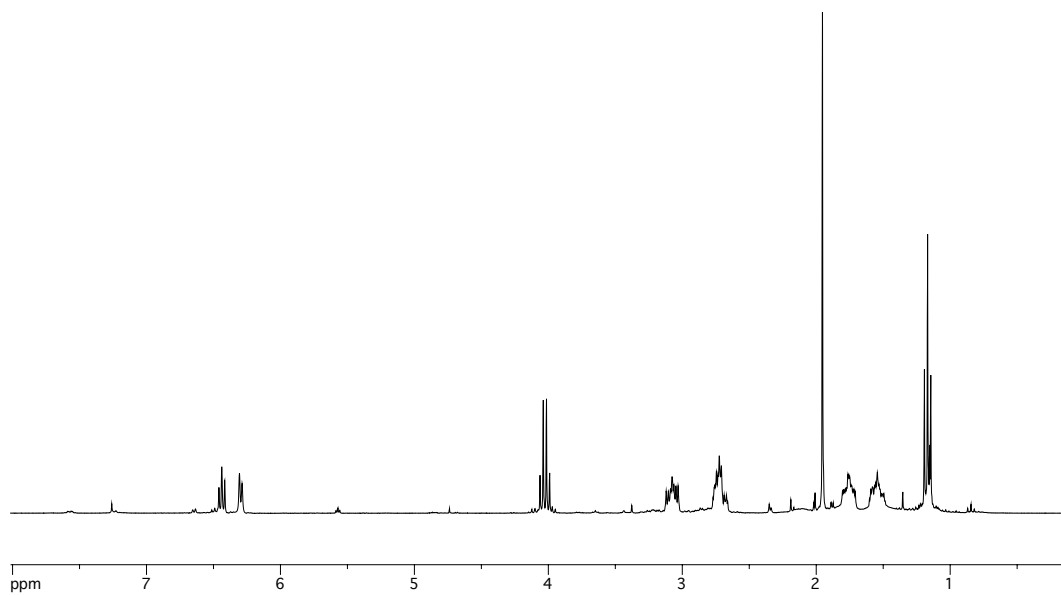


Figure 8.20. ^1H NMR of 1-azabicyclo[2.2.2]oct-2-en-1-ium-1-yltrihydroborate (3.1)^{36,37}

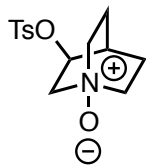


Figure 8.21. (1*S*,3*S*,4*S*)-3-(tosyloxy)quinuclidine 1-oxide (3.35)^{36,37}

3.31 (2g, 7.108mmol) was dissolved in Et₂O (35mL) and cooled to -78°C. O₃ was then bubbled through the system for 2 hours. The reaction was then flushed with argon and concentrated down. (**3.35**, 94%)

[JMG-1-207]

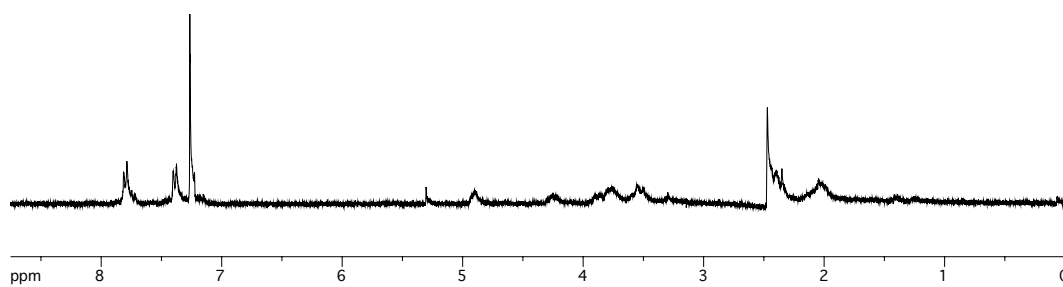


Figure 8.22. ^1H NMR of (1*S*,3*S*,4*S*)-3-(tosyloxy)quinuclidine 1-oxide (3.35)^{36,37}

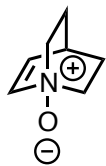


Figure 8.23. 1-azabicyclo[2.2.2]oct-2-ene 1-oxide (3.4)^{36,37}

3.35 (1.98g, 6.658mmol) was dissolved in THF (70mL) and cooled to -78°C. KOtBu (3g, 26.633mmol) was then added and the reaction was warmed to room temperature over 1 hour. The reaction was then concentrated and diluted with DCM and washed with bicarbonate and brine and dried over MgSO₄. (**3.4**, quant) [JMG-1-208]

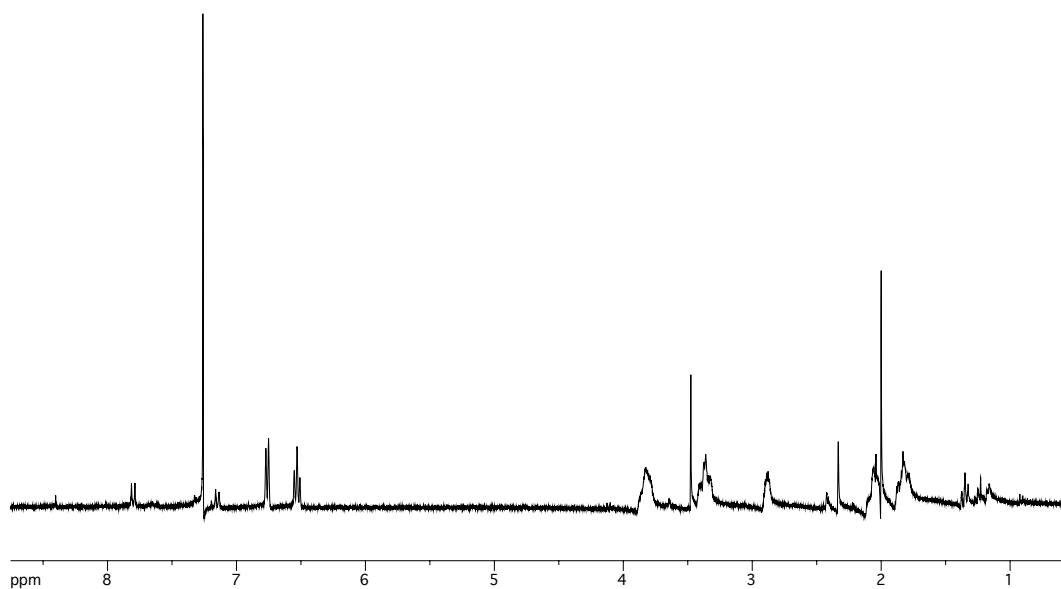


Figure 8.24. ^1H NMR of 1-azabicyclo[2.2.2]oct-2-ene 1-oxide (3.4)^{36,37}

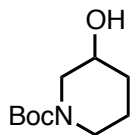


Figure 8.25. tert-butyl 3-hydroxypiperidine-1-carboxylate (3.43a)³⁴

To piperidin-3-ol (**3.43**, 500mg, 4.943mmol) was added EtOH (10ml, 0.5M) and then cooled to 0°C. Boc₂O (1.186g, 5.437mmol) and the reaction was allowed to warm to room temperature over 1 hour. The reaction was concentrated and pulled through a silica plug with 50-75% EtOAc/Hex.

[JMG-1-161-2]

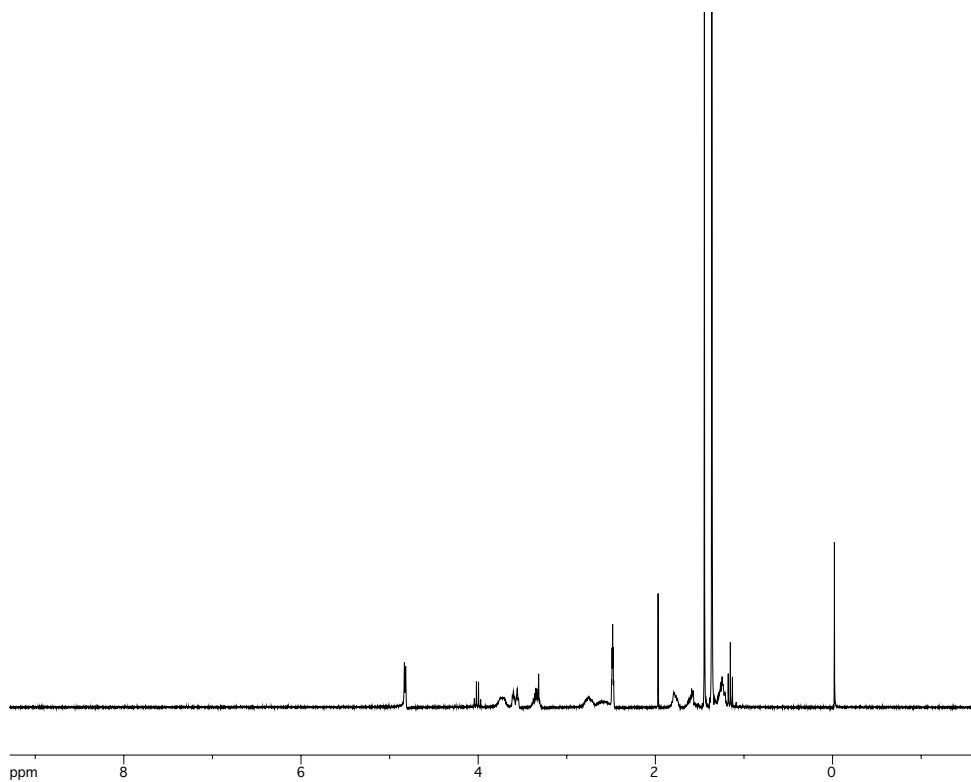


Figure 8.26. ^1H NMR of tert-butyl 3-hydroxypiperidine-1-carboxylate (3.43a)³⁴

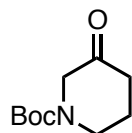


Figure 8.27. tert-butyl 3-oxopiperidine-1-carboxylate (**3.44**)^{34,40}

3.34a (17.11g, 85.014mmol) was dissolved in DCM (0.2M, 425mL) and cooled to 0°C. DMSO (15mL, 212.54mmol) was added in one portion, followed by P₂O₅ (60.3g, 212.54mmol). The reaction was then stirred for 30 minutes and the ice bath was removed and the reaction was stirred at room temperature for 1 hour. The reaction was then cooled back to 0°C and Et₃N (51mL, 365.56mmol) was added slowly over 10 minutes and then the reaction was stirred until the starting material had been consumed (~30 minutes). The reaction was then quenched slowly with 1M NaHSO₃ and extracted with DCM and then washed with brine and dried over Na₂SO₄.

[JMG-1-162]

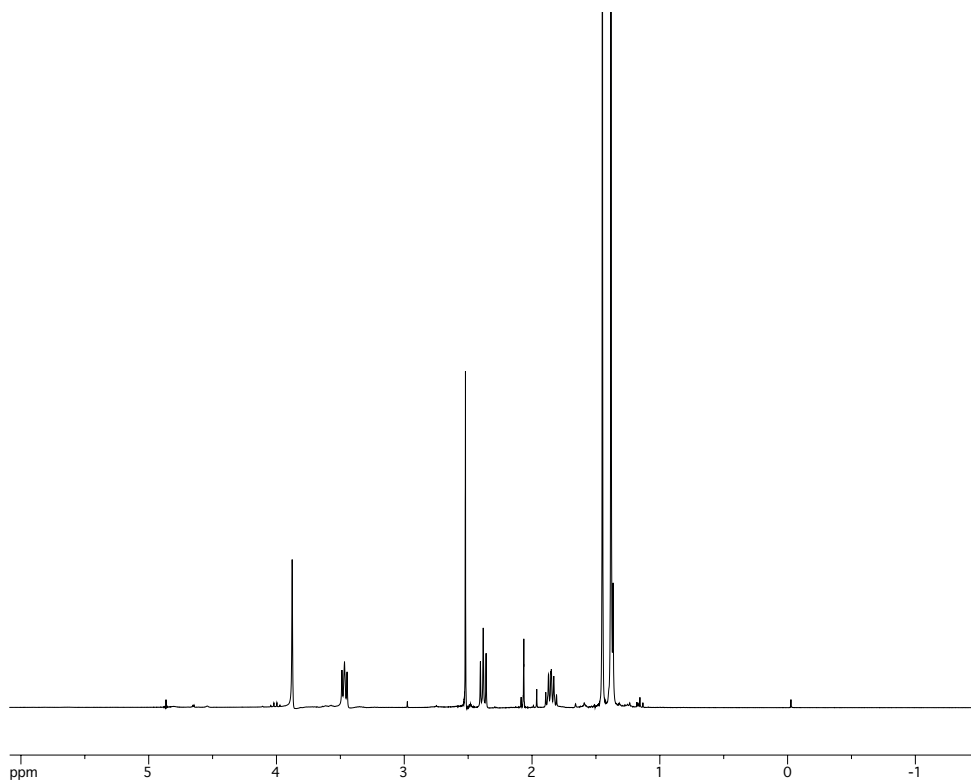


Figure 8.28. ^1H NMR of tert-butyl 3-oxopiperidine-1-carboxylate (3.44)^{34,40}

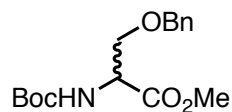


Figure 8.29. methyl 3-(benzyloxy)-2-((*tert*-butoxycarbonyl)amino)propanoate (3.48)⁴⁰

3.47 (2.0g, 10.245mmol) was dissolved in MeOH (15mL) and cooled to 0°C. SOCl₂ (1.7mL, 22.539mmol) was then added dropwise and the reaction was warmed to 40°C for 3.5 hours and then cooled to room temperature. The reaction was then concentrated and then redissolved in 1:1 THF:H₂O (34mL) and solid NaHCO₃ (1g) was added followed by Boc₂O (2.84g, 10.245mmol). The reaction was allowed to stir at room temperature overnight and was then diluted with EtOAc and washed with brine. The reaction was dried over Na₂SO₄ and concentrated. No purification was needed.

¹H-NMR (300 MHz; CDCl₃): δ 1.44 (s, 9H), 3.68 (dd, *J* = 9.2, 3.5 Hz, 1H), 3.74 (s, 3H), 3.86 (dd, *J* = 9.3, 3.1 Hz, 1H), 4.57-4.42 (m, 3H), 5.40 (d, *J* = 8.7 Hz, 1H), 7.37-7.25 (m, 5H).

[JMG-1-315]

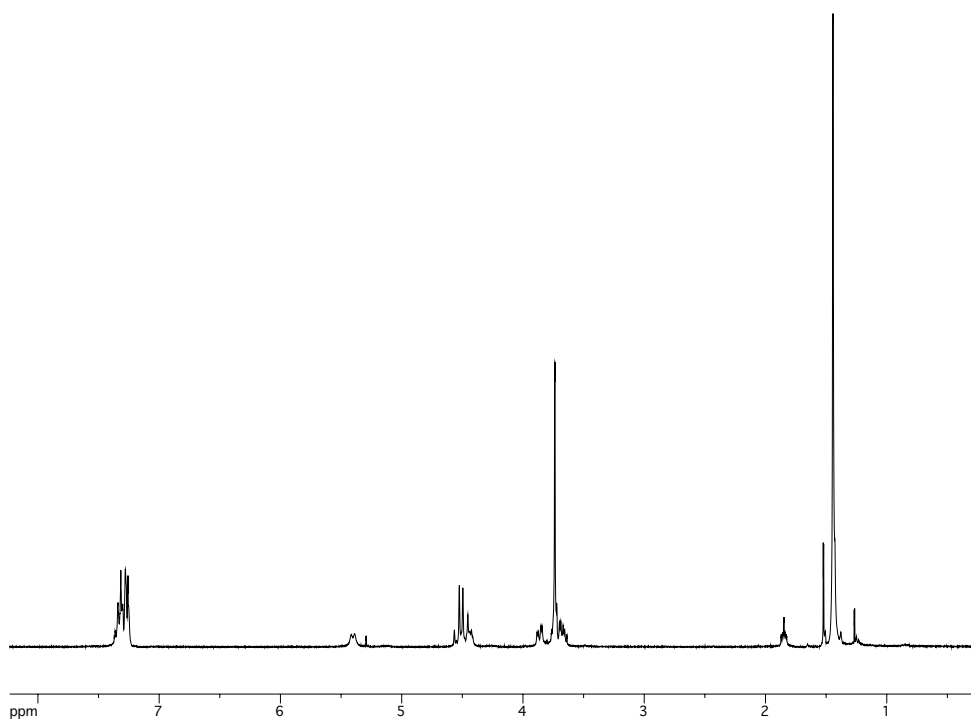


Figure 8.30. ^1H NMR of methyl 3-(benzyloxy)-2-((*tert*-butoxycarbonyl)amino)propanoate (3.48)⁴⁰

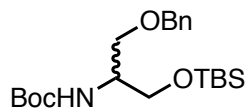


Figure 8.31. *tert*-butyl (1-(benzyloxy)-3-((*tert*-butyldimethylsilyl)oxy)propan-2-yl)carbamate (**3.49**)⁴⁰

3.48 (3.3g, 10.667mmol) was dissolved in THF (35mL) and cooled to 0°C. LiAlH₄ (607mg, 16.000mmol) was then added and the reaction was allowed to stir for 5 minutes. The reaction was then diluted with ether and 600μl H₂O were added, followed by 600μl of 15% NaOH, and then 1.8mL of H₂O. The reaction was allowed to warm to room temperature and stir for one hour whereby the salts were then filtered off over a pad of celite and the organics were dried over Na₂SO₄ and concentrated and then dissolved in DCM (30mL). TBSCl (2.5g, 16.706mmol) and imidazole (1.7g, 25.058mmol) were added and the reaction was allowed to stir at room temperature overnight. The reaction was then diluted with NH₄Cl_{aq} and extracted with DCM and dried over MgSO₄. Purification through a short silica plug with hexanes:EtOAc, 50:50 and then heating to 60°C while under vacuum (to get rid of TBSOH) gave the desired product (**4.39**) in 73% yield over two steps.

¹H-NMR (300 MHz; CDCl₃): δ 0.05 (s, 6H), 0.88 (s, 9H), 1.44 (s, 9H), 3.49 (dd, *J* = 9.1, 6.1 Hz, 1H), 3.64-3.58 (m, 2H), 3.74 (dd, *J* = 9.7, 3.6 Hz, 2H), 4.51 (s, 2H), 7.34-7.31 (m, 5H).

[JMG-1-319-1]

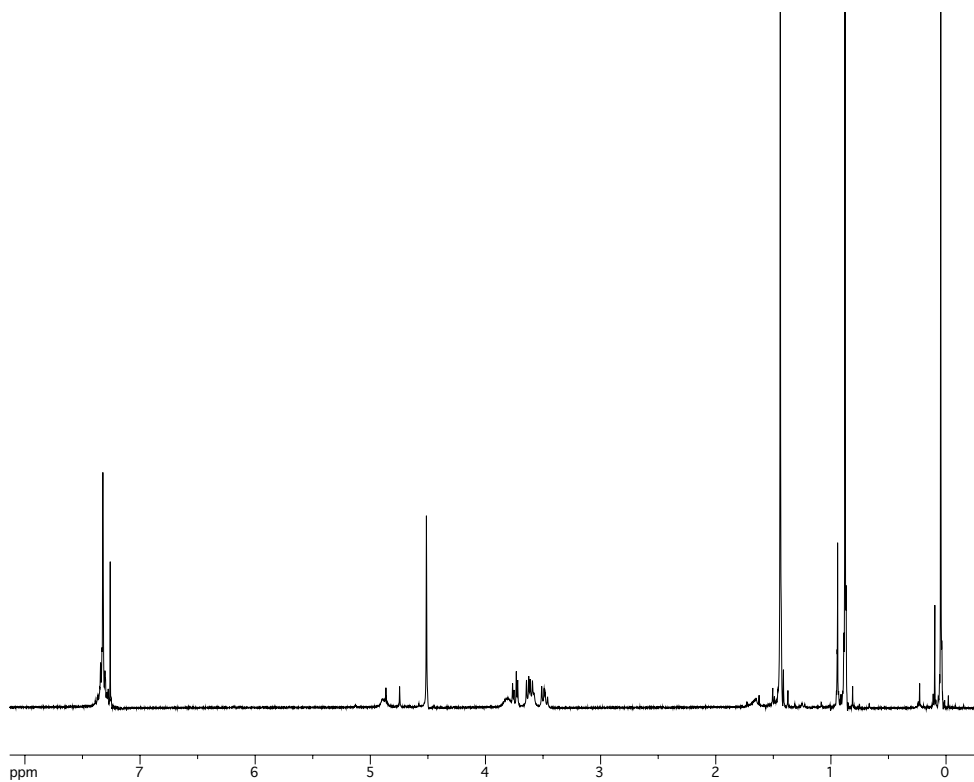


Figure 8.32. ^1H NMR of *tert*-butyl (1-(benzyloxy)-3-((*tert*-butyldimethylsilyl)oxy)propan-2-yl)carbamate (3.49)⁴⁰

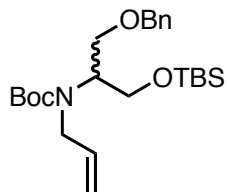


Figure 8.33. *t*-Bu-allyl(1-(benzyloxy)-3-((TBS)oxy)propan-2-yl)carbamate (**3.50**)⁴⁰

DMF (23mL) and NaH (60%wt, 273mg, 6.825mmol) were cooled to 0°C. **3.49** (1.8g, 4.550mmol) in DMF (5mL) were added and the reaction was stirred for 15 minutes. Allyl-Br (905μl, 10.465mmol) was then added and the reaction was allowed to warm to room temperature and stir for 24 hours. The reaction was then quenched with H₂O (30mL) and then the reaction as diluted with EtOAc and extracted with NH₄Cl_{aq} and dried over Na₂SO₄. Purification via column chromatography, hexanes:EtOAc, 85:15, gave **3.50** in 98% yield.

¹H-NMR (300 MHz; CDCl₃): δ 0.03 (s, 6H), 0.87 (s, 9H), 1.43 (s, 9H), 3.94-3.60 (m, 6H), 4.49 (d, *J* = 3.9 Hz, 2H), 5.12-5.03 (m, 2H), 5.85-5.77 (m, 1H), 7.36-7.28 (m, 5H).

[JMG-1-321]

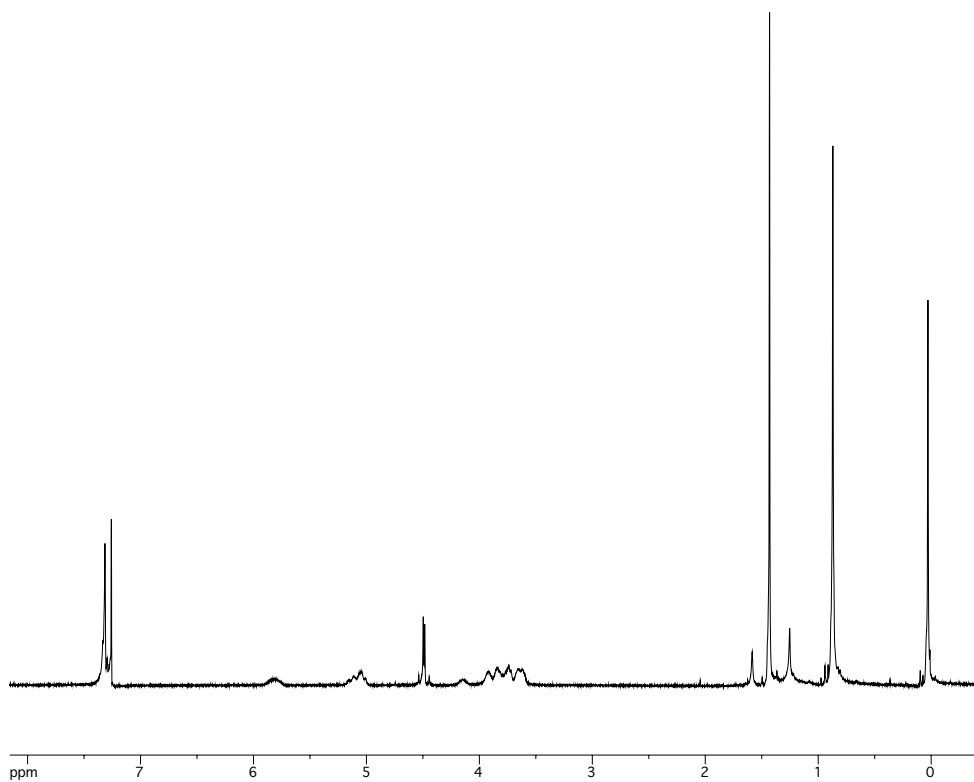


Figure 8.34. ^1H NMR of *t*-Bu-allyl(1-(BnO)-3-((TBS)oxy)propyl)carbamate (3.50)⁴⁰

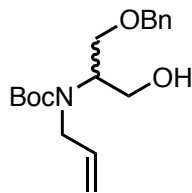


Figure 8.35. *t*-Bu-allyl(1-(BnO)-3-hydroxypropyl)carbamate (3.50a**)**⁴⁰

3.50 (1.95g, 4.476mmol) was dissolved in THF (4mL) and TBAF (14mL, 13.862mmol) was added. The reaction was stirred for 3 hours at room temperature. The reaction was then quenched with $\text{NH}_4\text{Cl}_{\text{aq}}$ and extracted with EtOAc and dried over Na_2SO_4 . Column chromatography, hexanes:EtOAc, 70:30 provided the desired alcohol (**3.50a**) in 56% yield.

^1H NMR (300MHz, CDCl_3): 1.44 (s, 9H), 3.74 (m, 7H), 4.51 (s, 2H), 5.08 (m, 2H), 5.78 (m, 1H), 7.32 (m, 5H).

[JMG-1-326]

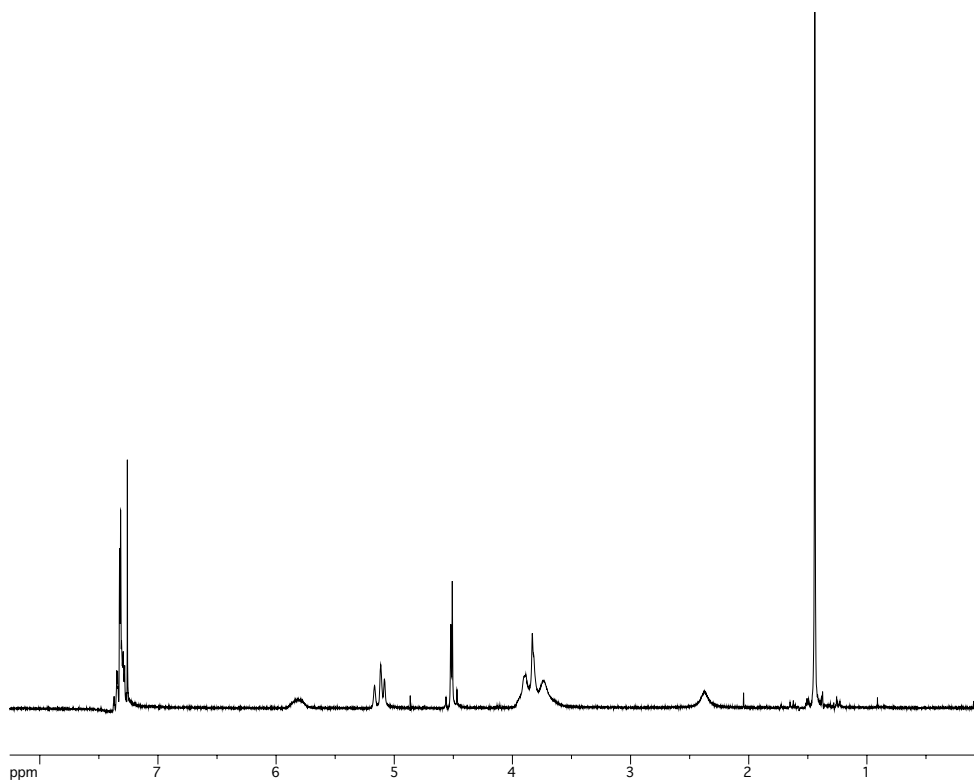


Figure 8.36. ^1H NMR of *t*-Bu-allyl(1-(BnO)-3-hydroxypropan-2-yl)carbamate (3.50a)⁴⁰

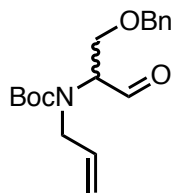


Figure 8.37. t-Bu-allyl(1-(BnO)-3-oxopropan-2-yl)carbamate (3.51)⁴⁰

DCM (2mL) and (COCl)₂ (253μl, 2.950mmol) were cooled to -78°C. DMSO (419μl, 12.290mmol) was then added and the reaction was stirred for 30 minutes. **3.50a** (790mg, 2.458mmol) in DCM (2mL) was then added and the reaction was stirred for 1 hour. Et₃N (1.7mL, 12.290mmol) was then added and the reaction was warmed to 0°C and stirred for 1 hour and then quenched with H₂O and extracted with DCM and dried over Na₂SO₄. Column chromatography, hexanes:EtOAc, 90:10, gave the desired aldehyde (**3.51**) in 42% yield.

¹H NMR (300MHz, CDCl₃): (rotomers) 1.35, 1.45 (s, 9H), 3.71 (m, 4H), 4.14 (dd, 1H, *J* = 15, 69), 4.47 4.54 (s, 2H), 5.12 (m, 2H), 5.78 (m, 1H), 7.31 (m, 5H), 9.50, 9.54 (s, 1H).

[JMG-1-327-1]

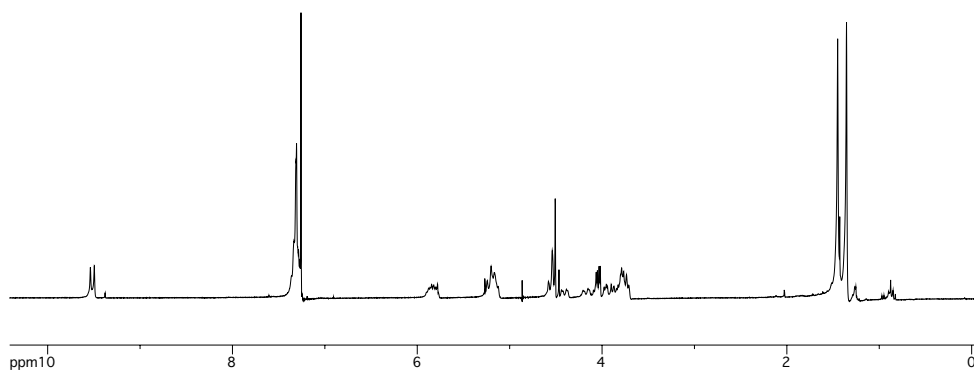


Figure 8.38. ^1H NMR of *t*-Bu-allyl(1-(BnO)-3-oxopropan-2-yl)carbamate (3.51)⁴⁰

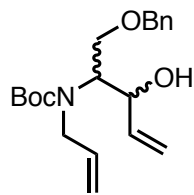


Figure 8.39. *t*-Bu-allyl(1-(BnO)-3-hydroxypent-4-en-2-yl)carbamate (3.52)⁴⁰

To a flamed round bottom under argon was added **3.51** (300mg, 1.033mmol) and THF (10.5mL). The solution was then cooled to 0°C and vinyl-MgBr (1.2mL, 1.137mmol) was added. The reaction was stirred for 2 hours at room temperature and then quenched with H₂O. Column chromatography, hexanes:EtOAc, 90:10 gave the desired alcohol (**3.52**) in 73% yield.

¹H NMR (300MHz, CDCl₃): 1.43 (s, 9H), 3.64 (m, 5H), 4.41 (m, 3H), 5.08 (m, 3H), 5.29 (d, 1H, *J* = 15), 5.71 (m, 2H), 7.31 (m, 5H).

[JMG-1-330]

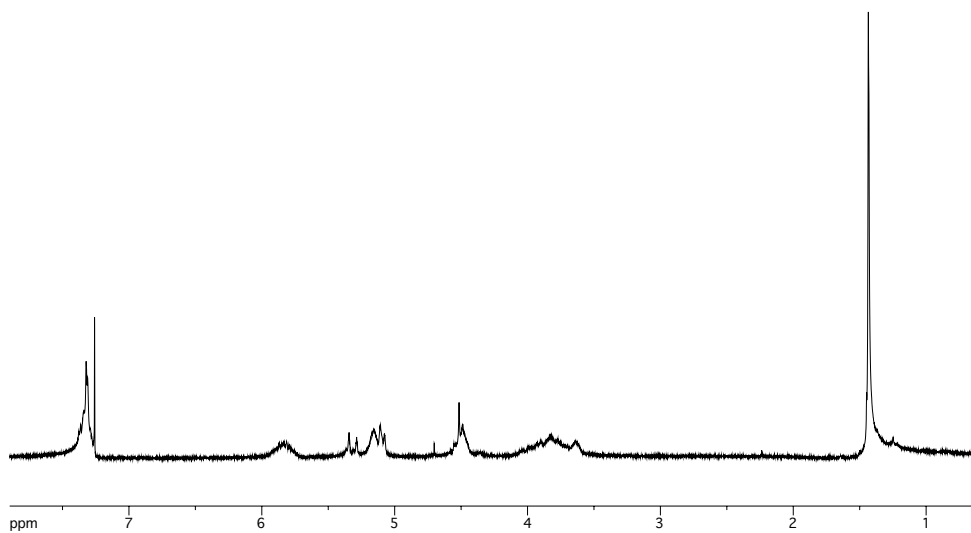


Figure 8.40. ^1H NMR of *t*-Bu-allyl(1-(BnO)-3-hydroxypentenyl)carbamate (3.52)⁴⁰

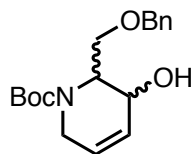


Figure 8.41. *t*-Bu-6-((BnO)methyl)dihydropyridine carboxylate (3.53)⁴⁰

To a flamed round bottom flask under argon was added **3.52** (261mg, 0.751mmol) and degassed DCM (20mL). Grubbs 2G (32mg, 0.038mmol) was then added and the reaction was stirred at room temperature overnight. The reaction was quenched with H₂O (10mL) and stirred for 1 hour. The biphasic mixture was washed with brine and separated and dried over Na₂SO₄. Column chromatography, hexanes:EtOAc, 65:35, gave the desired alcohol (**3.53**) in 15% yield.

HRMS calcd for C₁₈H₂₆NO₄ (M+H)⁺: 320.1862, found: 320.1856.

¹H NMR (300MHz, CDCl₃): 1.45 (s, 9H), 3.07 (m, 1H), 3.36 (d, 1H, *J* = 18), 3.50 (t, 1H, *J* = 9), 3.75 (t, 1H, *J* = 6), 4.04 (d, 1H, *J* = 6), 4.46 (m, 3H), 5.64 (m, 2H), 7.31 (s, 5H).

[JMG-1-333-2]

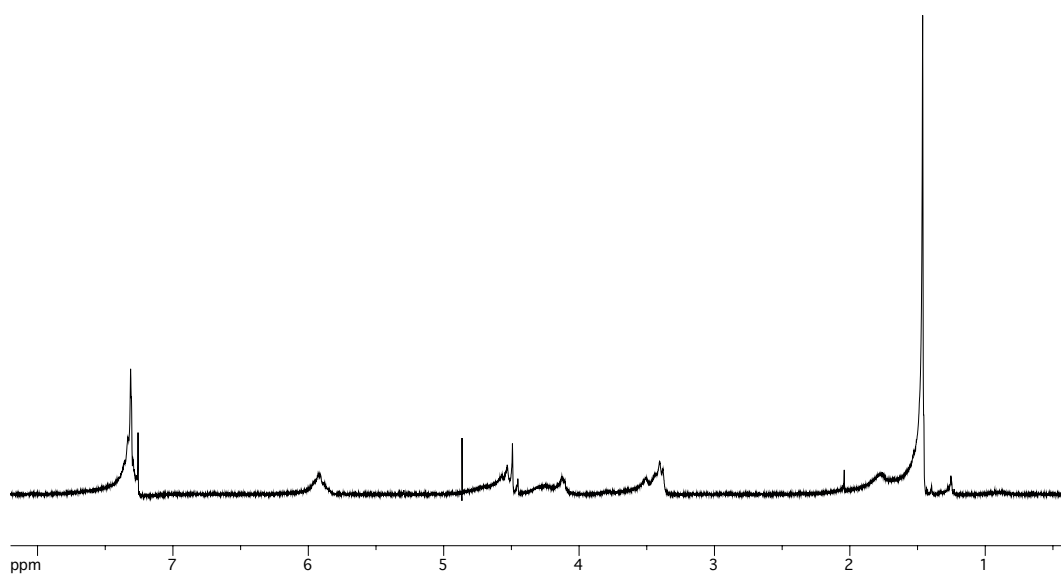


Figure 8.42. ^1H NMR of *t*-Bu-6-((BnO)methyl)dihydropyridine carboxylate (3.53)⁴⁰

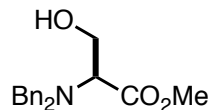


Figure 8.43. (S)-methyl 2-(dibenzylamino)-3-hydroxypropanoate (3.57)^{41,186}

3.56 (2g, 12.855mmol) was dissolved in THF (100mL) and DMSO (1.6M) and benzyl bromide (6.5g, 38.565mmol) was added followed by sodium bicarbonate (4.3g, 51.420mmol). The reaction was refluxed for 15 hours and then cooled to room temperature and diluted with water. The reaction was then extracted with EtOAc and washed with brine (200mL) and purified via column chromatography, hexanes: EtOAc, 85:15 to afford **3.57** (84%).

[JMG-1-397]

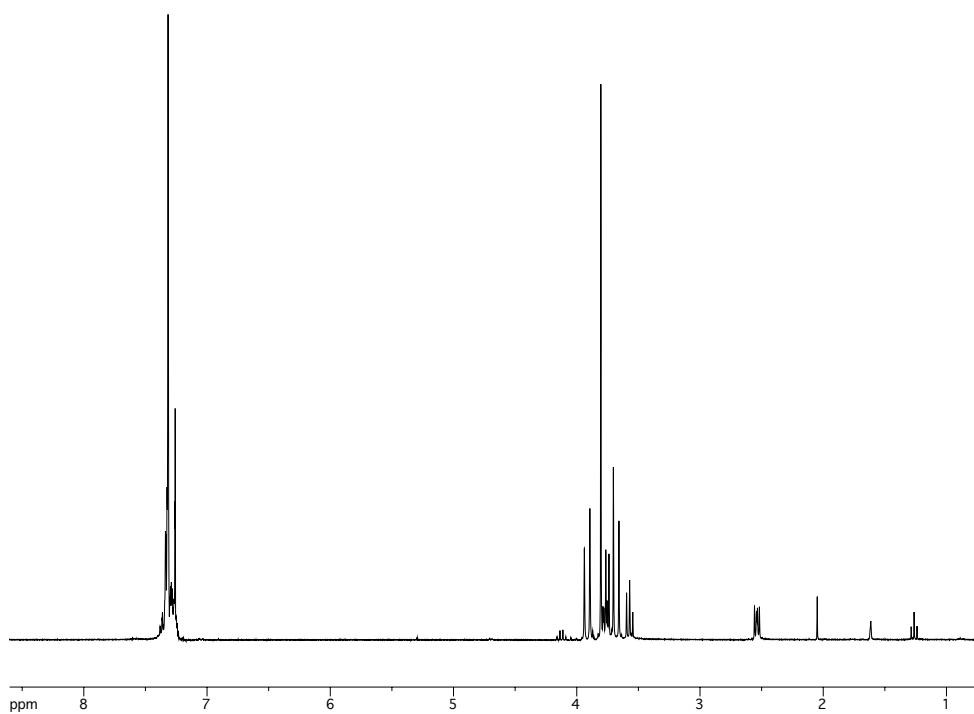


Figure 8.44. ^1H NMR of (S)-methyl 2-(dibenzylamino)-3-hydroxypropanoate (3.57)^{41,186}

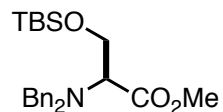


Figure 8.45. (S)-methyl 3-((TBSO)-2-(dibenzylamino)propanoate (3.58)^{41,186}

3.57 (3.3g, 10.823mmol) was dissolved in DMF (100mL) and imidazole (1.1g, 16.235mmol) and TBSCl (2.12g, 14.070mmol) were added and stirred overnight. The reaction was quenched with $\text{NH}_4\text{Cl}_{\text{aq}}$ (100mL) and extracted with EtOAc and washed with brine (2 X 100mL), dried over Na_2SO_4 , concentrated and purified via column chromatography, hexanes:EtOAc, 85:15. The resulting oil was heated (neat) to 60°C with stir bar while being under high vacuum overnight to remove the TBSOH impurity.

[JMG-1-444]

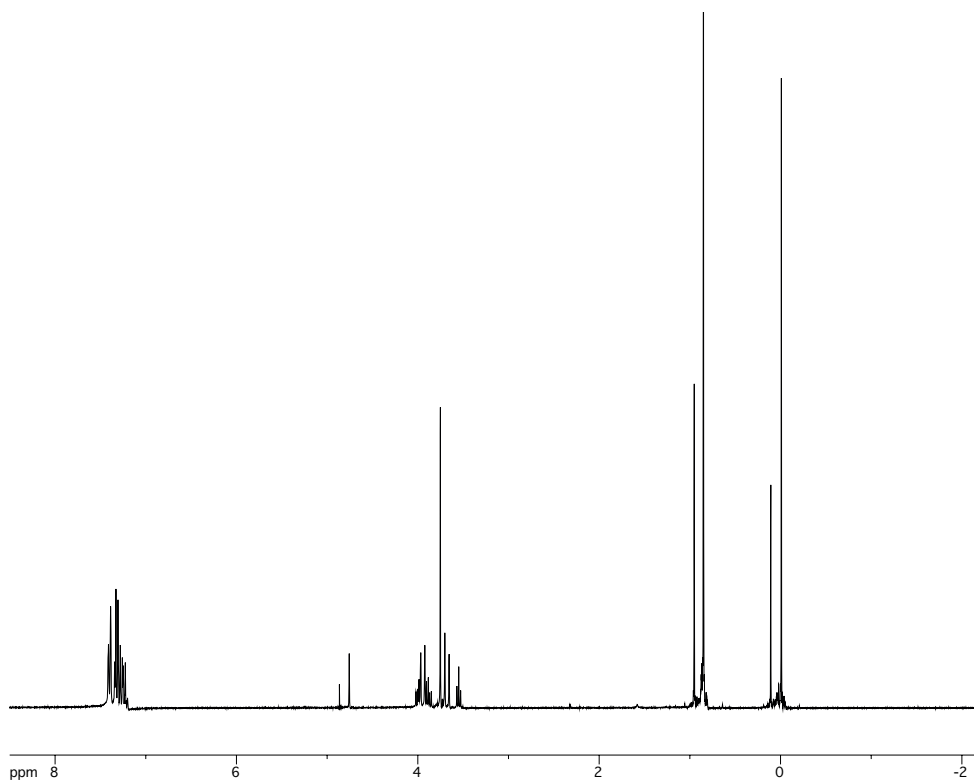


Figure 8.46. ^1H NMR of (S)-methyl 3-((TBSO)-2-(dibenzylamino)propanoate (3.58)^{41,186}

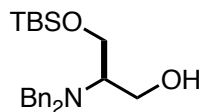


Figure 8.47. (R)-3-((TBSO)-2-(dibenzylamino)propan-1-ol (**3.59**)^{41,186}

3.58 (4.5g, 10.831mmol) and ether (50mL) were cooled to 0°C and LiBH₄ (955mg, 43.324mmol) was added followed by MeOH (1mL). The ice bath was removed and the reaction was heated to reflux for 3 hours, then cooled and quenched with NH₄Cl_{aq} (dropwise). The mixture was extracted with EtOAc and washed with brine (2 X 100mL). No purification was needed (**3.59**, 62%).

[JMG-1-399-2]

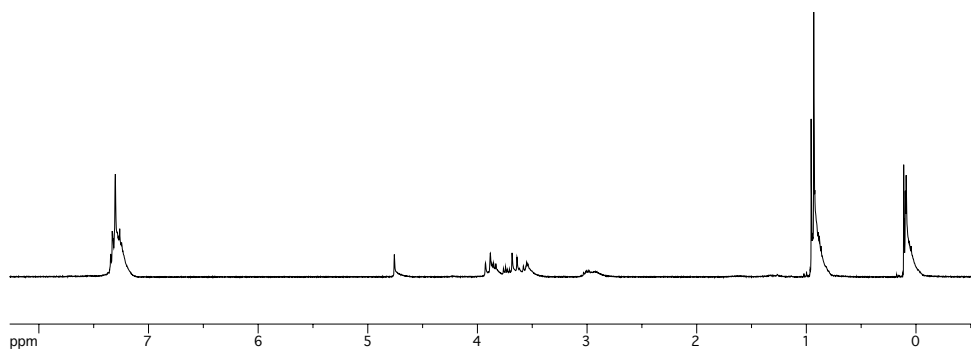


Figure 8.48. ^1H NMR of (S)-methyl 3-((TBSO)-2-(dibenzylamino)propanoate (3.58)^{41,186}

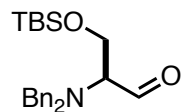


Figure 8.49. (S)-3-((TBSO)-2-(dibenzylamino)propanal (3.60)^{41,186}

DCM (4mL) was cooled to -78°C and thionyl chloride (13.858mmol) was added. DMSO (30.488mmol) was then added and stirred at -78°C for 10 minutes. **3.59** (6.929mmol) was dissolved in DCM (3mL) and added dropwise to reaction. The reaction was allowed to stir for 15 minutes and then Et₃N (62.362mmol) was added and stirred at -78°C for 1 hour. The reaction was then warmed to room temperature and quenched with water and extracted with DCM, dried over Na₂SO₄, and concentrated. (55%)

[JMG-1-400]

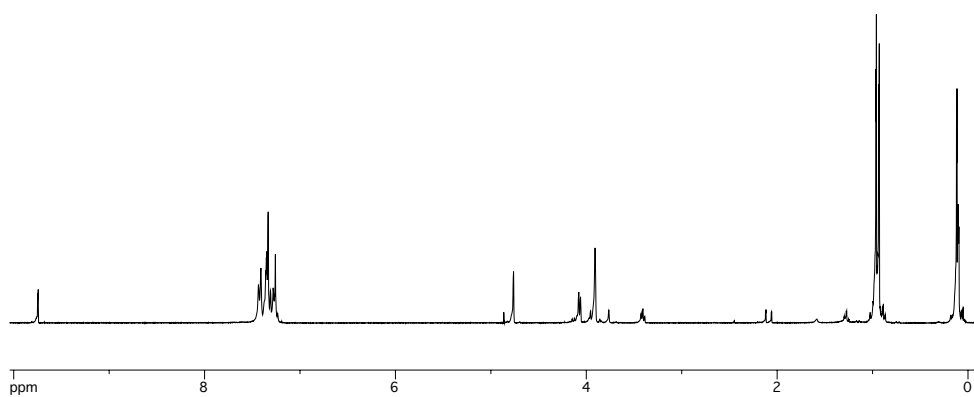


Figure 8.50. ^1H NMR of (S)-3-((TBSO)-2-(dibenzylamino)propanal (3.60)^{41,186}

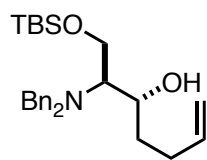


Figure 8.51. (2S,3R)-1-((TBSO)-2-(dibenzylamino)hept-6-en-3-ol (**3.61**)^{41,186}

3.60 (268mg, 0.699mmol) in Et₂O (3.5mL) was cooled to 0°C under argon in a flame dried round bottomed flask. Homo-allyl-MgBr (3mL, 1.397mmol) was added and stirred for 1 hour. The reaction was then quenched with NH₄Cl_{aq} and extracted with Ether and dried over Na₂SO₄. (65%)

[JMG-1-411]

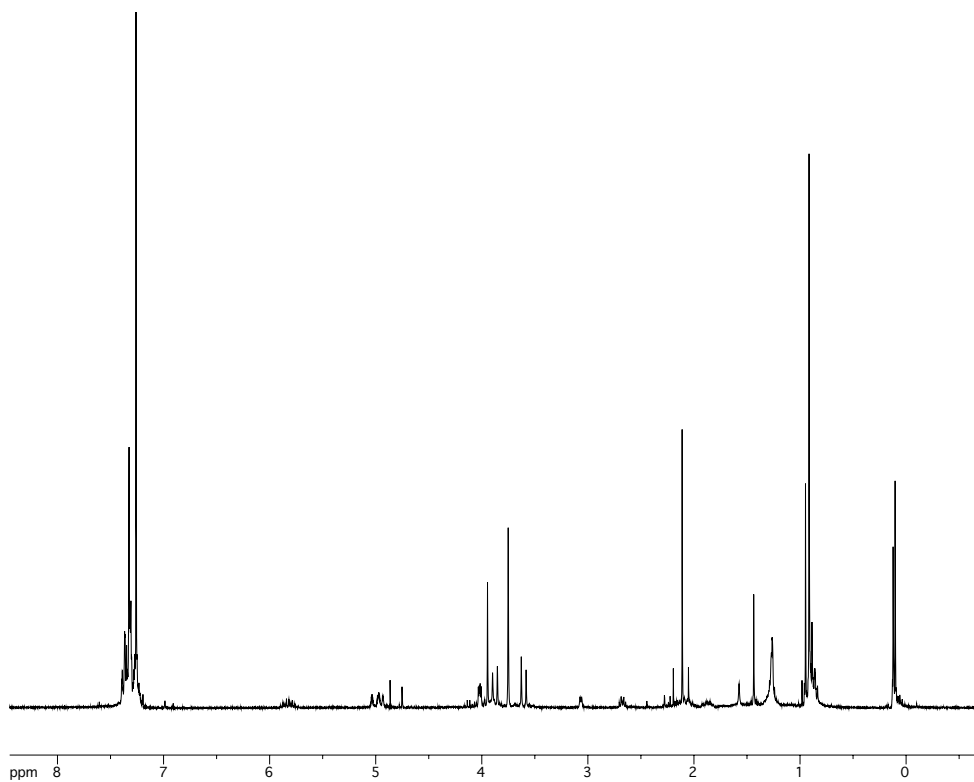


Figure 8.52. ^1H NMR of (2S,3R)-1-((TBSO)-2-(dibenzylamino)hept-6-en-3-ol (3.61)^{41,186}

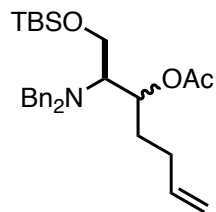


Figure 8.53. (2S)-1-((TBSO)-2-(dibenzylamino)hept-6-en-3-yl acetate (3.62)^{41,186}

To **3.61** (2.51g, 5.708mmol) was added DCM (60mL, 0.1M). Ac₂O (1.5mL, 15.698mmol) and DMAP (2.1g, 17.124mmol) were then added. The reaction was stirred at room temperature and monitored by TLC. The reaction was then worked up with NH₄Cl_{aq} and dried over Na₂SO₄ and ran through a plug to purify. (88%)

[JMG-1-418]

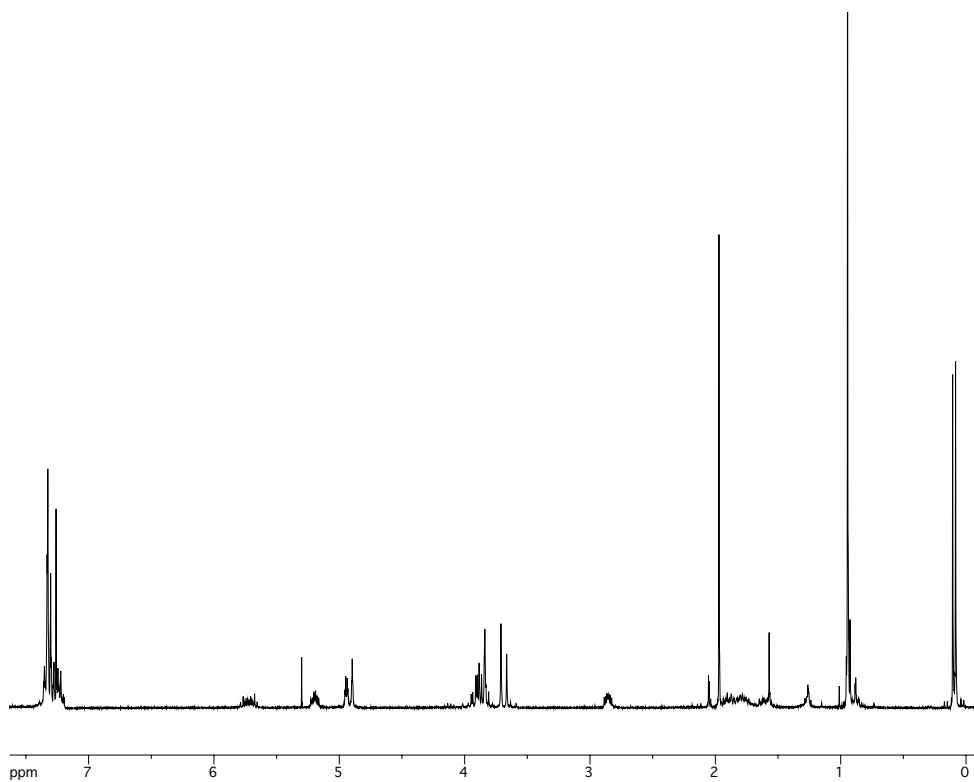


Figure 8.54. ^1H NMR of (2S)-1-(TBSO)-2-(dibenzylamino)heptenyl acetate (3.62)^{41,186}

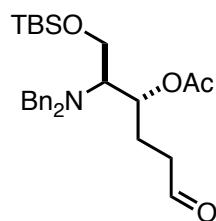


Figure 8.55. (2S,3R)-1-(TBSO)-2-(dibenzylamino)-6-oxohexan-3-yl acetate (3.63)^{41,186}

To **3.62** (1.024g, 2.1169mmol) was added acetone (5.5mL), water (1mL) then NMO (1.24g, 10.585mmol) at room temperature. OsO₄ (600μL-5% solution in toluene, 0.106mmol, 5mol%). The reaction was then stirred at room temperature overnight. A saturated solution of Na₂SO₃ was then added to the mixture and it was extracted with EtOAc and the organic layer was dried over Na₂SO₄ and concentrated and taken on to the next step. The crude diol was then dissolved in DCM (11mL) and added in one portion to a stirring suspension of SiO₂ gel (4g) and NaIO₄ (2g) in DCM (11mL) at 0°C. The reaction was allowed to stir at 0°C for 1 hour and was then filtered through a silica plug and washed with DCM. (60%)

[JMG-1-436crude]

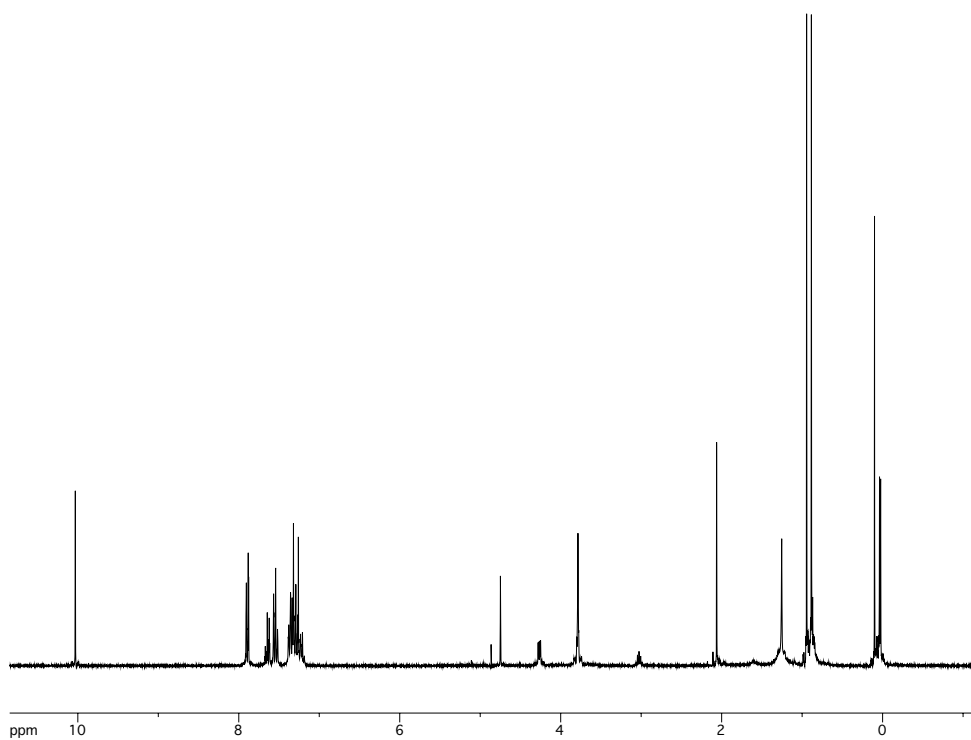


Figure 8.56. ^1H NMR of (TBSO)-2-(dibenzylamino)oxohexanyl acetate (3.63)^{41,186}

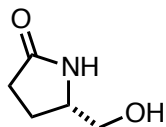


Figure 8.57. (S)-5-(hydroxymethyl)pyrrolidin-2-one (3.87)¹⁸⁷

To a solution of **3.86** (5g, 38.724mmol) was added MeOH (45mL) and the reaction mixture was then cooled to -20°C and SOCl₂ (3.1mL, 42.596mmol) was then added dropwise. The reaction was then warmed to room temperature and stirred for 1 hour. The reaction was then concentrated down taken on to the next step immediately. To a solution of crude ester was added EtOH (52mL) and the reaction was cooled to 0°C. NaBH₄ (1.6g, 40.660mmol) was then added in portions. The reaction was then stirred at 0°C for 30 minutes and warmed to room temperature and stirred for 1.5 hours. The reaction was then acidified to pH=3 with concentrated HCl and then concentrated down. The crude mixtures was taken up in CHCl₃ and filtered through a Celite plug and subsequently purified by column chromatography, DCM: MeOH, 9:1.

HRMS calcd for C₅H₁₀NO₂ (M+H)⁺: 116.0712, found: 116.0734.

¹H-NMR (400 MHz; CD₃OD): δ 1.90 (dddd, *J* = 13.0, 9.8, 6.4, 5.0 Hz, 1H), 2.22 (dddd, *J* = 13.0, 9.7, 8.3, 6.9 Hz, 1H), 2.48-2.34 (m, 2H), 3.47 (dd, *J* = 11.3, 5.5 Hz, 1H), 3.57 (dt, *J* = 7.5, 3.9 Hz, 2H), 3.80 (dq, *J* = 8.6, 4.5 Hz, 1H). ¹³C NMR (101 MHz; cd₃od): δ 22.29, 29.64, 57.09, 64.09, 180.32

[JMG-3-161, JMG-3-161C13]

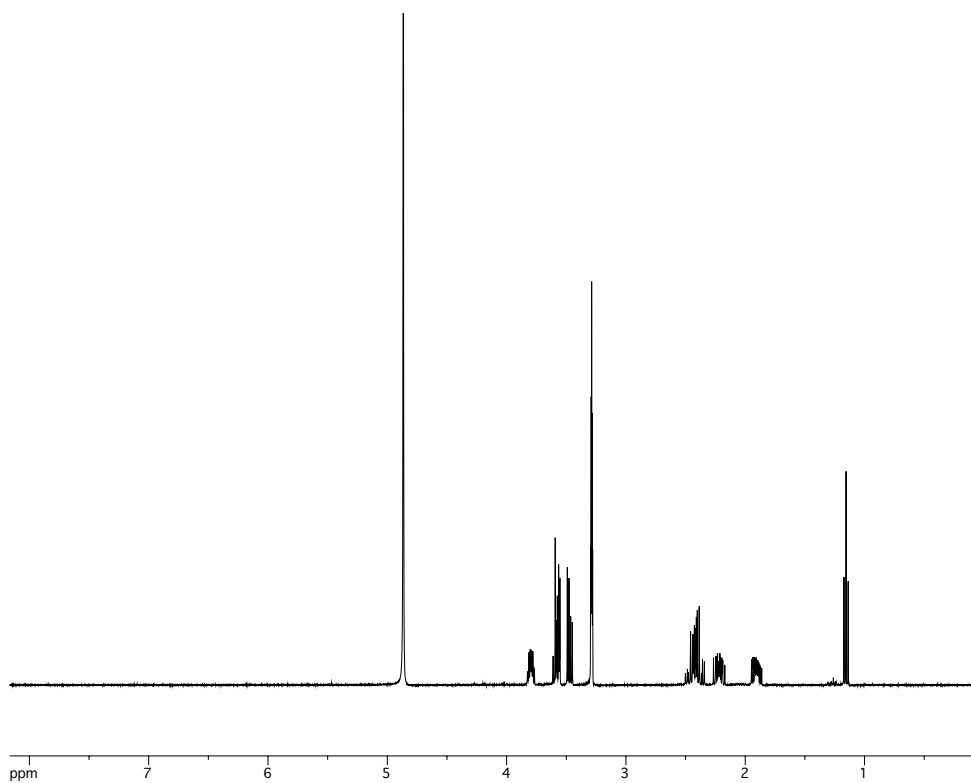


Figure 8.58. ^1H NMR of (S)-5-(hydroxymethyl)pyrrolidin-2-one (3.87)¹⁸⁷

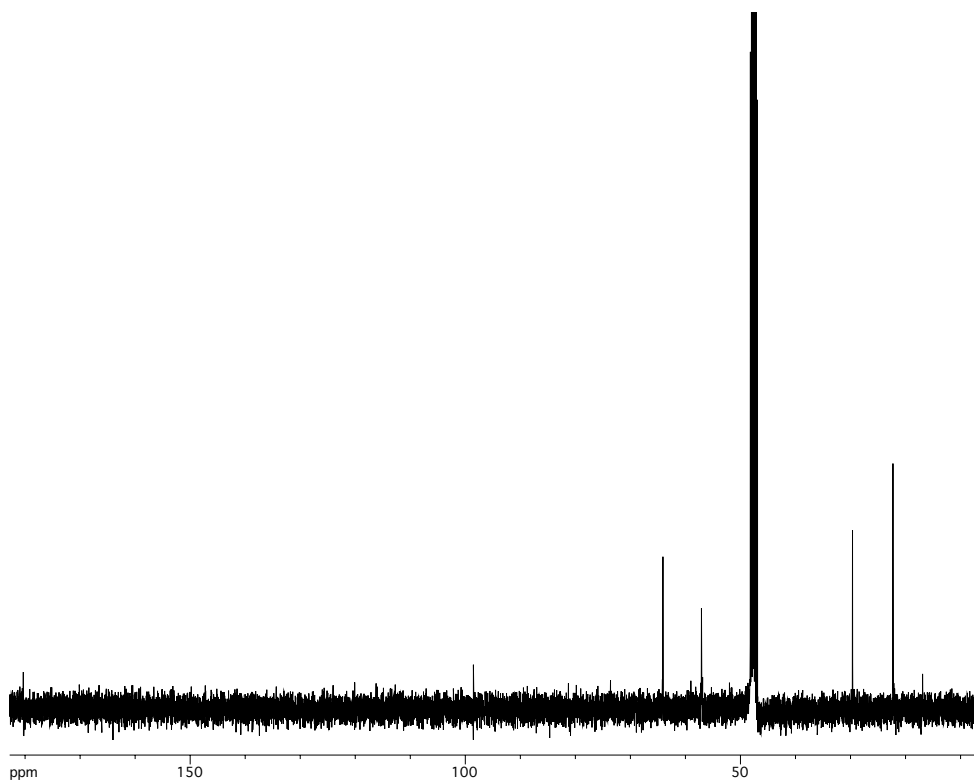


Figure 8.59. ^{13}C NMR of (S)-5-(hydroxymethyl)pyrrolidin-2-one (3.87)¹⁸⁷

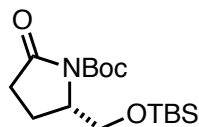


Figure 8.60. (S)-5-((TBSO)methyl)pyrrolidin-2-one (3.88)¹⁸⁷

3.87 (4.46g, 38.739mmol) was dissolved in DMF (0.12M) and cooled to 0°C. Imidazole (6.6g, 96.847mmol) and TBSCl (8.8g, 58.108mmol) were then added. The reaction was stirred for 1 hour. The reaction was then diluted with EtOAc and washed with bicarbonate and brine and dried over Na₂SO₄. Material was pushed through a silica plug with DCM:MeOH: 97/3. And redissolved in Pyridine (60mL). Boc₂O (5.8g, 26.505mmol) and DMAP (1.6g, 26.505mmol) were added and the reaction was stirred at room temperature overnight. The reaction was then concentrated and dissolved in EtOAc and washed with NH₄Cl_{aq} then bicarbonate, then brine and dried over Na₂SO₄ and concentrated. Purification via column chromatography yielded the desired product (**3.88**) (75% over 2 steps).

HRMS calcd for C₁₆H₃₁NO₄SiNa (M+Na)⁺: 352.1920, found: 352.1914.

¹H-NMR (300 MHz; CDCl₃): δ 0.01 (d, *J* = 4.2 Hz, 6H), 0.85 (s, 9H), 1.50 (s, 9H), 2.10-1.98 (m, 2H), 2.34 (ddd, *J* = 17.5, 9.5, 2.5 Hz, 1H), 2.68 (ddd, *J* = 17.6, 10.8, 10.1 Hz, 1H), 3.66 (dd, *J* = 10.4, 2.3 Hz, 1H), 3.89 (dd, *J* = 10.4, 3.9 Hz, 1H), 4.14 (dq, *J* = 6.5, 2.0 Hz, 1H). ¹³C NMR (75 MHz; CDCl₃): δ -5.37, 18.40, 21.35, 26.03, 28.29, 32.59, 59.11, 64.51, 82.90, 150.24, 175.23

[JMG-2-75-3, JMG-2-75-3C13]

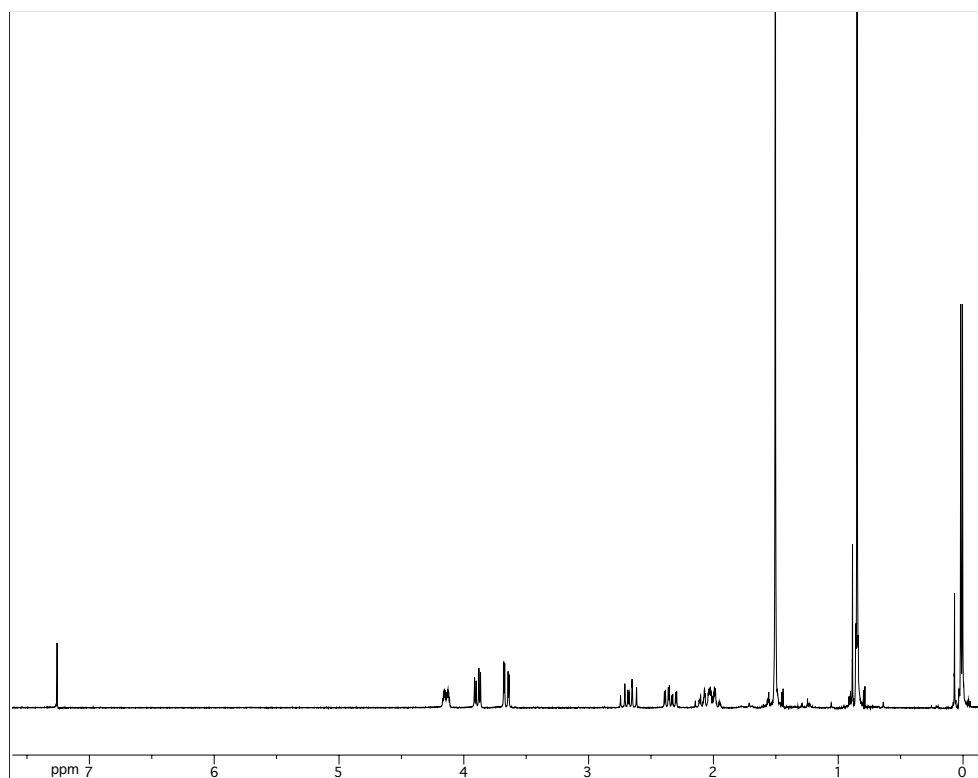


Figure 8.61. ^{13}C NMR of (S)-5-(TBSO)methylpyrrolidin-2-one (3.88)¹⁸⁷

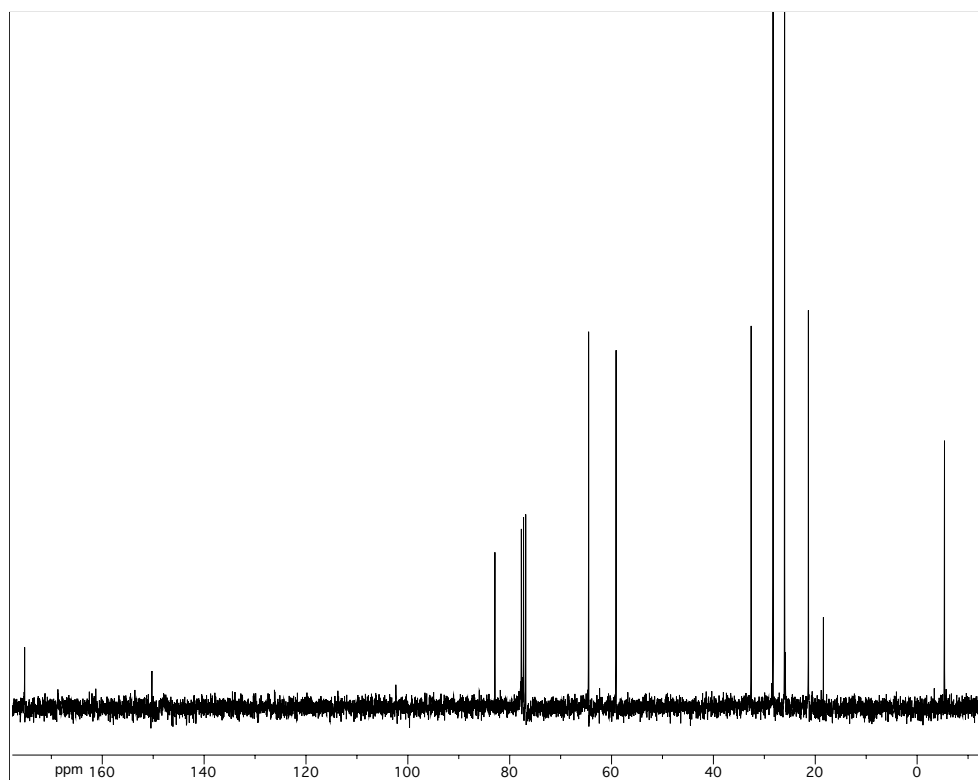


Figure 8.62. ^{13}C NMR of (S)-5-(TBSO)methylpyrrolidin-2-one (3.88)¹⁸⁷

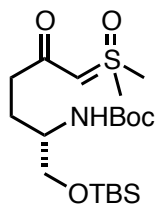


Figure 8.63. Tert-butyldimethylsilylether-sulfoxonium ylide (3.89)⁴³

(CH₃)₃SOCl (683mg, 5.310mmol), KOtBu (596mg, 5.310mmol) and THF (0.22M) were refluxed for 2 hours and cooled to room temperature. **3.88** (500mg, 1.517mmol) was then added and stirred at room temperature for an additional 2 hours. The reaction was then washed with water and EtOAc and dried over Na₂SO₄. Purification via column chromatography, DCM:MeOH, 10:1, gave the desired sulfoxonium ylide (**3.89**, 34%).

HRMS calcd. for C₁₉H₄₀NO₅SSi (M+H)⁺: 422.2324, found 422.2400.

¹H-NMR (400 MHz; CDCl₃): δ -0.00 (s, 6H), 0.84 (s, 9H), 1.39 (s, 9H), 1.78-1.69 (m, 2H), 2.19 (tt, *J* = 14.8, 7.4 Hz, 2H), 3.35 (d, *J* = 3.5 Hz, 6H), 3.54 (s, 2H), 4.35 (s, 1H), 4.75 (s, 1H). ¹³C NMR (101 MHz; CDCl₃): δ 0.03, 23.76, 31.37, 32.97, 33.91, 42.69, 47.67, 57.27, 70.54, 74.80, 84.31, 161.06, 195.72

[JMG-3-170, JMG-3-170C13]



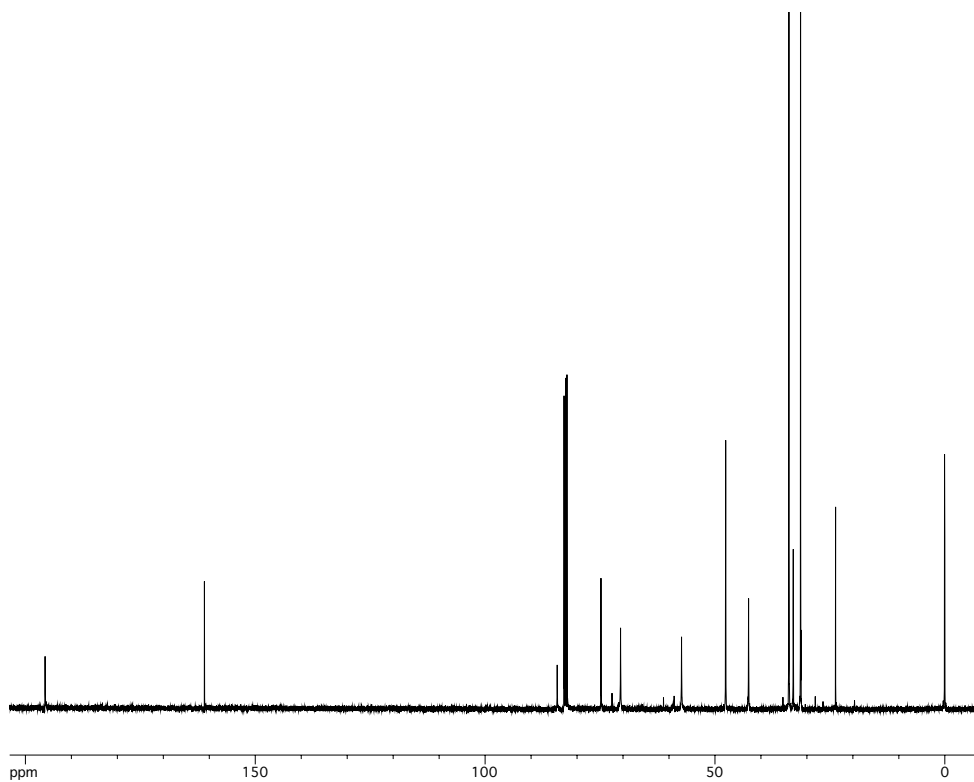


Figure 8.65. ^{13}C NMR of Tert-butyldimethylsilylether-sulfoxonium ylide (3.89)⁴³

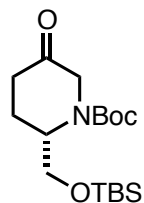


Figure 8.66. (*S*)-tert-butyl 2-(TBSO)methyl-5-oxopiperidine-1-carboxylate (3.90)⁴³

Degassed DCE (5mL) was heated to 70°C with [Ir(COD)Cl]₂ (4mg, 0.005mmol). **3.89** (209mg, 0.496mmol) was then dissolved in degassed DCE (5mL) and added via syringe pump to Ir solution over 18 hours. Reaction was pulled down and purified via column chromatography (4-10%).

HRMS calcd for C₁₇H₃₃NO₄SiNa (M+Na)⁺: 366.2077, found: 366.2067.

[JMG-2-34]

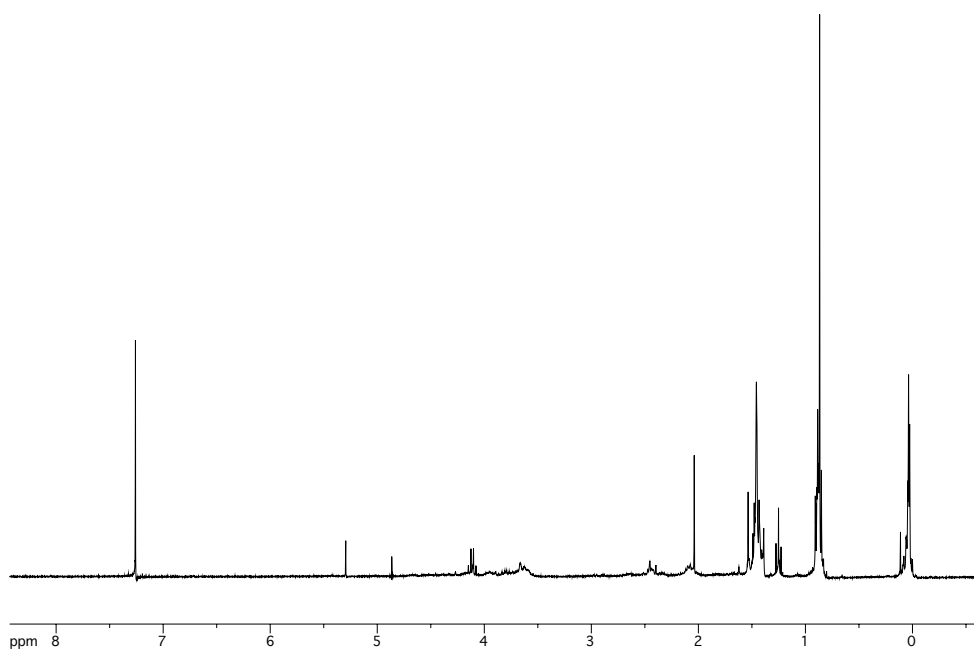


Figure 8.67. ^1H NMR of (*S*)-*t*-Bu 2-(TBSO)methyl)oxopiperidinecarboxylate (3.90)⁴³

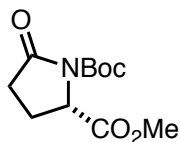


Figure 8.68. (S)-1-*tert*-butyl 2-methyl 5-oxopyrrolidine-1,2-dicarboxylate (3.91)

To the starting amide (**3.86**) (15.489mmol) was added MeOH (0.8M) and the solution was cooled to 0°C. SOCl₂ (17.038mmol) was added dropwise. The solution was warmed to room temperature and stirred for 2 hours. The reaction was slowly quenched by the addition of solid sodium bicarbonate until the exotherm stopped. The reaction was then filtered through a plug of Celite and washed with MeOH. The reaction was concentrated down and CHCl₃ was added to crash out the product (although this is not needed and the slightly impure compound can be take on to the next step). To the methyl ester was added CH₃CN (1M), followed by DMAP (10mol%, 1.151mmol), and Boc₂O (11.621mmol) and the reaction was stirred at room temperature overnight. The reaction was then concentrated and diluted with EtOAc, and washed with NaHSO₄ (10%) followed by brine and then dried over Na₂SO₄. Purification via column chromatography, hexane:EtOAc, 50:50, afforded a yellowish colored product (**3.91**). (63% over 2 steps)

HRMS calcd for C₁₁H₁₇NO₅Na (M+Na)⁺: 266.1004, found: 266.1013.

¹H-NMR (400 MHz; CDCl₃): δ 1.42 (s, 9H), 1.97 (ddt, *J* = 13.2, 6.4, 3.3 Hz, 1H), 2.31-2.20 (m, 1H), 2.42 (ddd, *J* = 17.5, 9.4, 3.7 Hz, 1H), 2.61-2.52 (m, 1H), 3.72 (s, 3H), 4.55 (dd, *J* = 9.4, 3.0 Hz, 1H). ¹³C NMR (101 MHz; CDCl₃): δ 21.46, 27.89, 31.11, 52.51, 58.79, 83.59, 149.24, 171.79, 173.14 [JMG-2-184, JMG-2-184C13]

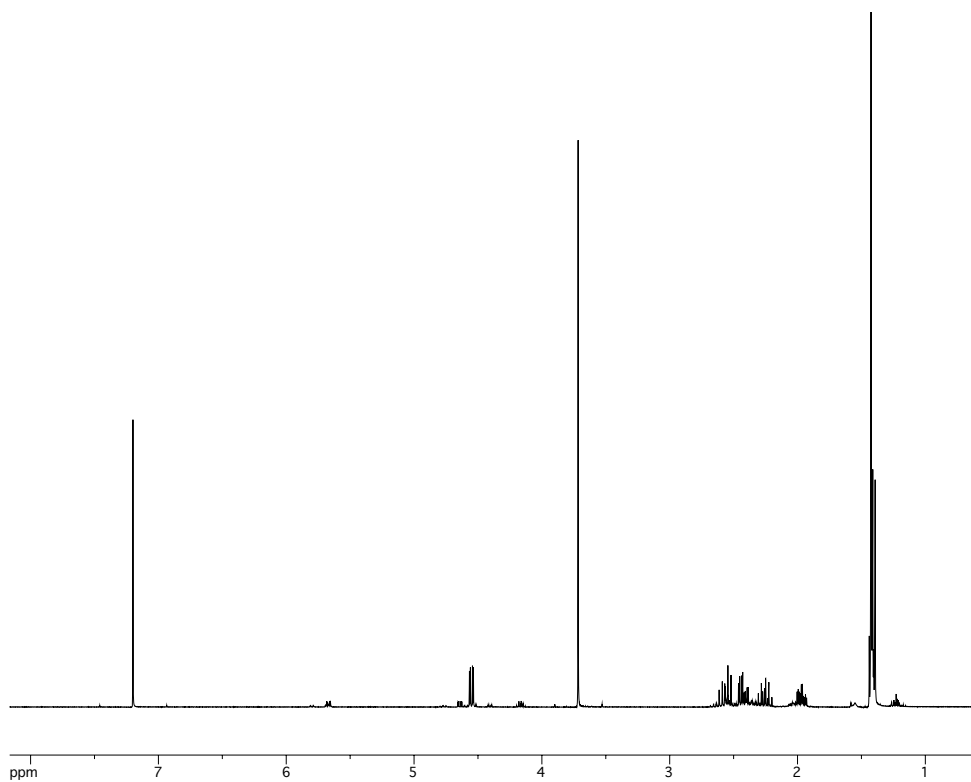


Figure 8.69. ^1H NMR (S)-1-*tert*-butyl methyl oxopyrrolidine-1,2-dicarboxylate (3.91)

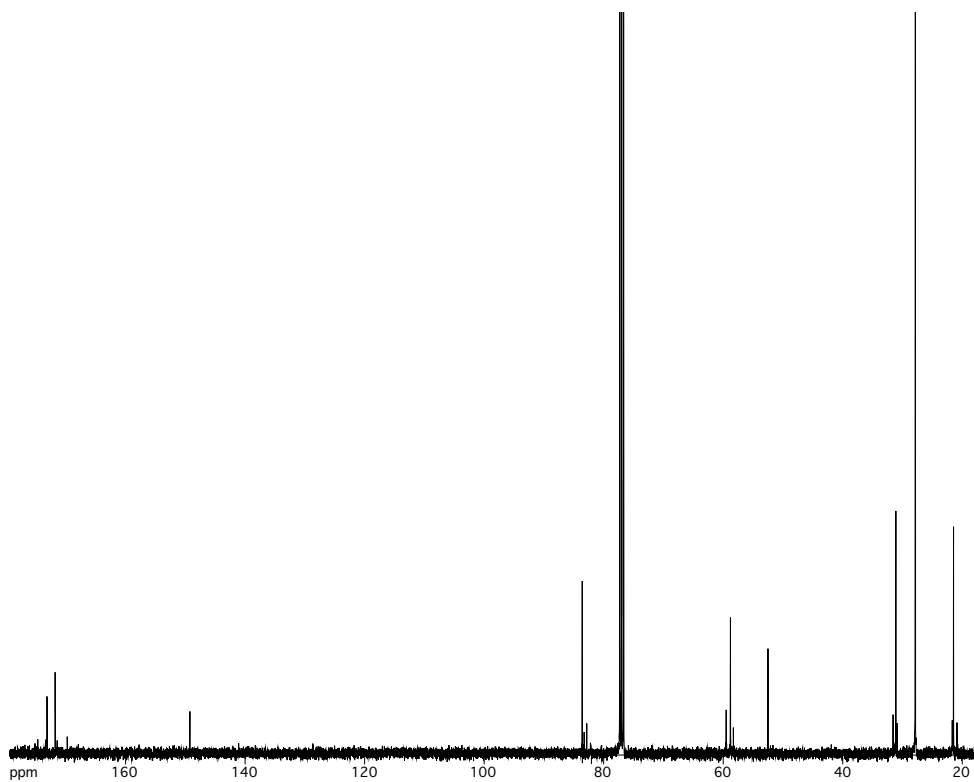


Figure 8.70. ^{13}C NMR (S)-1-*tert*-butyl methyl oxopyrrolidine-1,2-dicarboxylate (3.91)

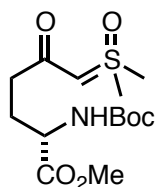


Figure 8.71. Methylester Sulfoxonium Ylide (3.92)⁴³

(CH₃)₃SOCl (3.5eq, 2.878mmol) and KO^tBu (3.5eq, 2.878mmol) and THF (0.2M) were refluxed for 2 hours. The mixture was allowed to cool to room temperature and then the **3.91** was added and the reaction was stirred an additional 2 hours at room temperature. After completion, the reaction was washed with water (100mL) and extracted with EtOAc and dried over Na₂SO₄ and concentrated giving the desired compound in yield following purification via column chromatography, DCM:MeOH, 10:1 (27%).

HMRS calcd. for C₁₄H₂₆NO₆S (M+H⁺): 336.1411, found 336.1477.

¹H-NMR (400 MHz; CDCl₃): δ 1.37 (s, 9H), 1.93-1.83 (m, 1H), 2.13-1.98 (m, 1H), 2.39-2.17 (m, 2H), 3.34 (s, 6H), 3.67 (s, 3H), 4.24-4.05 (m, 1H), 4.33 (bs, 1H), 5.40 (d, *J* = 7.8 Hz, 1H). ¹³C NMR (101 MHz; cdcl₃): δ 24.83, 28.32, 36.20, 42.20, 52.18, 53.35, 55.91, 69.62, 79.65, 82.39, 155.44, 170.98, 173.11, 188.87

[JMG-3-165, JMG-3-165C13]

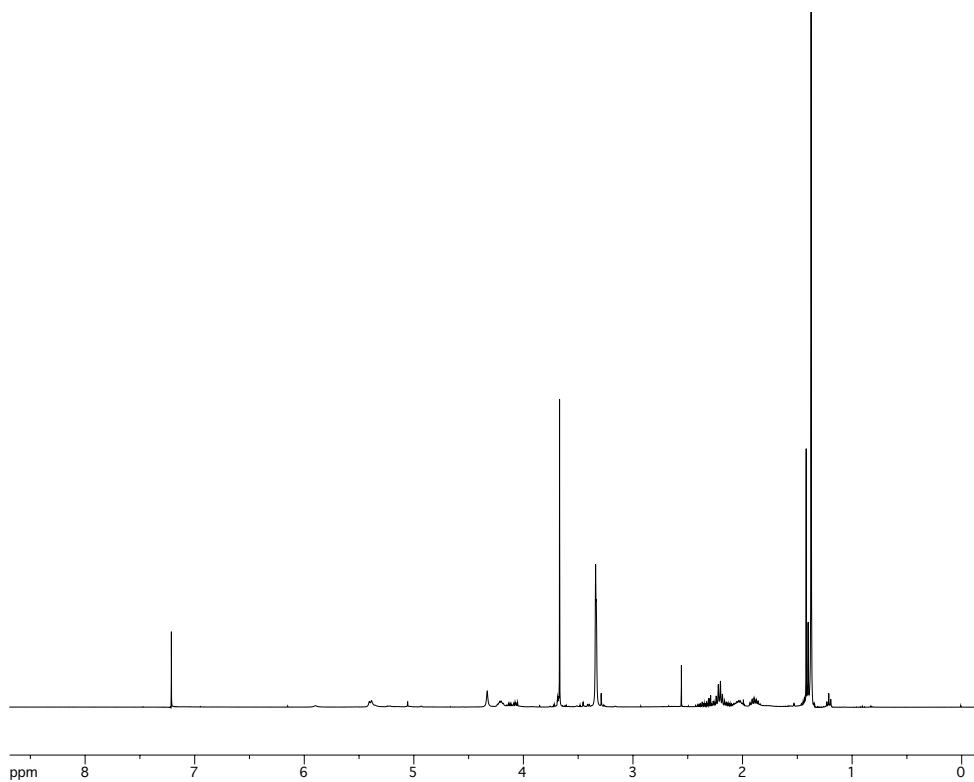


Figure 8.72. ^1H NMR of Methylester Sulfoxonium Ylide (3.92)⁴³

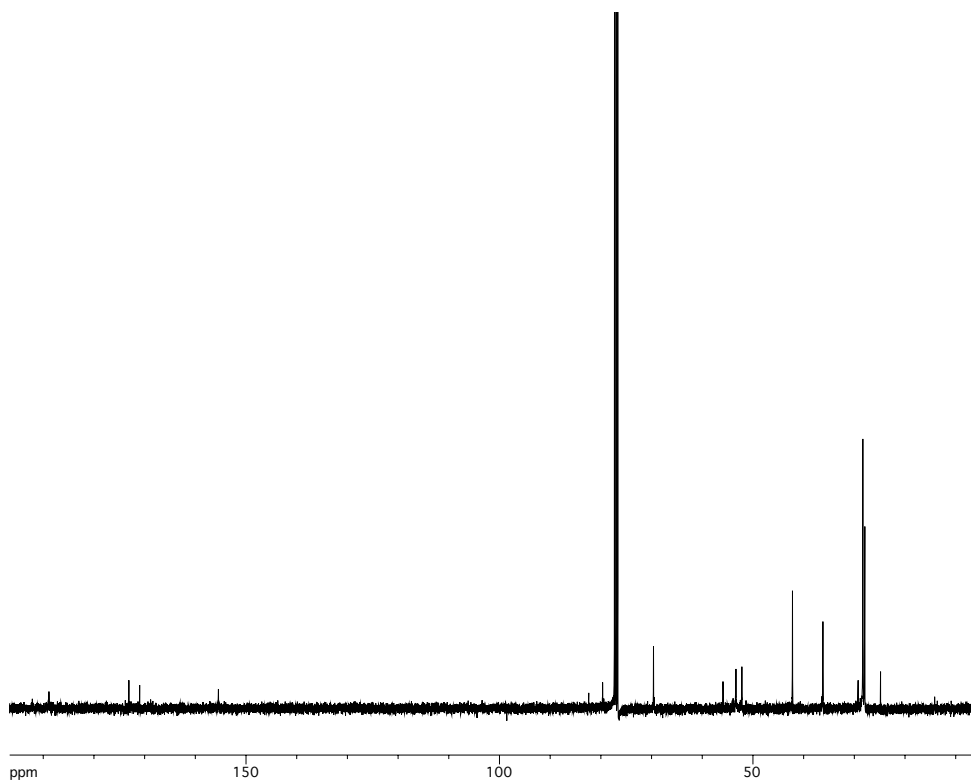


Figure 8.73. ^{13}C NMR of Methyl ester Sulfoxonium Ylide (3.92)⁴³

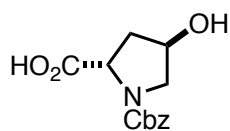


Figure 8.74. 1-((benzyloxy)carbonyl)-4-hydroxypyrrolidine-2-carboxylic acid (3.95)⁴⁵

To **3.94** (6.76g, 51.556mmol) in DCM (112mL) in a 3-neck round-bottomed flask under argon was added Hünigs base (27mL, 154.668mmol) followed by a slow addition of TMSCl (24.5mL, 193.335mmol) and the reaction was stirred vigorously for 1.5 hours. The reaction was then cooled to 0°C and CbzCl (7mL, 48.978mmol) was added. The reaction was sealed and warmed to room temperature overnight. The reaction was then transferred to a single neck round bottomed flask and concentrated and dissolved in 2.5% sodium bicarbonate solution and extracted into Et₂O. The aqueous layer was acidified to pH=2 with 1N HCl and then extracted with EtOAc and dried over Na₂SO₄ and concentrated to give the desired product (**3.95**) without further purification (82%).

[JMG-2-135, JMG-2-135C13]

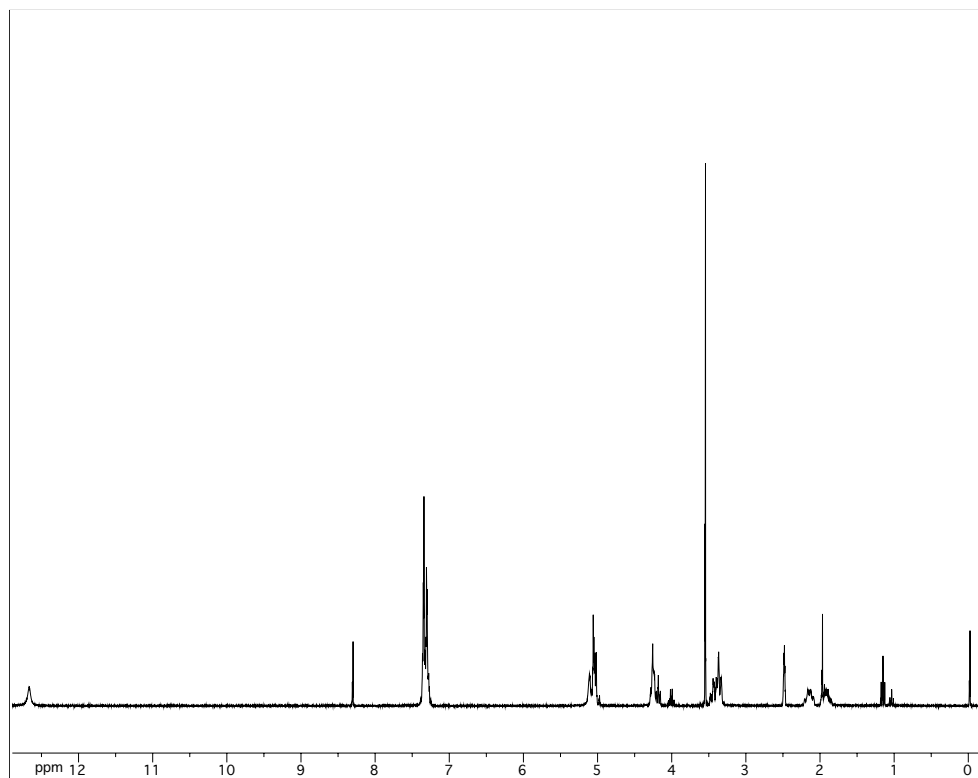


Figure 8.75. ^1H NMR of 1-((BnO)carbonyl)hydroxypyrrolidinecarboxylic acid (3.95)⁴⁵

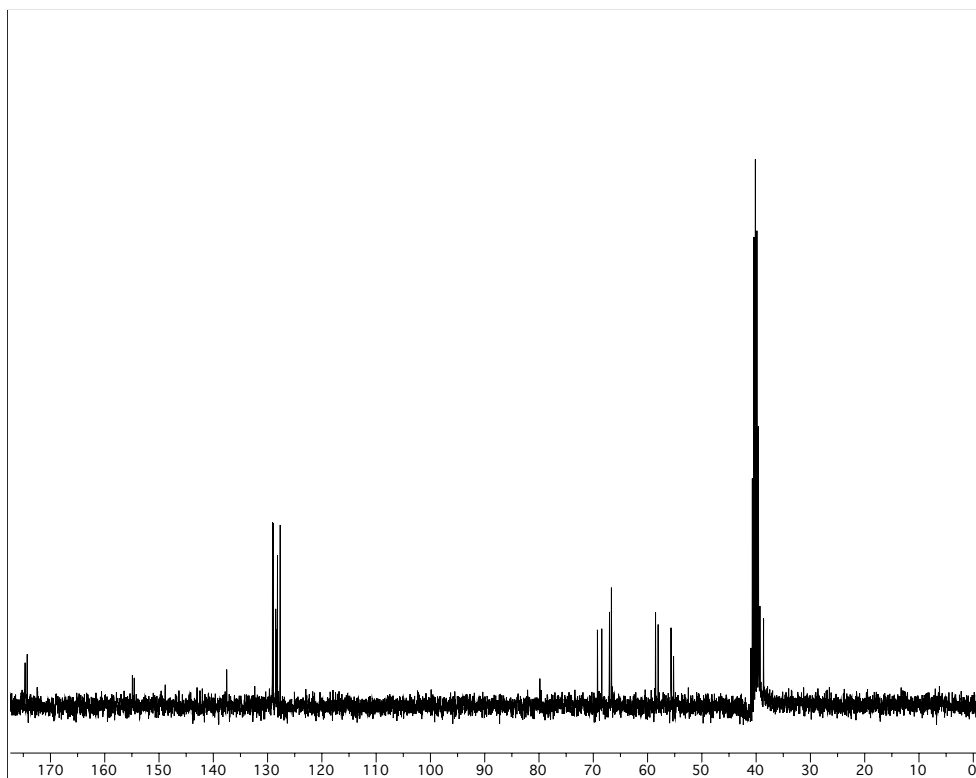


Figure 8.76. ^{13}C NMR of 1-((BnO)carbonyl)hydroxypyrrolidinecarboxylic acid (3.95)⁴⁵

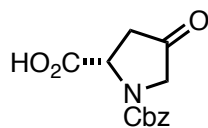


Figure 8.77. (S)-1-benzyl 2-tert-butyl 4-oxopyrrolidine-1,2-dicarboxylate (3.96)⁴⁵

Jones Reagent: Dissolve CrO_3 (4.54g, 45.389mmol) in 2.6mL concentrated H_2SO_4 , then cool to 0°C and add, CAUTIOUSLY, 5.7mL of water.

3.95 was dissolved in acetone, (110mL, 0.05M) and cooled to 0°C . Jones reagent was cannulated into the SM/acetone solution over 10 minutes and the reaction was stirred for 3 hours. The reaction was then cooled back to 0°C and MeOH was added to quench the remaining Jones reagent. Filtration and purification via column chromatography yielded the desired product (quant).

[JMG-2-136, JMG-2-136C13]

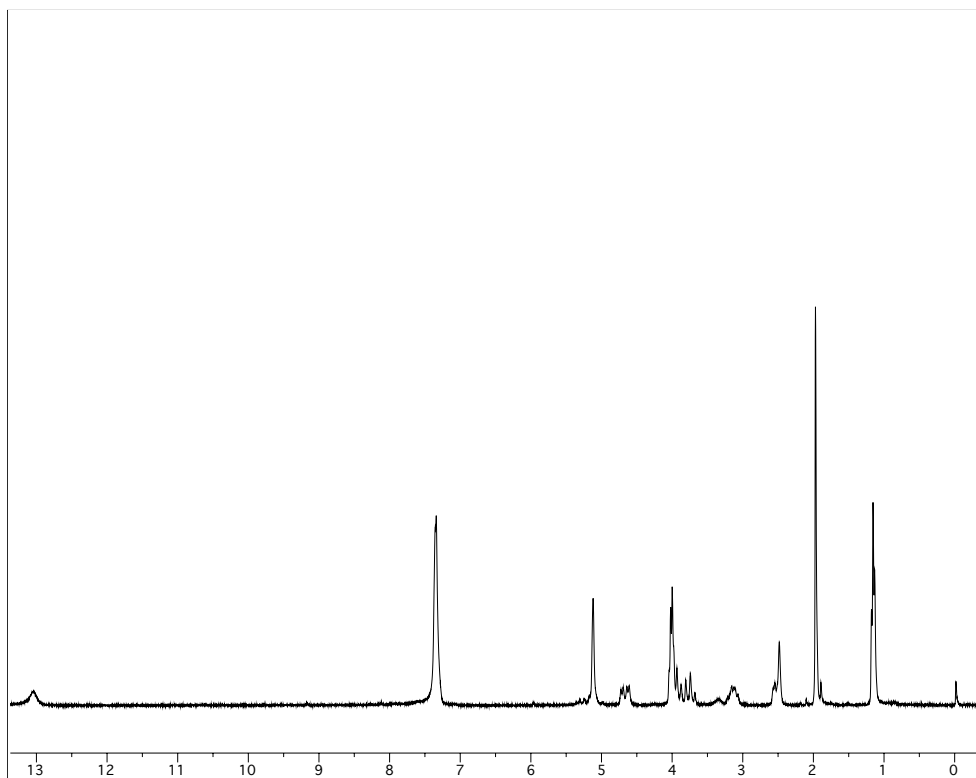


Figure 8.78. ^1H NMR of (S)-1-benzyl tert-butyl oxopyrrolidine dicarboxylate (3.96)⁴⁵

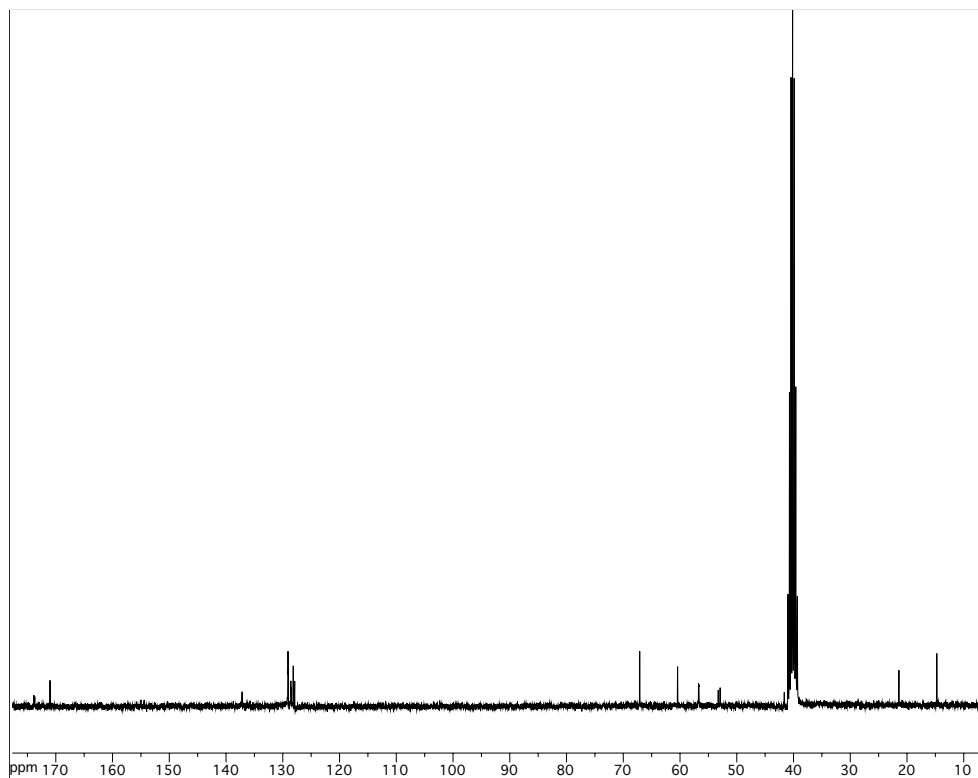


Figure 8.79. ^{13}C NMR of (S)-1-benzyl tert-butyl oxopyrrolidine dicarboxylate (3.96)⁴⁵

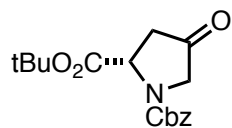


Figure 8.80. (S)-1-benzyl 2-*tert*-butyl oxopyrrolidine-2-carboxylate (3.97)^{45,188}

3.96 (200mg, 0.760mmol) was dissolved in *t*BuOH (500 μ l, 1.159mmol) and MgCl₂ (7mg, 0.076mmol) and Boc₂O (216mg, 0.988mmol) were added and the reaction was heated to 40°C for overnight. Reaction was then cooled to room temperature and water (50mL) and EtOAc was added and the mixture was extracted and dried over MgSO₄, (24%).

[JMG-2-153]

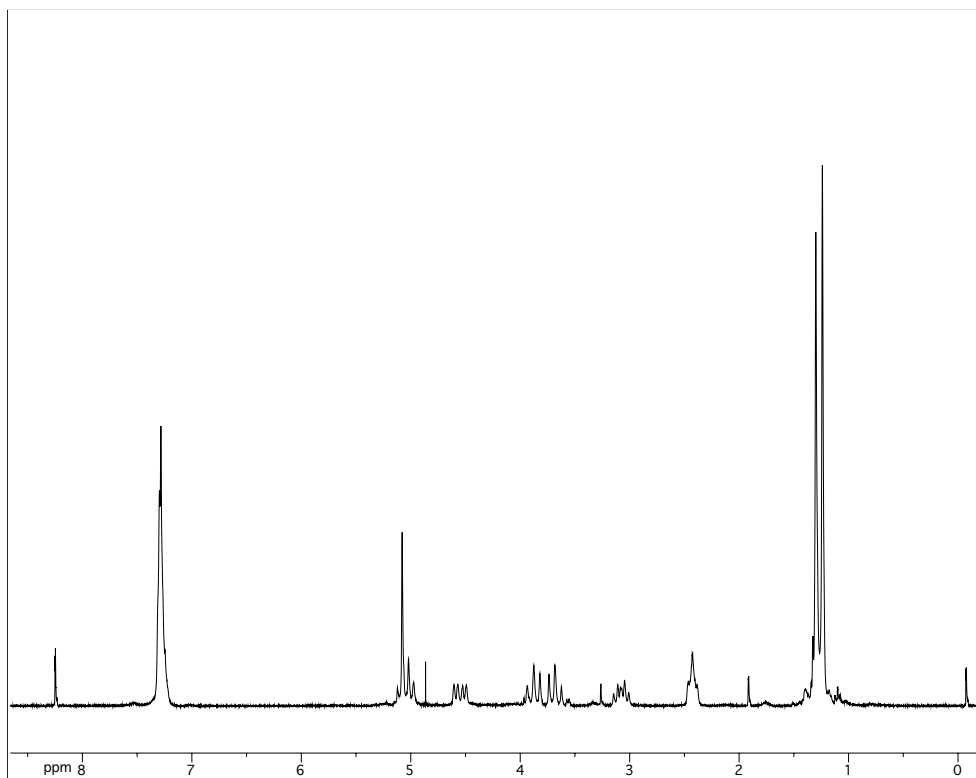


Figure 8.81. ^1H NMR of (S)-1-benzyl *tert*-butyl oxopyrrolidine dicarboxylate (3.97)^{45,188}

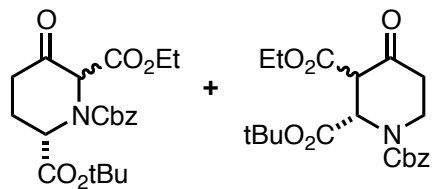


Figure 8.82. (6S)- tricarboxylate (3.98) & (2S)- tricarboxylate (3.99)⁴⁵

3.97 (147mg, 0.460mmol) was dissolved in Et₂O (0.25M) and was cooled to 5°C and BF₃•Et₂O (60μl, 0.483mmol) was added followed by EDA (73μl, 0.690mmol). The ice bath was removed and the reaction was allowed to stir at room temperature for 1 hour. The reaction was the diluted with Et₂O and washed with NH₄Cl, then brine and dried over MgSO₄, (15.25%).

HRMS calcd for C₂₁H₂₈NO₇Na (M+Na)⁺: 428.1866, found: 428.1674

[JMG-2-158T, JMG-2-158TC13]

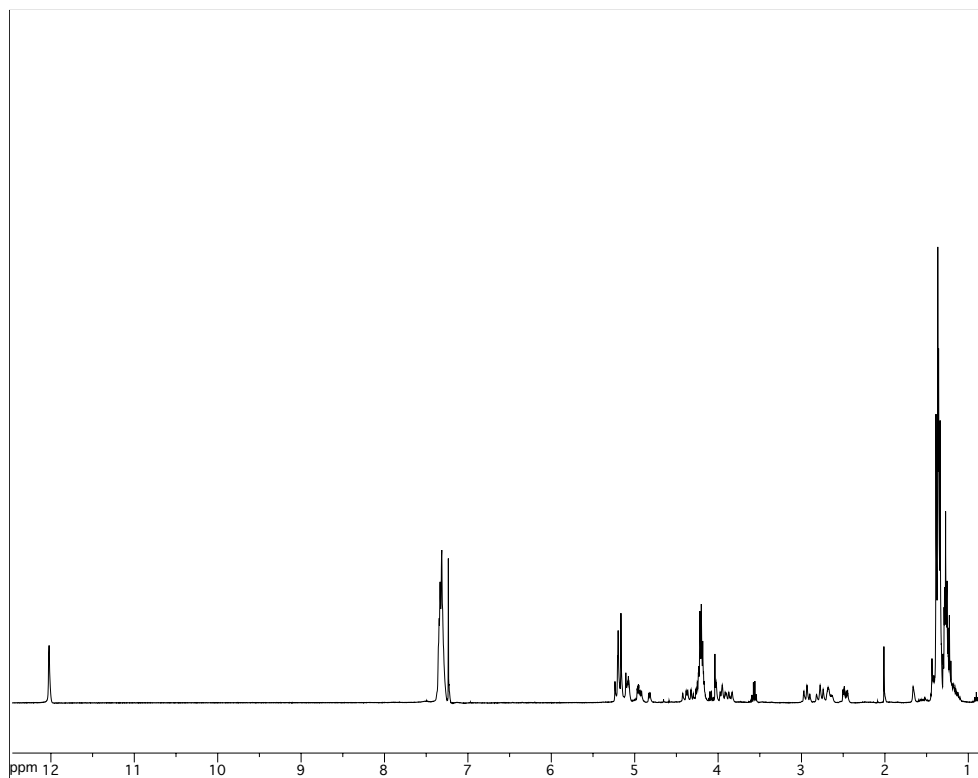


Figure 8.83. ^1H NMR of (6S)- tricarboxylate (3.98) & (2S)- tricarboxylate (3.99)⁴⁵

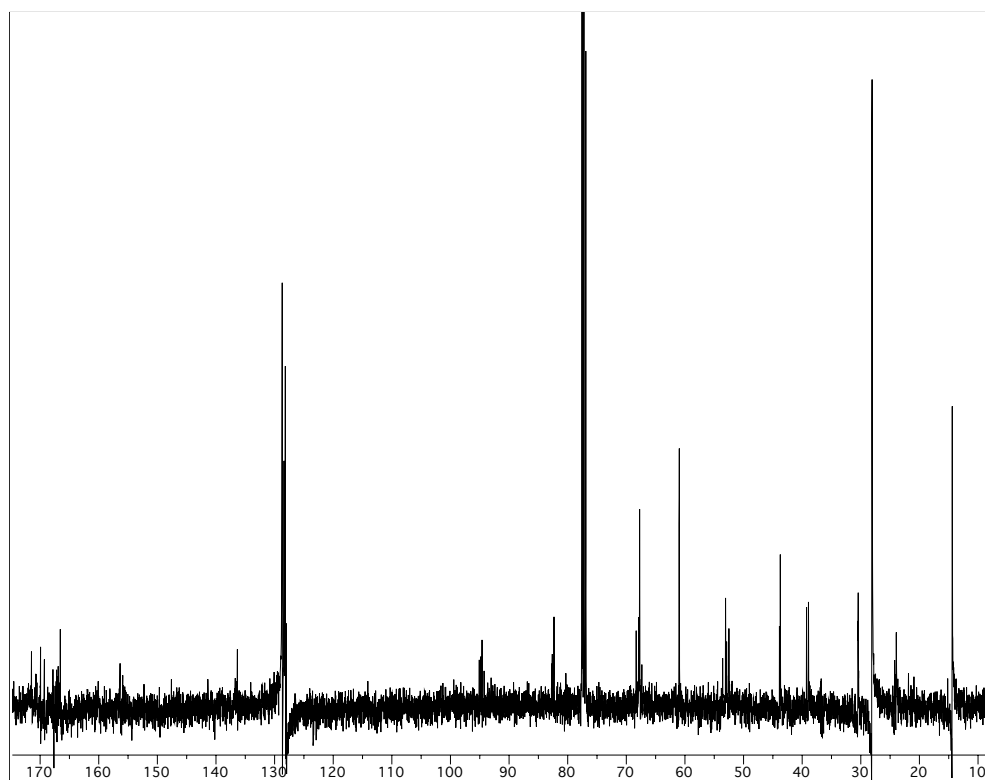


Figure 8.84. ^{13}C NMR of (6S)- tricarboxylate (3.98) & (2S)- tricarboxylate (3.99)⁴⁵

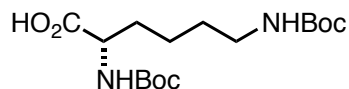


Figure 8.85. (S)-2,6-bis((tert-butoxycarbonyl)amino)hexanoic acid (3.101)⁴⁶

To L-Lysine (**3.100**) (5g, 27.369mmol), in water and dioxane (0.18M each) was added Boc_2O (12.5g, 60.212mmol) and NaOH (3.3g, 109.476mmol). The reaction was refluxed at 60°C for 6 hours. After the reaction was allowed to cool to room temperature, it was concentrated down and then diluted with EtOAc and 2N HCl was added until the solution was acidic. The organic layer was then washed with $\text{NaHSO}_4(\text{sat})$ (200mL) and then the aqueous layer was extracted with CHCl_3 . The organic layers were combined and dried over Na_2SO_4 . The crude product (**3.101**) was taken on to the next step without further purification.

[JMG-2-208, JMG-2-208C13]

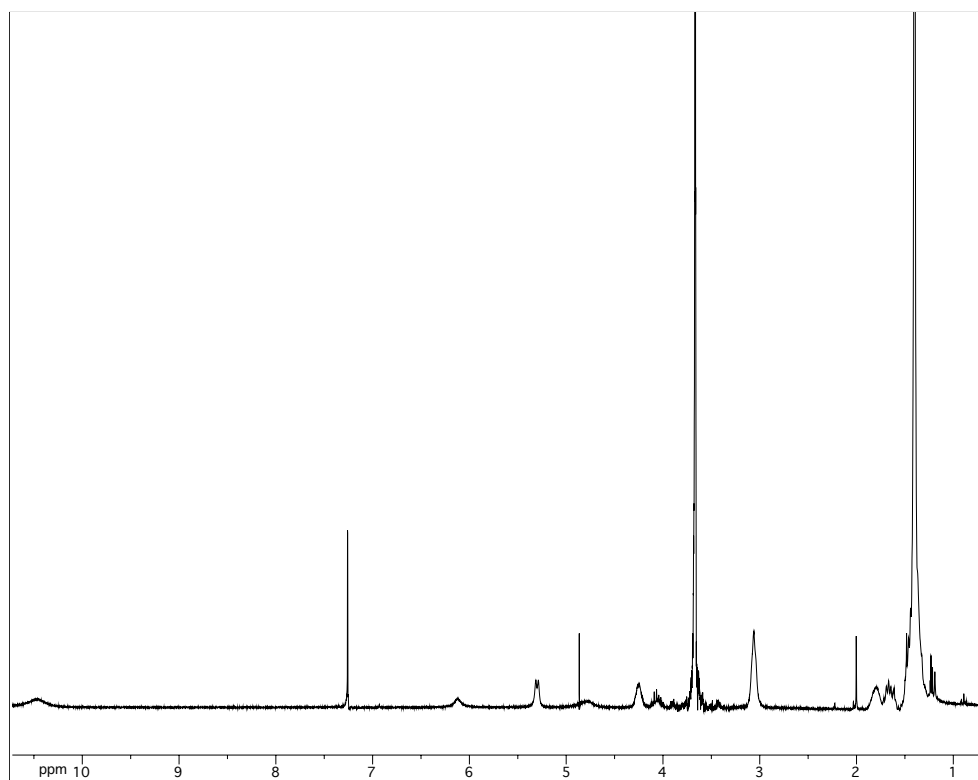


Figure 8.86. ^1H NMR of (S)-2,6-bis((Boc)amino)hexanoic acid (3.101)⁴⁶

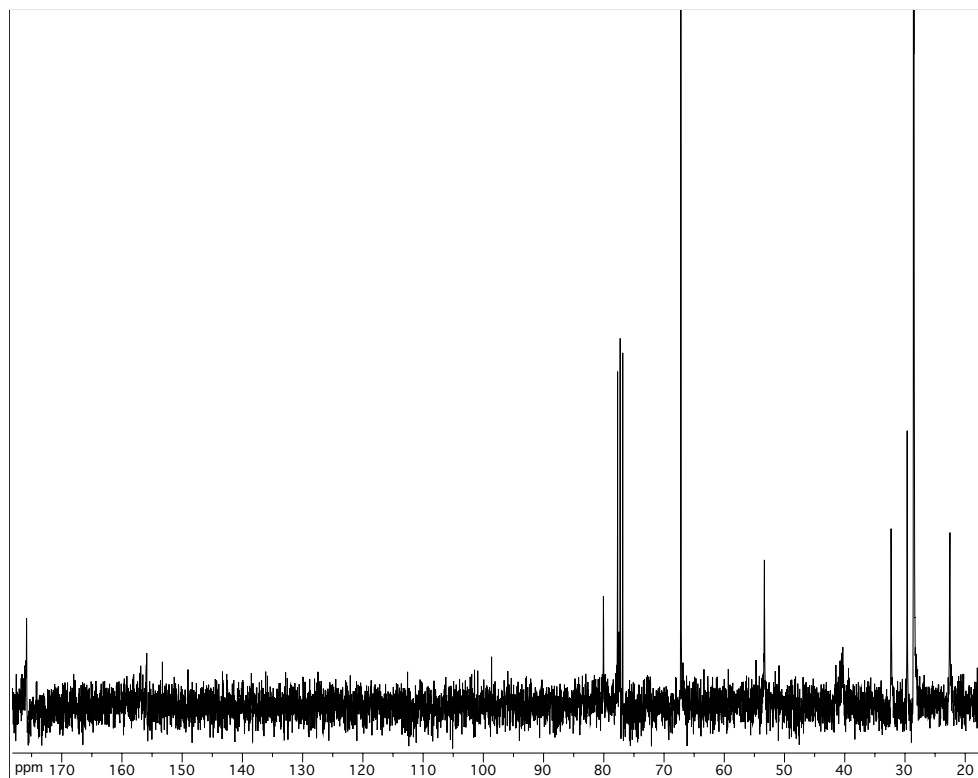


Figure 8.87. ^{13}C NMR of (S)-2,6-bis((Boc)amino)hexanoic acid (3.101)⁴⁶

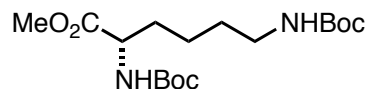


Figure 8.88. (S)-methyl 2,6-bis((Boc)amino)hexanoate (3.102**)**⁴⁶

To starting acid (**3.101**) (5.71g, 16.434mmol) and DMF (0.5M) at 0°C was added KHCO_3 (3.3g, 32.966mmol), and MeI (1.6mL, 24.724mmol). The ice bath was removed and the reaction was stirred at room temperature overnight. The reaction was then diluted with EtOAc and washed with water (2 x 200mL) then brine (3 x 100mL) and dried over Na_2SO_4 and concentrated. Purification via column chromatography, hexanes:EtOAc, 70:30 provided the desired methyl ester (**3.102**, 80%).

[JMG-2-211DMSO]

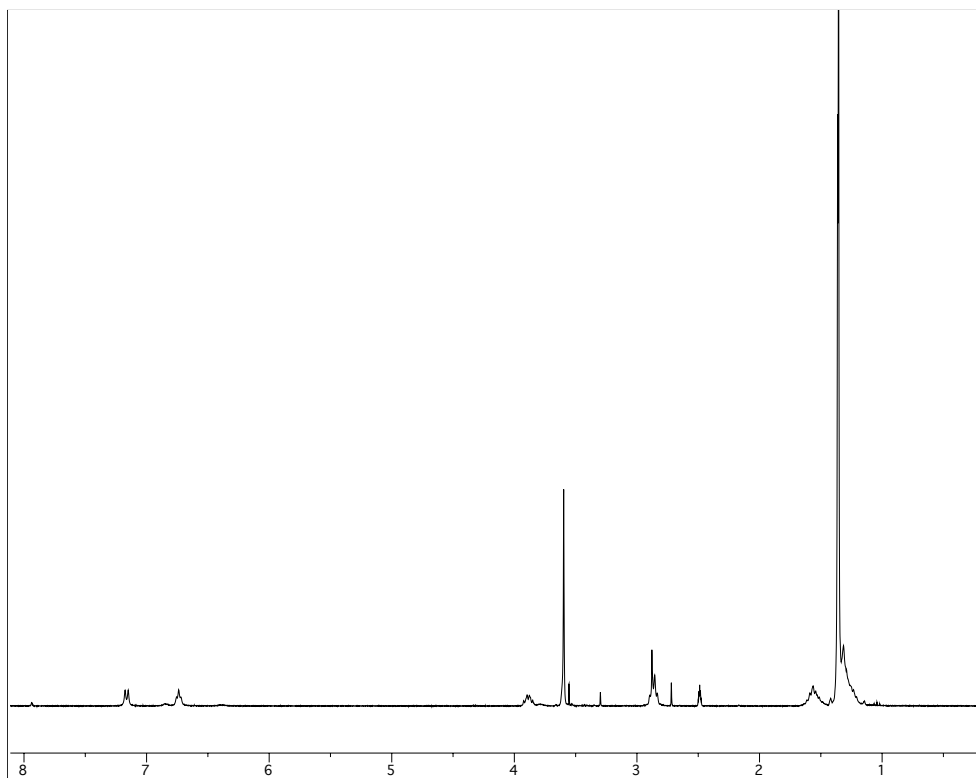


Figure 8.89. ^1H NMR of (S)-methyl 2,6-bis((Boc)amino)hexanoate (3.102)⁴⁶

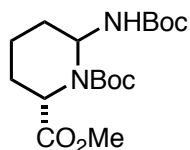


Figure 8.90. Dicarboxylate (3.103)⁴⁶

To the fully protected L-Lysine (**3.102**) (1g, 2.774mmol) was added a saturated solution of NaOAc in AcOH (12mL). To this solution was added $\text{Mn}(\text{OAc})_2 \cdot 4\text{H}_2\text{O}$ (50mg, 0.194mmol). Acetic peracid (2.2mL) was then added dropwise (VERY slowly) over several hours. The reaction was allowed to stir until SM was consumed. The reaction was then dumped into a 50:50 mix of EtOAc:hexane and the aqueous layer was removed and further washed with hexanes. The combined organic layers were then washed with water and then brine and the dried over Na_2SO_4 and then concentrated (67% combined).

[JMG-2-215-S1, JMG-2-215-S1C13]

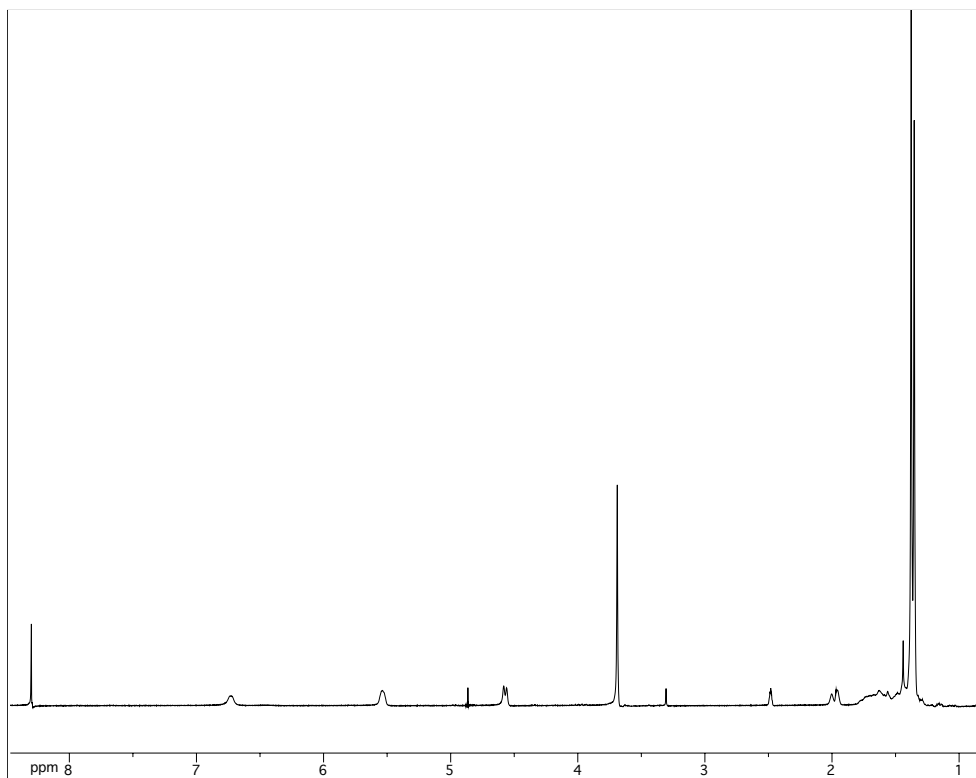


Figure 8.91. ^1H NMR of Dicarboxylate (3.103)⁴⁶

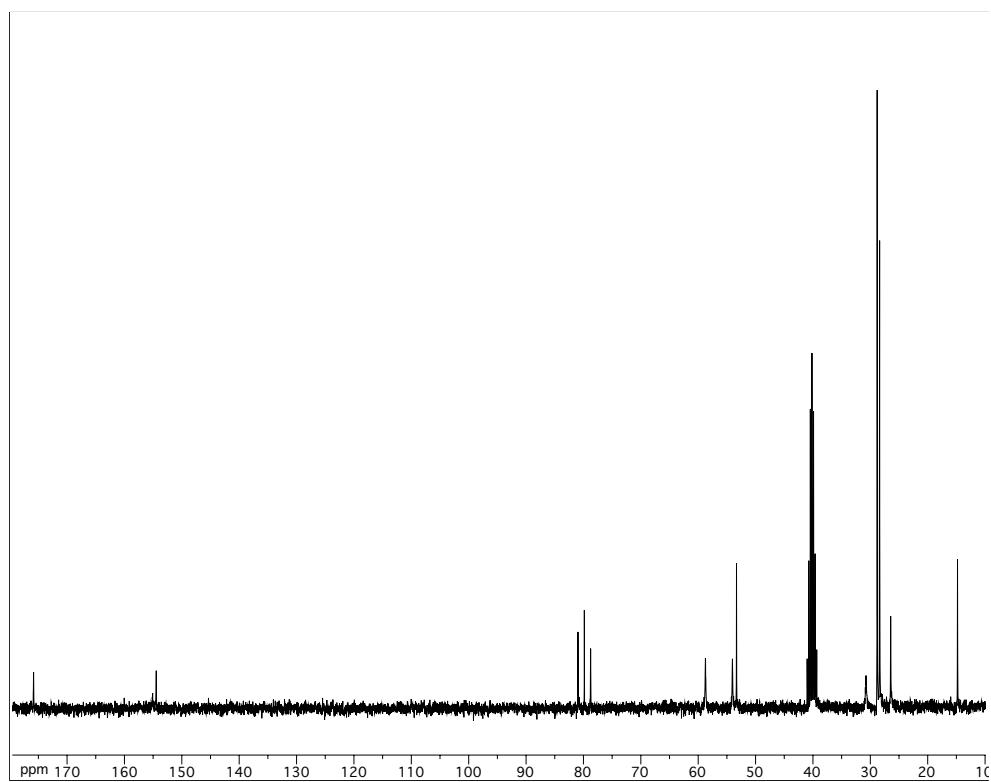


Figure 8.92. ^{13}C NMR of Dicarboxylate (3.103)⁴⁶

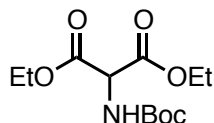


Figure 8.93. Diethyl-2-((Boc)amino)malonate (3.107)⁴⁸

To starting malonate (**3.106**) (25g, 118.125mmol) was added dioxane (200mL) followed by 1N NaOH (120mL). The reaction mixture was cool to 0°C and then Boc₂O (25.8g, 118.125mmol) in 50mL dioxane was added. The reaction was allowed to warm to room temperature and stirred overnight. The reaction was then concentrated and diluted with EtOAc (300mL) and washed with NH₄Cl_{aq}(300mL), then brine (300mL) and dried over Na₂SO₄. The crude product was taken on to the next step without purification (~81%).

[JMG-2-253]

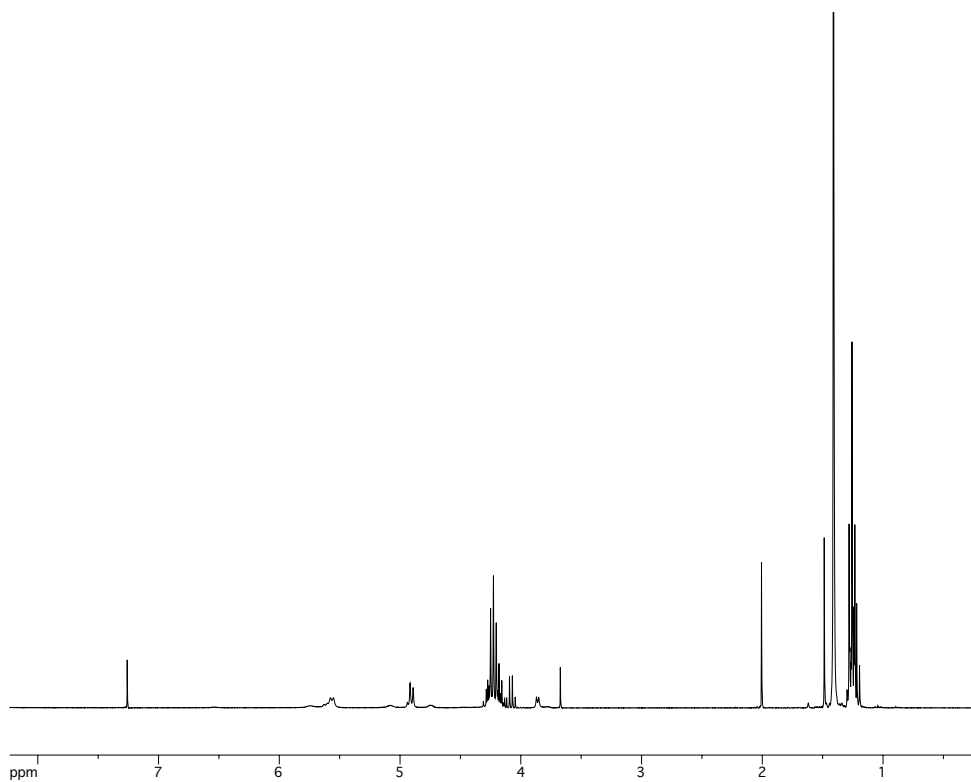


Figure 8.94. ^1H NMR of Diethyl-2-((Boc)amino)malonate (3.107)⁴⁸

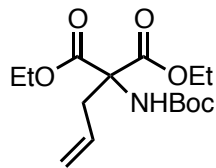


Figure 8.95. Diethyl 2-allyl-2-((Boc)amino)malonate (3.108)⁴⁸

To the starting Boc protected malonate (**3.107**) (31.28g, 113.622mmol) was added ethanol (30mL). Sodium metal (3.13g, 136.346mmol) that had been dissolved in 150mL of ethanol was then cannulated into the reaction and stirred for 30 minutes. Allyl bromide (9.8mL, 113.622mmol) was added and the system was refluxed at 85°C for 4 hours. The reaction was then concentrated and diluted in EtOAc (300mL) and washed with $\text{NH}_4\text{Cl}_{\text{aq}}$ (300mL) and then brine (300mL). The organic extracts were dried over Na_2SO_4 and concentrated and taken on to the next step without purification (80%).

[JMG-2-254]

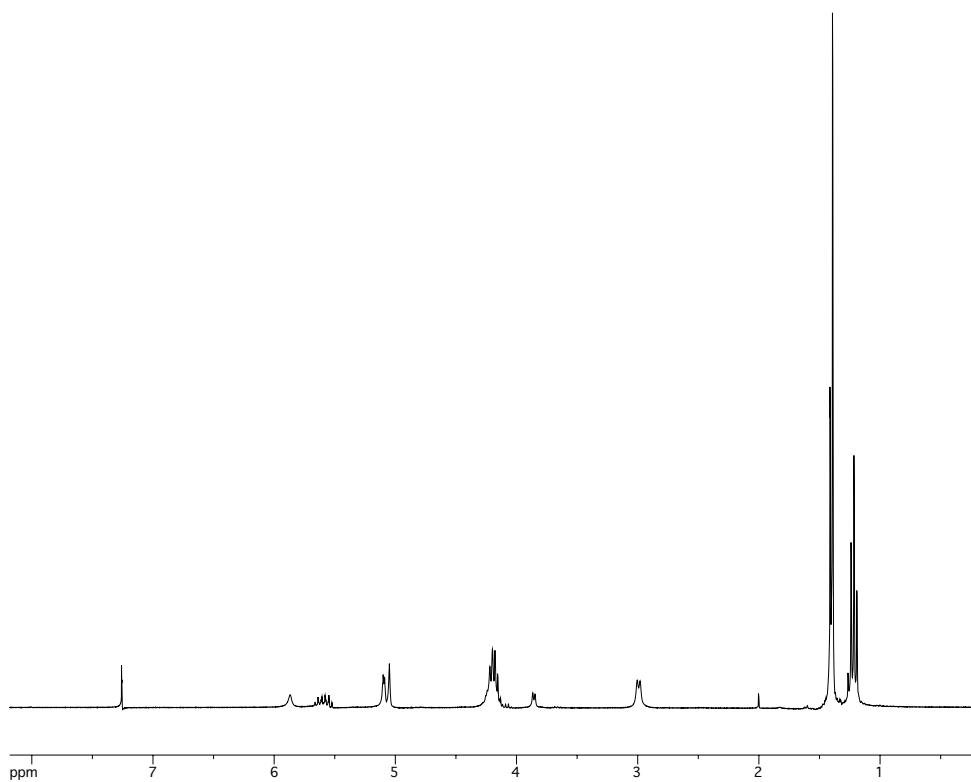


Figure 8.96. ^1H NMR of Diethyl 2-allyl-2-((Boc)amino)malonate (3.108)⁴⁸

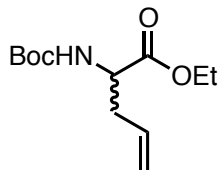


Figure 8.97. Ethyl 2-((tert-butoxycarbonyl)amino)pent-4-enoate (3.109)⁴⁸

3.108 (19g, 60.259mmol) was dissolve in EtOH (40mL) and 1N NaOH (40mL). The reaction was then stirred at room temperature for 16 hours. The reaction was then acidified to pH~3 with 1N HCl and then concentrated down and diluted with EtOAc (200mL). The reaction was then extracted with brine (150mL), dried over Na₂SO₄, concentrated and redissolved in xylenes and refluxed over night. The reaction was then concentrated and extracted with EtOAc and brine to afford racemic N-Boc-allylglycine ethylester. The crude product was taken on to the resolution without further purification (89%).

[JMG-2-264-R2]

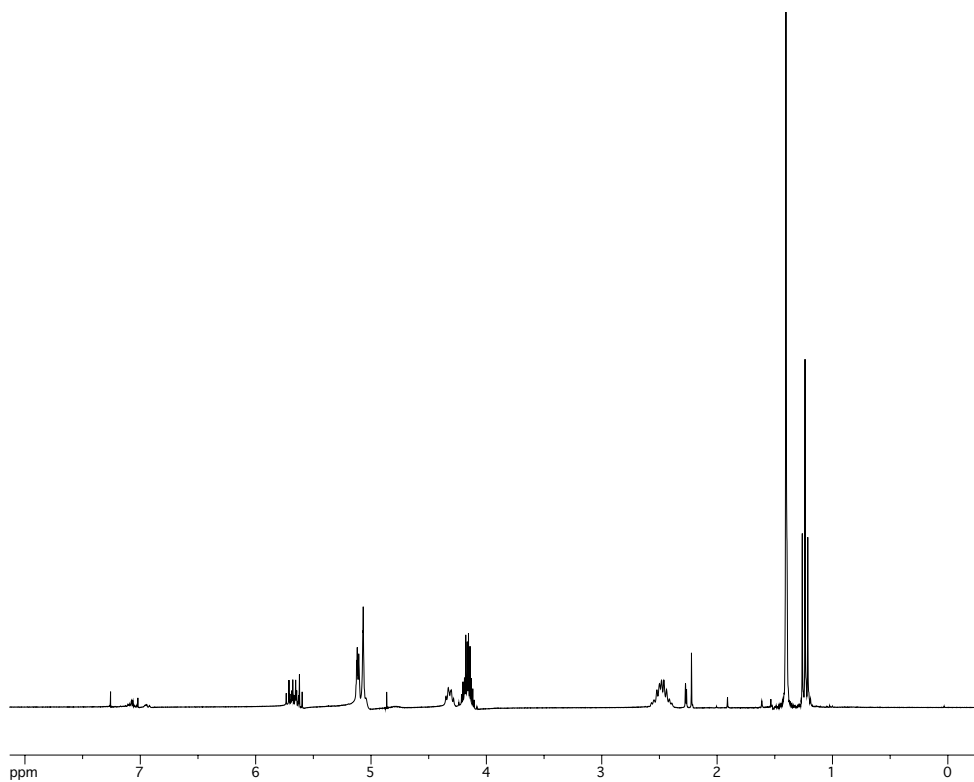


Figure 8.98. ^1H NMR of Ethyl 2-((tert-butoxycarbonyl)amino)pent-4-enoate (3.109)⁴⁸

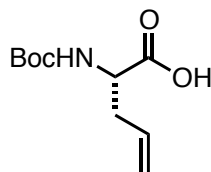


Figure 8.99. (*S*)-2-((*tert*-butoxycarbonyl)amino)pent-4-enoic acid (**3.110**)⁴⁸

To the racemic malonate (**3.109**) (6.04g, 24.825mmol) was added a phosphate buffer (pH=8, 415mL) and α -chymotrypsin (30mg, 75units/mg). The reaction was kept at 37°C and 1N NaOH was added dropwise to maintain the pH of the system at 7-8 overnight. The reaction was then extracted with EtOAc several times. The aqueous layer was then acidified with 2N HCl to pH=3 and was extracted with EtOAc (3 X 100mL). The organic layer was dried over Na₂SO₄ and concentrated to yield (*S*)-N-Boc-allylglycine (**3.110**, 84%, 94%ee).

[JMG-2-271]

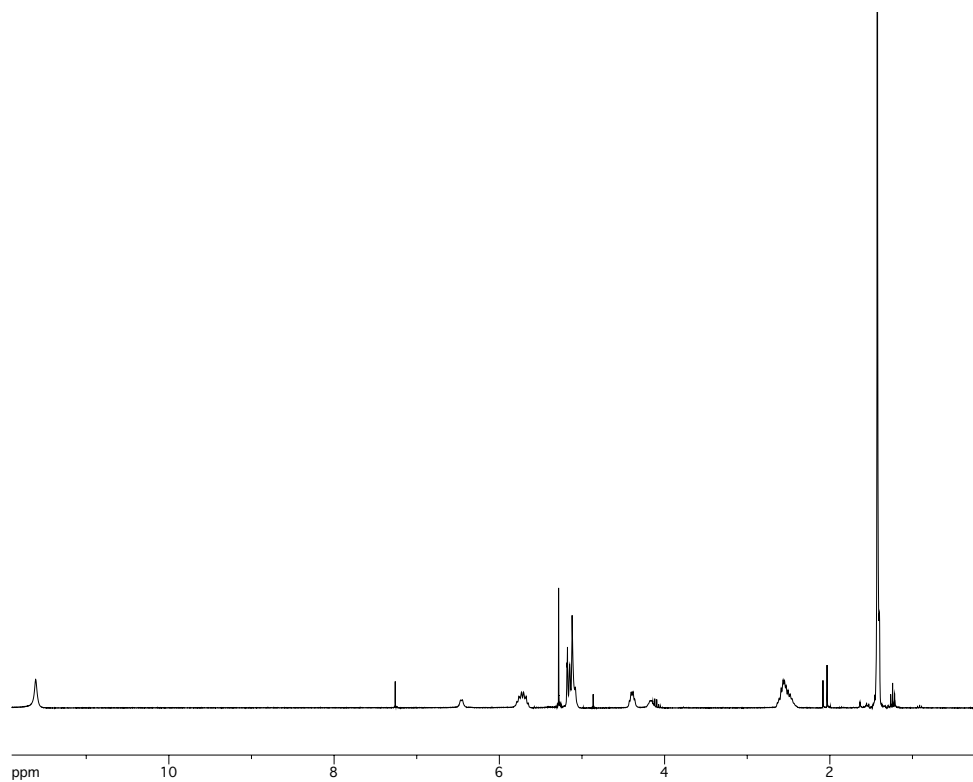


Figure 8.100. ^1H NMR of (S)-2-((Boc)amino)pent-4-enoic acid (3.110)⁴⁸

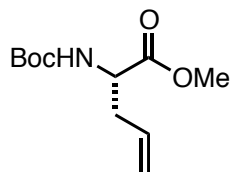


Figure 8.101. (S)-methyl 2-pent-4-enoate (3.111)⁴⁸

The free acid (**3.110**) (612mg, 2.843mmol) was dissolved in acetone (0.1M, 28mL) and K_2CO_3 (569mg, 5.686mmol) and MeI (265 μ l, 4.265mmol) were added and the reaction was allowed to stir at room temperature over night. The reaction was then concentrated and diluted with EtOAc and washed with sodium bicarbonate (100mL) then brine (100mL) and dried over Na_2SO_4 and concentrated. The crude mixture was dry loaded onto SiO_2 and run through a plug with hexanes:EtOAc (50:50) to afford the methyl ester (**3.111**) in 63% yield.

[JMG-2-272, JMG-2-272C13]

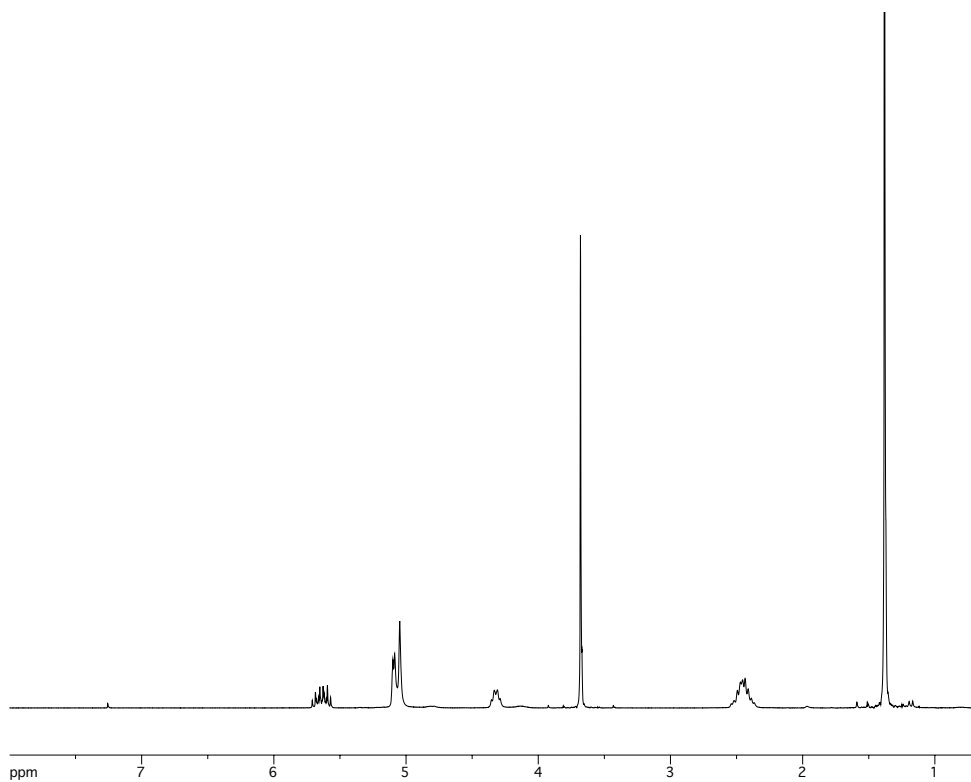


Figure 8.102. ^1H NMR of (S)-methyl 2-pent-4-enoate (3.111)⁴⁸

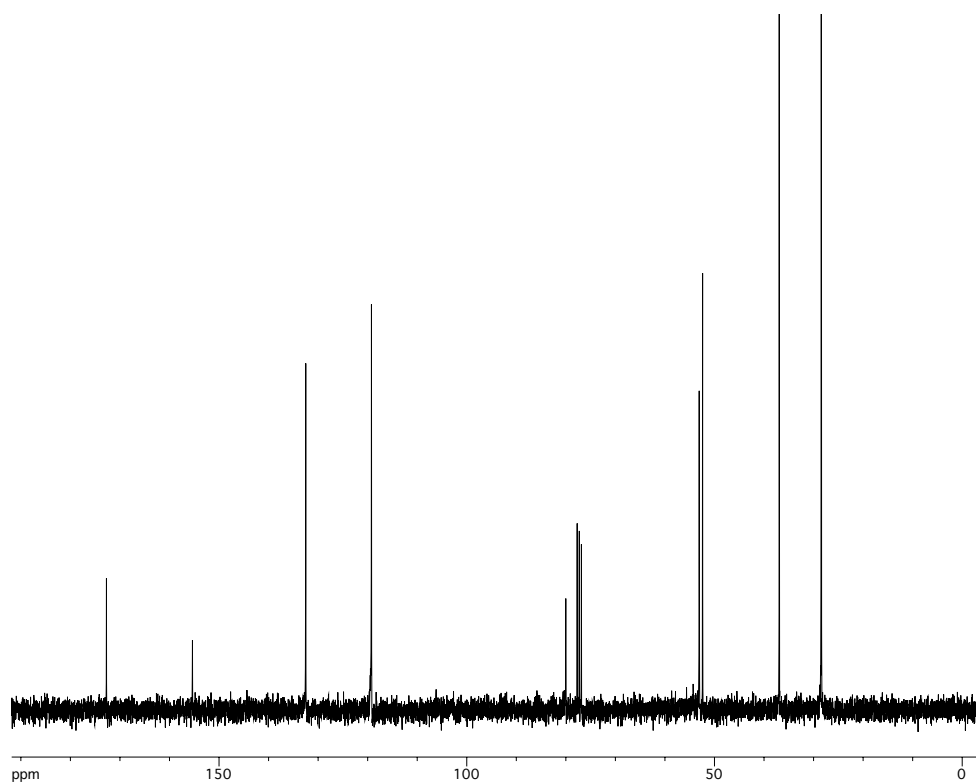


Figure 8.103. ^{13}C NMR of (*S*)-methyl 2-pent-4-enoate (3.111)⁴⁸

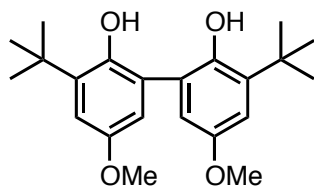


Figure 8.104. 3,3'-di-tert-butyl-5,5'-dimethoxy-[1,1'-biphenyl]-2,2'-diol (**3.114**)⁴⁹

$K_3Fe(CN)_6$ (9.14g, 27.741mmol) and KOH (5.56g, 99.035mmol) was dissolved in water (150mL). To the starting phenol (**3.113**) (5g, 27.741mmol) was added MeOH (150mL) and the water/iron mixture previously made was added drop-wise over 1 hour at room temperature. After the addition was complete, the reaction was stirred for an additional 2 hours at room temperature. 90mL of water was then added and the reaction was extracted with EtOAc. The aqueous layer was then extracted with Et_2O (3 x 200mL). The organic layers were combined and extracted with brine (2 X 200mL) and dried over Na_2SO_4 (95%).

[JMG-2-266]

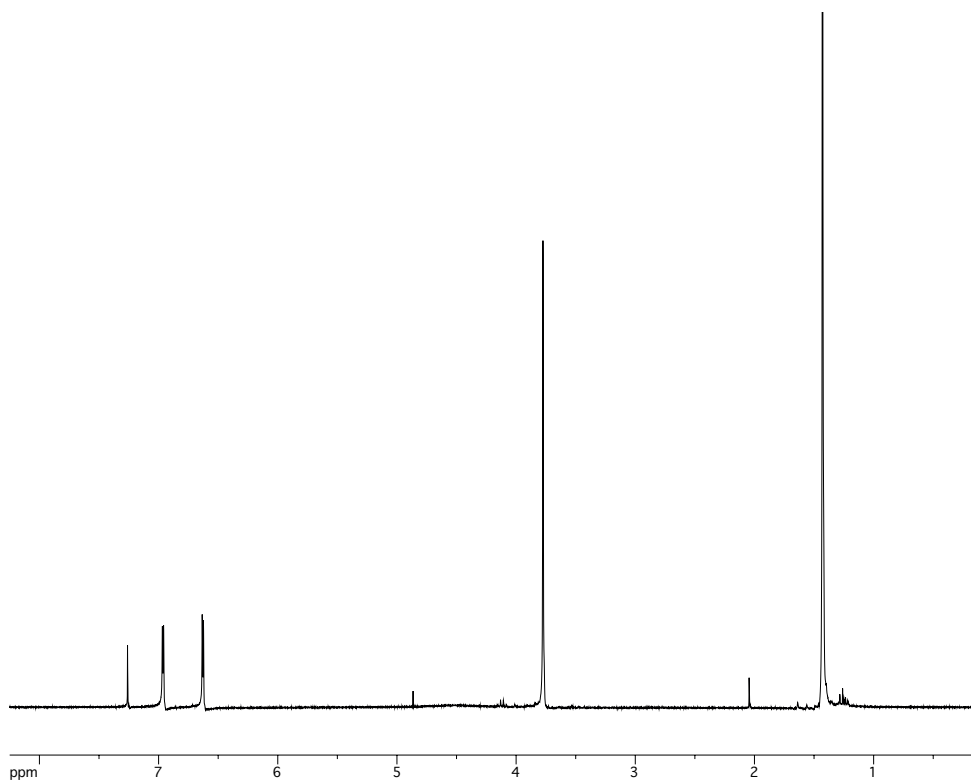


Figure 8.105. ^1H NMR of 3,3'-di-tert-butyl-5,5'-dimethoxy-[1,1'-biphenyl]-2,2'-diol (3.114)⁴⁹

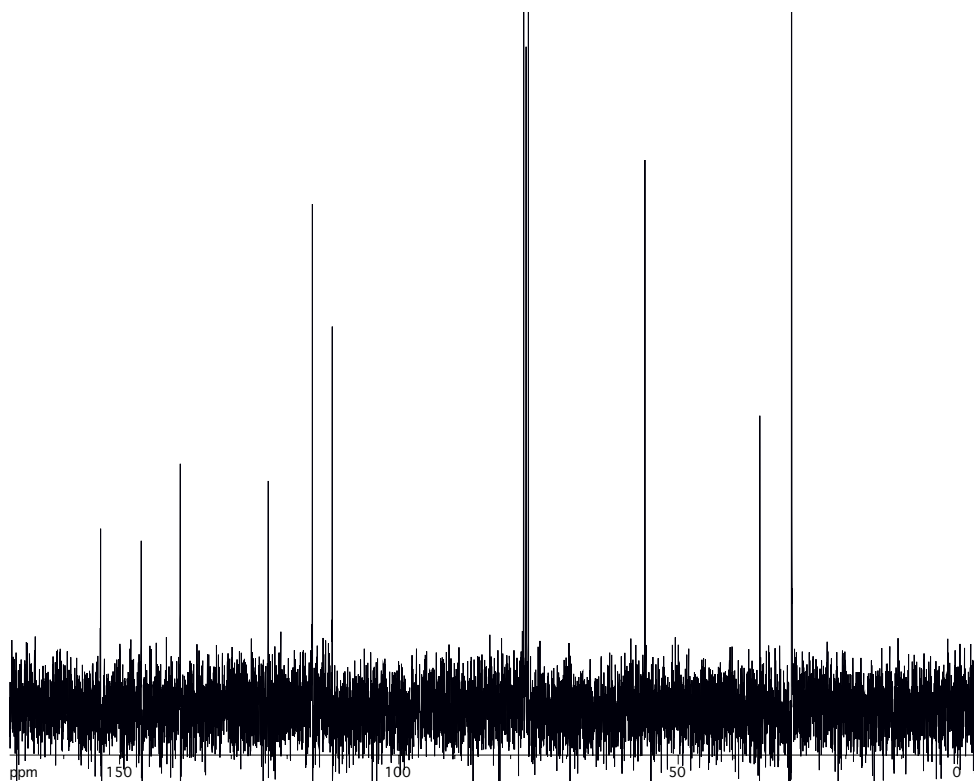


Figure 8.106. ^{13}C NMR of 3,3'-di-tert-butyl-5,5'-dimethoxy-[1,1'-biphenyl]-2,2'-diol (3.114)⁴⁹

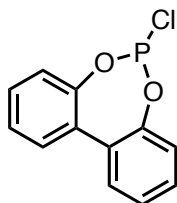


Figure 8.107. 6-chlorodibenzo[d,f][1,3,2]dioxaphosphepine (3.116)¹⁸⁹

To **3.115** (5g, 26.851mmol) was added PCl_3 (9mL) the reaction was heated to reflux for 2 hours and then the excess PCl_3 was vacuum distilled off (had to heat system to 200°C). The crude material was immediately taken on to the next step without purification (64% crude).

[JMG-2-268]

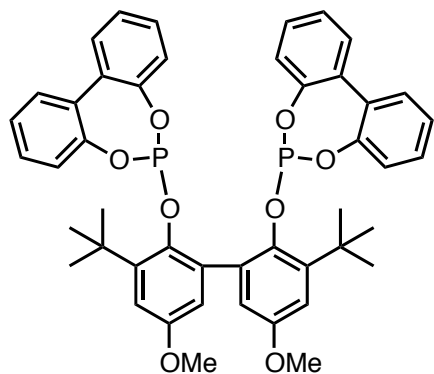


Figure 8.108. BIPHENPHOS Ligand (3.117)¹⁸⁹

The diphenol (**3.114**) (3g, 8.369mmol) was dissolved in toluene (45mL) and Et₃N (9.3mL, 66.952mmol) was added. This solution was then added to the diphenyl phosphorous chloride (**3.116**) (4.19g, 16.738mmol) in toluene (2mL) at -40°C over 15 minutes. The reaction was then stirred at room temperature overnight. Water was then added (15mL) and the reaction was filtered and the precipitate was washed with water (4 X 15mL) and dried overnight. The solid was then recrystallized from CH₃CN to give a white solid (**3.117**, 88%).

[JMG-2-269]

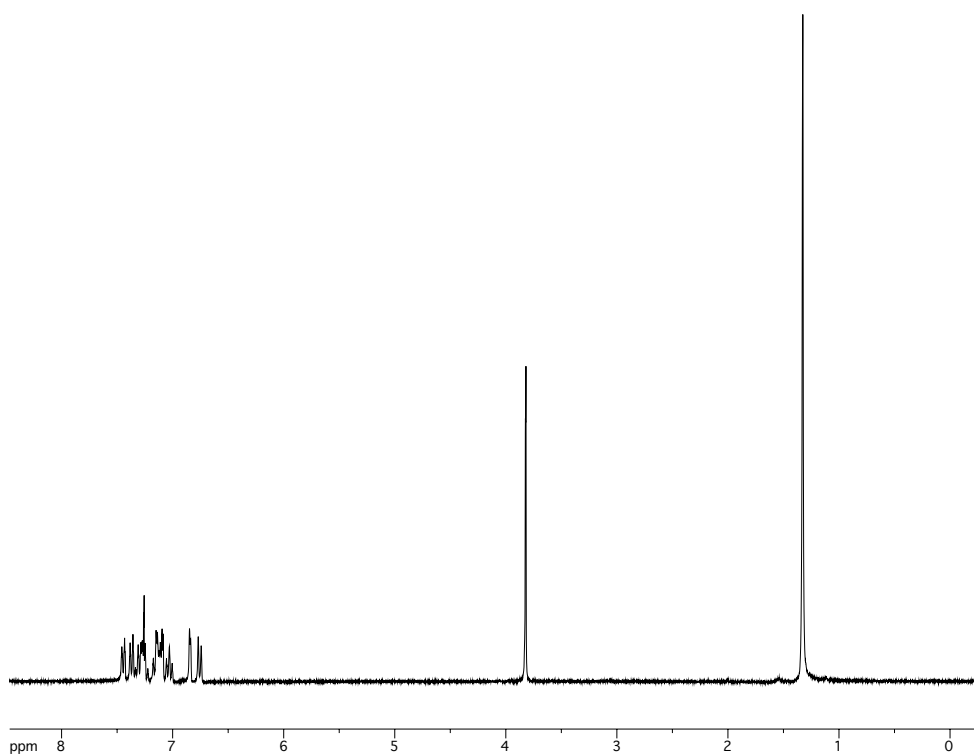


Figure 8.109. ^1H NMR of BIPHENPHOS Ligand (3.117)¹⁸⁹

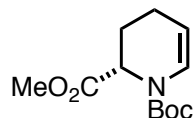


Figure 8.110. (S)-1-tBu 2-methyl 3,4-dihydropyridine dicarboxylate (3.104)³

Rh(acac)(CO)₂ (5mg, 0.019mmol, 1mol%) and BIPHENPHOS (**3.117**) (30mg, 0.038mmol, 2 mol%) were dissolved in THF (10mL) in a bomb and the system was purged with argon. Allylglycine (**3.111**) (430mg, 1.876mmol) was then added in THF (3mL). The system was closed and purged with CO 3X's and then pressurized to 30psi with CO followed by an additional 30psi of H₂. The system was placed behind a blast shield and heated to 65°C over night. The reaction was then cooled to room temperature and concentrated and run through a plug, hexanes:EtOAc, 85:15 to afford pure enamine **3.104**. (85-90%)

[JMG-2-273DMSO]

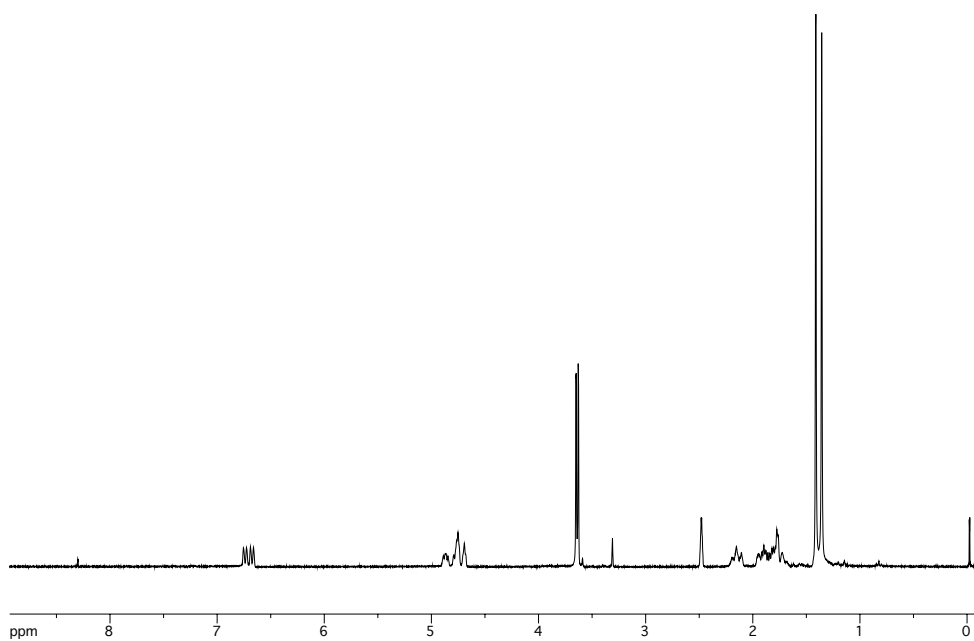


Figure 8.111. ^1H NMR of (S)-1-tBu 2-methyl dihydropyridine dicarboxylate (3.104)³

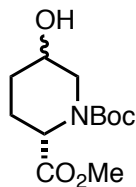


Figure 8.112. (2S)- hydroxypiperidine dicarboxylate (3.105)⁴⁷

To **3.104** (160mg, 0.663mmol) in DCM (5mL) at -78°C was added $\text{BH}_3 \cdot \text{SMe}_2$ (2M in THF, 350mL) and the reaction was then warmed to room temperature and stirred for 4 hours. The reaction was then concentrated down and THF (5mL) was added followed by TMO (269mg, 3.581mmol) and the system was refluxed for 15 minutes. The reaction was then diluted with EtOAc and washed with water (30mL) and extracted with EtOAc (3 x's 20mL) and dried over Na_2SO_4 and concentrated. Purification via column chromatography, hexanes:EtOAc, 50:50, gave the desired compound (**3.105**) as a sys/trans mixture in 83% yield.

[JMG-2-279 (300MHz), JMG-2-274C13 (100MHz)]

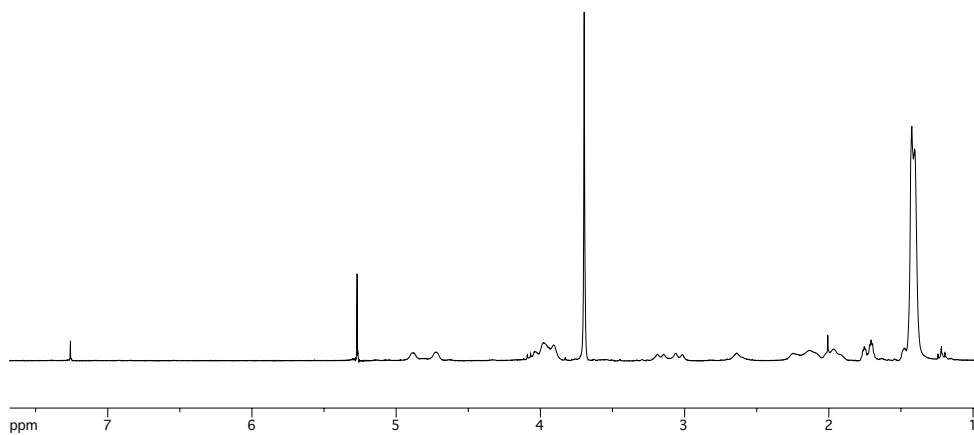


Figure 8.113. ^1H NMR of (2S)- hydroxypiperidine dicarboxylate (3.105)⁴⁷

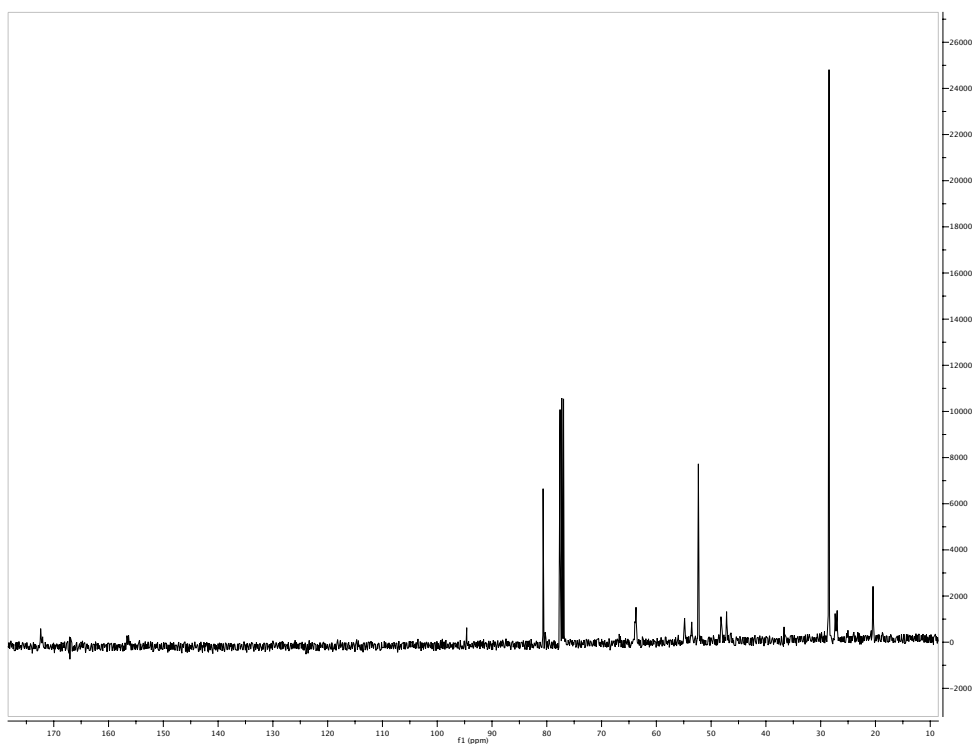


Figure 8.114. ^{13}C NMR of (2S)- hydroxypiperidine dicarboxylate (3.105)⁴⁷

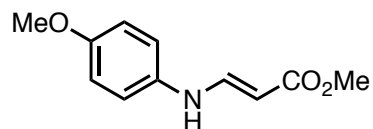


Figure 8.115. Methyl 3-((4-methoxyphenyl)amino)acrylate (3.118)⁵⁰

To **3.12** (10g, 81.202mmol) and MeOH (200mL) was added methyl propiolate (7.25mL, 81.202mmol). The reaction as stirred at room temperature for 16 hours. The reaction was then concentrated down and dissolved in HOT EtOAc and then filtered through a silica plug. The filtrate was then concentrated down to give **3.118** (4.72g, 39%) as a silvery fluffy solid.

[JMG-2-231]

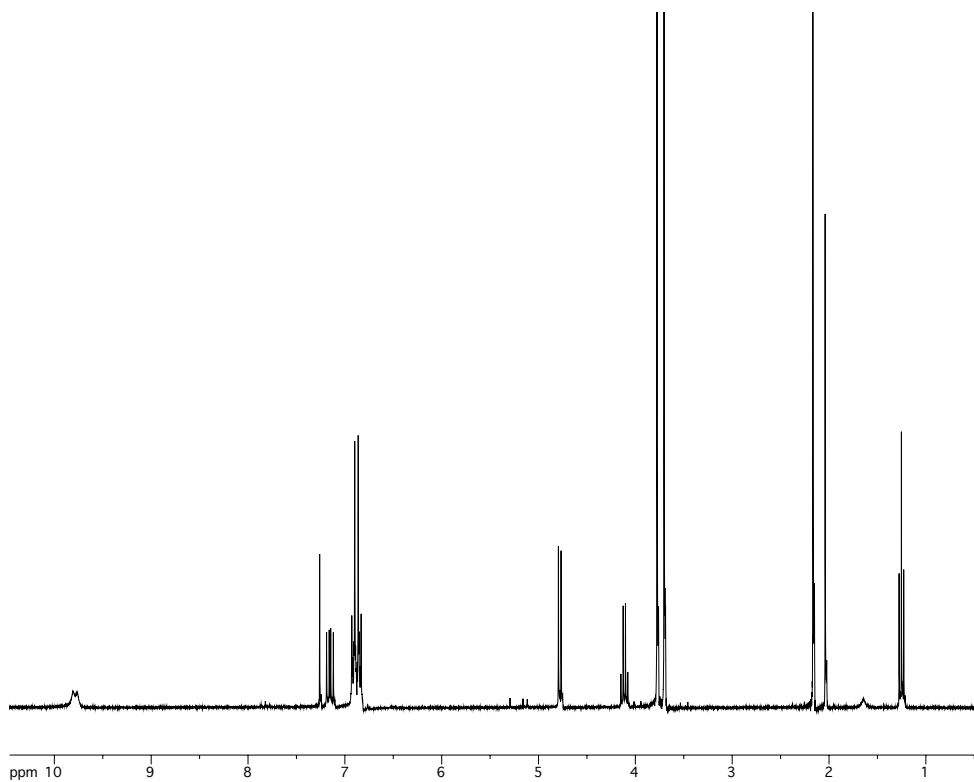


Figure 8.116. ^1H NMR of Methyl 3-((4-methoxyphenyl)amino)acrylate (3.118)⁵⁰

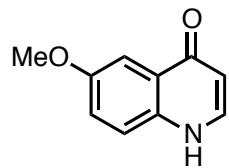


Figure 8.117. 6-methoxyquinolin-4(1H)-one (3.119)⁵⁰

Diphenyl ether (60mL) was heated to 260°C and **3.118** (1g, 4.825mmol) was added and the reaction was stirred at 260°C for an additional 30 minutes. The reaction was then cooled and diluted with hexanes and then filtered. The solid was then washed with Et₂O and dried under high vacuum. (84%)

[JMG-2-313]

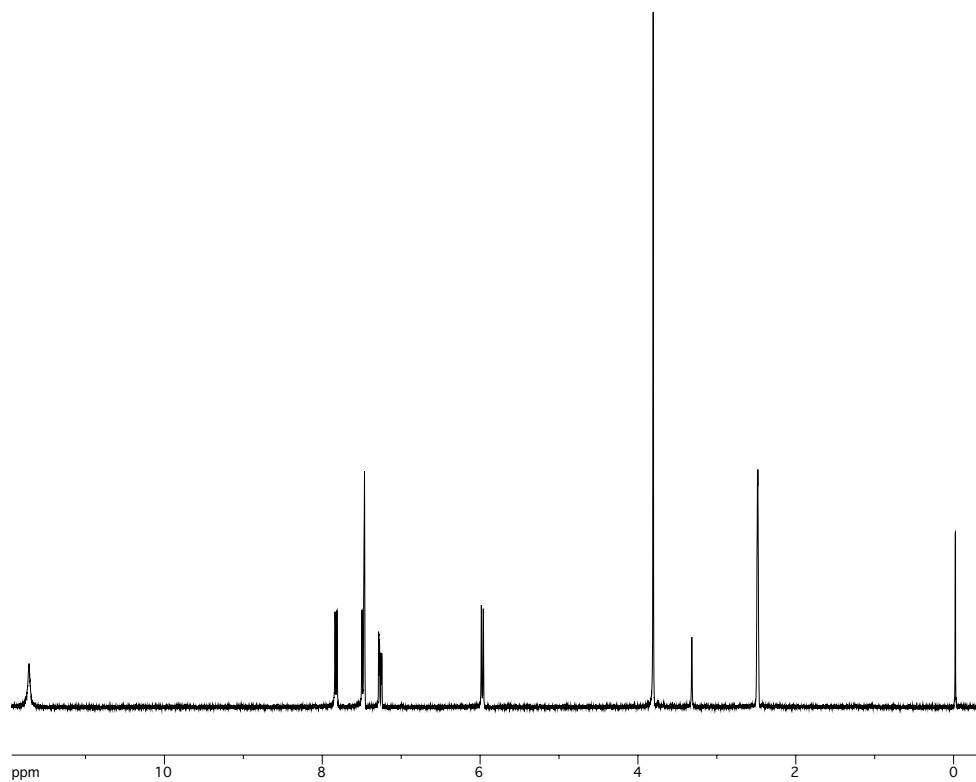


Figure 8.118. ^1H NMR of 6-methoxyquinolin-4(1H)-one (3.119)⁵⁰

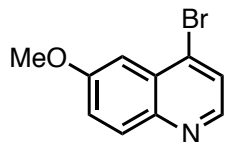


Figure 8.119. 4-bromo-6-methoxyquinoline (3.81)⁵⁰

To **3.119** (108mg, 0.571mmol) in DMF (2.5mL) at 0°C was added PBr₃ (60μl, 0.641mmol) and the reaction was stirred at room temperature for 1 hour. Ice chunks were then added and the reaction was allowed to stir for 30 minutes. The reaction was then extracted with sodium bicarbonate (50mL) and DCM and dried over Na₂SO₄ and purified via column chromatography to give **3.81** (~30%)

[JMG-2-354-S3]

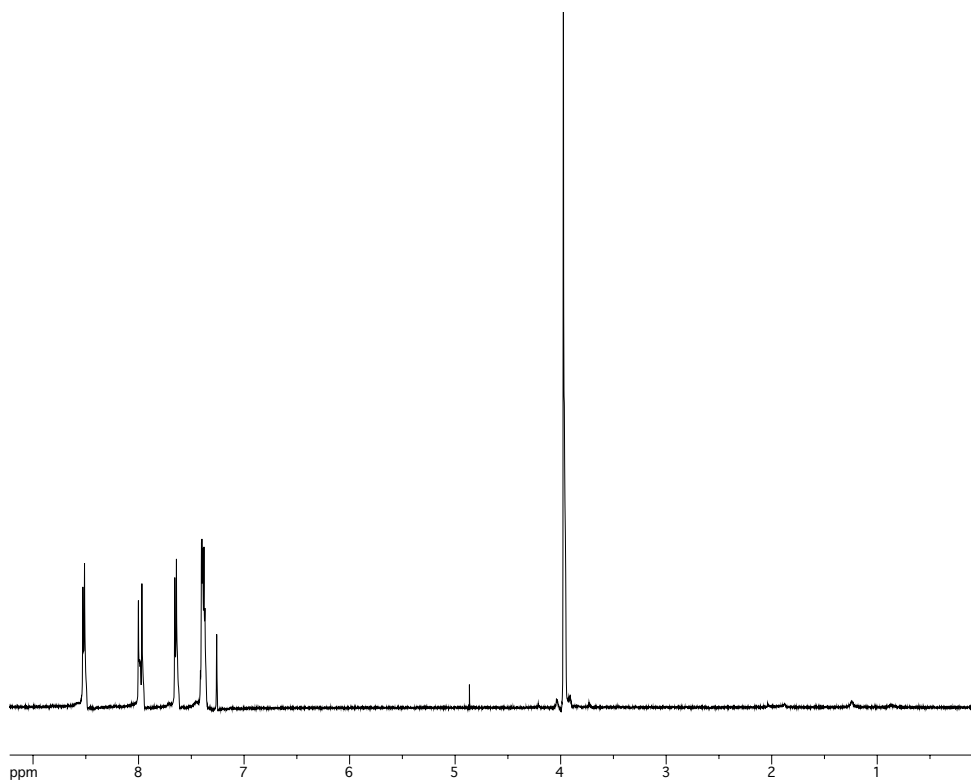


Figure 8.120. ^1H NMR of 4-bromo-6-methoxyquinoline (3.81)⁵⁰

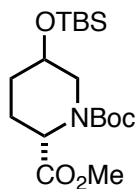


Figure 8.121. (2S)-5-((TBSO)piperidine dicarboxylate (3.120)

To **3.105** (657mg, 2.534mmol) was added DMF (25mL) and TBSCl (571mg, 3.801mmol) and imidazole (517mg, 7.601mmol) and the reaction was stirred overnight at room temperature. The reaction was then diluted with EtOAc and washed with H₂O (100mL) and then brine (100mL) and extracted and dried over Na₂SO₄ and purified via column chromatography.

HRMS calcd for C₁₈H₃₅NO₅Si: 396.1282, found: 396.1278

¹H-NMR (400 MHz; CDCl₃): δ 0.00 (d, *J* = 10.3 Hz, 6H), 0.83 (s, 9H), 1.40 (s, 9H), 1.56 (dt, *J* = 13.7, 2.8 Hz, 1H), 1.88 (d, *J* = 12.4 Hz, 1H), 2.16 (tdd, *J* = 13.6, 5.9, 4.0 Hz, 1H), 3.03 (m, 1H), 3.67 (s, 3H), 3.86-3.81 (m, 2H), 4.92-4.56 (m, 1H). ¹³C NMR (75 MHz; CDCl₃): δ -4.76, 18.24, 20.66, 25.93, 28.52, 48.24, 52.25, 53.29, 64.36, 80.06, 155.51, 172.71

[JMG-2-298, JMG-2-298C13]

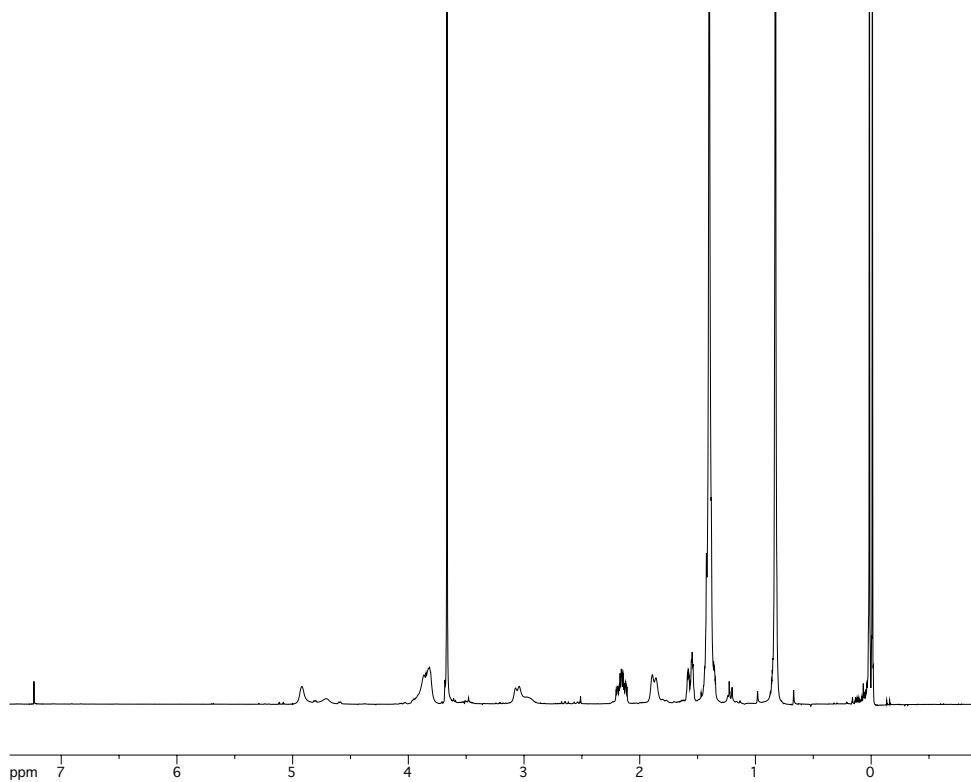


Figure 8.122. ^1H NMR of (2S)-5-((TBSO)piperidine dicarboxylate (3.120)

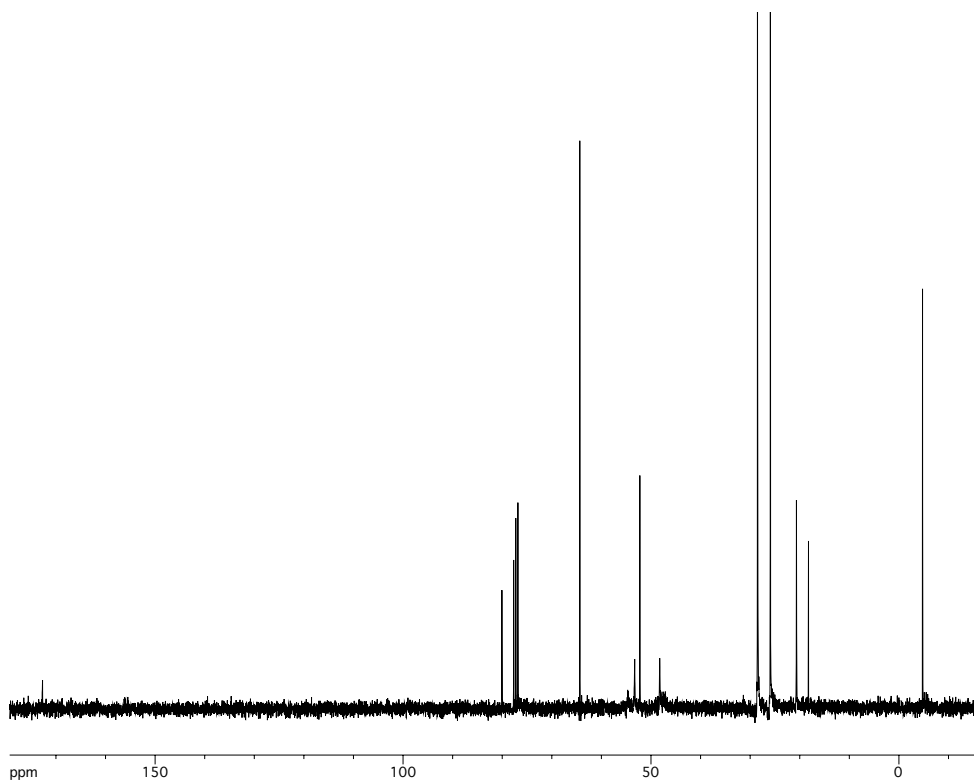


Figure 8.123. ^{13}C NMR of (2*S*)-5-((TBSO)piperidine dicarboxylate (3.120)

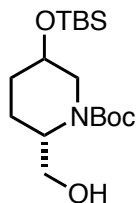


Figure 8.124. (2S)-((TBSO)-2-(hydroxymethyl)piperidine-1-carboxylate (3.121)

To crude **3.120** was added THF (50mL) and it was cooled to 0°C. LiAlH₄ (960mg, 25.340mmol) was then added and the reaction was stirred for 1 hour at room temperature. The reaction was then diluted with Et₂O cooled back down to 0°C and 1mL of H₂O was added, followed by 1mL of 15% NaOH, and 3mL of H₂O. The reaction was then allowed to stir for 1 hour and the salts were filtered off and rinsed with Et₂O and then the organics were concentrated and dried over MgSO₄. Purification via silica plug yielded 312mg of **3.121** (36% over 2 steps).

¹H NMR (300MHz, CDCl₃): 0.01 (s, 3H), 0.04 (s, 3H), 0.85 (s, 9H), 1.42 (s, 9H), 1.58 (m, 3H), 1.95 (m, 1H), 2.99 (d, 1H, *J* = 12), 3.56 (m, 1H), 3.68 (m, 3H), 4.17 (m, 1H).

[JMG-2-375]

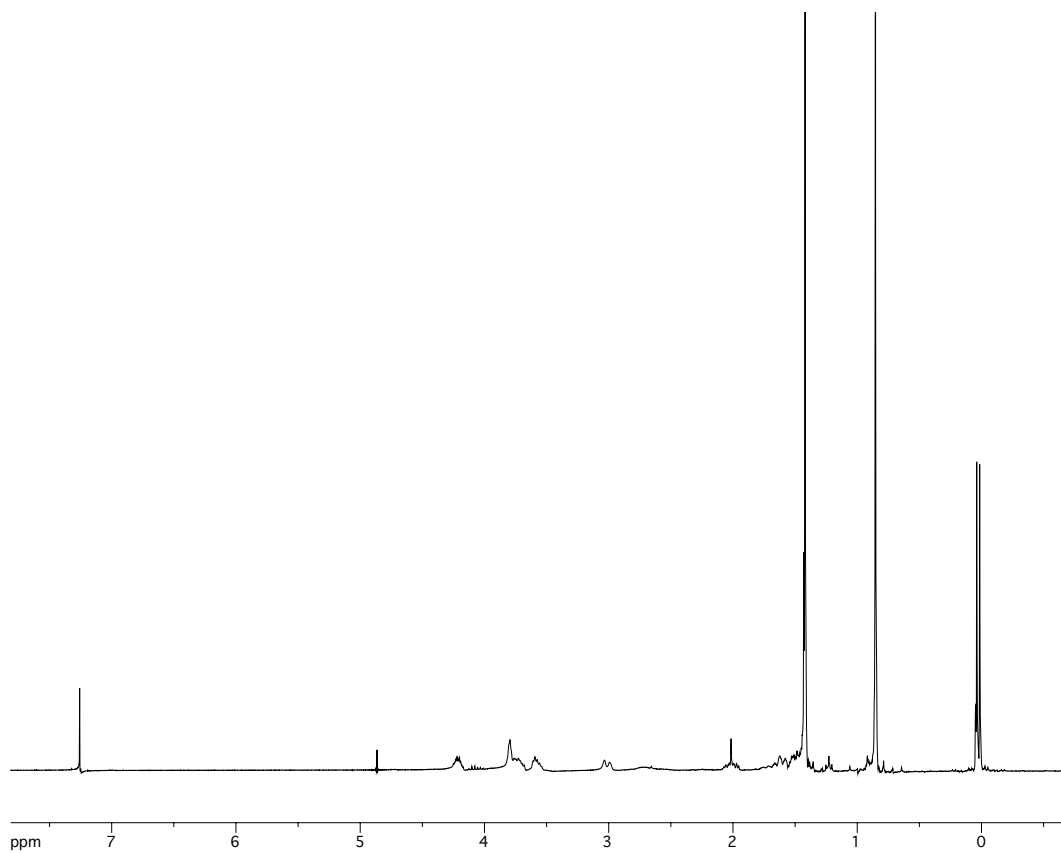


Figure 8.125. ^1H NMR of (2S)- ((TBSO)-2-piperidine-1-carboxylate (3.121)

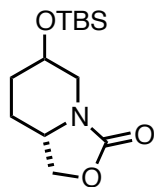


Figure 8.126. (8*S*)- tetrahydro-1*H*-oxazolo[3,4-*a*]pyridin-3(5*H*)-one (**3.123**)

To **3.121** (250mg, 0.723mmol) was added DCM (8mL) followed by CBr₄ (480mg, 1.447mmol) then PPh₃ (380mg, 1.447mmol), and Et₃N (300μl, 2.169mmol). The reaction was allowed to stir at room temperature overnight. The reaction was then diluted with DCM and washed with brine and dried over Na₂SO₄ and concentrated and purified to give **3.123** (quant).

HRMS calcd. for C₁₃H₂₆NO₃Si (M+H)⁺: 272.1682, Found: 272.1683.

¹H-NMR (300 MHz; CDCl₃): δ 0.03 (s, 6H), 0.84 (s, 9H), 1.21 (t, *J* = 7.1 Hz, 1H), 1.39 (t, *J* = 10.4 Hz, 2H), 1.87-1.82 (m, 1H), 2.00-1.96 (m, 1H), 2.59 (dd, *J* = 12.7, 10.1 Hz, 1H), 3.60-3.52 (m, 2H), 3.90-3.82 (m, 2H), 4.37 (t, *J* = 8.4 Hz, 1H).

¹³C NMR (75 MHz; CDCl₃): δ -4.56, 25.91, 29.32, 32.94, 48.17, 53.71, 66.71, 67.92, 157.05

[JMG-2-338, JMG-2-338C13]

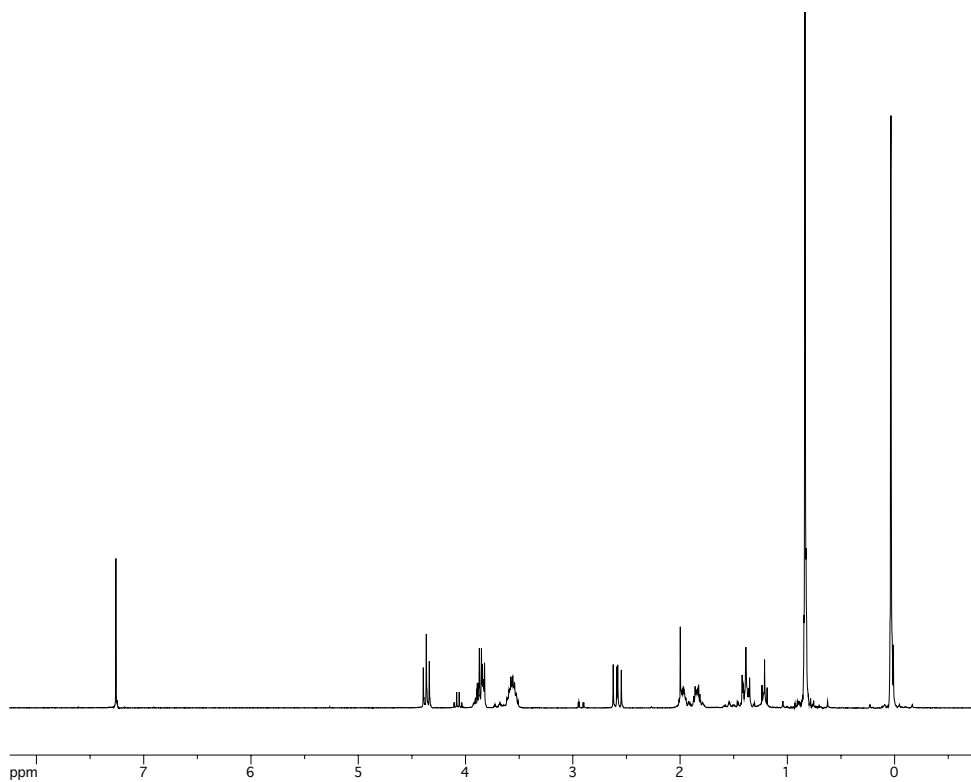


Figure 8.127. ^1H NMR of (8*S*)- tetrahydro-1*H*-oxazolo[4,5-*b*]pyridin-3(5*H*)-one (3.123)

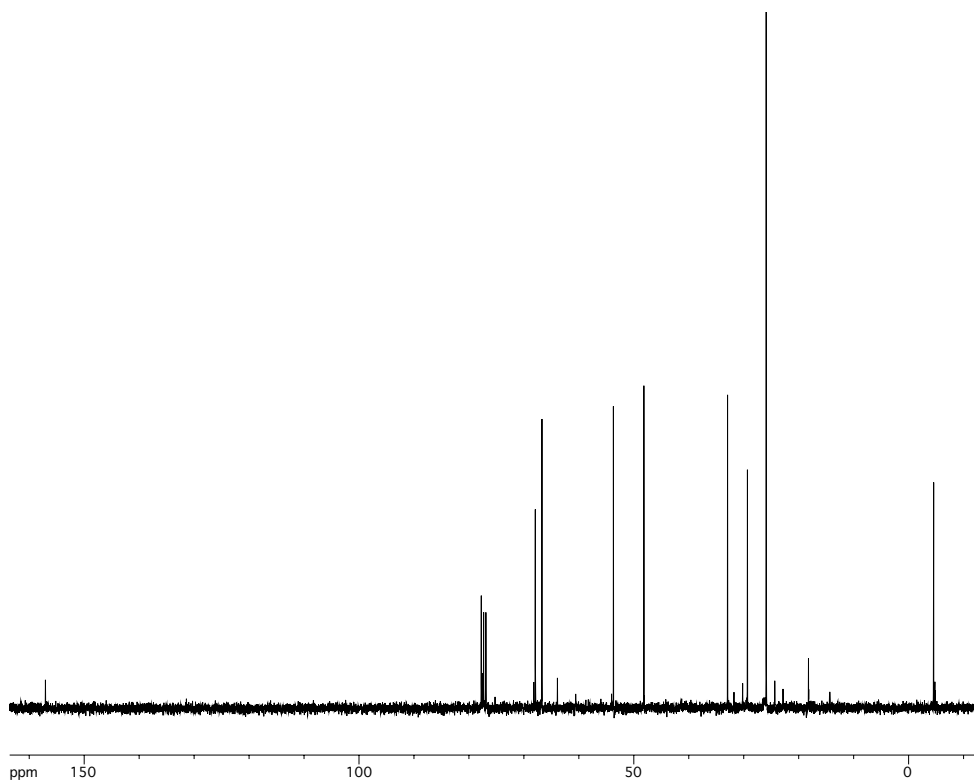


Figure 8.128. ^{13}C NMR of (8*S*)-tetrahydro-1*H*-oxazolopyridin-3(5*H*)-one (3.123)

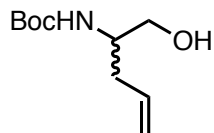


Figure 8.129. 1-hydroxypent-4-en-2-yl-carbamate (3.129a)

3.111 (300mg, 1.309mmol) and THF (30mL) were cooled to 0°C. LiAlH₄ (150mg, 3.926mmol) was added and the reaction was stirred at room temperature for 1 hour. The reaction was then quenched with 150μl water, 300μl 15% NaOH, and 150μl water. The reaction was then allowed to stir for 1 hour and the salts were filtered off through a pad of Celite and rinsed with Et₂O. The organics were dried over Na₂SO₄ and concentrated and purified via column chromatography. (93%)

HRMS calcd for C₁₀H₂₀NO₃ (M+H)⁺: 202.1443, found: 202.1463. ¹H-NMR (300 MHz; CDCl₃): δ 1.42 (s, 9H), 2.30-2.19 (m, 2H), 3.00 (bs, 1H), 3.67-3.54 (m, 3H), 4.81 (d, *J* = 6.5 Hz, 1H), 5.13-5.06 (m, 2H), 5.76 (ddt, *J* = 17.1, 10.1, 7.1 Hz, 1H). ¹³-C NMR (75 MHz; CDCl₃): δ 28.52, 36.16, 52.30, 65.36, 79.92, 118.24, 134.42, 156.63

[JMG-2-364, JMG-2-364C13]

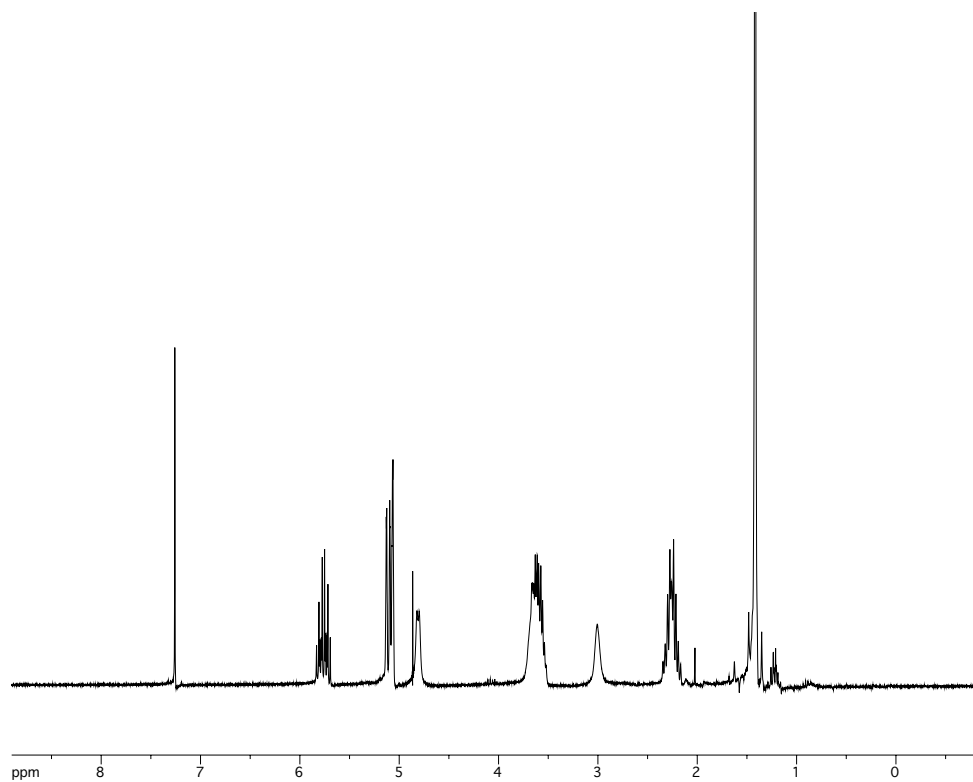


Figure 8.130. ^1H NMR of 1-hydroxypent-4-en-2-yl-carbamate (3.129a)

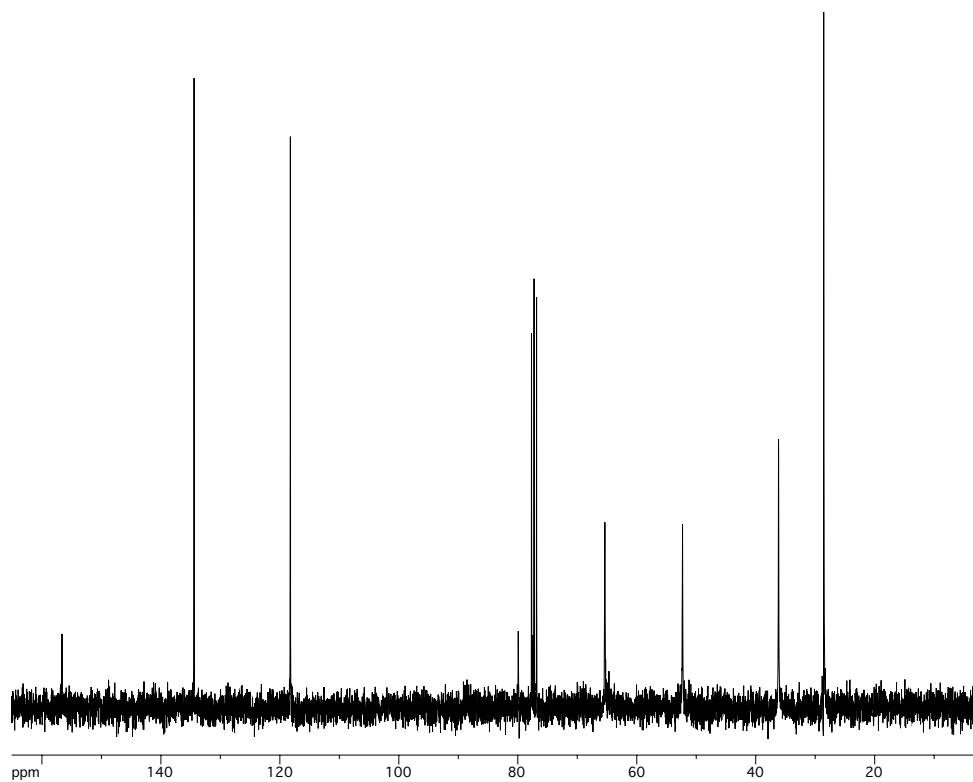


Figure 8.131. ^{13}C NMR of 1-hydroxypent-4-en-2-yl-carbamate (3.129a)

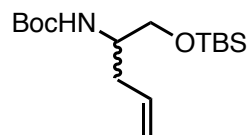


Figure 8.132. Pent-4-en-2-yl-carbamate (3.129)

3.129a (810mg, 4.025mmol) was dissolved in DMF (80mL) and TBSCl (908mg, 6.037mmol) and imidazole (821mg, 12.074mmol) were added. The reaction was allowed to stir at room temperature overnight. The reaction was then diluted with EtOAc and washed with $\text{NH}_4\text{Cl}_{\text{aq}}$ (2 X 100mL) then with brine (2 X 100mL) and dried over Na_2SO_4 (quant).

HRMS calcd for $\text{C}_{16}\text{H}_{33}\text{NO}_3\text{SiNa}$ ($\text{M}+\text{Na}$) $^+$: 338.2127, found: 338.2129. $^1\text{H-NMR}$ (300 MHz; CDCl_3): δ 0.02 (s, 6H), 0.88 (s, 9H), 1.42 (s, 9H), 2.30-2.23 (m, 2H), 3.62-3.56 (m, 3H), 4.69-4.66 (m, 1H), 5.11-5.02 (m, 2H), 5.76 (ddt, $J = 17.1, 10.1, 7.1$ Hz, 1H).

[JMG-2-419]

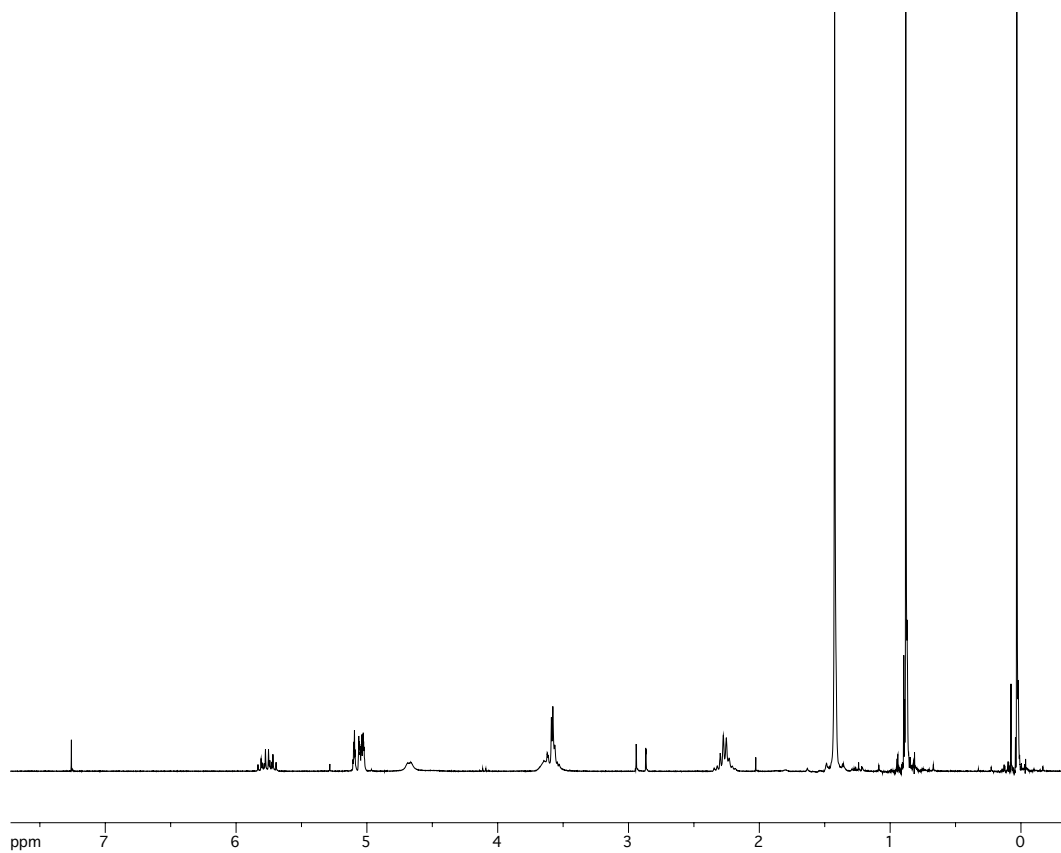


Figure 8.133. ^1H NMR of Pent-4-en-2-yl-carbamate (3.129)

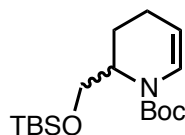


Figure 8.134. 3,4-dihydropyridine-1(2*H*)-carboxylate (3.130)

3.129 (300mg, 0.951mmol) was added to THF (10mL) in hydrogenation bomb. Rh(acac)CO (3mg, 1mol%) and BIPHENPHOS (15mg, 2mol%) was then added and the system was purged with CO, then pressurized to 30psi (CO). 30psi (H₂) was then added and the reaction was placed in an oil bath, behind a blast shield, and heated to 60°C overnight. The reaction was then cooled to room temperature and the pressure was released and then the reaction was concentrated. Purification via column chromatography gave the desired product **3.130**. (90%)

HRMS calcd for C₁₇H₃₃NO₃SiNa (M+Na)⁺: 350.2127, found: 350.2138.

¹H-NMR (300 MHz; CDCl₃): δ 0.04 (d, *J* = 3.2 Hz, 6H), 0.87 (s, 9H), 1.47 (s, 9H), 1.68-1.54 (m, 2H), 2.16-1.86 (m, 3H), 3.61-3.44 (m, 1H), 4.32-4.14 (m, 1H), 4.87-4.72 (m, 1H), 6.73 (dd, *J* = 38.5, 8.7 Hz, 1H).

[JMG-2-420]

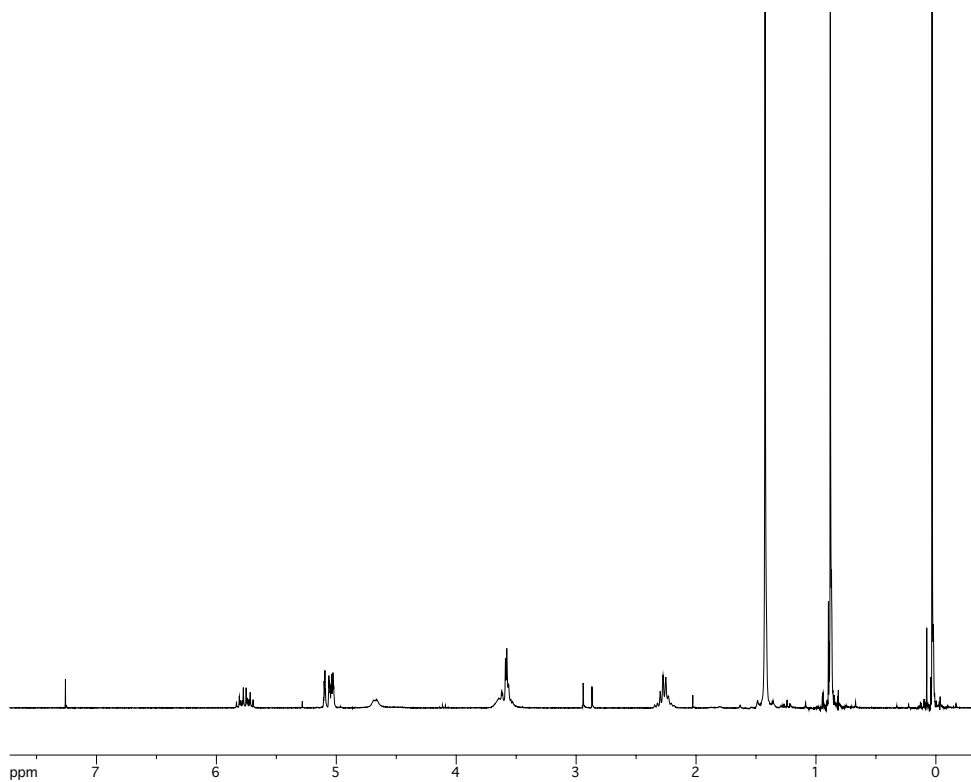


Figure 8.135. ^1H NMR of 3,4-dihydropyridine-1(2H)-carboxylate (3.130)

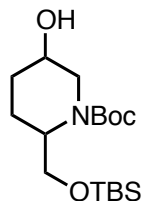


Figure 8.136. 5-hydroxypiperidine-1-carboxylate (3.131)

TO **3.130** (149mg, 0.454mmol) in DCM (15mL) at -78°C was added $\text{BH}_3 \cdot \text{SMe}_2$ (250 μL , 0.454mmol, 2M soln' in THF). The reaction was then warmed up to room temperature and allowed to stir for 2 hours. The reaction was then concentrated down and diluted with THF (15mL) and TMO (170mg, 2.275mmol) was added and the reaction was refluxed for 20 minutes. The reaction was then diluted with water and extracted with DCM and dried over Na_2SO_4 . No further purification was needed (75%).

HRMS calcd for $\text{C}_{17}\text{H}_{36}\text{NO}_4\text{Si}$ ($\text{M}+\text{H}$) $^+$: 346.2414, found: 346.2501.

^1H -NMR (300 MHz; CDCl_3): δ 0.02 (s, 6H), 0.86 (s, 9H), 1.43 (s, 9H), 1.73-1.52 (m, 2H), 1.97-1.77 (m, 1H), 2.98-2.93 (m, 1H), 3.68-3.55 (m, 2H), 4.17-3.90 (m, 3H). ^{13}C -NMR (75 MHz; CDCl_3): δ -5.22, 18.42, 18.66, 26.08, 28.64, 60.67, 60.95, 61.26, 64.64, 67.22, 79.92, 147.22

[JMG-2-421crude, JMG-2-421C13]

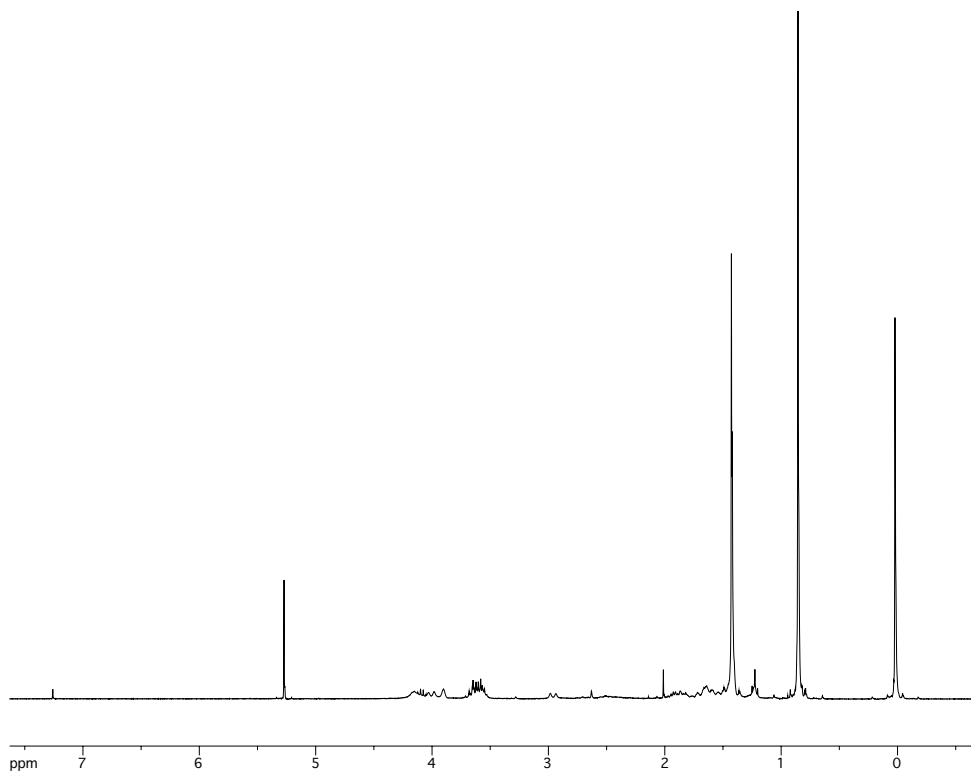


Figure 8.137. ^1H NMR of 5-hydroxypiperidine-1-carboxylate (3.131)

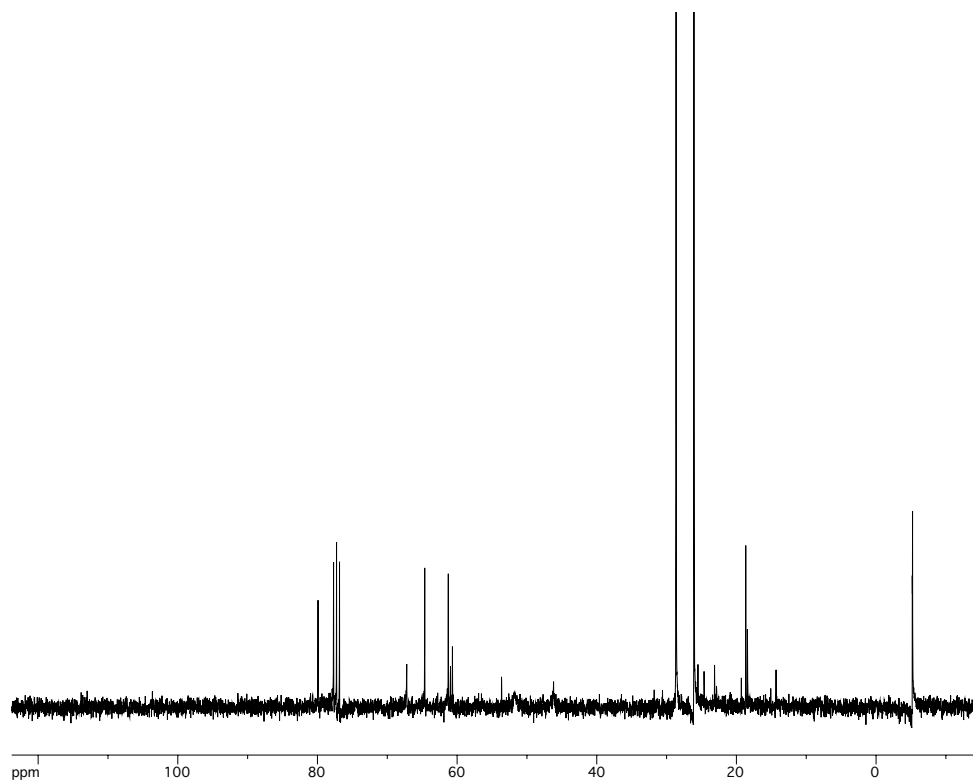


Figure 8.138. ^{13}C NMR of 5-hydroxypiperidine-1-carboxylate (3.131)

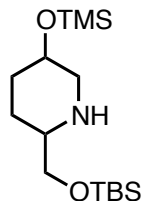


Figure 8.139. 5-((TMS)oxy)piperidine (**3.131a**)

To **3.131** (200mg, 0.579mmol) in DCM (12mL) was added 2,6-lutidine (405μl, 3.474mmol) and TMSOTf (840μl, 4.630mmol) and the reaction as stirred at room temperature for 1 hour. The reaction was then concentrated and purified via column chromatography, hexanes:EtOAc:Et₃N, 1:1:0.01 (34%)

HRMS calcd for C₁₅H₃₇NO₂Si₂ (M+H)⁺: 318.2285, found, 318.2281.

¹H-NMR (300 MHz; CDCl₃): δ 0.04 (s, 6H), 0.11 (s, 9H), 0.88 (s, 9H), 1.18-1.06 (m, 1H), 1.41-1.28 (m, 1H), 1.60-1.52 (m, 1H), 1.95-1.90 (m, 2H), 2.58-2.43 (m, 2H), 3.13 (ddd, *J* = 10.9, 4.6, 2.1 Hz, 1H), 3.35 (dd, *J* = 9.7, 8.3 Hz, 1H), 3.66-3.54 (m, 2H). ¹³-C NMR (75 MHz; CDCl₃): δ -5.17, 0.37, 18.55, 26.15, 27.38, 34.33, 54.16, 57.48, 67.62, 69.31

[JMG-2-425, JMG-2-425C13]

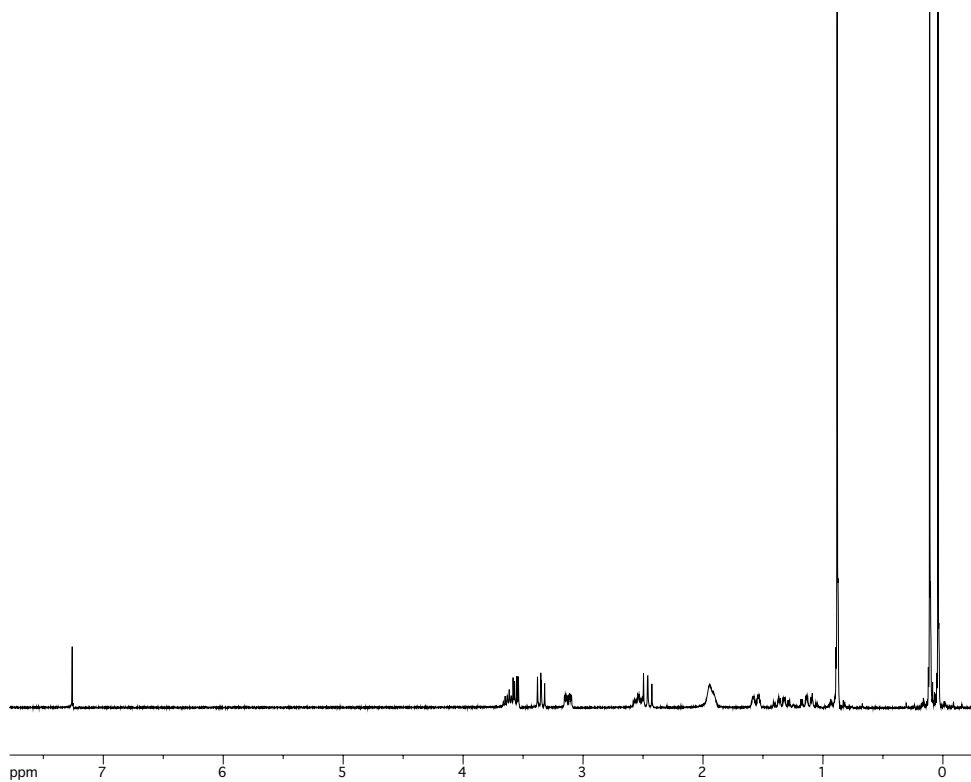


Figure 8.140. ^1H NMR of 5-((TMS)oxy)piperidine (3.131a)

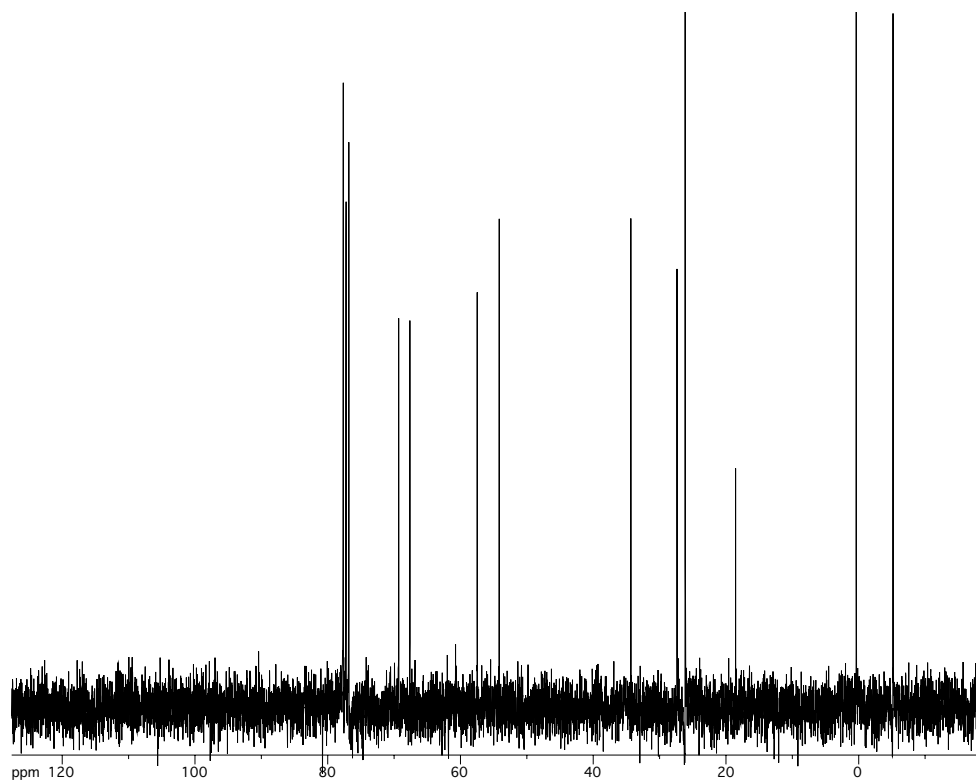


Figure 8.141. ^{13}C NMR of 5-((TMS)oxy)piperidine (3.131a)

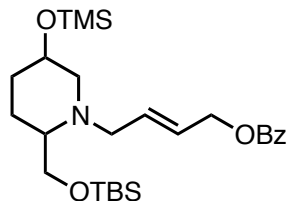


Figure 8.142. 5-((TMS)oxy)piperidin-1-yl)but-2-en-1-yl benzoate (**3.133**)

3.131a (167mg, 0.526mmol) was dissolved in DMF (6mL) and the allyl-I (**3.132**) (326mg, 1.078mmol) and K_2CO_3 (107mg, 1.078mmol), and Et_3N (150 μ l, 1.078mmol) were added. The reaction was allowed to stir for 48 hours while being protected from light. The reaction was then diluted with EtOAc and washed with bicarbonate and then brine and purified via column chromatography. (26%)

HRMS calcd for $C_{26}H_{45}NO_4Si_2Na$ ($M+Na$) $^+$: 514.2785, found: 514.2764.

1H -NMR (300 MHz; $CDCl_3$): δ 0.03 (s, 6H), 0.09 (s, 9H), 0.87 (s, 9H), 1.85-1.80 (m, 1H), 1.92-1.89 (m, 1H), 2.02 (t, J = 10.4 Hz, 1H), 2.24-2.20 (m, 1H), 2.95-2.90 (m, 1H), 3.11 (dd, J = 14.4, 7.0 Hz, 1H), 3.52-3.43 (m, 2H), 3.70-3.61 (m, 1H), 3.80 (dd, J = 10.4, 5.0 Hz, 1H), 4.80 (d, J = 5.7 Hz, 2H), 6.01-5.79 (m, 2H), 7.45-7.40 (m, 2H), 7.55 (tt, J = 7.4, 1.7 Hz, 1H), 8.06-8.03 (m, 2H). ^{13}C NMR (75 MHz; $CDCl_3$): δ -5.19, 0.36, 18.53, 26.15, 28.23, 34.05, 55.92, 60.58, 61.95, 65.21, 66.32, 68.49, 127.53, 128.53, 129.86, 131.33, 133.16, 166.53

[JMG-2-435-3, JMG-2-435C13]

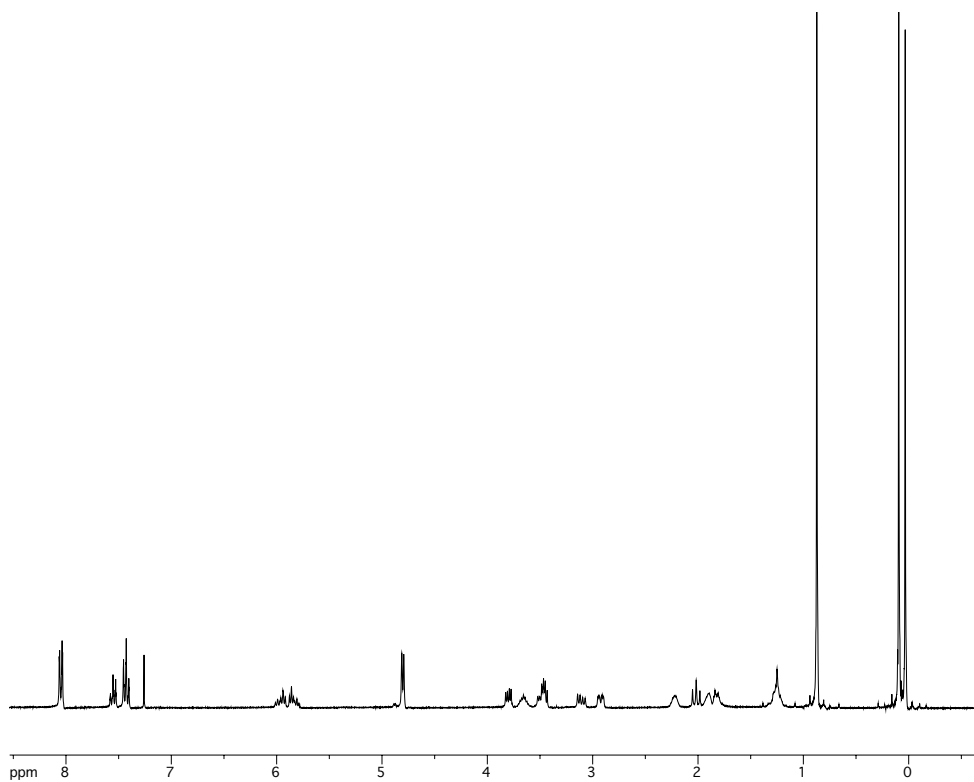


Figure 8.143. ^1H NMR of 5-((TMS)oxy)piperidin-1-yl)but-2-en-1-yl benzoate (3.133)

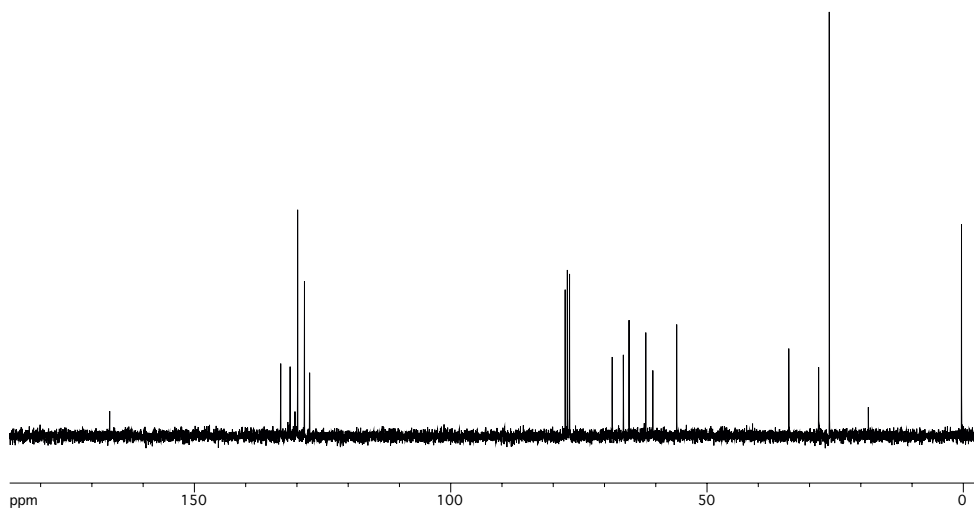


Figure 8.144. ^{13}C NMR of 5-((TMS)oxy)piperidin-1-yl)but-2-en-1-yl benzoate (3.133)

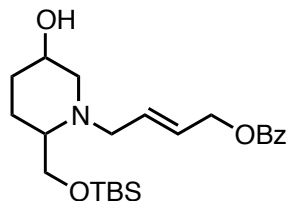


Figure 8.145. 5-(4-hydroxypiperidin-1-yl)but-2-en-1-yl benzoate (3.134)

Material from previous reaction (**3.133**) was diluted with THF (5mL) and stirred with 1N HCl for 20 minutes. The reaction was then extracted with CHCl_3 and dried over Na_2SO_4 . Purification via column chromatography yielded desired alcohol **3.134** (29%).

HRMS calcd for $\text{C}_{23}\text{H}_{38}\text{NO}_4\text{Si}$ ($\text{M}+\text{H}$) $^+$: 420.2570, found: 420.2564.

^1H -NMR (300 MHz; CDCl_3): δ 0.03 (s, 6H), 0.87 (s, 9H), 1.39-1.29 (m, 2H), 1.94-1.85 (m, 2H), 2.17-2.09 (m, 2H), 2.41-2.37 (m, 1H), 2.98 (dd, J = 10.9, 3.5 Hz, 1H), 3.16 (dd, J = 14.2, 6.4 Hz, 1H), 3.48 (ddd, J = 21.7, 12.3, 5.7 Hz, 2H), 3.74-3.70 (m, 1H), 3.82 (dd, J = 10.3, 5.1 Hz, 1H), 4.80 (d, J = 5.4 Hz, 2H), 5.85 (ddd, J = 20.4, 11.0, 4.2 Hz, 2H), 7.43 (t, J = 7.6 Hz, 2H), 7.55 (t, J = 7.4 Hz, 1H), 8.05 (d, J = 7.3 Hz, 2H). ^{13}C -NMR (75 MHz; CDCl_3): δ -5.18, 18.47, 26.13, 26.52, 32.08, 51.38, 56.29, 58.61, 61.39, 64.20, 65.21, 67.25, 127.47, 128.56, 129.86, 131.68, 133.20, 166.56

[JMG-2-462-1, JMG-2-462C13]

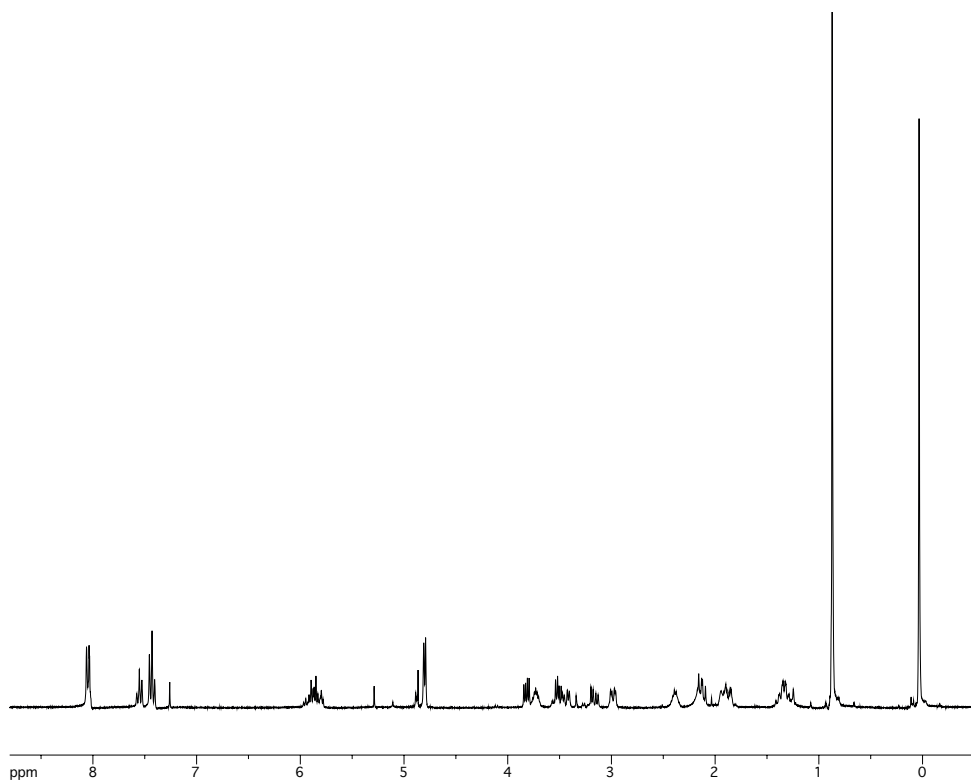


Figure 8.146. ^1H NMR of 5-(hydroxypiperidin-1-yl)but-2-en-1-yl benzoate (3.134)

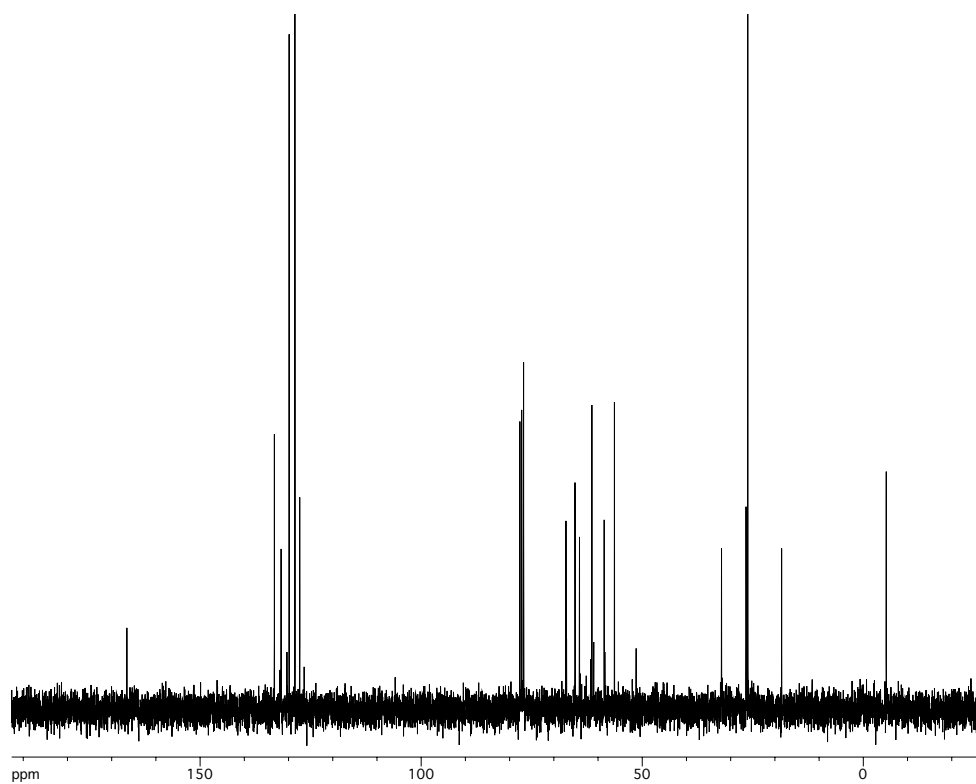


Figure 8.147. ^{13}C NMR of 5-hydroxypiperidin-1-yl)but-2-en-1-yl benzoate (3.134)

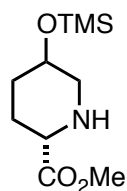


Figure 8.148. Piperidine-2-carboxylate (3.135)

3.105 (462mg, 1.702mmol) was dissolved in DCM (40mL) and at room temperature was added 2,6-lutidine (1.3mL, 11.286mmol) then TMSOTf (2.7mL, 15.052mmol) and the reaction was allowed to stir for 1 hour. The reaction was then concentrated down and purified via column chromatography, hexanes:EtOAc:Et₃N (1:1:0.01).

¹H-NMR (300 MHz; CDCl₃): δ 0.10 (s, 9H), 1.58-1.37 (m, 2H), 2.11-1.95 (m, 2H), 2.47-2.43 (m, 2H), 2.50 (d, *J* = 1.8 Hz, 1H), 3.13 (ddd, *J* = 11.7, 4.5, 1.8 Hz, 1H), 3.27 (dd, *J* = 10.8, 2.9 Hz, 1H), 3.60 (td, *J* = 9.8, 5.0 Hz, 1H), 3.71 (s, 3H). ¹³-C NMR (75 MHz; CDCl₃): δ 0.30, 28.60, 32.62, 34.05, 52.27, 58.07, 68.14, 173.68.

[JMG-2-400, JMG-2-400C13]

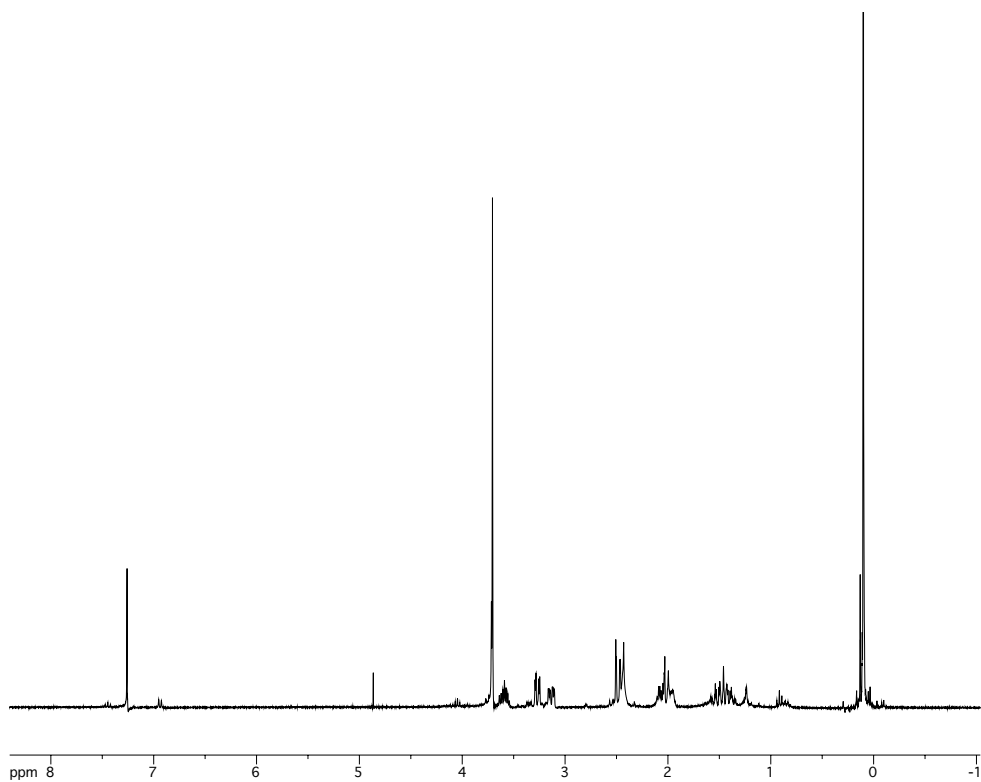


Figure 8.149. ^1H NMR of Piperidine-2-carboxylate (3.135)

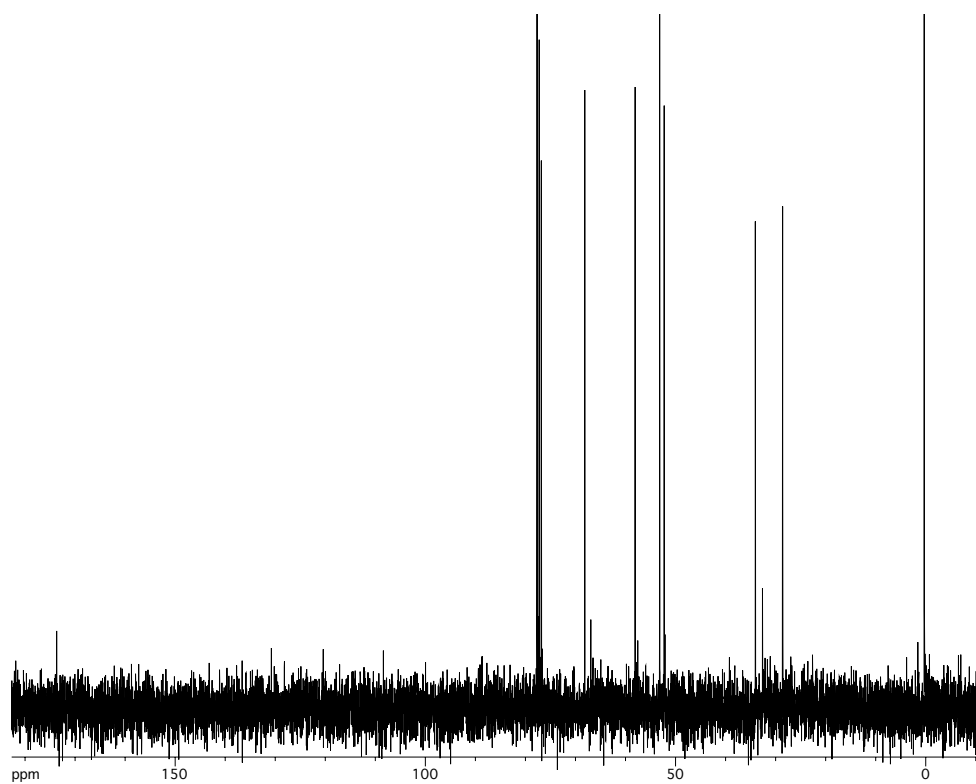


Figure 8.150. ^{13}C NMR of Piperidine-2-carboxylate (3.135)

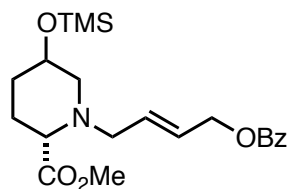


Figure 8.151. 5-((trimethylsilyl)oxy)piperidine-2-carboxylate (3.136)

3.135 (142mg, 0.614mmol), was dissolved in DMF (13mL). Allyl-I (**3.132**) (390mg, 1.258mmol), K_2CO_3 (174mg, 1.258mmol) and Et_3N (175 μ L, 1.258mmol) were then added and the reaction was allowed to stir for 24 hours while being protected from light. The reaction was then washed with saturated $Na_2S_2O_3$ (45mL) and extracted with EtOAc and then washed with brine (50mL). The reaction was then purified via column chromatography, hexanes:EtOAc, 87:3, to afford **3.136** (28%).

1H -NMR (300 MHz; $CDCl_3$): δ 0.08 (s, 9H), 1.34-1.22 (m, 1H), 1.74-1.62 (m, 1H), 1.95-1.88 (m, 3H), 2.94-2.84 (m, 2H), 3.08-3.03 (m, 1H), 3.27-3.20 (m, 1H), 3.71 (s, 3H), 3.79-3.73 (m, 1H), 4.79 (d, J = 5.3 Hz, 2H), 5.91-5.82 (m, 2H), 7.42 (t, J = 7.5 Hz, 2H), 7.54 (t, J = 7.4 Hz, 1H), 8.03 (d, J = 7.0 Hz, 2H). ^{13}C NMR (75 MHz; $CDCl_3$): δ 0.30, 28.30, 33.51, 52.46, 58.00, 59.02, 64.81, 65.40, 67.45, 128.54, 129.85, 133.20

[JMG-2-401-S2, JMG-2-401-S2C13]

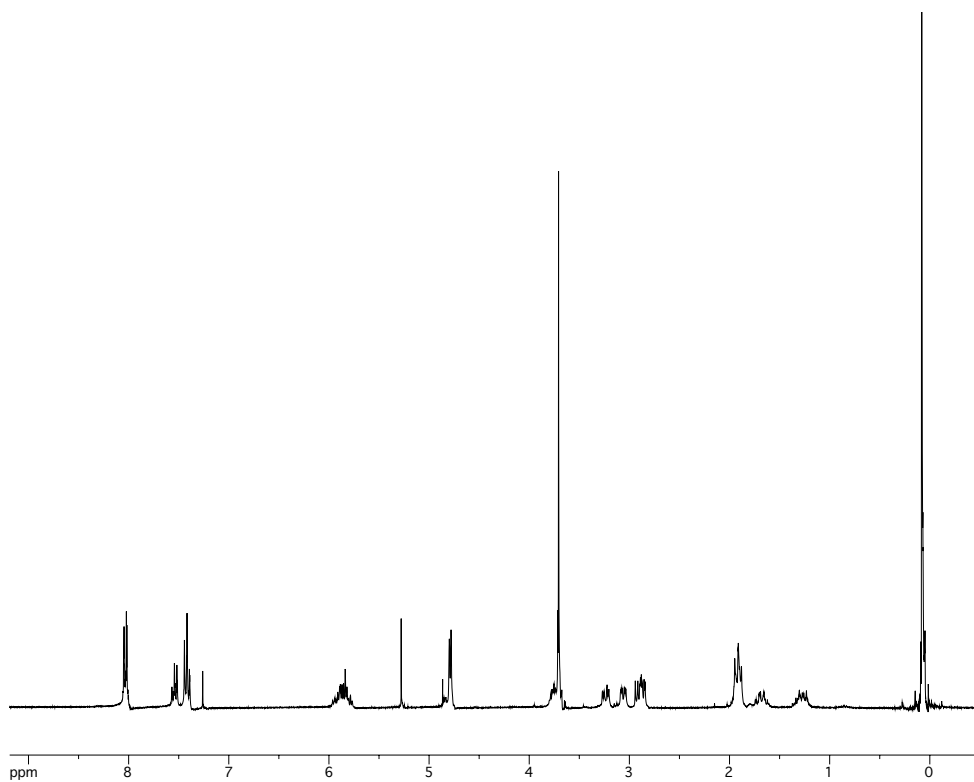


Figure 8.152. ^1H NMR of 5-((trimethylsilyl)oxy)piperidine-2-carboxylate (3.136)

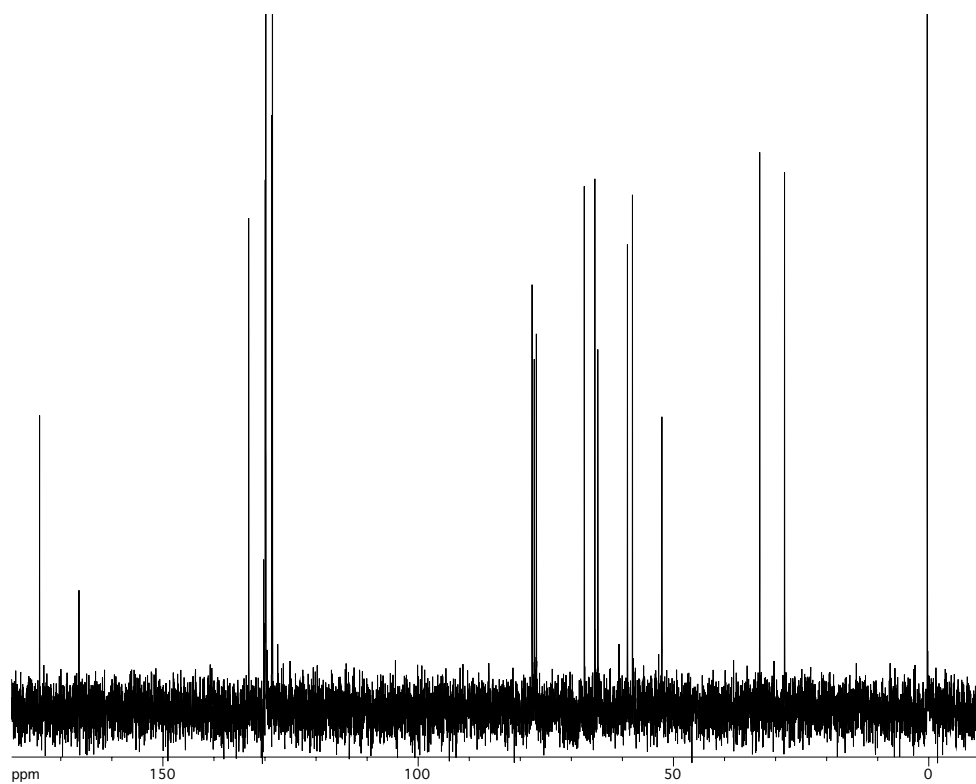


Figure 8.153. ^{13}C NMR of 5-((trimethylsilyl)oxy)piperidine-2-carboxylate (3.136)

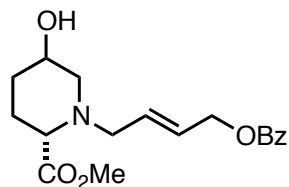


Figure 8.154. 5-hydroxypiperidine-2-carboxylate (3.136a)

3.136 (~190mg-contaminated with 2,6-lutidine from previous reactions) was stirred in THF (12mL), and 2N HCl (12mL) for 3 hours. The reaction was then extracted with CHCl_3 (50mL X 4) and purified via column chromatography to give 150mg of **3.136a**.

HRMS calcd for $\text{C}_{18}\text{H}_{23}\text{NO}_5$ ($\text{M}+\text{H}$) $^+$: 334.1634, found 334.1658. ^1H -NMR (300 MHz; CDCl_3): δ 1.62 (t, J = 12.1 Hz, 1H), 1.87 (d, J = 13.0 Hz, 1H), 2.08-1.99 (m, 1H), 2.76 (bs, 1H), 3.29 (m, 2H), 3.73 (s, 3H), 3.86-3.78 (m, 3H), 4.18-4.05 (m, 2H), 4.85 (d, J = 5.4 Hz, 2H), 6.12-5.99 (m, 1H), 6.28-6.14 (m, 1H), 7.46 (dd, J = 8.1, 6.9 Hz, 2H), 7.58 (t, J = 7.4 Hz, 1H), 8.10-8.00 (m, 2H). ^{13}C NMR (75 MHz; CDCl_3): δ 22.28, 53.06, 55.16, 57.17, 63.57, 64.12, 128.63, 128.70, 129.89, 130.32, 133.46, 166.34, 169.09

[JMG-2-490, JMG-2-490C13]

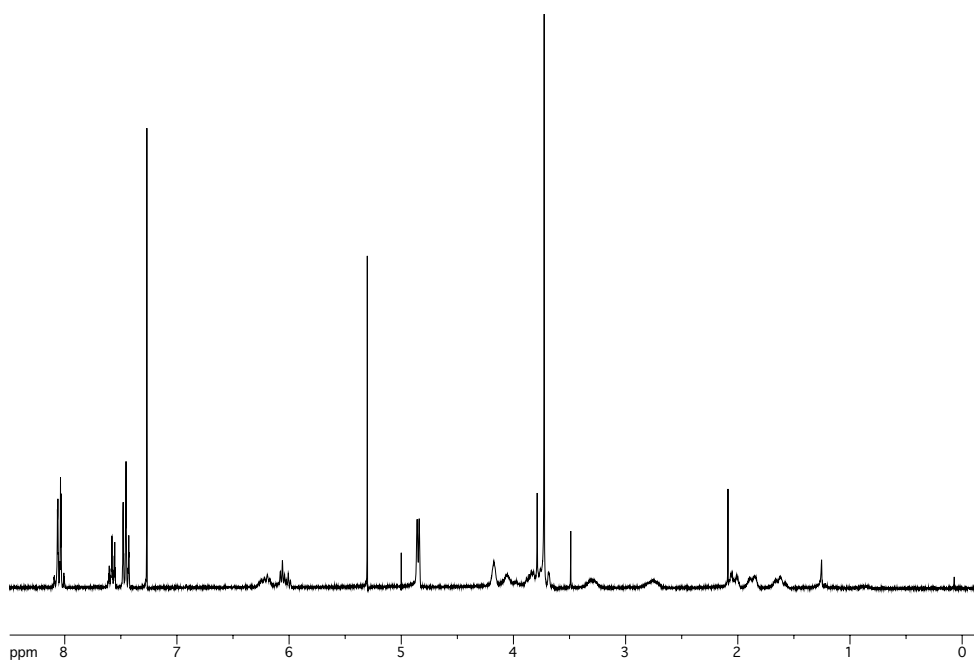


Figure 8.155. ^1H NMR of 5-hydroxypiperidine-2-carboxylate (3.136a)

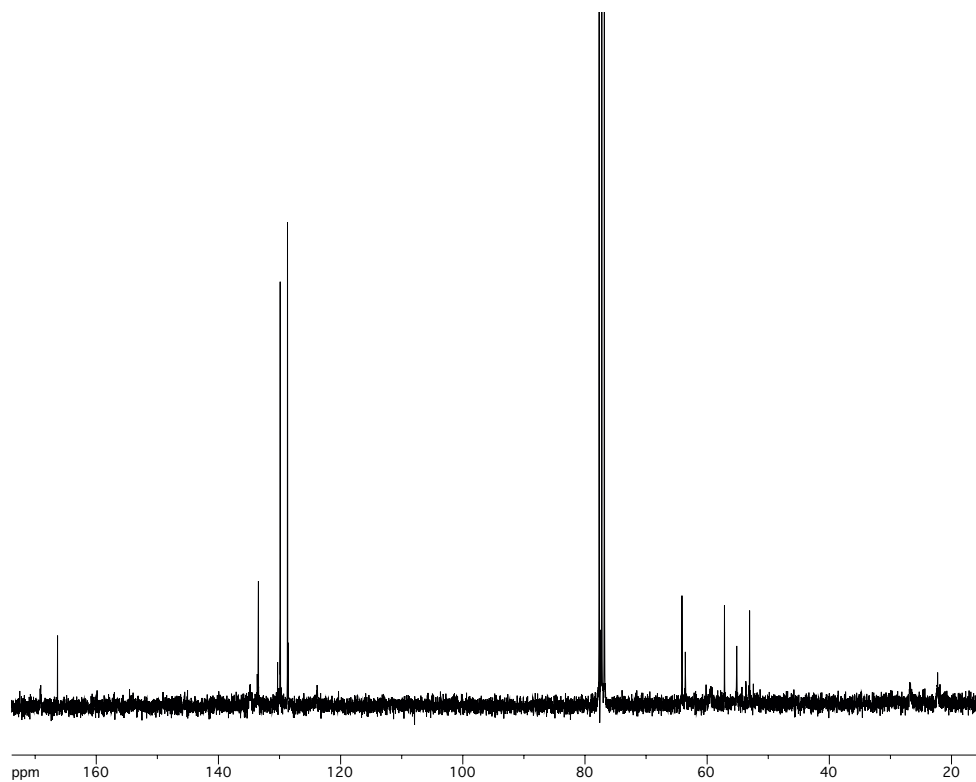


Figure 8.156. ^{13}C NMR of 5-hydroxypiperidine-2-carboxylate (3.136a)

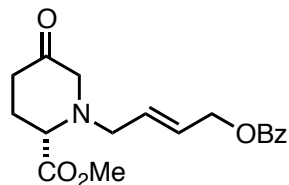


Figure 8.157. 5-oxopiperidine-2-carboxylate (3.137)

3.136a (130mg, 0.390mmol) in DCM (4mL) was cooled to -78°C . $(\text{COCl})_2$ (67 μL , 0.780mmol) was then added and stirred for 5 minutes. DMSO (97 μL , 1.365mmol) was then added and the reaction was stirred at -78°C for 20 minutes. Et_3N (380 μL , 2.730mmol) was then added and the reaction was stirred for 30 minutes at -78°C and then it was warmed to room temperature and quenched with water (15mL) and extracted with DCM. Purification via column chromatography yielded 74mg of **3.137**. (35% 2 steps).

$^1\text{H-NMR}$ (300 MHz; CDCl_3): δ 2.23-2.18 (m, 2H), 2.44 (dd, $J = 10.4, 4.7$ Hz, 2H), 3.21 (d, $J = 16.3$ Hz, 1H), 3.29 (t, $J = 4.9$ Hz, 2H), 3.59 (d, $J = 16.2$ Hz, 1H), 3.67 (t, $J = 4.9$ Hz, 1H), 3.72 (s, 3H), 4.80 (d, $J = 4.4$ Hz, 2H), 5.90-5.75 (m, 2H), 7.43 (t, $J = 7.5$ Hz, 2H), 7.56 (t, $J = 7.4$ Hz, 1H), 8.04 (d, $J = 7.1$ Hz, 2H). $^{13}\text{-C NMR}$ (75 MHz; CDCl_3): δ 26.34, 36.07, 51.89, 56.92, 59.11, 59.52, 64.78, 77.47 128.38, 128.85, 129.74, 130.57, 133.26, 166.47, 173.04, 206.79

[JMG-2-492-1, JMG-2-492C13]

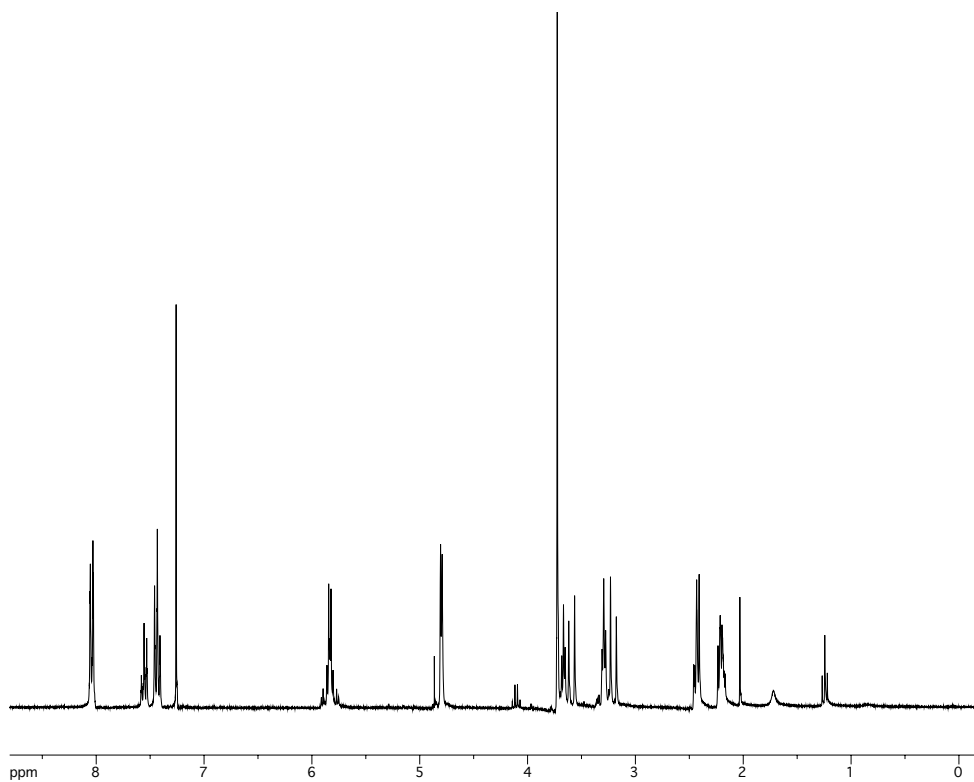


Figure 8.158. ^1H NMR of 5-oxopiperidine-2-carboxylate (3.137)

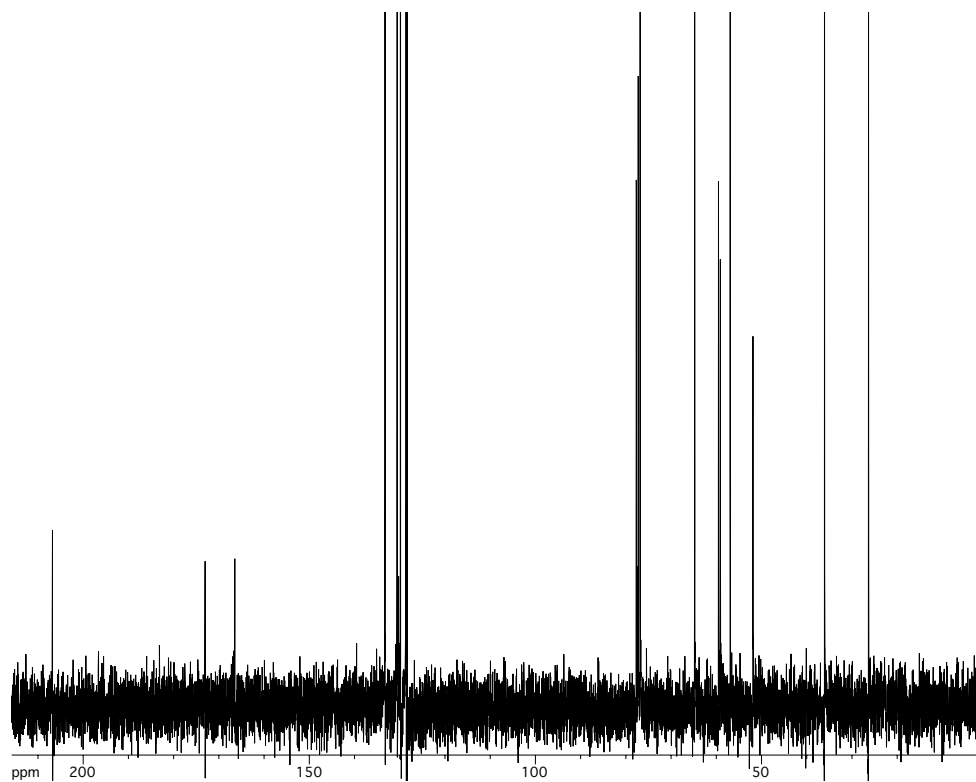


Figure 8.159. ^{13}C NMR of 5-oxopiperidine-2-carboxylate (3.137)

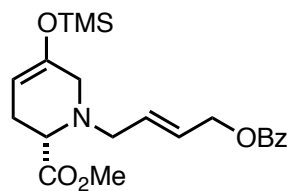


Figure 8.160. 1,2,3,6-tetrahydropyridine-2-carboxylate (3.138)

3.137 (74mg, 0.223mmol) in THF (3.5mL) was cooled under argon to -78°C . TMSCl (50 μl , 0.447mmol) and then LHMDs (450 μl , 0.447mmol, 1M soln') were added and the reaction was stirred at -78°C for 30 minutes and then stirred 15 minutes at 0°C . The reaction was then concentrated down and purified on a Davisil column with hexanes:EtOAc (80:20) to give 43mg of **3.138** (48%). Compound was immediately taken on to the cyclization reaction and further data was not obtained.

[JMG-2-493crude]

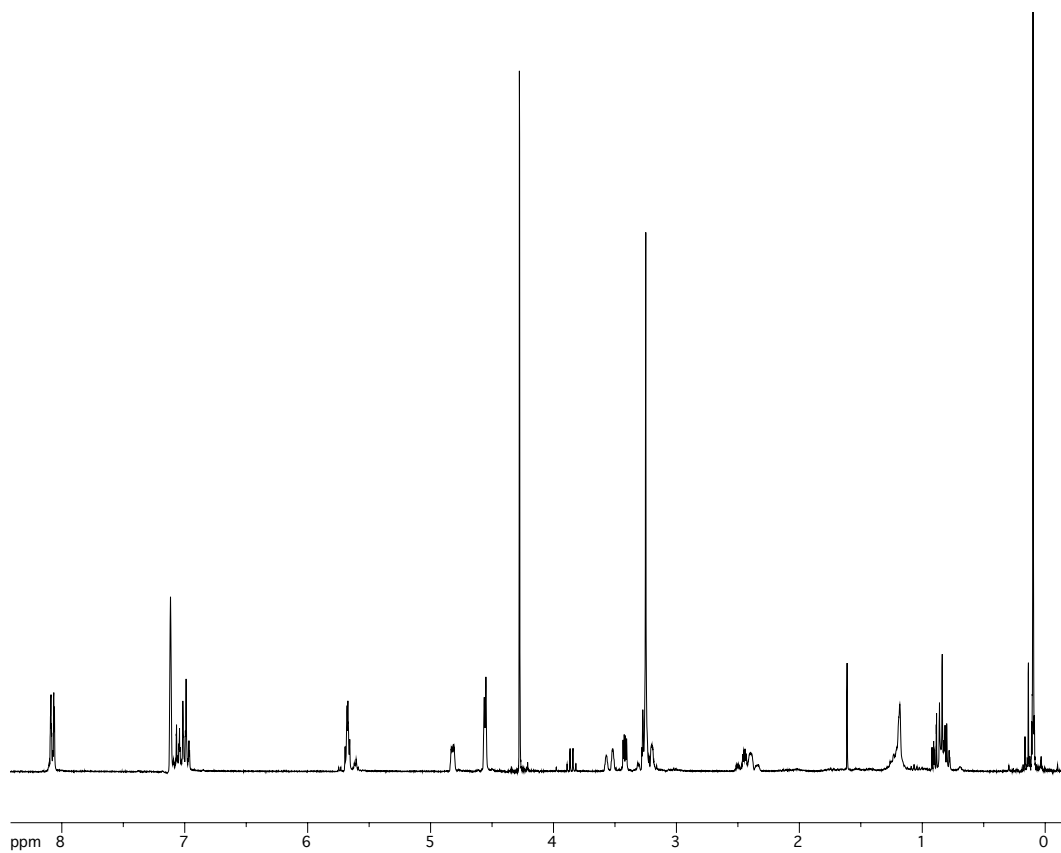


Figure 8.161. ^1H NMR of 1,2,3,6-tetrahydropyridine-2-carboxylate (3.138)

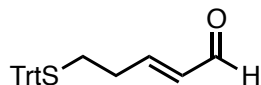


Figure 8.162. (*E*)-5-(tritylthio)pent-2-enal (**5.11**)⁵

TrtSH (5g, 18.090mmol) was dissolved in DCM (120mL) at room temperature. Et₃N (3.5mL, 25.326mmol) was added followed by acrolein (**5.9**) (1.7mL, 25.326mmol) and the reaction was stirred for 1 hour. The reaction was then concentrated and diluted with benzene (120mL). **5.10** (6.06g, 19.899mmol) was then added and the reaction was fitted with a D.S. trap and refluxed overnight. The reaction was the concentrated onto silica gel and run through a short plug of silica with hexanes:EtOAc, 50:50. The crude mixture was then concentrated and diluted with Et₂O, causing the desired product to crash out. The product was then filtered and dried (25%).

[JMG-3-91ppt]

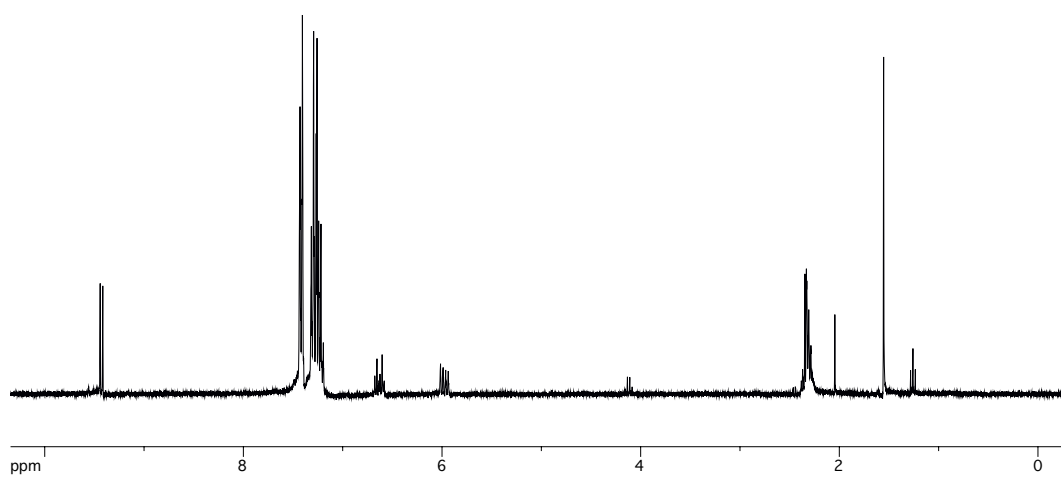


Figure 8.163. ¹H NMR of (*E*)-5-(tritylthio)pent-2-enal (5.11)⁵

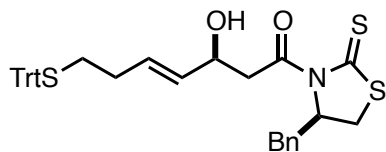


Figure 8.164. 3-hydroxy-7-(tritylthio)hept-4-en-1-one (5.13)⁵

Thiazolium thione (**5.12**) (1.5g, 5.975mmol) was dissolved in DCM (40mL) and TiCl_4 (734ml, 6.679mmo) was added. The reaction was cooled to -78°C and Hünig's base (1.2mL, 6.679mmol) was added dropwise and the reaction was stirred for 2 hours at -78°C . The aldehyde (**5.11**) (1.23g, 3.515mmol) was then added in DCM (5mL) and the reaction was stirred for 1 hour at -78°C . 50mL $\text{NH}_4\text{Cl}_{\text{aq}}$ was then added and the reaction was extracted with DCM (50mL X 2) and washed with brine and then dried over Na_2SO_4 and concentrated. The crude mixture of diastereomers was purified via column chromatography, hexanes:EtOAc, 95:5-75:25 to afford the desired diastereomer, **5.13**, in 56% yield.

[JMG-3-96]

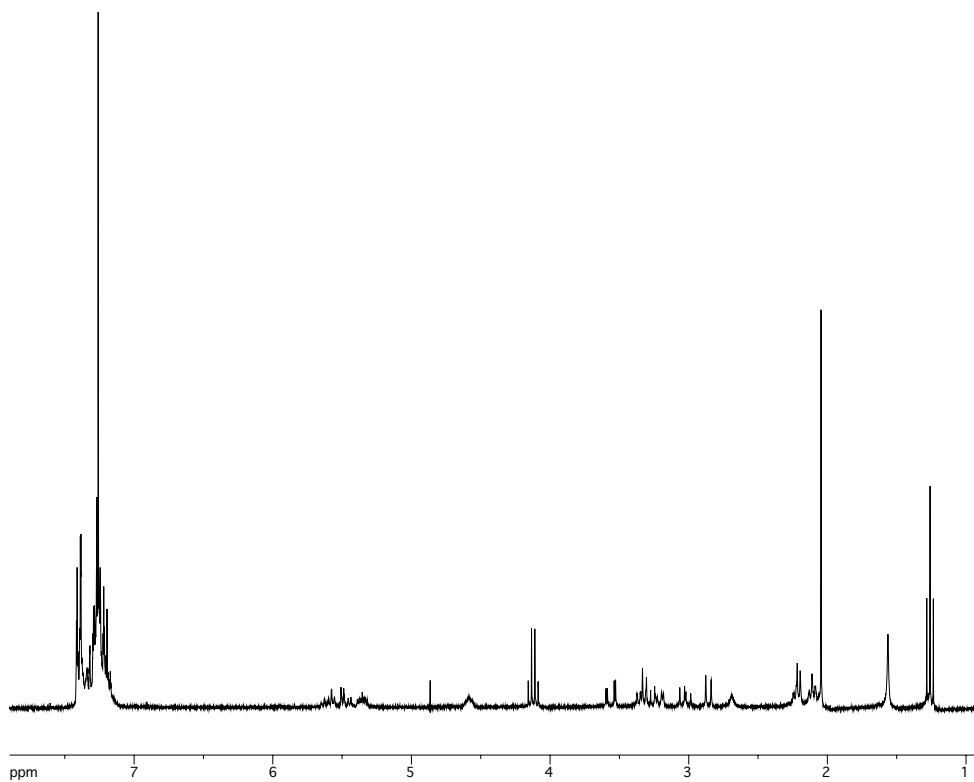


Figure 8.165. ^1H NMR of 3-hydroxy-7-(tritylthio)hept-4-en-1-one (5.13)⁵

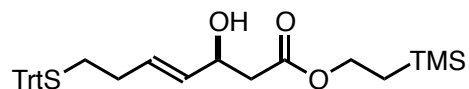


Figure 8.166. 3-hydroxy-7-(tritylthio)hept-4-enoate (5.5)⁵

To **5.13** (217mg, 0.356mmol) was added DCM (6mL). TMS-EtOH (510ml, 3.558mmol) was then added followed by imidazole (36mg, 0.534mmol). The reaction was allowed to stir at room temperature overnight. The reaction was then concentrated and purified via column chromatography, hexanes:EtOAc, 90:10 to afford the desire product, with excess TMS-EtOH in it. The crude mixture was then placed on high vacuum and heated to 40°C overnight to aid in the removal of the TMS-EtOH. The desired compound was isolated. Due to the presence of residual TMS-EtOH, excess reagents for the subsequent coupling reaction were used.

[JMG-3-52-2]

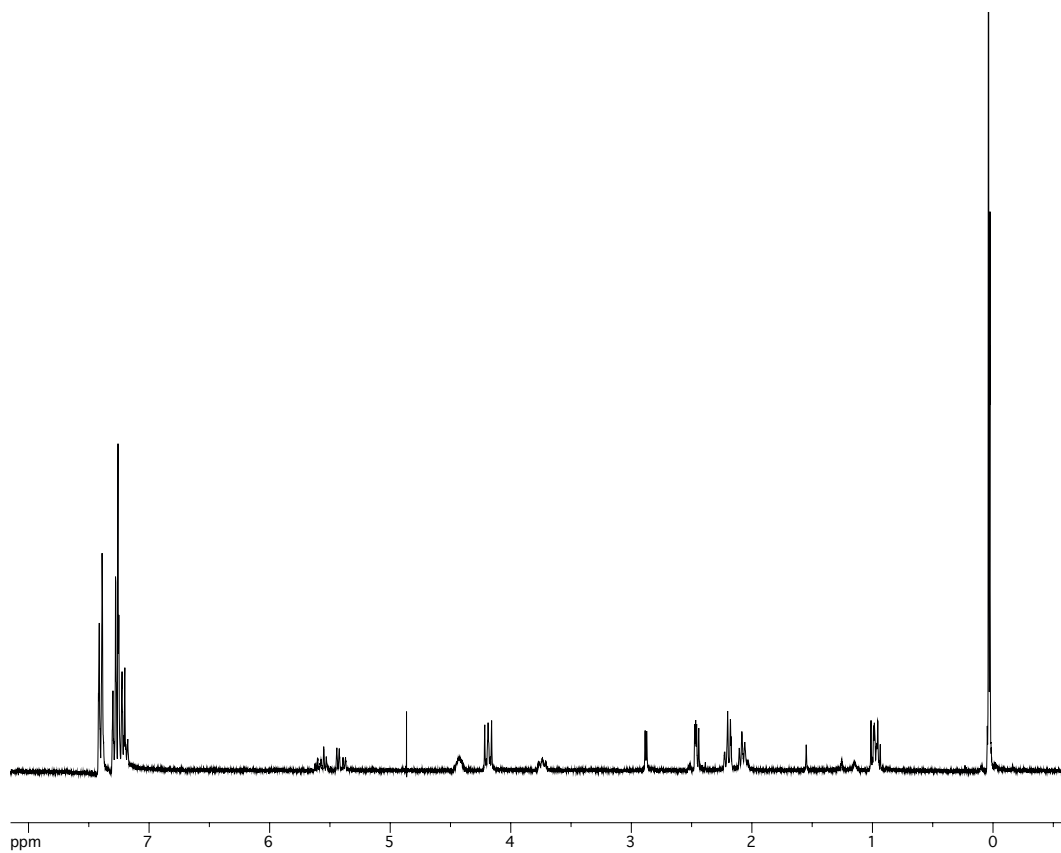


Figure 8.167. ^1H NMR of 3-hydroxy-7-(tritylthio)hept-4-enoate (5.5)⁵

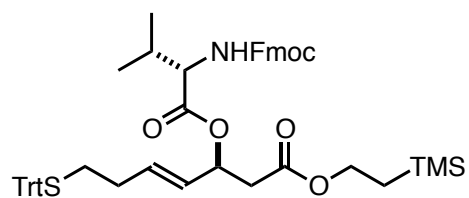


Figure 8.168. N-Fmoc-Val-7-(tritylthio)hept-4-enoate (5.14)⁵

5.5 (190mg, 0.366mmol) and Fmoc-L-Val-OH (621mg, 1.831mmol) were dissolved in DCM (8mL) and cooled to 0°C. EDCI (341mg, 2.196mmol) was added followed by DMAP (5mg, 0.037mmol) and Hünig's base (385ml, 2.196mmol). The reaction was allowed to warm to room temperature and stirred overnight. The reaction was then concentrated onto silica gel and purified via column chromatography, hexanes:EtOAc, 90:10 to afford desired product **5.14**. (65%)

[JMG-3-64-3]

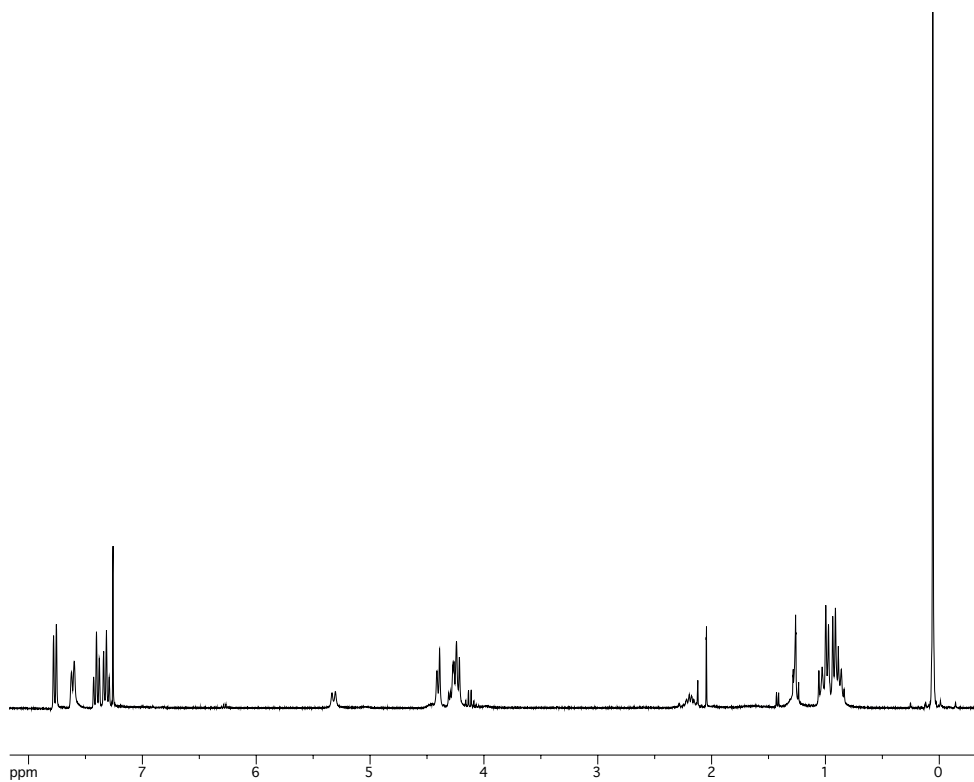


Figure 8.169. ^1H NMR of N-Fmoc-Val-7-(tritylthio)hept-4-enoate (5.14)⁵

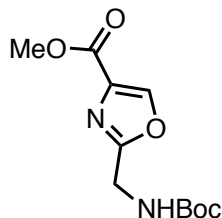


Figure 8.170. Oxazole (5.7)⁸⁵

Dipeptide (420mg, 1.520mmol) was dissolved in DCM (6mL) under argon and cooled to -78°C. DAST (241ml, 1.824mmol) in DCM (5mL) was then added dropwise and the reaction was stirred at -78°C for 1.5 hours. The reaction was then poured into sodium bicarbonate and extracted with DCM and dried over Na₂SO₄ and concentrated. The crude mixture was immediately dissolved in DCM (7.5mL) and BrCCl₃ (875ml, 9.050mmol) was added followed by DBU (1.35mL, 9.050mmol) and the reaction was allowed to stir at room temperature for 3 hours. The reaction was concentrated onto silica gel and purified via column chromatography with hexanes: EtOAc, 50:50, to give the desired product (74%).

[JMG-3-51]

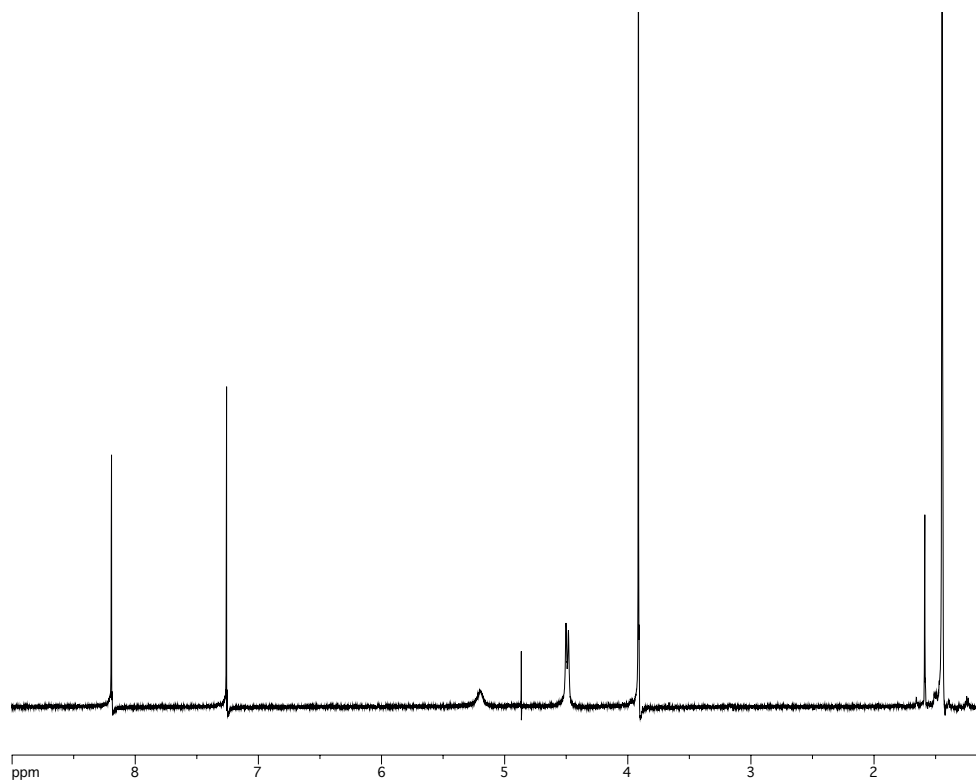


Figure 8.171. ^1H NMR of Oxazole (5.7)⁸⁵

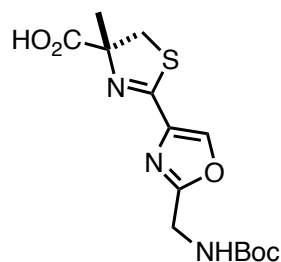


Figure 8.172. Thiazoline-Oxazole Acid (5.4)^{5,85}

To oxazole **5.7** (880mg, 3.436mmol) under argon at room temperature was added MeOH (90mL) then NH₄OH (20mL). The reaction was allowed to stir overnight. The reaction mixture was then concentrated and put under vacuum for several hours. The crude amide was then dissolved in DCM (120mL) and Et₃N (7.5mL, 53.068mmol) was added and the reaction was cooled to 0°C. POCl₃ (824mL, 8.845mmol) was then added dropwise and the reaction was allowed to warm to room temperature and stir for 16 hours. The reaction was then concentrated down and taken on immediately. To the crude material was added MeOH (60mL) then α-Me-Cys-OH·HCl (610mg, 3.554mmol) was added and the reaction was stirred at room temperature. Et₃N (2mL, 14.120mmol) was then added and the reaction was stirred overnight. The reaction was subsequently concentrated and purified through a silica plug providing **5.4** (72%). HRMS (ESI): *m/z* calcd. for C₁₄H₁₉N₃O₅S (M+H)⁺: 342.1124, found 342.1112. [α]_D = -3.46, c=0.005 in DCM. ¹H NMR (400MHz, CDCl₃) δ TMS: 1.47 (9H, s); 1.69 (3H, s); 3.34 (1H, d, *J* = 11.1); 3.88 (1H, d, *J* = 11.7); 4.50-4.51 (2H, m, *J* = 2.7); 5.29 (1H, bs); 8.20 (1H, s). ¹³C NMR (100.8MHz, CDCl₃) δ TMS: 24.02, 26.27, 37.83, 40.74, 80.44, 83.98, 134.65, 140.49, 155.49, 162.36, 162.50, 174.80. IR (n_{max}) 3321.20, 2978.02, 1711.95, 1625.16, 1165.44, 947.31 cm⁻¹ [JMG-3-109, JMG-3-109C13]

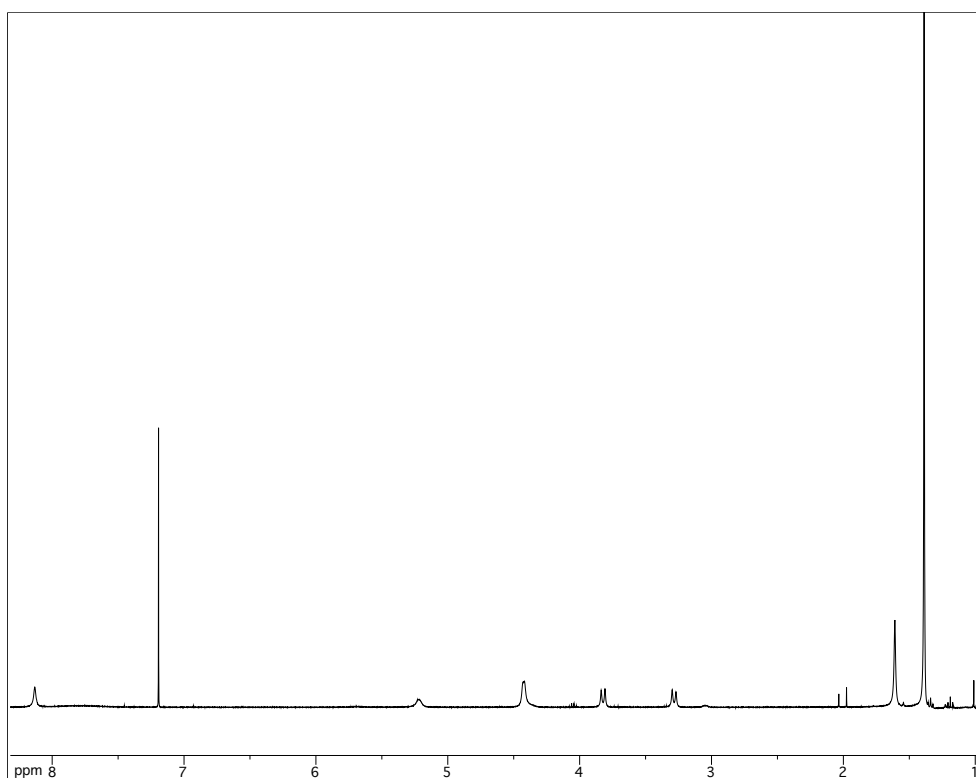


Figure 8.173. ^1H NMR of Thiazoline-Oxazole Acid (5.4)^{5,85}

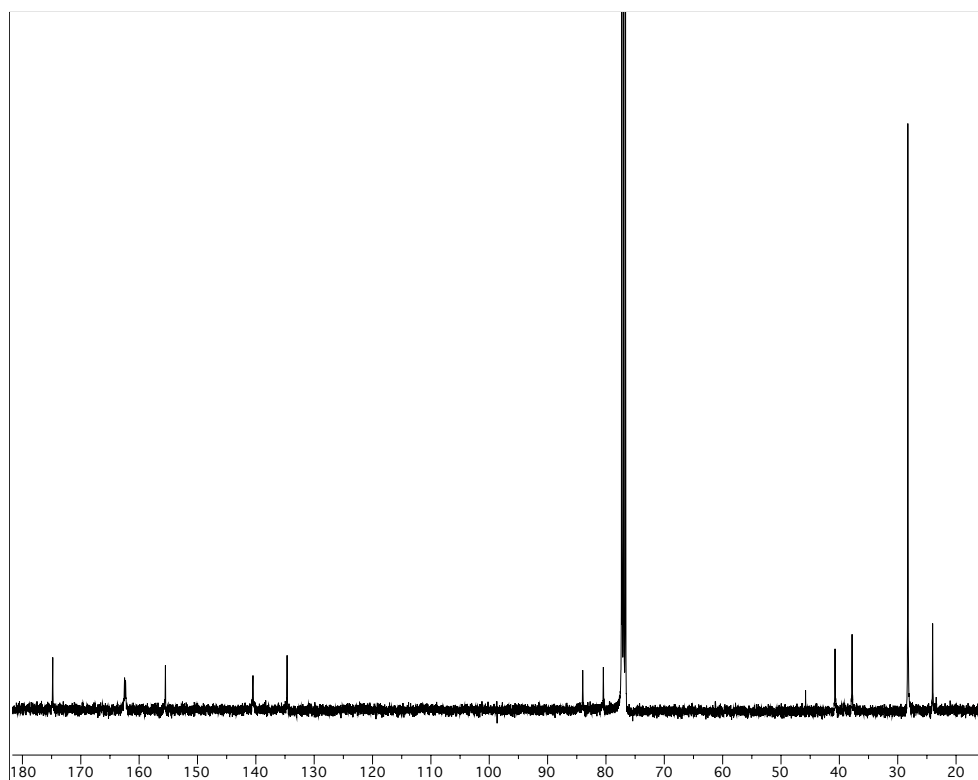


Figure 8.174. ^{13}C NMR of Thiazoline-Oxazole Acid (5.4)^{5,85}

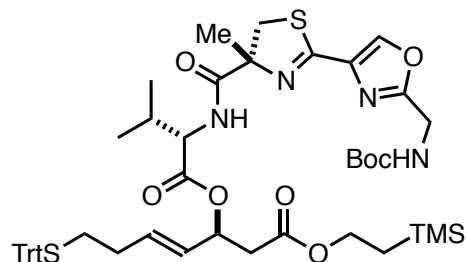


Figure 8.175. Thiiazoline-Oxazole Acycle Analog (5.3)^{5,85}

5.14 (880mg, 1.047mmol) was dissolved in CH₃CN (5.5mL) and Et₂NH (5.3mL) was added. The reaction was allowed to stir at room temperature for 3 hours and was then concentrated, dissolved in EtOAc and concentrated down two more times and then put under high vacuum overnight. The crude amine was then dissolved in DCM (15mL) and PyBOP (1.1g, 2.094mmol) was added and the solution as cooled to 0°C. Hünig's base (911ml, 5.235mmol) was then added and the reaction was stirred for 10 minutes. Thiiazoline-oxazole fragment (**5.4**) (360mg, 0.869mmol) was then added in DCM (10mL). The reaction was allowed to stir at room temperature for 5 hours and was then concentrated down onto silica gel and purified via column chromatography, hexanes:EtOAc, 93:7 to 70:30 to afford the desired acycle (**5.3**) in 91% yield.

HRMS (ESI): *m/z* calcd. for C₅₀H₆₄N₄O₈S₂Si (M+Na)⁺ 963.3833, found 963.3827. [α]_D = +30, c = 6 in CH₂Cl₂. ¹H-NMR (300 MHz; CDCl₃): δ 0.04 (s, 9H), 0.76 (d, *J* = 6.9 Hz, 3H), 0.83 (d, *J* = 6.8 Hz, 3H), 1.00-0.94 (m, 4H), 1.47 (s, 9H), 1.57 (s, 3H), 2.09-2.02 (m, 3H), 2.22-2.12 (m, 2H), 2.55 (dd, *J* = 15.8, 5.8 Hz, 1H), 2.69 (dd, *J* = 15.6, 7.8 Hz, 1H), 3.31 (d, *J* = 11.6 Hz, 1H), 3.78 (d, *J* = 11.5 Hz, 1H), 4.15 (ddd, *J* = 10.0, 7.1, 3.3 Hz, 3H), 4.50-4.44 (m, 2H), 5.15 (bs, 1H), 5.37 (dd, *J* = 15.6, 7.4 Hz, 1H), 5.66 (tt, *J* = 14.8, 7.3 Hz, 2H), 7.12 (d, *J* = 8.9 Hz, 1H), 7.41-7.20 (m, 5H), 8.10 (s, 1H). ¹³C NMR (75 MHz;

CDCl₃): δ -1.27, 17.51, 17.74, 19.27, 24.91, 28.54, 31.31, 31.55, 39.93, 41.42, 57.12, 63.33, 66.83, 71.97, 77.43, 85.49, 126.82, 128.07, 129.78, 134.07, 145.04, 162.12, 169.85, 170.50, 174.41. IR (n_{\max}) 3388.61, 2960.13, 1736.44, 1681.31, 1510.68, 1250.17, 1171.92 cm⁻¹

[JMG-3-67, JMG-3-67C13]

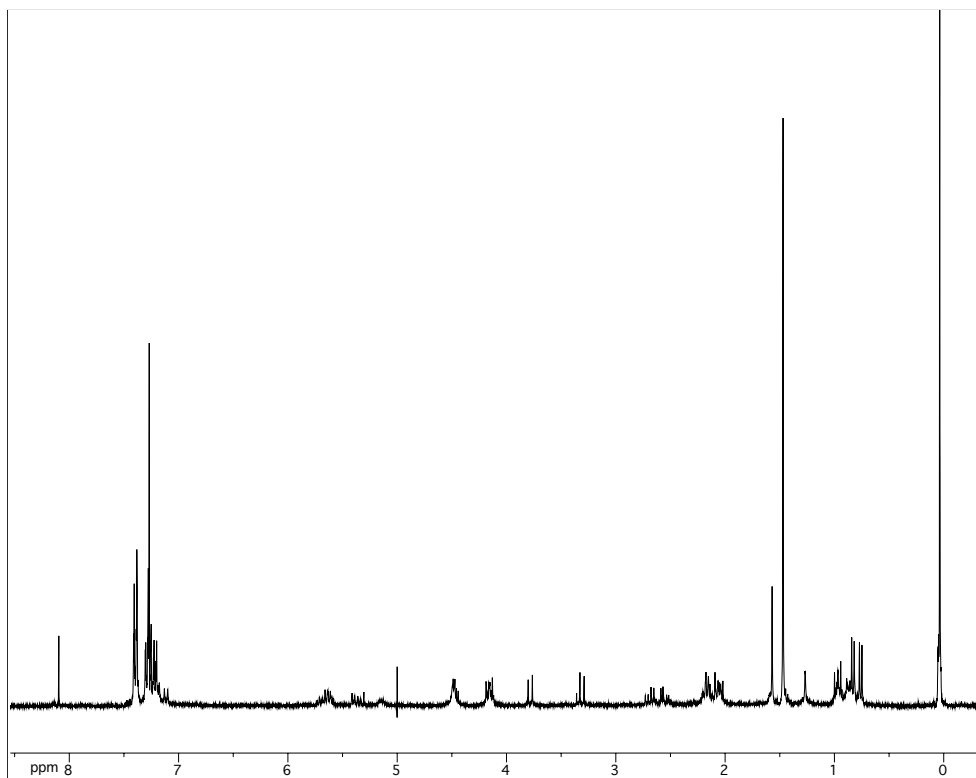


Figure 8.176. ^1H NMR of Thiazoline-Oxazole Acycle Analog (5.3)^{5,85}

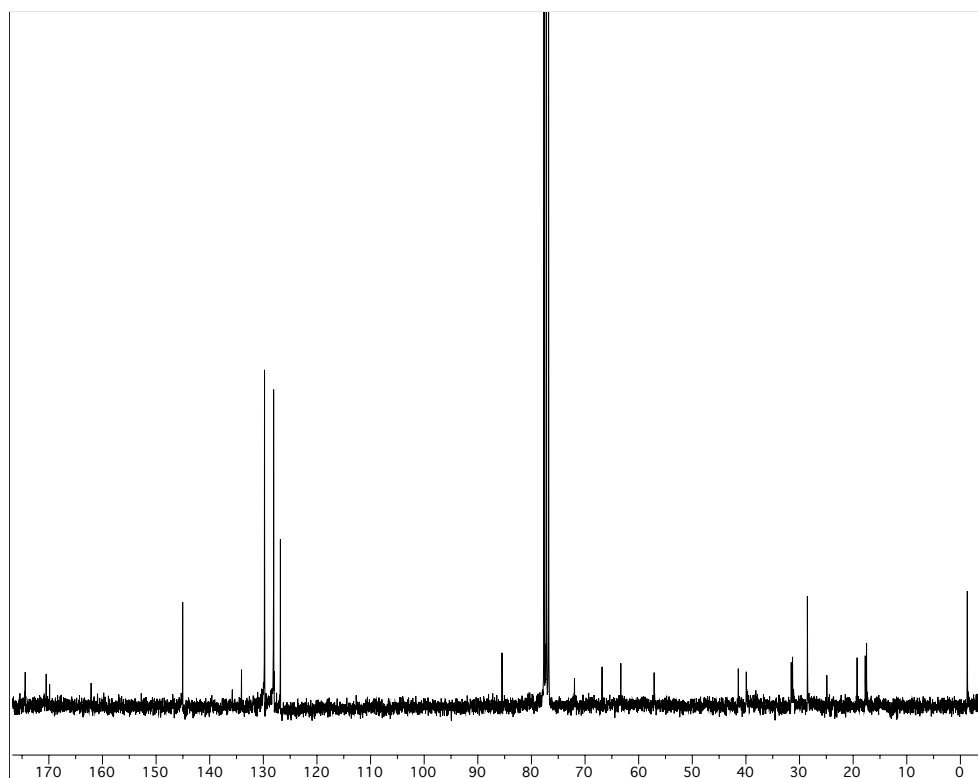


Figure 8.177. ^{13}C NMR of Thiazoline-Oxazole Acycle Analog (5.3)^{5,85}

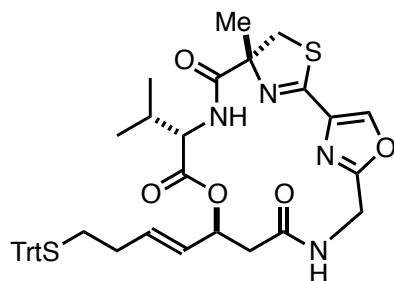


Figure 8.178. Thiiazoline-Oxazole Macrocycle Analog (5.2)

5.3 (433mg, 0.460mmol) was dissolved in DCM (15mL) and cooled to 0°C. TFA (1.5mL) was then added and the reaction was stirred at room temperature overnight. The reaction was then pulled down and pulled down again from DCM and placed under vacuum for several hours. The reaction was then dissolved in DCM (460mL) and cooled to 0°C and Hünig's base (640ml, 3.680mmol) was then added dropwise. T3P (400mg, 0.552mmol) was then taken up into a syringe with DMF (2mL) and added to the starting material via a syringe pump over 1 hour. The reaction was then allowed to stir at room temperature for 48 hours and was then concentrated down and diluted with EtOAc and washed with brine (3 X 30mL). Purification via column chromatography, hexanes:EtOAc, 50:50 gave the desired product (**5.2**) in 30-40% yield.

HRMS calcd for $C_{40}H_{42}N_4NaO_5S_2$ (M+Na)⁺ 745.2494, found 745.2486. $[\alpha]_D = +23$, $c = 0.04$ in CH_2Cl_2 . 1H (300 MHz, $CDCl_3$): 0.68 (6H, t, $J = 6.8$), 1.83 (3H, s), 1.94 (4H, m), 2.20 (2H), 2.64 (1H, dd, $J = 3.8, 16.0$), 2.75 (1H, dd, $J = 7.7, 15.9$), 3.24 (1H, d, $J = 11.3$); 3.79 (1H, dd, $J = 4.1, 17.5$), 4.00 (1H, d, $J = 11.3$), 4.46 (1H, dd, $J = 4.0, 8.6$), 4.76 (1H, dd, $J = 9.0, 17.3$), 5.53 (3H, m), 6.40 (1H, dd, $J = 4.2, 9.4$), 7.15 (1H, d, $J = 8.8$), 7.22 (10H, m), 7.37 (5H, m), 7.97 (1H, s). ^{13}C (75.5 MHz, $CDCl_3$): 17.72, 18.86, 24.20,

31.11, 31.59, 34.03, 37.25, 37.28, 41.31, 43.48, 58.68, 66.93, 71.78, 77.44, 84.10,
126.96, 128.18, 128.91, 129.80, 133.00, 135.30, 141.16, 144.88, 162.08, 163.34,
168.67, 170.32, 173.59. IR (n_{\max}) 3376.15, 2959.87, 1735.69, 1674.72, 1541.38,
1245.67 cm^{-1}

[JMG-3-69, JMG-3-69C13]

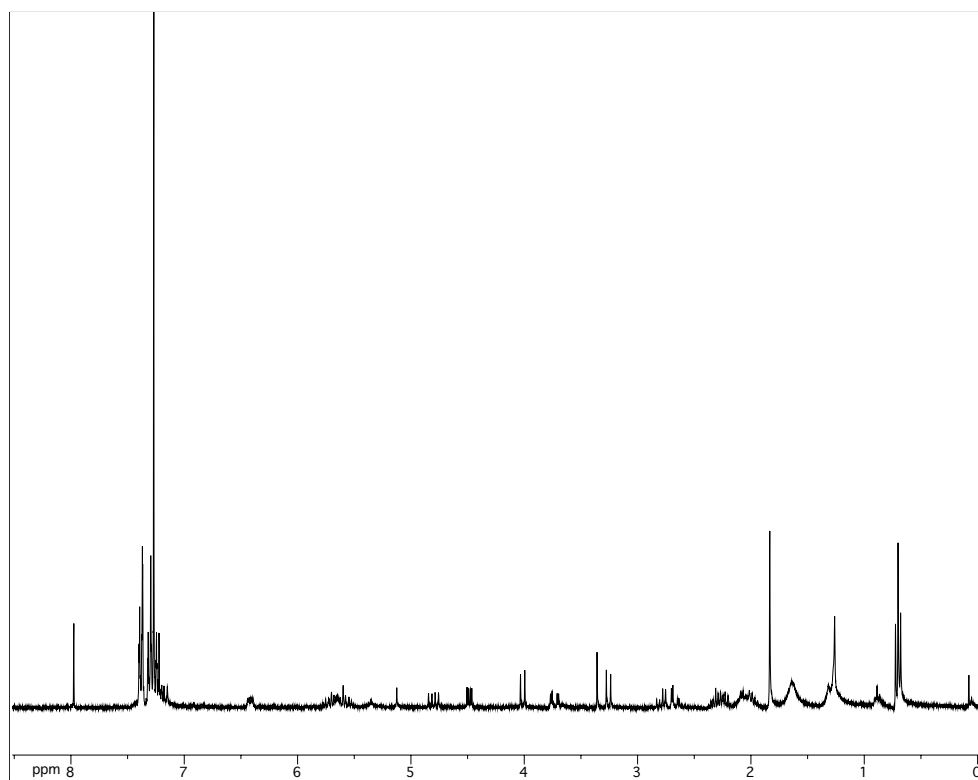


Figure 8.179. ^1H NMR of Thiazoline-Oxazole Macrocycle Analog (5.2)

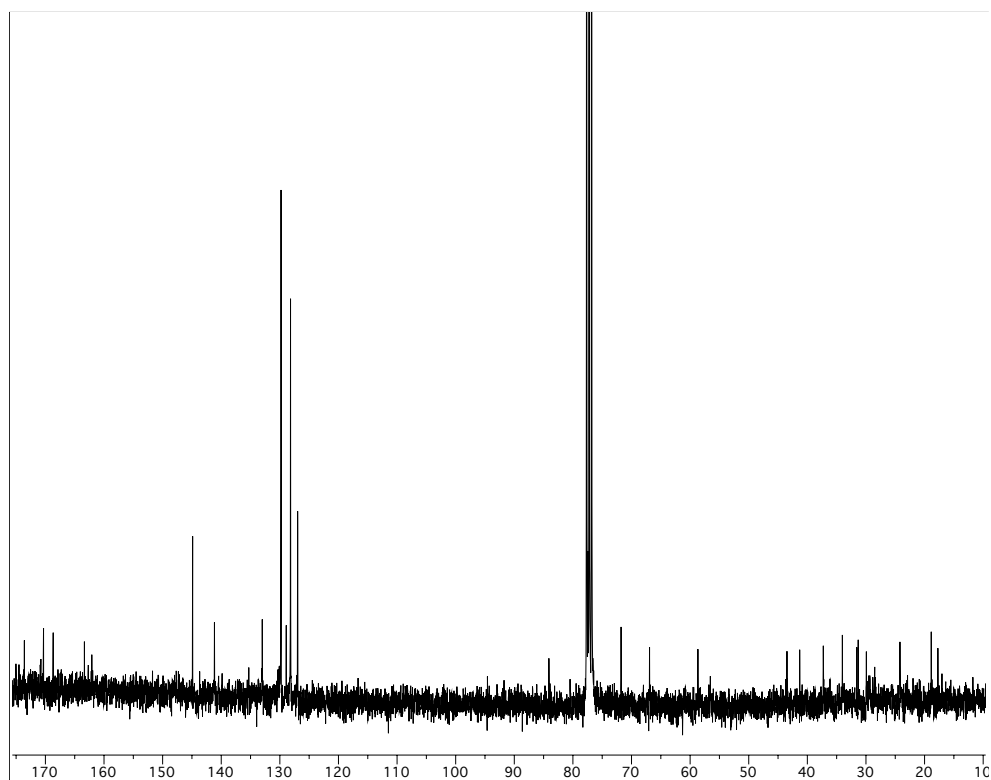


Figure 8.180. ^{13}C NMR of Thiazoline-Oxazole Macrocyclic Analog (5.2)

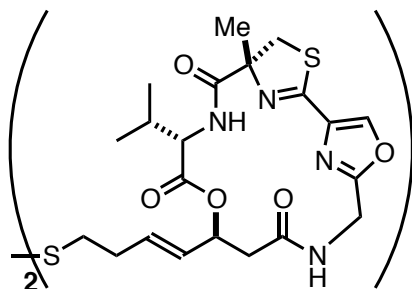


Figure 8.181. Thiazoline-Oxazole Dimer (5.15)

5.2 (128mg, 0.177mmol) in DCM (25mL) was cooled to 0°C. $i\text{Pr}_3\text{SiH}$ (75ml, 0.354mmol) was added and then TFA (885ml) was then added to the reaction at room temperature. The reaction was allowed to stir at room temperature for 2 hours and then was concentrated and purified via column chromatography, hexanes:EtOAc, 50:50 then 100% EtOAc to give the desired dimer (**5.15**) in 35% yield.

HRMS calcd. for $\text{C}_{42}\text{H}_{54}\text{N}_8\text{O}_{10}\text{S}_4\text{Na}$ ($\text{M}+\text{Na}$) $^+$: 981.2743, found: 981.2715. HRMS calcd. for $\text{C}_{42}\text{H}_{55}\text{N}_8\text{O}_{10}\text{S}_4$ ($\text{M}+\text{H}$) $^+$: 959.2924, found: 959.2906. $[\alpha]_{\text{D}} = +4$, $c = 0.005$ in CH_2Cl_2
 ^1H NMR (400 MHz, CDCl_3): 0.61 (3H, d, $J = 6.9$); 0.65 (3H, d, $J = 6.9$); 1.79 (3H, s); 2.02 (2H, m), 2.38 (2H, m); 2.67 (2H, t, $J = 7.4$); 2.85 (2H, dd, $J = 9.7, 16.6$); 3.20 (1H, d, $J = 11.4$); 3.93 (3H, m); 4.49 (1H, dd, $J = 3.6, 9.0$); 4.86 (1H, dd, $J = 9.4, 17.6$); 5.51 (1H, dd, $J = 7.1, 15.4$); 5.61 (1H, m); 5.82 (1H, m); 6.45 (1H, dd, $J = 3.8, 9.1$); 7.04 (1H, d, $J = 9.1$); 7.95 (1H, s). ^{13}C NMR (100.8 MHz, CDCl_3): 17.48, 18.97, 24.15, 29.93, 31.93, 34.46, 37.54, 37.97, 38.84, 40.56, 43.56, 58.44, 72.18, 77.46, 84.05, 128.74, 133.18, 135.28, 141.39, 162.21, 163.65, 165.99, 168.99, 170.57, 173.72. IR (n_{max}) 3336.37, 2925.71, 1736.10, 1676.07, 1620.05, 1501.02, 1244.86 cm^{-1}

[JMG-3-142, JMG-3-142C13]

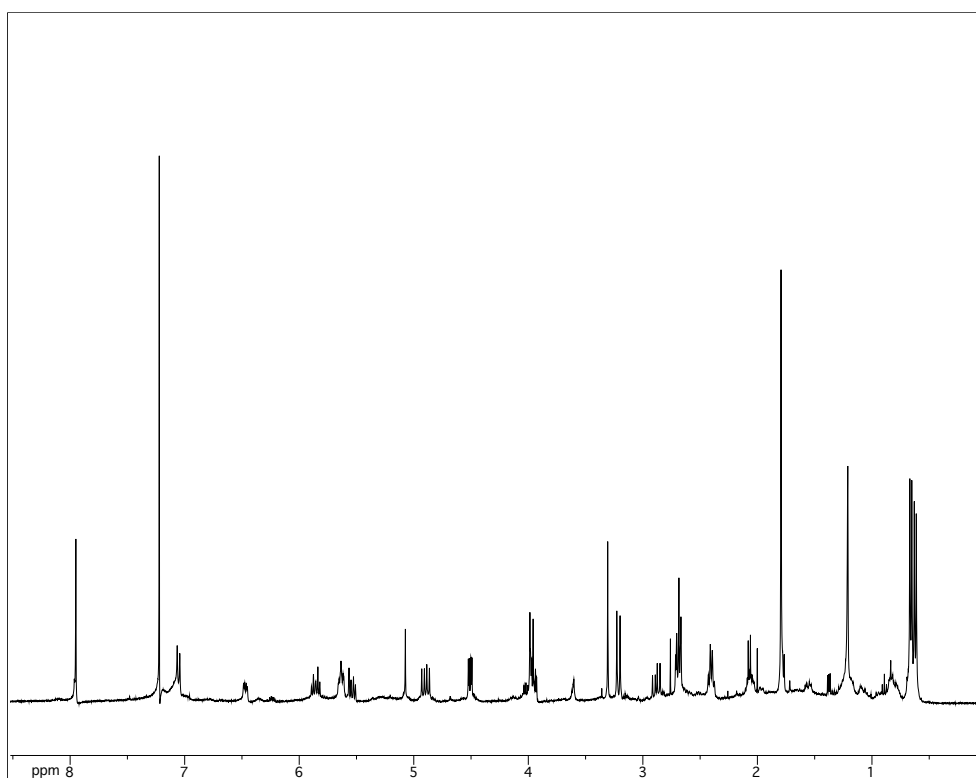


Figure 8.182. ^1H NMR of Thiazoline-Oxazole Dimer (5.15)

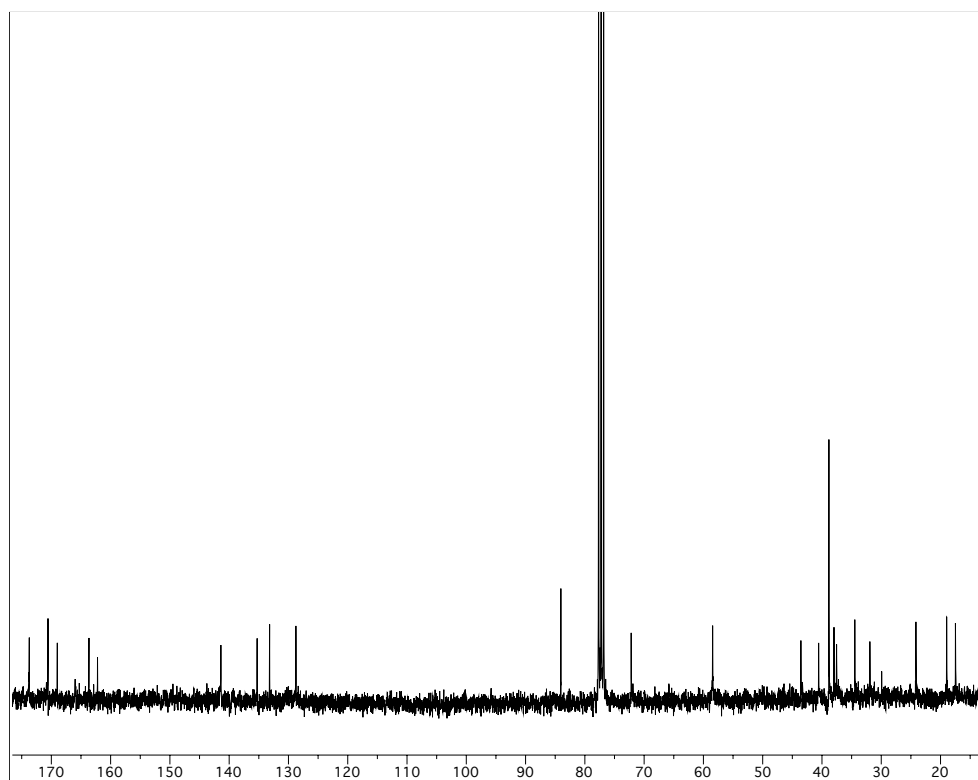


Figure 8.183. ^{13}C NMR of Thiazoline-Oxazole Dimer (5.15)

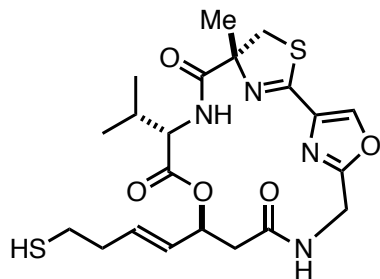


Figure 8.184. Thiiazoline-Oxazole Thiol Analog (5.16)^{5,85}

Macrocycle (**5.3**) (40mg, 0.055mmol) was dissolve in degassed DCM (7mL) and Et₃SiH (20ml, 0.111mmol) was added, followed by TFA (275ml). The reaction as stirred at room temperature for 1 hour and then pulled down and immediately purified via column chromatography, hexanes:EtOAc, 20:80 to 0:100, provided the desired thiol (**5.16**) in 83% yield. HRMS calcd for C₂₁H₂₉N₄O₅S₂ (M+H)⁺: 481.1579, found 481.1574. HRMS calcd for C₂₁H₂₈N₄NaO₅S₂ (M+Na)⁺: 503.1399, found 503.1389. [α]_D = +24, c = 0.8 in CH₂Cl₂ ¹H NMR (400MHz, CDCl₃): 0.65 (d, 3H, *J* = 6.9), 0.69 (d, 3H, *J* = 6.9), 1.84 (s, 3H), 2.08 (m, 1H), 2.34 (m, 2H), 2.56 (q, 2H, *J* = 7.3), 2.69 (dd, 1H, *J* = 3.1, 16.4), 2.87 (dd, 1H, *J* = 11.4), 3.24 (d, 1H, *J* = 11.6), 4.01 (d, 1H, *J* = 11.2), 4.02 (dd, 1H, *J* = 3.6, 17.6), 4.53 (dd, 1H, *J* = 3.7, 8.9), 4.94 (dd, 1H, *J* = 9.6, 17.6), 5.55 (ddt, 1H, *J* = 1.3, 6.8, 15.4), 5.66 (ddd, 1H, *J* = 2.8, 6.7, 9.4), 5.81 (dt, 1H, *J* = 7.3, 14.9), 6.21 (dd, 1H, *J* = 3.5, 9.4), 7.11 (d, 1H, *J* = 8.8), 7.99 (s, 1H). ¹³C NMR (100.8MHz, CDCl₃): 17.71, 19.18, 24.36, 30.17, 34.66, 36.75, 37.78, 40.99, 43.80, 58.68, 72.34, 77.63, 84.28, 99.17, 129.41, 132.99, 135.52, 141.62, 162.38, 163.68, 169.18, 170.86, 173.92. IR (n_{max}) 3374.08, 2960.18, 2530.09, 1734.46, 1671.79, 1505.02, 1247.74, 1038.66, 753.00 cm⁻¹ [JMG-3-182, JMG-3-182C13]

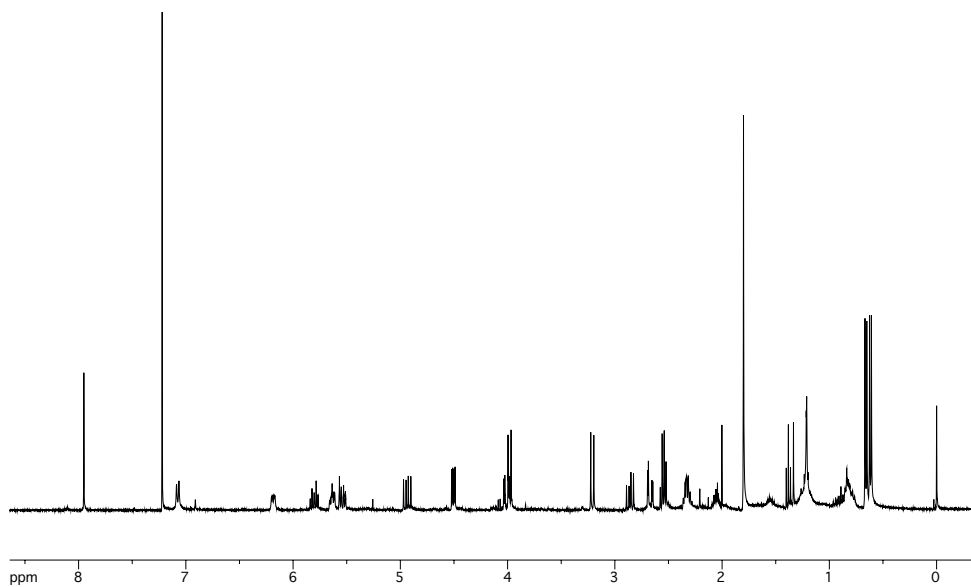


Figure 8.185. ^1H NMR of Thiazoline-Oxazole Thiol Analog (5.16)^{5,85}

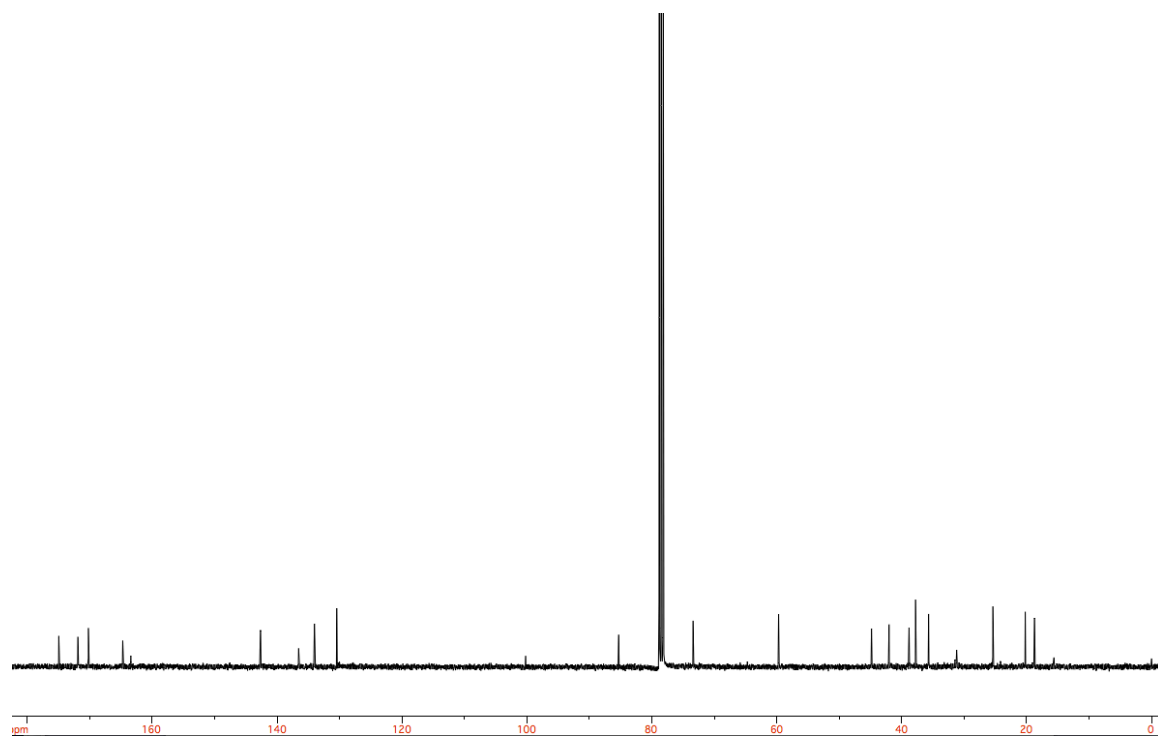


Figure 8.186. ^{13}C NMR of Thiazoline-Oxazole Thiol Analog (5.16)^{5,85}

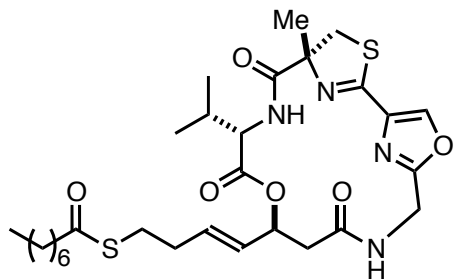


Figure 8.187. Thiazoline-Oxazole Thioester Analog (5.1)^{5,85}

Macrocycle (**5.3**) (40mg, 0.055mmol) was dissolve in degassed DCM (7mL) and Et₃SiH (20μl, 0.111mmol) was added, followed by TFA (275μl). The reaction as stirred at room temperature for 1 hour and then pulled down and immediately dissolved in 7mL of degassed DCM. Octanoyl chloride (600ml, 3.300mmol) was added, followed by Et₃N (900μl, 4.950mmol). The reaction was stirred at room temperature overnight and then filtered over Celite and concentrated down and put onto a column and purified with 75% EtOAc to 100%. Then p-TLC was performed with 100% EtOAc, giving 9mg of product (**5.1**) (27%).

HRMS calcd for C₂₉H₄₃N₄O₆S₂ (M+H)⁺: 607.2624, found: 607.2628. HRMS calcd for C₂₉H₄₂N₄NaO₆S₂ 629.2443, found: 629.2444. [α]_D = +18, c = 0.7 in CH₂Cl₂ ¹H NMR (400 MHz; CDCl₃): 0.65 (d, 3H, *J* = 6.9), 0.69 (d, 3H, *J* = 6.9), 0.88 (m, 3H), 1.28 (m, 9H), 1.65 (m, 2H), 1.85 (s, 3H), 2.1 (td, 1H, *J* = 3.5, 6.9), 2.33 (dt, 2H, *J* = 7.6, 15.4), 2.54 (t, 2H, *J* = 7.6), 2.69 (dd, 1H, *J* = 2.9, 16.51), 2.91 (t, 2H, *J* = 7.4), 3.25 (d, 1H, *J* = 11.4), 4.05 (m, 2H), 4.12 (q, 1H, *J* = 7.1), 4.55 (dd, 1H, *J* = 3.6, 8.9), 4.99 (dd, 1H, *J* = 9.7, 17.7), 5.55 (ddt, 1H, *J* = 1.3, 6.9, 15.5), 5.65 (m, 1H), 5.84 (m, 1H), 6.14 (dd, 1H, *J* = 4.3, 8.6), 7.09 (d, 1H, *J* = 9.1), 7.99 (s, 1H). ¹³C NMR (100.8MHz, CDCl₃): 14.02, 17.16,

18.66, 22.55, 24.70, 27.91, 28.88, 29.93, 34.02, 37.28, 40.31, 43.31, 44.13, 58.10,
71.91, 77.17, 128.42, 132.72, 141.18, 163.22, 168.64, 170.50, 173.39, 199.35. IR (n_{\max})
3302.06, 2918.74, 1735.94, 1677.30, 1541.73, 1242.57 cm^{-1}

[JMG-3-181-1-400, JMG-3-181-1C13]

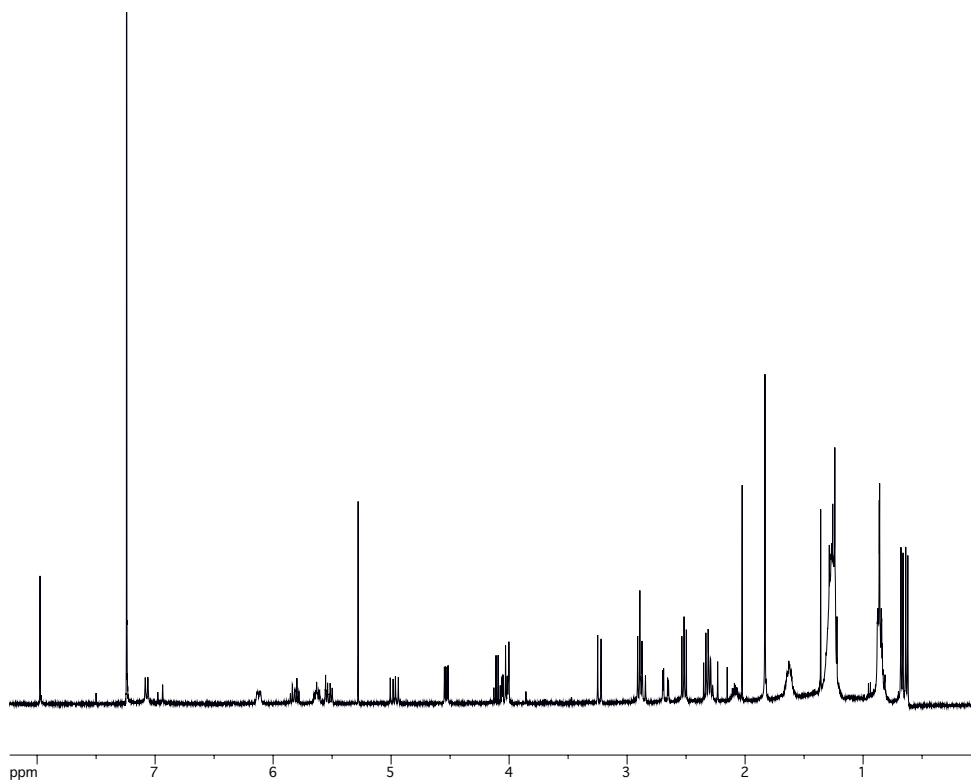


Figure 8.188. ^1H NMR of Thiazoline-Oxazole Thioester Analog (5.1)^{5,85}

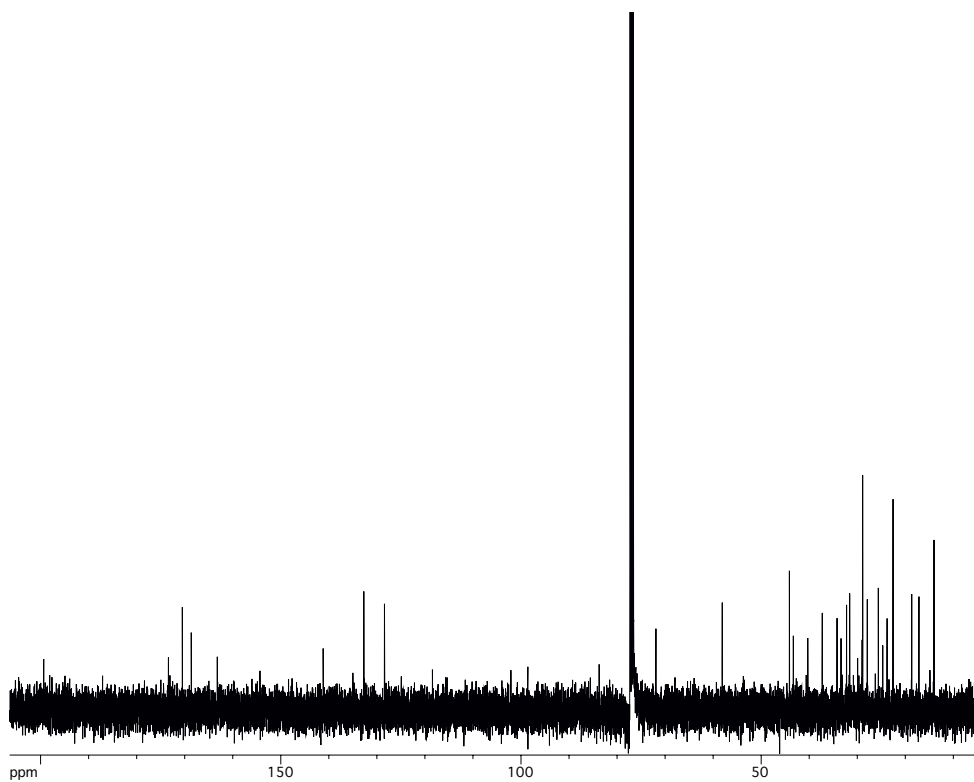


Figure 8.189. ^{13}C NMR of Thiazoline-Oxazole Thioester Analog (5.1)^{5,85}



Figure 8.190. Thiazole-peptide (5.23)^{5,85}

Thiazole acid **5.21** (355mg, 1.304mmol) was dissolved in DCM (50mL) and PyBOP (815mg, 1.565mmol) and α -Me-Ser-OMe (442mg, 2.607mmol) were added. Hünig's base (680 μ l, 3.912mmol) was added and the reaction was stirred overnight. The reaction was then concentrated down onto silica gel and purification with hexanes:EtOAc, 50:50 to 20:80 yielded **5.23** in (83%).

HRMS calcd for $C_{15}H_{24}N_3O_6S$ (M+H)⁺: 374.1396. found: 374.1400. $[\alpha]_D = -0.8$, $c = 2$ in $CHCl_3$. 1H -NMR (300 MHz; $CDCl_3$): δ 1.47 (s, 9H), 1.62 (s, 3H), 3.81 (s, 3H), 3.93 (d, $J = 11.5$ Hz, 1H), 4.17 (d, $J = 11.5$ Hz, 1H), 4.56 (d, $J = 6.2$ Hz, 2H), 5.50 (br, 1H), 7.96, 8.04 (s, 1H). ^{13}C -NMR (75 MHz; $CDCl_3$): δ 20.71, 28.55, 42.51, 53.23, 62.47, 66.65, 77.45, 124.46, 142.76, 149.34, 161.29, 170.08, 173.56. IR (ν_{max}) 3369.45, 3118.55, 2980.14, 1710.24, 1661.82, 1541.31, 1282.13, 1166.31 cm^{-1}

[JMG-3-160, JMG-3-160C13]

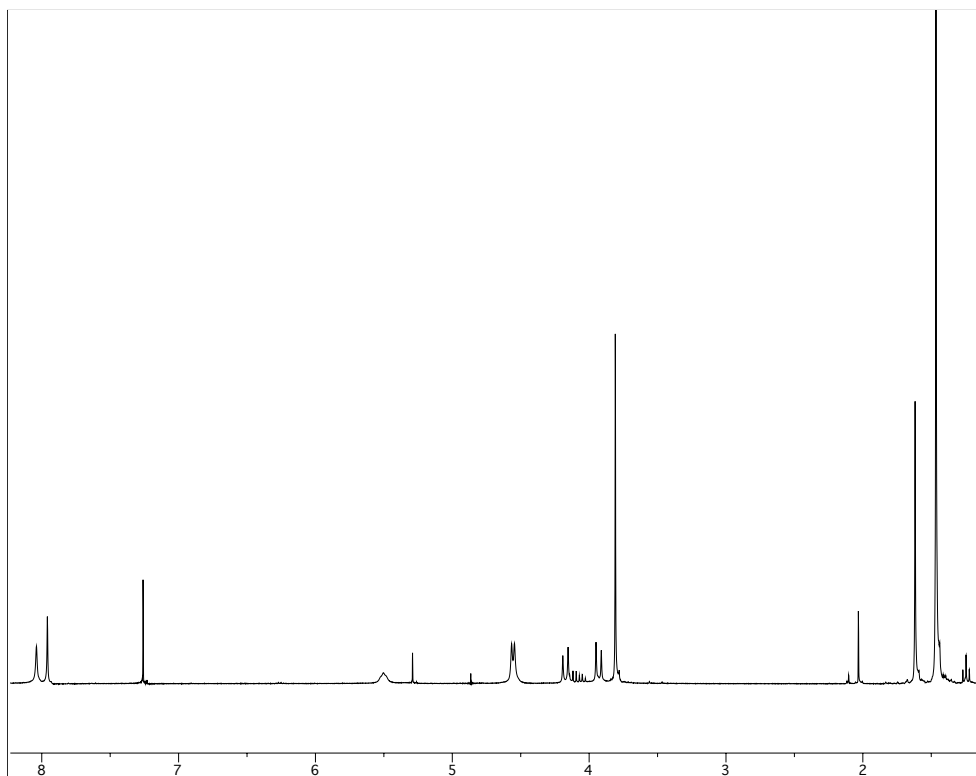


Figure 8.191. ^1H NMR of Thiazole-peptide (5.23)^{5,85}

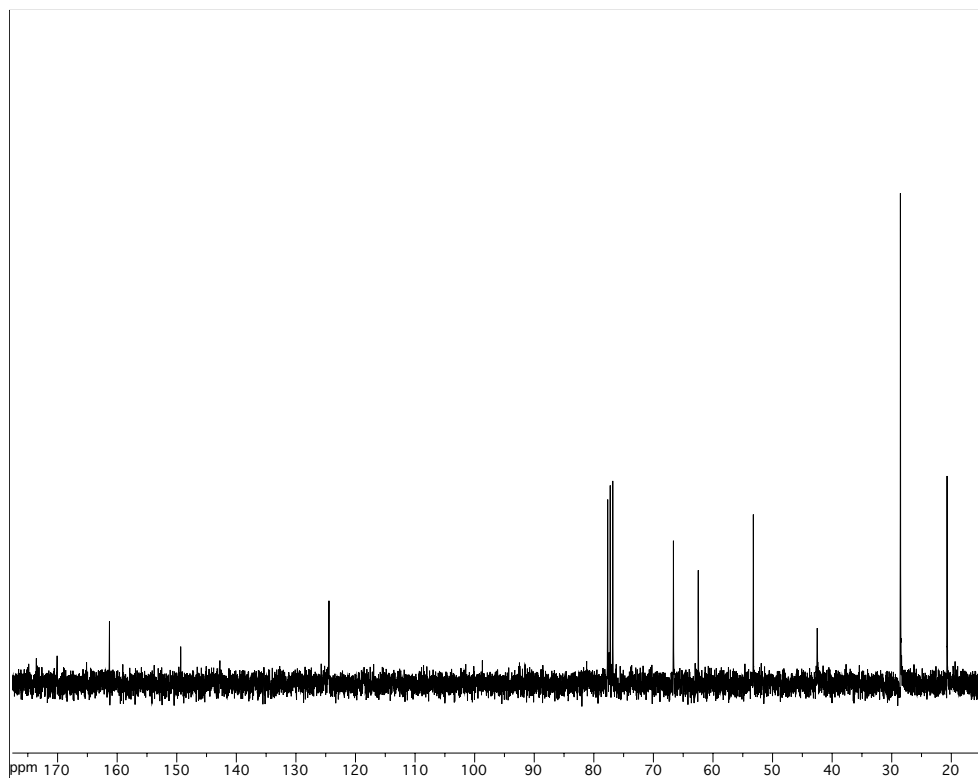


Figure 8.192. ^{13}C NMR of Thiazole-peptide (5.23)^{5,85}

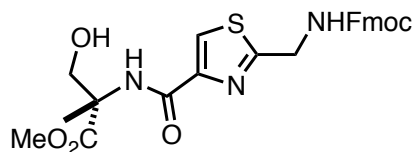


Figure 8.193. N-Fmoc-thiazole peptide (5.24)^{5,85}

5.23 (500mg, 1.339mmol) was dissolved in DCM (80mL) and cooled to 0°C. TFA (2mL, 26.779mmol) was then added and the reaction was stirred at room temperature overnight. The reaction was then concentrated down and then pulled down twice with toluene. The reaction mixture was then taken up in DCM and washed with about 15mL of brine. The organic layers were then dried over MgSO₄ and concentrated down. The crude mixture was then dissolved in DCM (80mL), cooled to 0°C and Fmoc-OSu (542mg, 1.607mmol) was added followed by Et₃N (375μl, 2.678mmol). The reaction was stirred at room temperature overnight and was then concentrated down onto silica gel and purified via column chromatography, hexanes:EtOAc, 50:50 to 100% EtOAc yielding the desired thiazole (**5.24**) in 35% yield.

HRMS calcd for C₂₅H₂₆N₃O₆S (M+H)⁺: 496.1542, found: 496.1532. [α]_D = +6.7, c = 4 in CHCl₃. ¹H-NMR (300 MHz; CDCl₃): δ 1.63 (s, 3H), 3.81 (s, 3H), 3.94 (d, *J* = 11.4 Hz, 1H), 4.26-4.17 (m, 2H), 4.50 (d, *J* = 6.7 Hz, 2H), 4.63 (d, *J* = 6.2 Hz, 1H), 5.79 (bs, 1H), 7.30 (t, *J* = 7.3 Hz, 2H), 7.40 (t, *J* = 7.5 Hz, 2H), 7.60 (d, *J* = 7.2 Hz, 1H), 7.76 (d, *J* = 7.4 Hz, 2H), 7.92 (d, *J* = 9.4 Hz, 1H), 8.04 (s, 1H). ¹³C NMR (75 MHz; CDCl₃): δ 13.94, 20.65, 42.74, 47.39, 53.25, 53.67, 62.50, 66.55, 67.38, 120.27, 124.57, 125.21, 127.32, 128.00, 141.56, 143.87, 149.41, 156.61, 161.16, 169.15, 173.56. IR(ν_{max}) 3367.48, 1725.53, 1657.25, 1541.81, 1222.44, 1056.31, 741.46 cm⁻¹

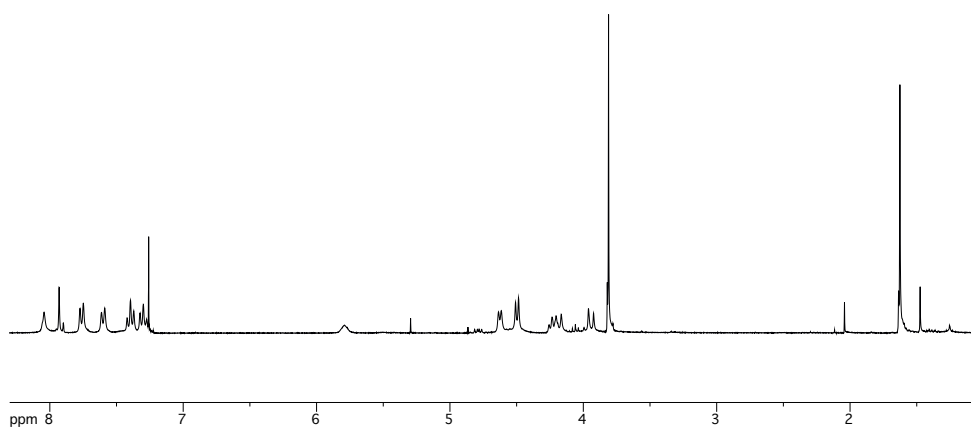


Figure 8.194. ^1H NMR of N-Fmoc-thiazole peptide (5.24)^{5,85}

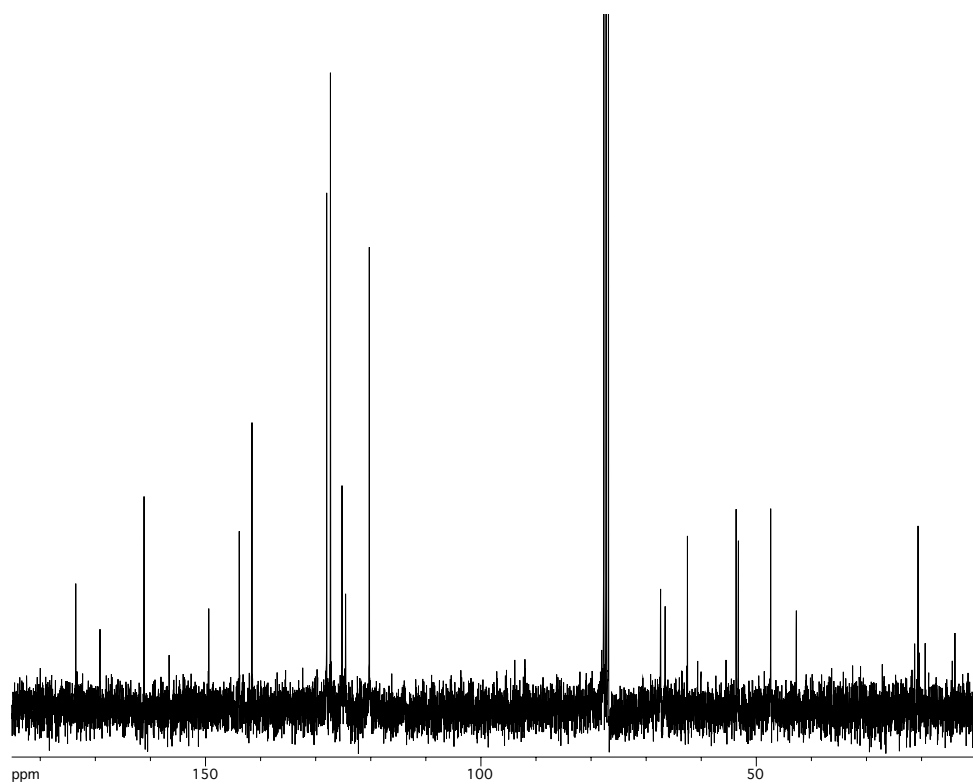


Figure 8.195. ^{13}C NMR of N-Fmoc-thiazole peptide (5.24)^{5,85}

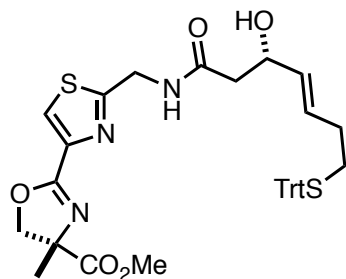


Figure 8.196. Oxazoline-thiazole-peptide (5.26)^{5,85}

Auxiliary (**5.13**) (588mg, 0.965mmol) was dissolved in DCM (24mL) and put under Argon. Oxazoline-Thiazole (**5.25**) (634mmol) was dissolved in DCM (6.5mL) with DMAP (12mg, 0.096mmol) and loaded into a syringe and added to the auxiliary over 1 hour at room temperature. The reaction was then allowed to stir overnight. The reaction was pulled down and purified via column chromatography provide the desired alcohol (**5.26**) in 41% yield.

HRMS calcd for $C_{36}H_{37}N_3NaO_5S_2$ ($M+Na$)⁺: 678.2072, found: 678.2077. $[\alpha]_D = +5$, $c = 2$ in $CHCl_3$. 1H -NMR (300 MHz; $CDCl_3$): δ 1.61 (s, 3H), 2.04 (q, $J = 6.3$ Hz, 2H), 2.21-2.16 (m, 2H), 2.40 (t, $J = 6.2$ Hz, 2H), 3.75 (s, 3H), 4.18 (d, $J = 8.8$ Hz, 1H), 4.43 (t, $J = 8.7$ Hz, 1H), 4.71 (t, $J = 3.0$ Hz, 2H), 4.82 (d, $J = 8.7$ Hz, 1H), 5.39 (dd, $J = 15.5, 6.2$ Hz, 1H), 5.58-5.49 (m, 1H), 7.40-7.18 (m, 15H), 7.89 (s, 1H). ^{13}C NMR (75 MHz; $CDCl_3$): δ 25.23, 31.54, 31.65, 40.96, 42.89, 53.09, 66.79, 69.22, 74.61, 76.56, 125.20, 126.82, 128.08, 129.77, 130.22, 132.48, 143.19, 145.05, 160.00, 172.19, 173.56. IR (ν_{max}) 3307.33, 3057.18, 2928.89, 1735.43, 1655.44, 1537.83, 1489.83, 1444.85, 701.40.

[JMG-3-100, JMG-3-100C13]

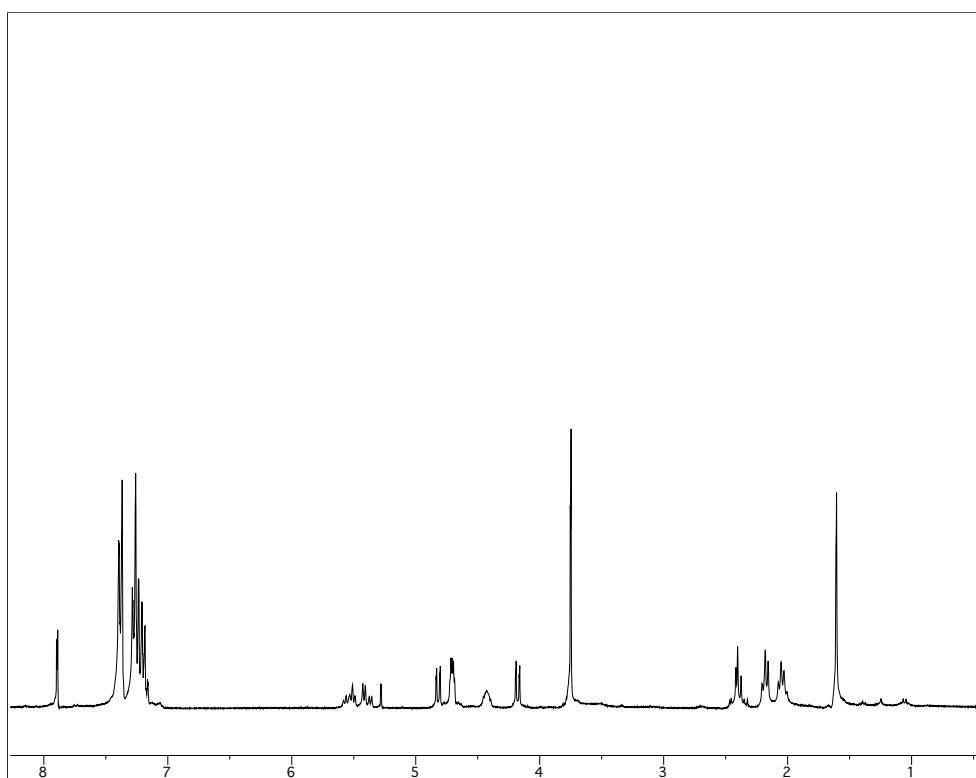


Figure 8.197. ^1H NMR of Oxazoline-thiazole-peptide (5.26)^{5,85}

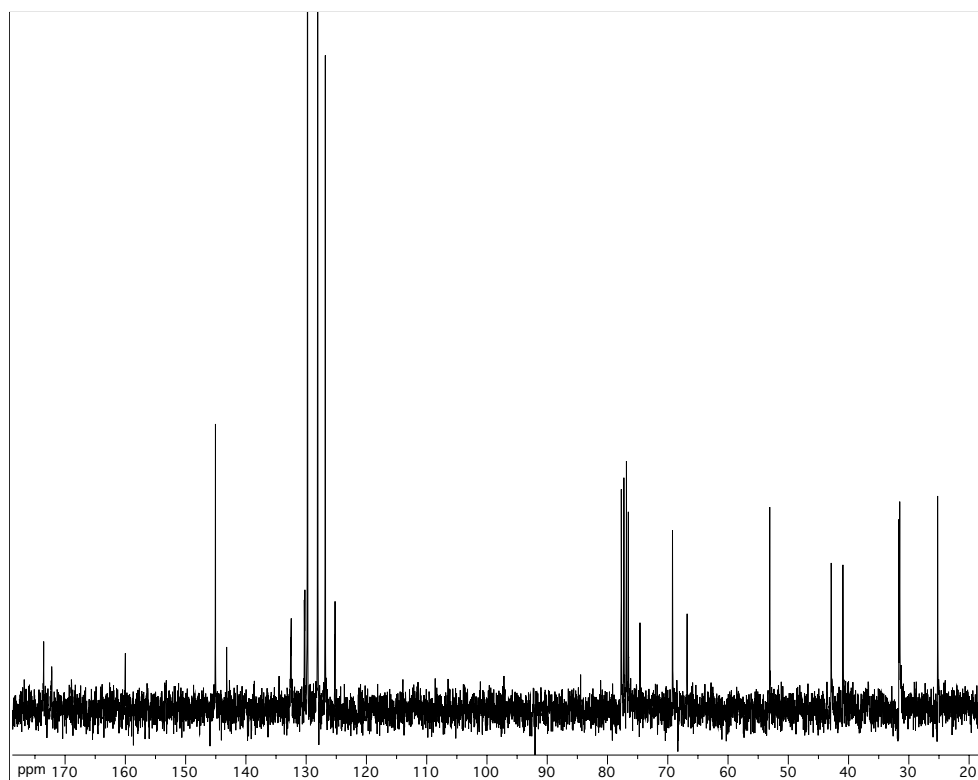


Figure 8.198. ^{13}C NMR of Oxazoline-thiazole-peptide (5.26)^{5,85}

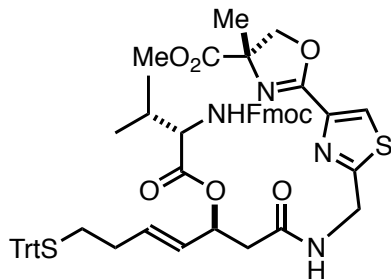


Figure 8.199. Oxazoline-Thiazole Acycle (5.19)^{5,85}

5.26 (173mg, 0.264mmol) and Fmoc-Val-OH (268mg, 0.791mmol) were dissolved in DCM (3mL) and cooled to 0°C. EDCI (152mg, 0.791mmol), DMAP (3mg, 0.026mmol) then Hünigs base (275μl, 1.582mmol) were added and the reaction was allowed to warm to room temperature and stirred overnight. The reaction was then concentrated and purified with 100% EtOAc to afford the desire product (**51.9**) in 67% yield. HRMS calcd for C₅₆H₅₆N₄NaO₈S₂: 999.3437, found: 999.3448. $[\alpha]_D = +13$, c = 3 in CHCl₃. ¹H-NMR (300 MHz; CDCl₃): δ 0.84 (d, *J* = 6.9 Hz, 3H), 0.89 (d, *J* = 6.9 Hz, 3H), 1.60 (s, 3H), 2.08-1.99 (m, 3H), 2.20-2.14 (m, 2H), 2.57-2.55 (m, 2H), 3.75 (s, 3H), 4.10-4.05 (m, 1H), 4.21-4.14 (m, 2H), 4.37-4.33 (m, 2H), 4.72 (t, *J* = 6.0 Hz, 2H), 4.80 (d, *J* = 8.7 Hz, 1H), 5.44-5.36 (m, 1H), 5.67-5.59 (m, 2H), 6.76-6.71 (m, 1H), 7.32-7.20 (m, 13H), 7.38 (d, *J* = 7.6 Hz, 8H), 7.56 (d, *J* = 7.5 Hz, 2H), 7.76-7.74 (m, 2H), 7.87 (s, 1H). ¹³C NMR (75 MHz; CDCl₃): δ 18.05, 19.22, 25.20, 31.53, 41.33, 47.36, 53.02, 59.59, 66.84, 67.28, 72.47, 74.66, 120.19, 125.14, 125.27, 126.85, 127.31, 127.73, 127.94, 128.09, 129.78, 134.24, 141.51, 143.94, 145.02, 156.59, 160.00, 169.17, 171.39, 173.60. IR (ν_{max}) 3295.78, 2961.26, 1735.92, 1655.71, 1527.83, 1209.69, 741.18. [JMG-3-105, JMG-3-105C13]

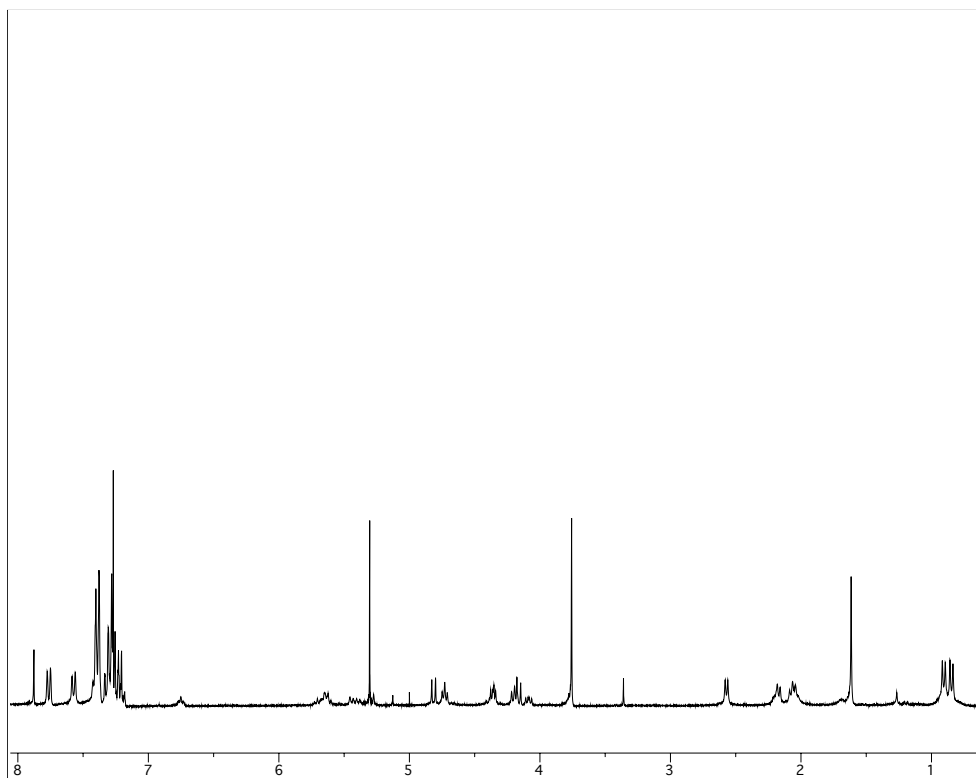


Figure 8.200. ^1H NMR of Oxazoline-Thiazole Acycle (5.19)^{5,85}

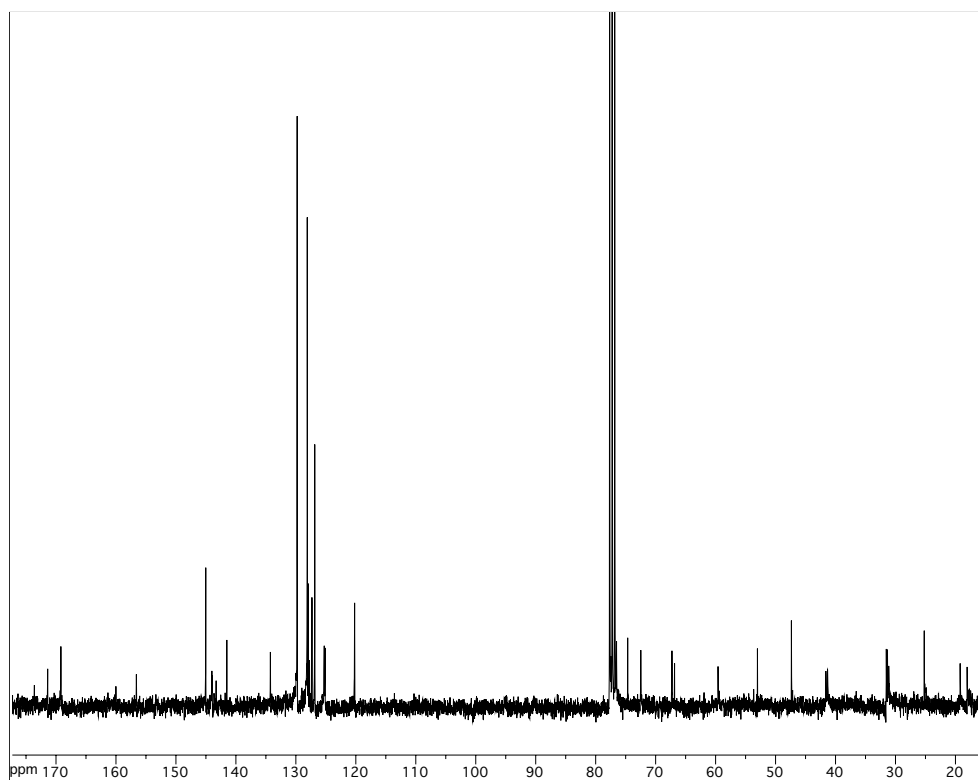


Figure 8.201. ^{13}C NMR of Oxazoline-Thiazole Acycle (5.19)^{5,85}

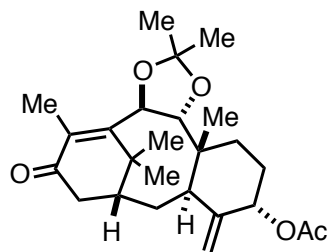


Figure 8.202. Taxoid 7.8

7.7 (200mg, 0.532mmol) was dissolved in DCM (14mL) and Ac₂O (140μl, 1.466mmol) was then added followed by DMAP (200mg, 1.598mmol) and the reaction was stirred at room temperature for 1 hour. The reaction was then pulled down onto silica gel and purified via column chromatography, hexanes:EtOAc, 70:30 to provide the desired compound (**7.8**) in 59% yield. HRMS calcd for C₂₅H₃₆NaO₅ (M+Na)⁺: 439.2460, found: 439.2456.

¹H-NMR (300 MHz; acetone-d₆): δ 0.90 (s, 3H), 1.17 (s, 3H), 1.41 (s, 3H), 1.46 (s, 3H), 1.64 (s, 3H), 1.69 (m, 2H), 1.85-1.67 (m, 7H), 1.85-1.76 (m, 3H), 1.87 (s, 3H), 1.92 (dd, *J* = 5.9, 2.3 Hz, 1H), 2.05 (dd, *J* = 4.4, 2.2 Hz, 1H), 2.07 (s, 3H), 2.27 (td, *J* = 6.1, 2.1 Hz, 1H), 2.84-2.82 (m, 2H), 2.91 (dd, *J* = 19.5, 7.3 Hz, 1H), 4.37 (d, *J* = 9.3 Hz, 1H), 4.86 (d, *J* = 1.2 Hz, 1H), 4.93 (d, *J* = 9.3 Hz, 1H), 5.17 (s, 1H), 5.27 (d, *J* = 2.9 Hz, 1H).

[JMG-1-86]

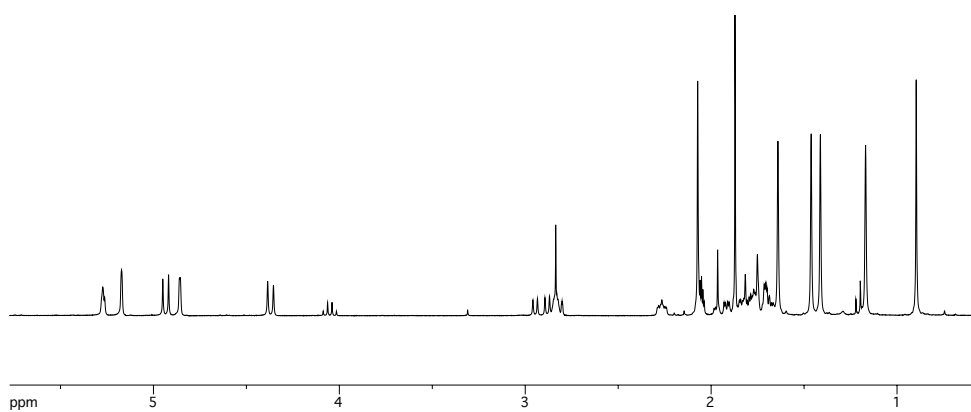


Figure 8.203. ^1H NMR of Taxoid 7.8

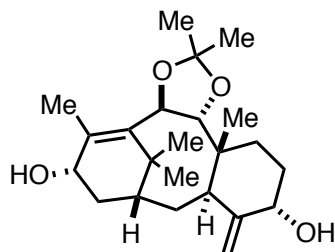


Figure 8.204. Taxoid 7.6

7.5 (2g, 5.944mmol) was dissolved in EtOAc (35mL) and a catalytic amount of TsOH was added followed by 2,2-DMP (11mL, 89.161mmol). The reaction was allowed to stir at room temperature for 3 hours. 15% NaOH (30mL) was then added and the reaction was extracted and the organics were washed with brine and then dried over Na₂SO₄. Filtration through a silica plug with hexanes:EtOAc, 50:50 gave desired acetonide **7.6** in 86% yield. HRMS calcd for C₂₃H₃₇O₄ (M+H)⁺: 377.2692, found: 377.2687.

¹H-NMR (300 MHz; acetone-d₆): δ 0.83 (s, 3H), 0.96 (s, 3H), 1.35 (d, *J* = 0.4 Hz, 3H), 1.39 (s, 3H), 1.50 (s, 3H), 1.81-1.58 (m, 7H), 1.93-1.87 (m, 1H), 2.05 (s, 3H), 2.85-2.74 (m, 1H), 3.27 (dt, *J* = 3.4, 1.6 Hz, 1H), 4.14 (d, *J* = 9.4 Hz, 1H), 4.27 (t, *J* = 2.6 Hz, 1H), 4.36-4.31 (m, 1H), 4.66 (t, *J* = 1.3 Hz, 1H), 4.90 (d, *J* = 9.4 Hz, 1H), 5.03 (d, *J* = 1.1 Hz, 1H).

[JMG-1-115]

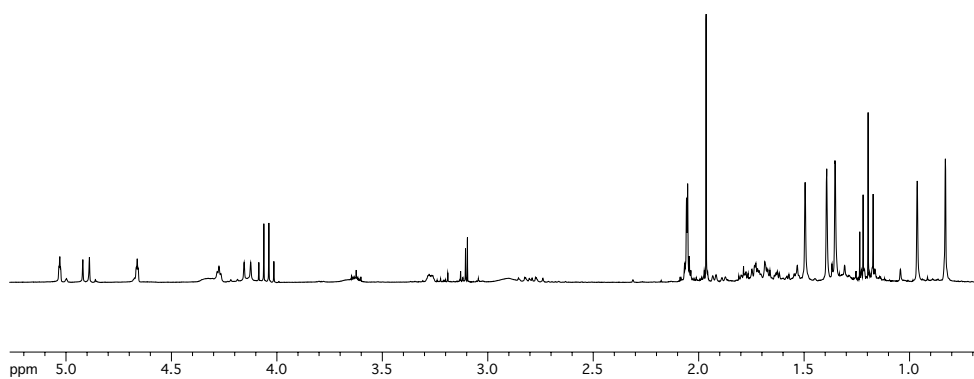


Figure 8.205. ^1H NMR of Taxoid 7.6

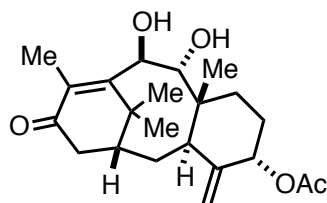


Figure 8.206. Taxoid 7.10

7.8 (5g, 13.146mmol) was dissolved in THF (130mL) and 0.1M HCl (130mL) was added. The reaction was allowed to stir at room temperature overnight and the reaction was then extracted with EtOAc and the organics were washed with brine and dried over Na₂SO₄. Purification through a short silica plug gave the desired diol (**7.10**) in 57% yield.

HRMS calcd for C₂₂H₃₃O₅ (M+H)⁺: 377.2328, found: 377.2319.

¹H-NMR (300 MHz; acetone-d₆): δ 0.93 (s, 3H), 1.15 (s, 3H), 1.60 (s, 3H), 1.76-1.64 (m, 3H), 1.85-1.79 (m, 2H), 1.86 (s, 3H), 2.03 (s, 3H), 2.06 (dd, *J* = 4.4, 2.2 Hz, 1H), 2.17-2.13 (m, 1H), 2.89-2.81 (m, 2H), 2.99 (dd, *J* = 4.1, 1.6 Hz, 1H), 4.11-4.03 (m, 2H), 4.52 (d, *J* = 3.1 Hz, 1H), 4.87-4.82 (m, 2H), 5.12 (s, 1H), 5.24 (t, *J* = 2.7 Hz, 1H).

[JMG-1-157ck]

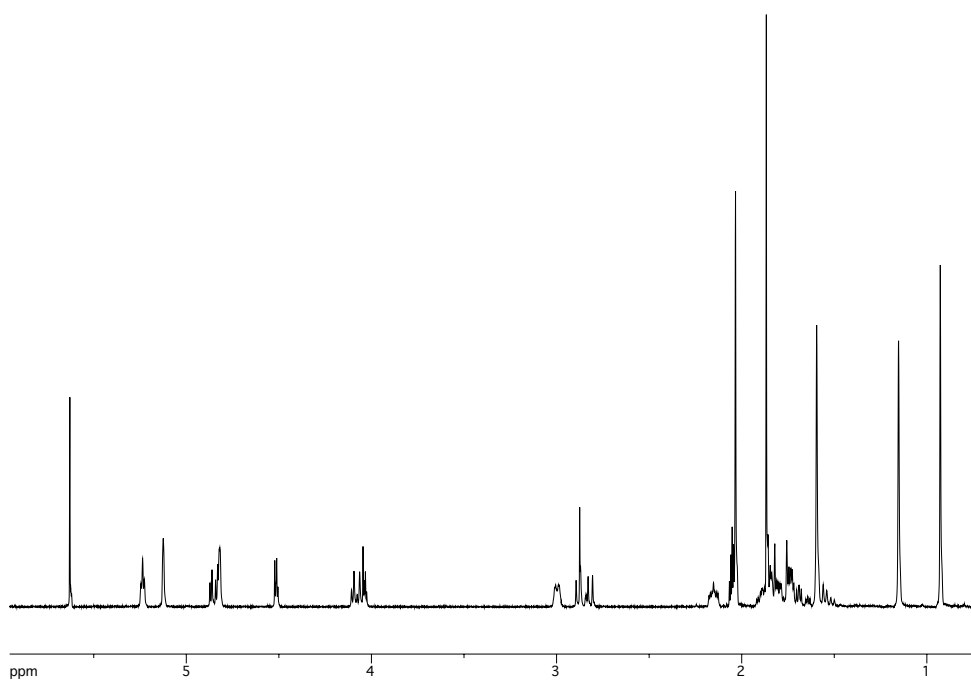


Figure 8.207. ^1H NMR of Taxoid 7.10

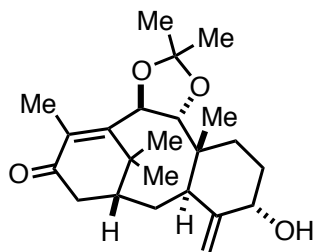


Figure 8.208. Taxoid 7.7

7.6 (1.79g, 4.754mmol) was dissolved in DCM (50mL) and MnO_2 (6.2g, 71.309mmol) was added. The reaction was stirred at room temperature overnight and was then filtered through a pad of Celite and concentrated. No further purification was needed and the desired ketone (**7.7**) was isolated in 42% yield.

HRMS calcd for $\text{C}_{23}\text{H}_{35}\text{O}_4$ ($\text{M}+\text{H}$) $^+$: 375.2535, found 375.2531.

^1H -NMR (300 MHz; acetone- d_6): δ 0.87 (s, 3H), 0.87 (s, 3H), 1.12 (s, 3H), 1.40 (s, 3H), 1.44 (s, 3H), 1.57-1.51 (m, 1H), 1.75-1.65 (m, 2H), 1.89-1.80 (m, 3H), 2.07-2.01 (m, 6H), 2.22-2.17 (m, 1H), 2.86-2.76 (m, 2H), 3.18-3.16 (m, 1H), 3.86 (dd, $J = 2.2, 1.1$ Hz,), 4.22-4.20 (m, 1H), 4.34 (d, $J = 9.3$ Hz, 1H), 4.64 (d, $J = 1.0$ Hz, 1H), 4.99-4.92 (m, 2H).

[JMG-1-220]

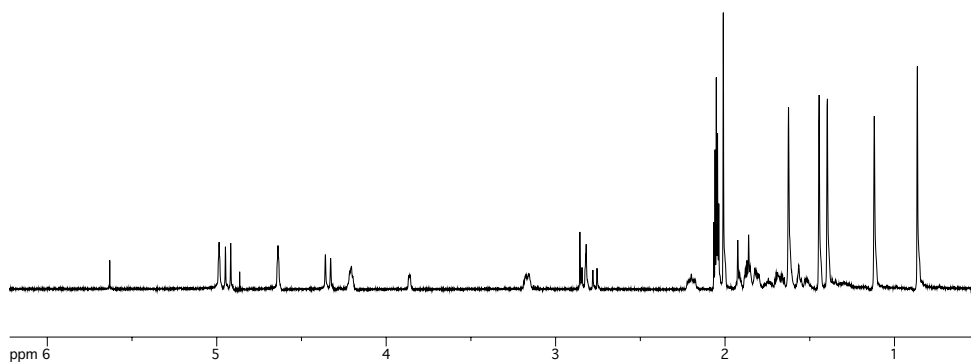


Figure 8.209. ^1H NMR of Taxoid 7.7

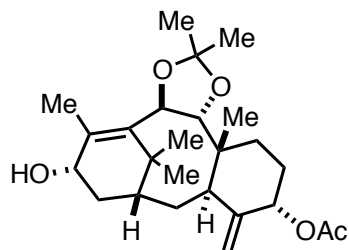


Figure 8.210. Taxoid 7.14

7.14 (820mg, 1.969mmol) was dissolved in THF (20mL) and a few drops of MeOH. The solution was then cooled to 0°C and NaBH₄ (1.5g, 39.371mmol) was added. The reaction was warmed to room temperature and stirred for 24 hours. The reaction was then quenched slowly with NH₄Cl_{aq} and extracted with EtOAc. Purification yielded the desired alcohol in 23% yield.

HRMS calcd for C₂₅H₃₉O₅ (M+H)⁺: 419.2797, found 419.2791.

¹H-NMR (300 MHz; aceton-d₆): δ 0.83 (s, 4H), 0.97 (s, 3H), 1.28 (m, 3H), 1.35 (s, 3H), 1.39 (s, 3H), 1.50 (s, 3H), 1.93-1.53 (m, 8H), 1.97 (s, 3H), 2.82-2.77 (m, 1H), 2.89 (s, 1H), 3.27 (t, *J* = 1.5 Hz, 1H), 3.67 (d, *J* = 10.1 Hz, 1H), 4.15-4.12 (m, 2H), 4.37-4.27 (m, 2H), 4.66 (d, *J* = 1.2 Hz, 1H), 4.90 (d, *J* = 9.4 Hz, 1H), 5.03 (d, *J* = 1.1 Hz, 1H).

[JMG-1-221-4]

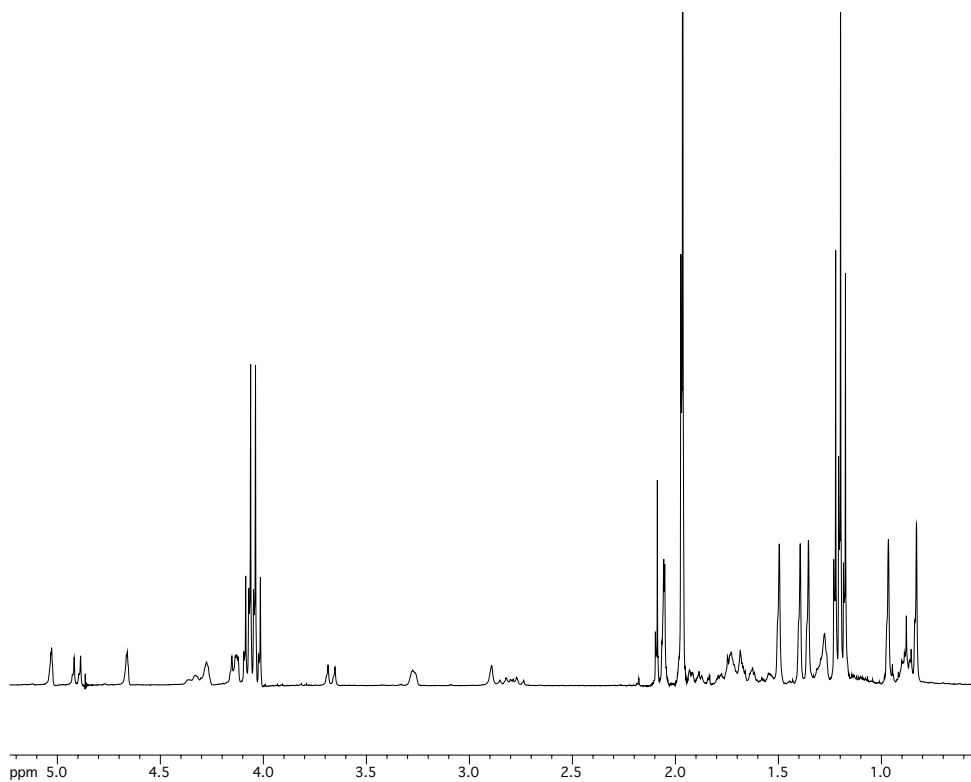


Figure 8.211. ^1H NMR of Taxoid 7.14

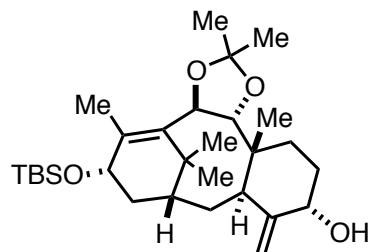


Figure 8.212. Taxoid 7.11

7.6 (486mg, 1.291mmol) was dissolved in DMF (13mL). TBSCl (234mg, 1.549mmol) and imidazole (350mg, 5.164mmol) were added the reaction was allowed to stir at room temperature overnight. The reaction as then quenched with $\text{NH}_4\text{Cl}_{\text{aq}}$ and extracted with EtOAc and then the organics were washed several times with brine and then dried over Na_2SO_4 . Purification yielded the desired compound in 85% yield.

HRMS calcd for $\text{C}_{29}\text{H}_{51}\text{O}_4\text{Si}$ ($\text{M}+\text{H}$) $^+$: 491.3557, found: 491.3552.

^1H -NMR (400 MHz; CDCl_3): δ 0.07 (d, J = 11.6 Hz, 3H), 0.80 (s, 3H), 0.87 (s, 9H), 0.96 (s, 3H), 1.16 (dd, J = 14.8, 4.2 Hz, 1H), 1.39 (s, 3H), 1.43 (s, 3H), 1.47 (s, 3H), 1.89-1.50 (m, 6H), 2.66 (dt, J = 14.8, 9.5 Hz, 1H), 2.66 (dt, J = 14.8, 9.5 Hz, 1H), 3.18 (s, 1H), 4.12 (d, J = 9.3 Hz, 1H), 4.23 (s, 1H), 4.49-4.47 (m, 1H), 4.66 (s, 1H), 4.89 (d, J = 9.4 Hz, 1H), 5.05 (s, 1H).

[JMG-2-230]

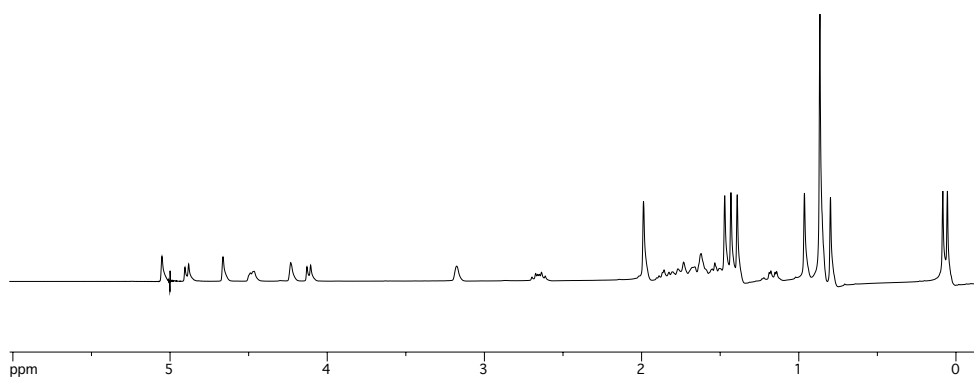


Figure 8.213. ^1H NMR of Taxoid 7.11

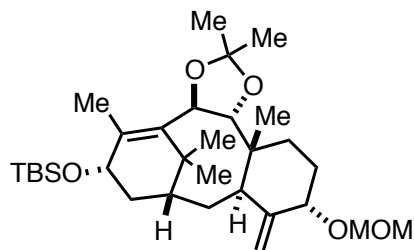


Figure 8.214. Taxoid 7.15

7.11 (20mg, 0.041mmol) was dissolved Hünig's base (1mL) and MOMCl (80μl, 0.815mmol) was added. The reaction was heated to 80°C for 3 days. The reaction was then cooled to room temperature and concentrated and then ran through a short silica plug.

HRMS calcd for $C_{31}H_{54}NaO_5Si$ ($M+Na$)⁺: 557.3638, found. 557.3631.

¹H-NMR (300 MHz; CDCl₃): δ 0.09-0.03 (m, 9H), 0.86 (d, J = 2.5 Hz, 6H), 0.91 (s, 8H), 1.10 (s, 3H), 1.25 (s, 3H), 1.40 (s, 3H), 1.45 (s, 3H), 1.54 (s, 3H), 1.57 (s, 2H), 1.78-1.59 (m, 6H), 1.98 (d, J = 1.2 Hz, 2H), 2.58-2.46 (m, 1H), 2.79-2.77 (m, 1H), 3.32 (s, 2H), 4.20 (t, J = 11.4 Hz, 2H), 4.55-4.49 (m, 2H), 4.79-4.69 (m, 1H), 4.86 (t, J = 8.4 Hz, 2H), 5.07 (s, 1H).

[JMG-2-96]

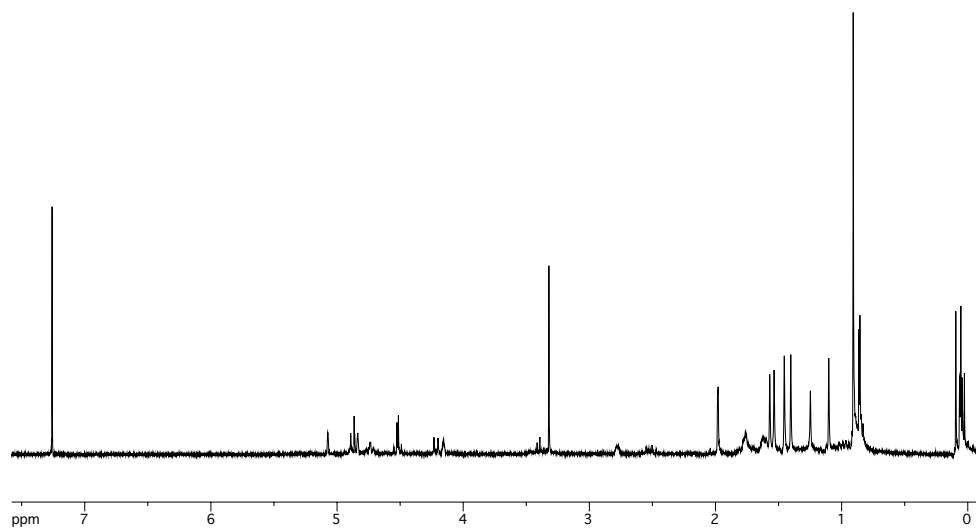


Figure 8.215. ^1H NMR of Taxoid 7.15

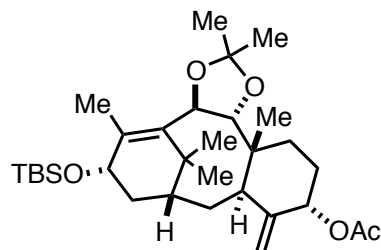


Figure 8.216. Taxoid 7.13

7.11 (660mg, 1.342mmol) was dissolved in DCM (35mL) and pyridine (2.5mL) and then Ac₂O (350μl, 3.691mmol) was added, followed by DMAP (491mg, 4.026mmol). The reaction was allowed to stir at room temperature overnight and the reaction was worked up with sodium bicarbonate (40mL) and washed with EtOAc and dried over Na₂SO₄ to give the desired product in 25% yield.

HRMS calcd for C₃₁H₅₂NaO₅Si (M+Na)⁺: 555.3482, found 555.3478.

¹H-NMR (300 MHz; CDCl₃): δ 0.06 (d, *J* = 6.8 Hz, 6H), 0.85 (s, 3H), 0.89 (s, 11H), 1.15 (s, 3H), 1.41 (s, 3H), 1.46 (s, 3H), 1.55 (s, 3H), 1.69-1.60 (m, 9H), 2.04 (s, 3H), 2.09 (s, 3H), 2.47 (dt, *J* = 14.2, 9.4 Hz, 1H), 2.77-2.75 (m, 1H), 4.26 (d, *J* = 9.6 Hz, 1H), 4.87-4.79 (m, 3H), 5.18 (s, 1H), 5.33 (s, 1H).

[JMG-2-152T]

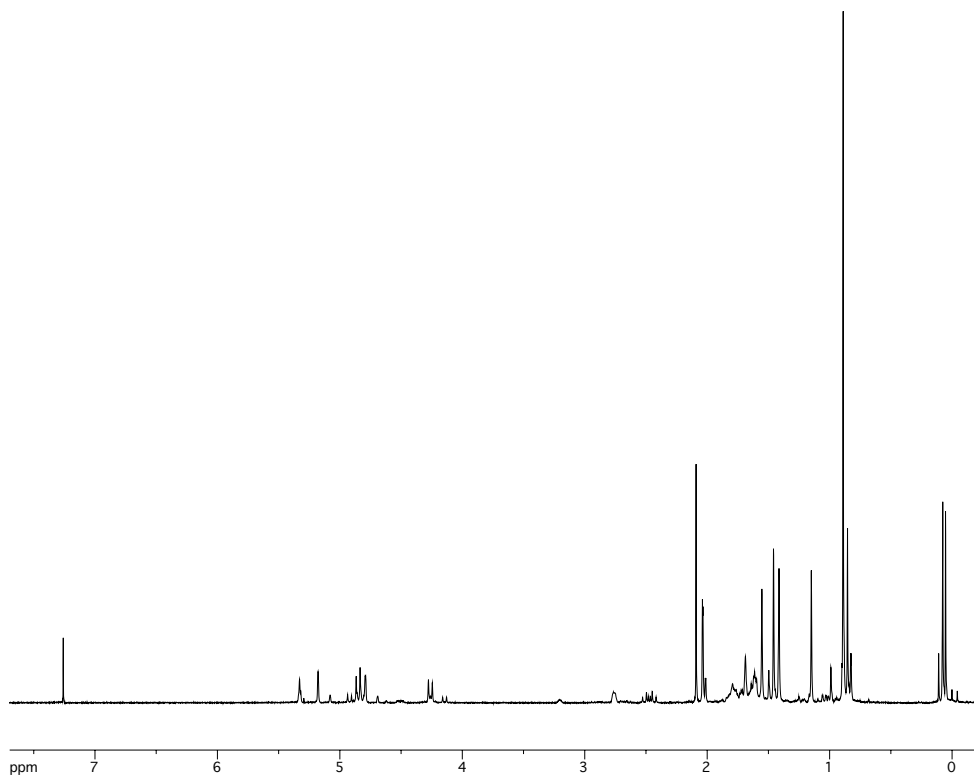


Figure 8.217. ^1H NMR of Taxoid 7.13

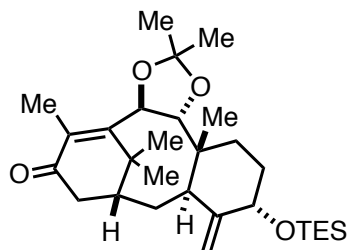


Figure 8.218. Taxoid 7.16

7.7 (20mg, 0.053mmol) was dissolved in DCM (7mL) and the reaction was cooled to 0°C. 2,6-lutidine (60ul, 0.530mol) and TESOTf (60ul, 0.265mmol) were then added and the reaction was stirred for 30 minutes. The reaction as then worked up with NH₄Cl_{aq} and extracted with DCM and dried over Na₂SO₄. The desired compound was isolated in 81% yield.

HRMS calcd for C₂₃H₃₃NaO₃ (M+Na)⁺: 380.2327, found 380.2325.

¹H-NMR (300 MHz; acetone-d₆): δ 0.62-0.52 (m, 7H), 0.69-0.62 (m, 5H), 0.95-0.86 (m, 12H), 1.02-0.96 (m, 8H), 1.14 (s, 3H), 1.29-1.27 (s, 3H), 1.40-1.36 (m, 3H), 1.44 (d, *J* = 3.9 Hz, 3H), 1.63-1.61 (m, 3H), 1.92-1.67 (m, 6H), 2.08-2.03 (m, 12H), 2.25-2.20 (m, 1H), 2.89-2.83 (m, 5H), 3.01-2.98 (m, 1H), 4.27-4.21 (m, 2H), 4.34 (d, *J* = 9.3 Hz, 1H), 4.67 (d, *J* = 0.2 Hz, 1H), 4.91 (d, *J* = 9.4 Hz, 1H), 5.03 (s, 1H).

[JMG-1-430-2]

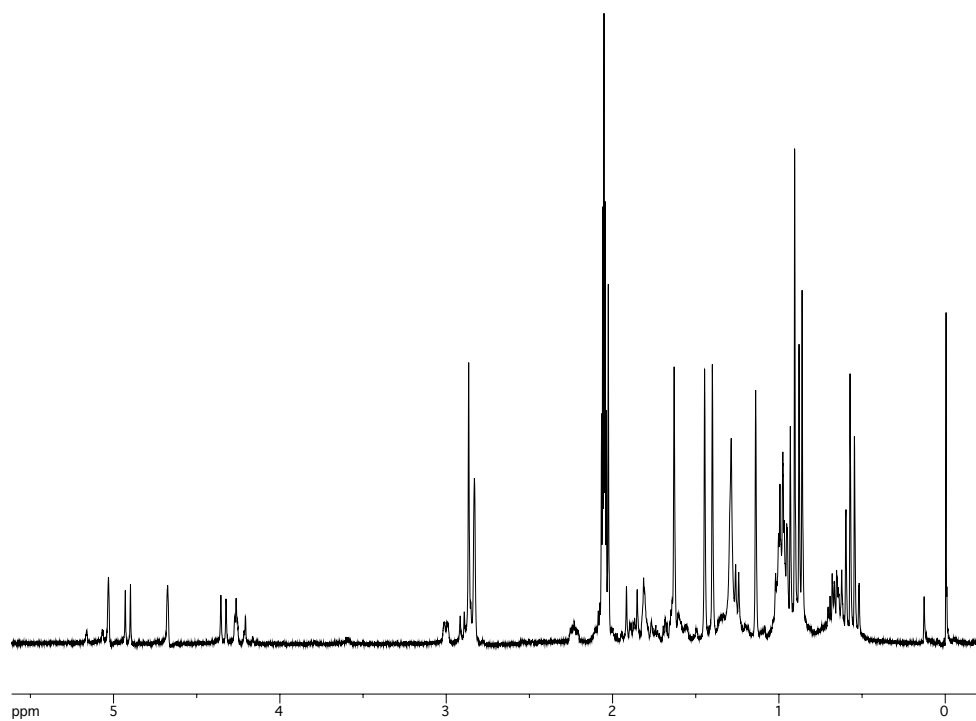


Figure 8.219. ^1H NMR of Taxoid 7.16

Appendix 1: Publications

Cite this: *Nat. Prod. Rep.*, 2012, **29**, 683

www.rsc.org/npr

REVIEW

The early stages of taxol biosynthesis: An interim report on the synthesis and identification of early pathway metabolites

Jennifer Guerra-Bubb,^a Rodney Croteau^b and Robert M. Williams^{*ac}

Received 14th February 2012

DOI: 10.1039/c2np20021j

Covering: 1966 to 2012

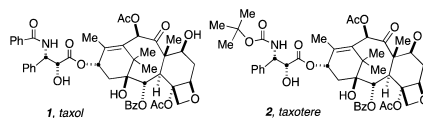
The biosynthesis of the anti-cancer drug taxol (paclitaxel) has required the collaborative efforts of several research groups to tackle the synthesis and labeling of putative biosynthetic intermediates, in concert with the identification, cloning and functional expression of the biosynthetic genes responsible for the construction of this complex natural product. Based on a combination of precursor labeling and incorporation experiments, and metabolite isolation from *Taxus* spp., a picture of the complex matrix of pathway oxygenation reactions following formation of the first committed intermediate, taxa-4(5),11(12)-diene, is beginning to emerge. An overview of the current state of knowledge on the early stages of taxol biosynthesis is presented.

- 1 Introduction
- 2 Taxadiene synthase
 - 2.1 Mechanism of taxadiene synthase
 - 2.2 Overproduction of taxadiene
- 3 Efforts toward biosynthetic intermediates to probe the 5 α -hydroxylase pathway
 - 3.1 Synthesis of taxa-4(5),11(12)-diene (5) and taxa-4(20),11(12)-diene (4)
 - 3.2 Synthesis of taxa-4(20),11(12)-dien-5 α -ol (26)
 - 3.3 Elucidation of the mechanism of taxadiene hydroxylase
 - 3.4 Over-production of taxa-4(20),11(12)-dien-5 α -ol
- 4 Syntheses of lightly functionalized taxoids
 - 4.1 Synthesis of taxa-4(20),11(12)-dien-2 α ,5 α -diol
 - 4.2 Synthesis of taxa-4(20),11(12)-dien-2 α ,10 β -diol-5 α -acetate from a Japanese yew-derived taxadien-tetraol
- 5 Deoxygenation of taxusin
 - 5.1 Attempt to deoxygenate taxusin at C-13
- 6 Subsequent biosynthetic transformations of the 5-hydroxytaxadiene core
 - 6.1 10 β - and 13 α -hydroxylase
 - 6.2 2 α - and 7 β -hydroxylase
 - 6.3 Uncharacterized hydroxylases
 - 6.4 Biosynthetic conversion to the 5,14-diol: A case of aberrant metabolism
- 7 Studies on the formation of the oxetane ring

- 8 C13 Acylation: Final step in the biosynthesis of taxol
- 9 Conclusion
- 10 Acknowledgements
- 11 References and notes

1 Introduction

Clinical oncologists, biologists and chemists have been irresistibly drawn to taxol¹ (**1**, paclitaxel) and its semi-synthetic congener taxotere (**2**) due to their promising spectrum of anti-neoplastic activity, unique mechanism of action, and the synthetic challenge that the complex, and densely functionalized ring system poses (Fig. 1).^{2–9} Taxol was first isolated from the bark of the Pacific yew, *Taxus brevifolia* Nutt.¹⁰ Unfortunately, the yew is slow growing and is primarily found in environmentally sensitive areas of the Pacific Northwest, and stripping the tree of its bark kills the yew. It takes three trees to obtain ~10 kg of bark from which 1 g of taxol can be isolated.⁷ FDA approval of taxol for the treatment of advanced ovarian cancer² has created a severe supply and demand problem. Collection of renewable *Taxus* sp. needles and clippings has attenuated this problem somewhat, but as the drug becomes more widely adopted, particularly for use earlier in the course of cancer

Fig. 1 The structure of taxol (**1**) and taxotere (**2**).

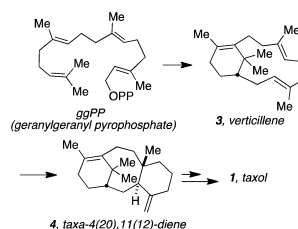
^aDepartment of Chemistry, Colorado State University, Fort Collins, Colorado 80523, USA. E-mail: rwmw@lamar.colostate.edu

^bInstitute of Biological Chemistry, Washington State University, Pullman, WA, 99164-6340, USA

^cUniversity of Colorado Cancer Center, Aurora, Colorado

intervention and for new therapeutic applications, pressure on the yew population is likely to increase worldwide. Alternative means of taxol production are being vigorously pursued since cost and availability will continue to be significant issues.

To date, totally synthetic methods have fallen short as an alternative source for taxol production,^{11–25} due to the complex structure of taxol that mandates lengthy and expensive synthetic routes. A method that has proven viable is the semi-synthesis of taxol from 10-deacetylbaicatin III, a renewable, which is isolated from the needles of yew species.^{3,7} The commercial supply of taxol and semi-synthetic precursors will have to increasingly rely on biological methods of production. This can be reasonably achieved by: (1) extraction from intact *Taxus* plants, (2) *Taxus* cell culture,²⁶ or (3) microbial systems.^{27–35} In order to produce large quantities of taxol or a pharmacophoric equivalent by semi-synthetic approaches, or perhaps by genetically engineered biosynthetic methods, it is essential to gain a better understanding of the detailed biosynthetic pathways^{26–37} in *Taxus* sp.



Scheme 1 The early biosynthetic proposal from ggPP to taxol.

In 1966, Lythgoe and coworkers proposed a biosynthetic pathway in which the tricyclic carbon framework of the taxoids was envisioned to arise by the sequential intramolecular cyclizations of the double bonds of geranylgeranyl pyrophosphate (ggPP) to 1(*S*)-verticillene (3) and then to taxa-4(20),11(12)-diene (4, Scheme 1).^{38,39}

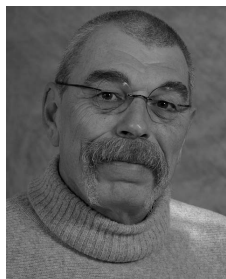
Our highly collaborative program has been aimed at manipulating taxoid biosynthesis at the genetic level in cell culture; as such, the slow steps in the biosynthetic pathway need to be elucidated. Since ggPP serves as a starting material for many other biosynthetic pathways,^{40–44} any number of the steps may be rate-limiting in the secondary metabolic flux to taxol. As a first step toward targeting the slow steps in the biosynthesis of taxol, we deployed several parallel strategies involving: (1) the biosynthetic production of lightly oxygenated taxoids using synthetic, tritium-labeled substrates; (2) total synthesis and isotopic labeling of pathway metabolites; (3) isolation and structure determination of pathway intermediates; (4) identification, cloning and functional expression of the biosynthetic genes; (5) incorporation of candidate pathway metabolites into taxol *in vivo* and; (6) mechanistic studies on the individual pathway enzymes.

We discovered that the “Lythgoe taxadiene” (4) is not the first committed intermediate on the taxoid biosynthetic pathway, but rather that taxa-4(5),11(12)-diene (5, Scheme 2) is the major



Jennifer Guerra-Bubb

Jennifer M. Guerra-Bubb graduated from the University of Kansas in 2007 with a B.S. in Chemistry and a minor in Mathematics. She is currently pursuing a Ph.D. in Chemistry under the guidance of Professor Robert M. Williams, wherein her work has focused on the synthesis of analogs of known HDAC inhibitors.



Rodney Croteau

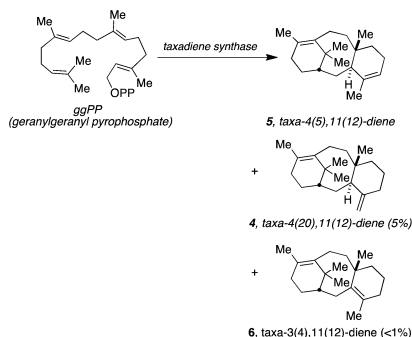
Rodney Croteau, Fellow of the Institute of Biological Chemistry and Regents' Professor at Washington State University, obtained his B.S. (1967) and Ph.D. (1970) degrees at the University of Massachusetts, Amherst. An early interest in natural products chemistry led to postdoctoral study in plant biochemistry at Oregon State University (with W. D. Loomis) and at Washington State University (with P. E. Kolattukudy) where he joined the faculty in 1975. His research

deals broadly with the origin and function of terpenoids in plants, including the monoterpenes, sesquiterpenes and diterpenes involved in chemical defense and communication, and that constitute the essential oils and resins used in pharmaceuticals, flavors and fragrances, and as industrial raw materials. His areas of interest range from biosynthetic pathway elucidation for complex terpenoids such as taxol, to enzyme structures and mechanisms, to the regulation of terpenoid metabolism.



Robert M. Williams

Robert M. Williams received a B.A. (Chemistry, 1975) from Syracuse University (Ei-ichi Negishi), the Ph.D. (1979) at MIT (W. H. Rastetter) and was a post-doc at Harvard (1979–80; R. B. Woodward/Yoshito Kishi). He joined Colorado State University in 1980 and named University Distinguished Professor in 2002. Significant awards include the ACS Cope Scholars Award (2002) and the ACS Ernest Guenther Award in the Chemistry of Natural Products (2011). His interdisciplinary research program (>280 publications) at the chemistry-biology interface concerns the synthesis, biosynthesis and the chemical biology of biomedically significant natural products.



Scheme 2 Products of recombinant taxadiene synthase.

metabolite.^{45–52} This was demonstrated by a total synthesis^{51,52} of both **4** and **5** and administration of synthetic ¹³C-labeled taxa-4(20),11(12)-diene (**4**) to microsomes of *Taxus canadensis*.⁴⁷ Cross-over experiments and the lack of detectable biotransformation of the Lythgoe diene (**4**) in *Taxus* microsomes had initially cast considerable doubt on the intermediacy of this substance in taxoid biosynthesis.⁵⁰ On the other hand, using ggPP as a substrate, taxa-4(5),11(12)-diene (**5**) has been shown to be the primary product of taxadiene synthase, an enzyme recently characterized, and the corresponding gene cloned and functionally expressed.^{45–48} However, recent results from our laboratories have revealed that recombinant taxadiene synthase indeed produces ~5% of the Lythgoe diene (**4**) plus <1% percent of the 3,4-diene isomer (**6**).⁵⁰

2 Taxadiene synthase

Taxadiene synthase from *Taxus* species catalyzes the first committed step in the biosynthesis of taxol and related taxoids by the cyclization of the universal diterpenoid precursor (*E,E,E*)-geranylgeranyl diphosphate (ggPP) to the parent hydrocarbon taxa-4(5),11(12)-diene (**5**). Following the remarkable one-step construction of taxadiene, an extended and complex series of oxygenation and acylation reactions ensue, culminating in the production of taxol.^{45,53} Taxadiene synthase, which has been isolated from both yew saplings⁴⁶ and cell cultures,⁵⁴ catalyzes a slow, but apparently not rate limiting step in the taxol biosynthetic pathway.⁵⁴ A cDNA encoding the taxadiene synthase from *T. brevifolia* has been obtained by a homology-based PCR cloning method.⁴⁸ A truncated version of the preprotein, in which the plastidial targeting peptide of the preprotein has been deleted, has been functionally expressed in *Escherichia coli* and shown to resemble the native enzyme in kinetic properties.⁵⁵ Native taxadiene synthase is constituted of 862 amino acids with a molecular weight of 98.3 kDa. The recombinant enzyme (after deletion of the plastid-targeting sequence) is constituted of 783 amino acids and has a molecular weight of ~80 kDa. Over-expression of the truncated, recombinant synthase has been successfully accomplished in *E. coli*. This significant milestone has made available sufficient amounts of the enzyme, and the enzyme products, to permit a more detailed study of the

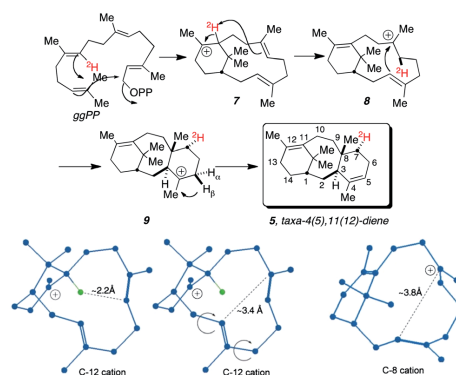
electrophilic cyclization reaction cascade. Recently, the X-ray crystal structure of a truncated variant of taxadiene synthase was reported by Koksai and coworkers.⁵⁶

2.1 Mechanism of taxadiene synthase

In collaboration with the Coates laboratory (University of Illinois) and the Floss laboratory (University of Washington), we have determined the fascinating mechanism of the “one-step” cyclization of ggPP to taxa-4(5),11(12)-diene (**5**) as shown in Scheme 3.⁵⁰

The Coates lab focused on the stereochemistry of the A-ring formation⁵⁷ and demonstrated that, as expected, the pyrophosphate-bearing carbon atom undergoes a clean Walden inversion, and that the attack of the C11/C12 π -system on the incipient cation to form the A-ring quaternary center is an antarafacial reaction. Our group has focused on the stereochemistry and mechanistic implications of the unprecedented migration of the C11 hydrogen atom to C7.⁵⁰ The Floss lab synthesized the requisite deuterated ggPP substrate (shown in Scheme 3) and this substrate was converted into taxadiene *via* soluble recombinant synthase from *Taxus cuspidata*. We observed >90% retention of deuterium at C7 in taxadiene (**5**). Our laboratory elucidated the stereochemistry of the deuterium migration by 2D NMR and 1D TOCSY and has unambiguously established that the deuterium atom migrates to the α -face of C-7. The observation that the deuterium transfer from C11 to C7 occurs with such a high degree of isotopic retention, coupled with the exclusive transfer to the α -face of C7, suggests that the mechanism for the transfer of the deuterium from C11 to C7 occurs *intramolecularly*. Such an intramolecular proton transfer during an olefin-cation cyclization reaction is highly unusual.⁵⁰

Of further interest, is the facial bias of the final C8/C3 olefin-cyclization. Considering the known relative stereochemistry of the taxoid B/C ring juncture, the C3/C4 π -system *must* attack the putative C8 cation (**8**) formed immediately following the C11/C7 proton migration, from the *same face* to which the newly installed proton at C7 migrated. Molecular modeling of this process, which formally involves a criss-cross of bond



Scheme 3 The mechanism of taxadiene synthase.⁵⁰

formation across the C7/C8 π -system, proved quite insightful. The molecular model of the C8 cation suggests that, upon pyramidalization at C7 and fashioning of the C11/C12 olefin, the conformation of the 12-membered ring twists, relative to that of the C12 cation, rocking the C3/C4 π -system into the correct facial orientation for capture of the C8 cation, establishing the *trans*-fused B/C ring juncture.

Taxadiene synthase is therefore a remarkable terpene cyclase that appears to function by non-covalent binding and ionization of the substrate ggPP and mediates an enantio- and face-selective polyolefin-cation cascade, involving the formation of three carbon-carbon bonds, three stereogenic centers, and the loss of a hydrogen atom in "a single step". The apparently unassisted C-11/C-7 intramolecular proton transfer mechanism of taxadiene synthase is seemingly rare in this regard, and suggests that this enzyme type is capable of mediating complex olefin-cation cyclizations, with absolute stereochemical fidelity, by conformational control alone. These provocative experimental results have provided important insight into the molecular architecture of the first dedicated step of taxol biosynthesis that creates the taxane carbon skeleton. We further note that these observations have broad relevance and implications for the general mechanistic capability of the large family of terpenoid cyclization enzymes that catalyze related electrophilic reaction cascades.

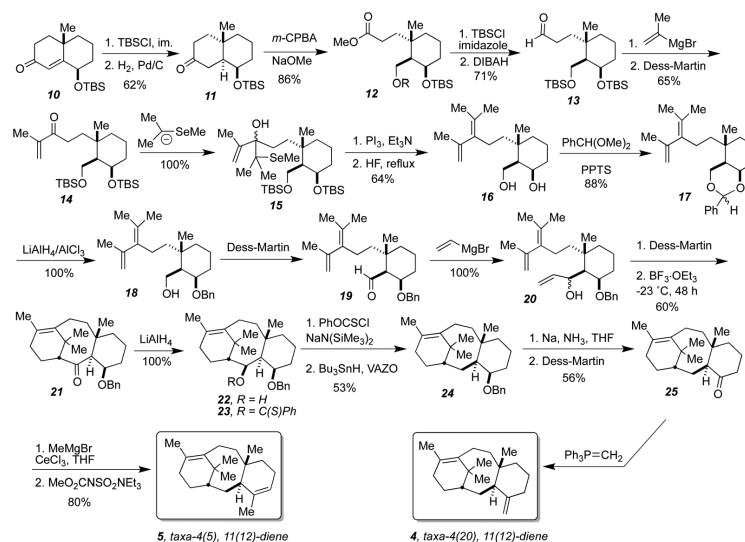
2.2 Overproduction of taxadiene

With the production of large scale advanced intermediates en route to taxol being quite limited, work towards developing routes aimed at overproduction of metabolites have been explored. Developments in metabolic engineering, as well as synthetic biology, have enabled new avenues for the

overproduction of complex natural products through the optimization of microbial hosts.^{58,59} Using a partitioned metabolic pathway utilizing the upstream methylerythritol-phosphate (MEP) forming IPP and the heterologous downstream terpenoid forming pathway, Ajikumar *et al.* reported that they were successfully able to develop a multivariate-modular approach towards metabolic-pathway engineering and were able to increase titers of taxadiene to a $\sim 1 \text{ g L}^{-1}$, essentially a 15 000-fold increase in an *E. coli* strain.⁶⁰ Additionally, Boghigian, *et al.*, have compared the heterologous production of taxadiene in two lineages of *E. coli*, K and B.⁶¹ Boghigian was able to show that the K-derivative outperformed the B-derivative and probed this finding by applying global transcript profiling to the two strains, thus revealing notable differences in pyruvate metabolism and central metabolism. Further studies demonstrated that temperature had a significant effect on taxadiene production and that indole inhibited the growth of both strains, which was consistent with their earlier observations.⁶¹

Metabolic engineering has also been applied in the realm of overexpressing natural product metabolites to help foster a more amenable route toward taxadiene production.⁶² Boghigian identified targets both within and outside of the isoprenoid precursor pathway and then tested them for over-expression in a heterologous *E. coli* host.⁶² The use of an algorithm for identifying over-expression targets is unique, since most metabolic engineering efforts have used computational methods to model cellular metabolism.

Collectively, the use of both heterologous hosts and metabolic engineering are paving the way for the over-expression of taxadiene synthase and future endeavors of developing routes toward the overexpression of downstream taxol pathway genes.



Scheme 4 The total synthesis of taxa-4(5),11(12)-diene (**5**) and taxa-4(20),11(12)-diene (**4**).

3 Efforts toward biosynthetic intermediates to probe the 5 α -hydroxylase pathway

3.1 Synthesis of taxa-4(5),11(12)-diene (5) and taxa-4(20),11(12)-diene (4)

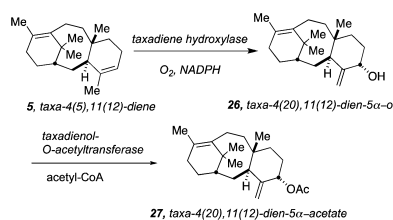
The total syntheses of taxa-4(20),11(12)-diene (4) and taxa-4(5),11(12)-diene (5) are outlined in Scheme 4. Synthetic access to these substrates (albeit in racemic form) has proven to be critical in penetrating the early stages of taxol biosynthesis. After evaluating several alternatives, we decided to adapt a route originally devised by Shea and Davis,^{63,64} that relied on the use of an intramolecular Diels-Alder (IMDA) cyclization reaction forming the A-B-ring system with an aromatic C-ring. This strategy was also explored by Jenkins and coworkers^{65–67} to access a model A-B/(saturated) C-ring system containing the C-19 methyl group with the correct relative stereochemistry, but devoid of functionality in the C-ring. This IMDA approach for the synthesis of the taxadienes (4 and 5) was easily employed by installing a functional group at C-4 in the C-ring for the ultimate installation of the C-20 carbon atom and the 4(20)- or 4(5)-double bonds. The synthesis illustrated in Scheme 4 closely parallels the Jenkins synthesis with the important difference being the early introduction of a hydroxyl group in the C-ring precursor, which ultimately became the functionalized C-4 carbon of the taxadienes.

The key intermediate in this synthesis proved to be ketone 25, which could be elaborated into the “Lythgoe diene” (4) by a simple Wittig reaction or, alternatively, to taxa-4(5),11(12)-diene (5) by a Grignard-dehydration sequence (this procedure also gives 4). The late-stage installation of the C-20 carbon atom by either approach turned out to be very significant, in that we were readily able to introduce tritium, deuterium and/or ¹³C at C-20 by the appropriate choice of relatively inexpensive, commercially available, isotopically labeled versions of methyl iodide.

3.2 Synthesis of taxa-4(20),11(12)-dien-5 α -ol (26)

We have further established that the first hydroxylation product in the taxol pathway is taxa-4(20),11(12)-dien-5 α -ol (26, Scheme 5) through total synthesis and bioconversion of this substance into taxol, 10-deacetylbaccatin III and cephalomannine *in vivo* in *Taxus brevifolia*.⁶⁸ Furthermore, a synthetic sample of taxa-4(20),11(12)-dien-5 α -acetate (27) has been used to establish that, following hydroxylation of 5 to 26, the next step in the pathway appears to be acetylation of 26 to acetate 27.⁶⁹ The Croteau lab has cloned and expressed taxa-4(20),11(12)-dien-5 α -ol-O-acetyl transferase from *Taxus canadensis* in *E. coli*.⁶⁹

Due to the very low yield of natural taxadiene obtainable from biological sources (an extract from 750 kg of *Taxus brevifolia* bark powder yielded⁴⁵ ~1 mg of 85% pure 5) and the remaining uncertainty as to the sequence of hydroxylation reactions to taxoids,^{45–48,70–73} synthetic access to these isotopically labeled tricyclic diterpenes has become essential for several reasons: (1) synthesis provides radio-labeled substrates from which pathway metabolites can be made by enzymatic biotransformation and; (2) the synthetic metabolites facilitate the identification, isolation and structure elucidation of new pathway metabolites that

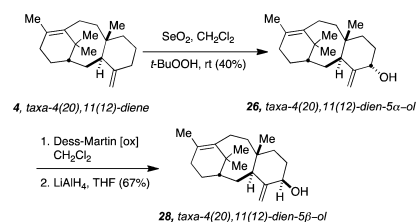


Scheme 5 Early hydroxylation and acetylation steps.

are produced biosynthetically in very tiny amounts. The second point was amply demonstrated by our synthesis of taxa-4(20),11(12)-dien-5 α -ol (26) which preceded the identification and isolation of this substance from *Taxus brevifolia*.^{71–73} Indeed, the identification of this substance as a biosynthetic intermediate would have proven far more difficult if the synthetic reference sample were not available. The first point has also been amply demonstrated, since synthetic, tritium-labeled 26 and the corresponding acetate 27 have served as key substrates from which numerous intermediate hydroxylation products (diol, triol, tetraol and pentaol) have been produced biosynthetically. It should also be noted that taxol has now been identified in several strains of microorganisms,^{27–35} and our laboratory has provided samples of stable- and radio-isotopically labeled taxadienes to numerous other laboratories interested in identifying pathway intermediates to taxoids produced in other biological systems.

The synthesis of taxa-4(20),11(12)-dien-5 α -ol (26) is illustrated in Scheme 6 and proceeds *via* selenium dioxide oxidation of the synthetic Lythgoe diene (4). We observed exclusive formation of the naturally configured 5 α -alcohol (26) from this reaction whose stereochemistry was confirmed by extensive 2D NMR analysis (¹H, nOe, DQF-COSY, HMQC, HMBC). To interrogate the possible intermediacy of the corresponding β -alcohol diastereomer 28, synthetic 26 was oxidized to the corresponding C-5 ketone with Dess-Martin periodinane and stereoselectively reduced with lithium aluminum hydride to deliver 28. This authentic, synthetic sample made it possible to interrogate taxadiene hydroxylase for the possible production of trace amounts of this diastereomer, which was not observed.

Preparative incubations of synthetic C20-[³H]-taxadiene (5) with *Taxus* microsomes were next carried out to accumulate sufficient biosynthetic product (~3 nmol) for full spectrum



Scheme 6 The synthesis of taxadiene 5 α - and 5 β -ols (26 and 28).

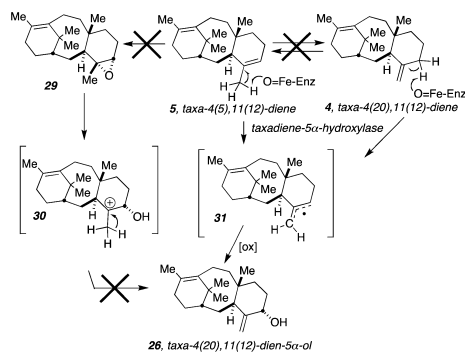
GC-MS analysis. Comparison of GC retention time and mass spectral fragmentation pattern of the TLC-purified biosynthetic product to those of authentic taxa-4(20),11(12)-dien-5 α -ol (**26**) indicated that the two compounds were identical. Final experimental corroboration was secured through the conversion of the purified, tritium-labeled biosynthetic product (42.8 nCi) to the corresponding 3,5-dinitrobenzoate ester (90% yield), which was diluted with authentic (\pm)-taxa-5(20),11(12)-dien-5 α -yl dinitrobenzoate, and recrystallized to constant specific activity and melting point (4.67 ± 0.09 nCi μmol^{-1} , m.p. 171 °C, dec.). These analyses, including quantitative evaluation of the radiochemical crystallization studies, revealed that a minimum of 87% of the oxygenation product of taxa-4(5),11(12)-diene (**5**) is taxa-4(20),11(12)-dien-5 α -ol (**26**).

We were also able to detect low levels of **26** as a natural metabolite in *Taxus* sp. bark extract. Thus, radiochemically-guided fractionation of a *T. brevifolia* bark extract (0.25 μCi of (\pm)-[20- ^3H]taxa-4(20),11(12)-dien-5 α -ol diluted into an extract of 250 kg dry bark) utilizing argentation TLC, and reverse-phase chromatography, before and after alkaline hydrolysis of half of the extract, followed by GC-MS analysis of the partially purified product, demonstrated the alcohol to be present in the 5–10 μg kg^{-1} range and ester(s) of **26** to be present in the 25–50 μg kg^{-1} range.

3.3 Elucidation of the mechanism of taxadiene hydroxylase

We have examined the interesting mechanistic question regarding the cytochrome P450 mediated conversion of taxa-4(5),11(12)-diene (**5**) into taxa-4(20),11(12)-dien-5 α -ol (**26**) with a contrathermodynamic allylic transposition.⁶⁸ We designed an experiment to discern if the cytochrome P450 hydroxylation of taxa-4(5),11(12)-diene (**5**) to taxa-4(20),11(12)-dien-5 α -ol (**26**) proceeds through an epoxide intermediate or an allylic radical species. No isomerization of taxa-4(5),11(12)-diene (**5**) to the 4(20),11(12)-diene isomer (**4**) (or *vice versa*) was observed in *Taxus* sp. microsomes (or *Spodoptera* microsomes enriched in the recombinant 5 α -Hydroxylase)⁶⁸ under standard assay conditions but in the absence of NADPH or in the absence of O_2 , or in the presence of CO, 100 μM miconazole, or 100 μM clotrimazole (all conditions under which hydroxylation activity is negligible), nor was isomerization observed in boiled controls containing all cofactors and reactants. Similarly, no interconversion of either positional isomer was observed in the presence of Mg^{+2} , NAD^+ , NADH, NADP^+ , or flavin cofactors, at pH values from 4–10. From these studies, we concluded that taxa-4(5),11(12)-diene (**5**) is not appreciably isomerized to taxa-4(20),11(12)-diene (**4**) under physiological conditions, and that the migration of the double bond from the 4(5)- to the 4(20)-position in the process of taxadienol formation is an inherent feature of the cytochrome P450 oxygenase reaction with taxa-4(5),11(12)-diene (**5**) as substrate. It is of further interest to note that taxa-4(20),11(12)-diene (**4**) is but a minor natural product of *Taxus* sp. formed by taxadiene synthase that is an adventitious, yet efficient, substrate for the 5 α -hydroxylase.

Previous efforts to evaluate the 5 α -hydroxylation reaction by the native enzyme, by search for an epoxide intermediate and through the use of [20- $^3\text{H}_3$]taxa-4(5),11(12)-diene to examine a kinetic isotope effect (KIE) on the deprotonation step, failed



Scheme 7 The mechanism of taxadiene hydroxylase.⁶⁸

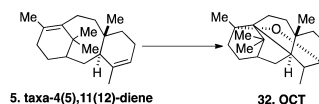
to distinguish between two reasonable mechanistic possibilities.⁷¹

The two mechanistic manifolds that were considered involve: (1) preliminary conversion of the 4(5)-double bond of taxa-4(5),11(12)-diene (**5**) to the corresponding 4(5)-epoxide (**29**), followed by ring-opening to carbenium ion species **30** and β -proton elimination from the C20 methyl group to yield the allylic alcohol product (**26**) or, (2) an alternate route involving cytochrome P450-mediated abstraction of hydrogen radical from the C20 methyl of the substrate (**5**) to yield the allylic radical (**31**) to which oxygen is added at C5 yielding **26** (Scheme 7).

The utilization of the isomeric taxa-4(20),11(12)-diene (**4**) by the hydroxylase, with efficiency comparable to that of the natural substrate, would appear to rule out an intermediate epoxide (**29**) in the reaction cycle. These results instead suggest a mechanism involving abstraction of a hydrogen radical from C20 for **5** (or from C5 in the case of the 4(20)-isomer **4**), leading to the common intermediate, allylic radical **31**, followed by oxygen insertion selectively from the 5 α -face of this radical intermediate to accomplish the net oxidative rearrangement. It also appears that the somewhat tighter binding of the 4(20)-isomer substrate (**4**) may be a reflection that this isomer more closely mimics the allylic radical intermediate.⁶⁸

3.4 Over-production of taxa-4(20),11(12)-dien-5 α -ol

As with the studies on the overproduction of taxadiene, Ajikumar and coworkers have also engineered a P450-based oxidation to convert taxadiene to taxa-4(20),11(12)-dien-5 α -ol.⁶⁰ The engineered strain of *E. coli* improved the production of taxa-4(20),11(12)-dien-5 α -ol some 2400-fold over Dejong's yeast alternative.⁷⁴ Interestingly, work towards the metabolic engineering of taxa-4(20),11(12)-dien-5 α -ol formation in tobacco



Scheme 8 Production of a novel taxane, OCT.

demonstrated that a novel taxane was also being produced as a by product (Scheme 8, **32**).⁷⁵

Rontein and coworkers reported that the rearrangement of taxadiene to OCT is mediated by CYP725A4 and does not rely on additional enzymes or factors.⁷⁵ Furthermore, it was also demonstrated by Ajikumar and coworkers that the production of OCT (**32**) is likely due to the functional plasticity of the 5- α -hydroxylase with its chimeric CYP450 enzymes.⁶⁰

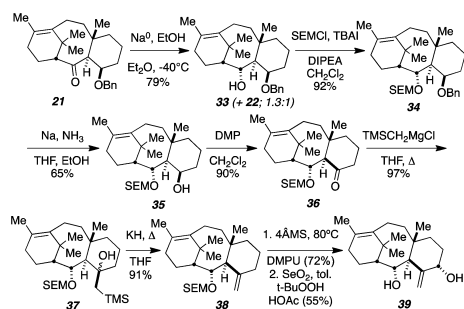
4 Syntheses of lightly functionalized taxoids

To approach subsequent biosynthetic steps considered to involve hydroxylation and acylation of the taxane core,⁷⁶ lightly oxygenated taxoids bearing the C5-hydroxyl group were prepared to evaluate them as bioconversion intermediates in *Taxus* cell feeding studies and as substrates for both native and recombinant enzymes from *Taxus*.

4.1 Synthesis of taxa-4(20),11(12)-dien-2 α ,5 α -diol

We have completed a synthesis of the 2 α ,5 α -diol (**39**) as shown in Scheme 9 utilizing the Shea-Jenkins type II IMDA construction⁷⁷ that was developed and refined in the course of our first total synthesis of taxa-4(5),11(12)-diene (**5**).^{51,52,63-67} The key issue came down to devising a means to reduce the ketone moiety of **21** to the 2 α -alcohol.

During the course of synthetic studies on taxol, Wender¹² reported the dissolving metal reduction of a substrate structurally related to **21** affording a mixture of α - and β -epimeric alcohols. Indeed, reduction of ketone **21** (Na⁰/EtOH/Et₂O) resulted in a 1.3 : 1 separable mixture (flash column silica gel chromatography) of **22** and **33** respectively in 58% yield, along with unreacted starting material (13%). We found that when the reduction of **21** is conducted at -40 °C the ratio **22**:**33** can be reversed to 1:1.3 and the yield increased to 79% (Scheme 9). This synthesis provided the first authentic specimen of this material and proved invaluable in identifying this material as a component of *Taxus* tissue extracts,⁷⁷ but its role as a biosynthetic pathway intermediate is presently uncertain and may be verified by radio labeling and incorporation experiments.



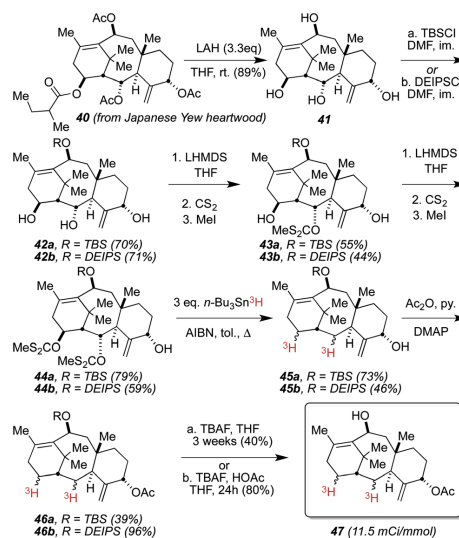
Scheme 9 The synthesis of taxa-4(20),11(12)-dien-2 α ,5 α -diol (**39**).

4.2 Synthesis of taxa-4(20),11(12)-dien-2 α ,10 β -diol-5 α -acetate from a Japanese yew-derived taxadien-tetraol

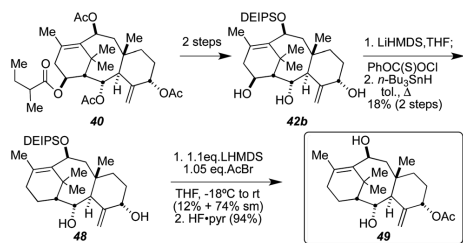
Extensive effort was expended on devising totally synthetic approaches to lightly oxygenated taxoids bearing oxygen atoms at C5 and also at either C9 and/or C10 but without success.⁷⁸ We then turned to semi-synthetic approaches using naturally occurring taxoid shunt metabolites that accumulate in *Taxus* sp. heartwood. We acquired over 100 kg of Japanese yew heartwood from a wood sculptor in Japan (Hida Ichii Ittoubori Kyoudou Kumiai of The Engraving Craftsman Association, Japan; see Fig. 2) and have extracted more than 3.5 grams of



Fig. 2 A small sculpture made from Japanese Yew by Hida Ichii Ittoubori Kyoudou Kumiai of The Engraving Craftsman Association, Japan.



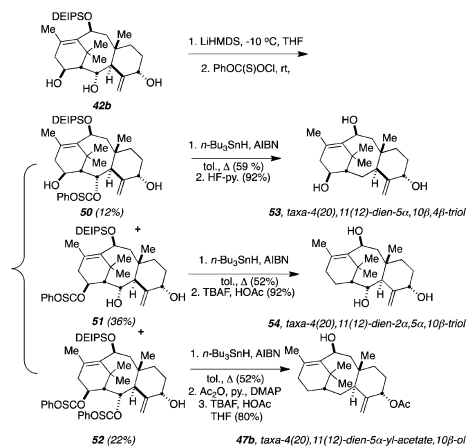
Scheme 10 The synthesis of tritiated taxa-4(20),11(12)-dien-5 α -yl-acetate-10 β -ol (**47**).⁷⁹



Scheme 11 The synthesis of taxa-4(20),11(12)-dien-5α-yl-acetate-2α,10β-diol (**49**).⁸⁰

2α,5α,10β-triacetoxy-14β-(2-methyl)-butyryloxytaxa-4(20),11-diene (**40**) as a raw material for the preparation of a host of lightly oxygenated taxoids. We have completed the semi-synthesis of taxa-4(20),11(12)-dien-5α-yl-acetate-10β-ol (**47**)⁷⁹ and taxa-4(20),11(12)-dien-5α-yl-acetate-2α,10β-diol (**49**)⁸⁰ as shown in Schemes 10 and 11. Thus, selective manipulation of the hydroxyl groups of this substrate has led to the synthesis taxa-4(20)-11(12)-diene-5α-yl-acetate-10β-ol (**47**, Scheme 10) in tritium-labeled form in preparatively useful amounts. This has provided a key substrate that the Croteau laboratory has utilized for characterization of downstream hydroxylases. In a first pass, we prepared 32 mg of tritium-labeled **46** with a specific activity of 11.5 Ci mol⁻¹. The Barton deoxygenation protocol permitted the facile tritium labeling of these materials through the purchase of commercially available Bu₃Sn³H of high specific activity.

Using the same approach, we prepared taxa-4(20),11(12)-dien-5α-yl-acetate-2α,10β-diol (**49**).⁸⁰ Substrates bearing the 5α-acetate residue have proven particularly important and, in some cases, difficult to selectively prepare.



Scheme 12 The synthesis of the 5,10,14-triol; the 2,5,10-triol and the 5,10-diol.

For example, diol **49**, prepared by the radical deoxygenation of **42b** (Scheme 11), was subjected to a variety of acetylation conditions. After extensive work, it was found that treatment of **48** with LHMDS at -18 °C and careful addition of acetyl bromide, cleanly afforded the C-5 mono-acetate, although only in 12% isolated yield. Fortunately, unreacted **48** could be readily recovered in 74% yield. Removal of the silyl residue with HF·pyridine gave taxa-4(20),11(12)-dien-5α-yl-acetate-2α,10β-diol (**49**, Scheme 11).

Substrate **42b** turned out to be a very useful species for the preparation of several triols as well as constituting an alternate source of the 5,10-diol-mono-acetate (**47**) as shown in Scheme 12. The acylation of **42b** with phenylthionochloroformate, was non-regioselective giving a separable mixture of **50**, **51** and **52**. Tin hydride-based deoxygenation of each species provided the first authentic specimens of taxa-4(20),11(12)-dien-5α, 10β,14β-triol (**53**) and taxa-4(20),11(12)-dien-2α, 5α,10β-triol (**54**). Substitution of Bu₃Sn²H or Bu₃Sn³H provided the corresponding isotopomers.

Compound **47b** has also constituted an alternative and expedient source for the synthesis of tritiated C5-mono-acetate **27b** (Scheme 13). This has proven significant since the totally synthetic route initially devised to prepare **47** described above, requires extensive time and effort to repeat.⁷⁹

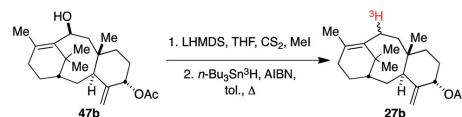
5 Deoxygenation of taxusin

Taxusin is an abundantly available taxoid that makes up a significant weight% of *Taxus* sp. heart wood. We obtained 5 kg of *Taxus brevifolia* heartwood chips from Prof. Croteau from which we extracted and purified 4.5 grams of taxusin and developed a tetraol protection strategy.

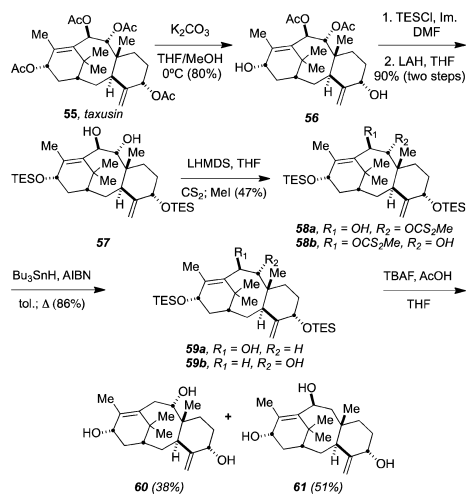
5.1 Attempt to deoxygenate taxusin at C-13

Despite considerable effort, we were unable to effect the deoxygenation of taxusin at C13 without concomitant migration of the 11(12)-bridgehead alkene. This would have provided convenient access to the 5,9-diol, 5,10-diol and 5,9,10-triol that are potential candidates as pathway metabolites. This approach has been abandoned in favor of the successful deoxygenation of a taxadien-tetraol obtained from Japanese yew heartwood described above.

Despite the failure to utilize taxusin to prepare C13-deoxytaxoids, we have developed deoxygenation strategies for the other hydroxyl residues at C9 and C10.⁸¹ Thus, treatment of taxusin with potassium carbonate in methanol, selectively removes the C5 and C13 acetate residues (**56**, Scheme 14). Protection of the C5 and C13 hydroxyl groups as the triethylsilyl (TES) ethers and LAH removal of the acetates furnished **57**. Xanthate formation gave a mixture of **58a** and **58b**, which could



Scheme 13 Alternative route to taxa-4(20),11(12)-diene-5α-acetate

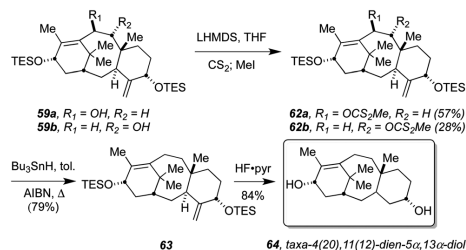


Scheme 14 The synthesis of the 5,9,13-triol and the 5,10,13-triol by deoxygenation of taxusin.

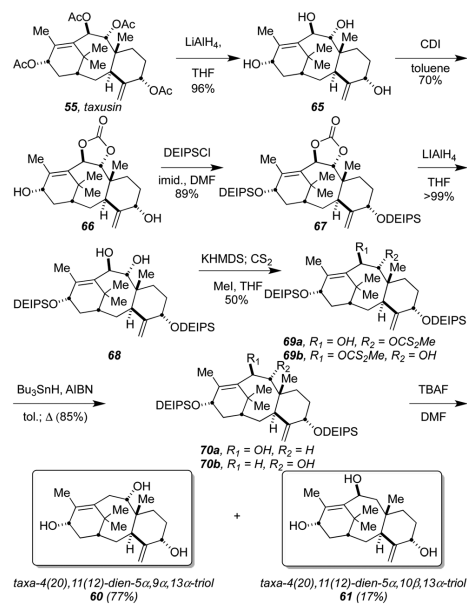
be subjected to radical deoxygenation and fluoride-based desilylation to produce taxa-4(20),11(12)-dien-5 α ,9 α ,13 α -triol (**60**) and taxa-4(20),11(12)-dien-5 α ,10 β ,13 α -triol (**61**).⁸¹

The mixture of **59a/b**, also provided an opportunity for the synthesis of the corresponding taxa-4(20),11(12)-diene-5 α ,13 α -diol (**64**). As shown in Scheme 15, **59a/b** was treated with LHMDS, carbon disulfide and methyl iodide to give a mixture of the xanthates **62a/b**, which could be separated on column but was used as a mixture in the following step. Barton deoxygenation of **62a/b** furnished the protected diol **63** in 79% yield. Final treatment of **63** with HF-pyridine complex afforded taxa-4(20),11(12)-diene-5 α ,13 α -diol (**64**).⁸¹

While this route provided the first authentic specimens of **60** and **64**, it proved to be capricious due to the lability of the *O*-TES ethers. As such, a more robust, second-generation synthesis was devised as shown in Scheme 16 where *O*-diethyl-*iso*-propylsilyl ethers (ODEIPS) were employed. In addition, we found that conversion of taxusin into the corresponding tetraol, followed by protection of the 9,10-diol unit as its cyclic carbonate proved advantageous and reproducible.⁸²



Scheme 15 The synthesis of taxa-4(20),11(12)-dien-5 α ,13 α -diol.

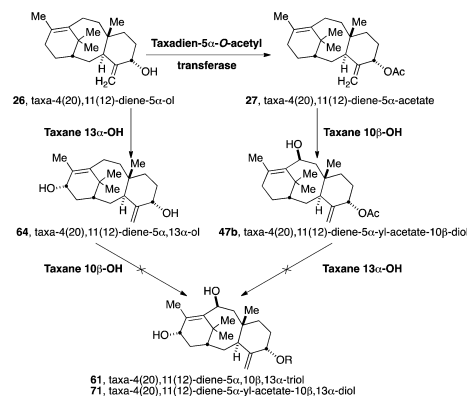


Scheme 16 Alternative syntheses of the 5,9,13-triol and the 5,10,13-triol by deoxygenation of taxusin.

6 Subsequent biosynthetic transformations of the 5-hydroxytaxadiene core

6.1 10 β - and 13 α -hydroxylase

The predicted second and third hydroxylation steps in the pathway are the 13 α - and 10 β -hydroxylations. The responsible



Scheme 17 13 α - and 10 β -hydroxylase

microsomal enzymes have been fully characterized, and the respective cytochrome P450 genes have been cloned.^{83,84} The enzymes, originally obtained from *T. cuspidata*,⁸³ show conversion of taxa-4(20),11(12)-diene-5 α -ol (**26**) (as well as its C20 tritium labeled isotope), to the subsequent diols, but 10 β -hydroxylase prefers taxa-4(20),11(12)-diene-5 α -acetate (**27**) (as well as its C20 tritium labeled isotope) as substrate and 13 α -hydroxylase prefers taxa-4(20),11(12)-diene-5 α -ol (**26**) (Scheme 17). The 13 α -hydroxylase was characterized as a member of the CYP725A gene family, whereas the 10 β -hydroxylase was determined to be of the CYP725A1 gene line. Subsequent attempts at hydroxylation of either the 10 β /13 α -diols to deliver the corresponding triol were unsuccessful with either of the 10 β /13 α -hydroxylases.⁸³

6.2 2 α - and 7 β -hydroxylase

Work towards the identification and characterization of the 2 α - and 7 β -hydroxylases utilized what is a presumed dead-end metabolite from yew heartwood, (+)-taxusin (**55**). This metabolite actually proved to be a useful surrogate to examine the oxygenations on route to taxol (**1**). Studies using (+)-taxusin (**55**) showed that it could be hydroxylated to give either 2 α -hydroxytaxusin (**73**) or 7 β -hydroxytaxusin (**72**) via their corresponding hydroxylases and that these two intermediates could be further elaborated with the opposing enzyme to give 2 α , 7 β -dihydroxytaxusin (**74**) (Scheme 18). Unfortunately, no structurally simpler taxoids could be utilized by these hydroxylases, suggesting that they function later in the biosynthesis of taxol.^{84,85}

Furthermore, the 2 α - and 7 β -hydroxylases genes have been cloned from *Taxus* species and are very similar to those of the CYP725A gene family. Studies show that both of these enzymes operate sequentially with 7 β -hydroxylation occurring first, and 2 α -hydroxylation occurring second.⁸⁵ Through catalytic as well

as binding studies,⁸⁶ it was found that 7 β -hydroxylase was not able to convert less functionalized taxadienes or highly substituted taxoids, which further supported the concept that 7 β -hydroxylation is an intermediate step in the biosynthetic pathway.

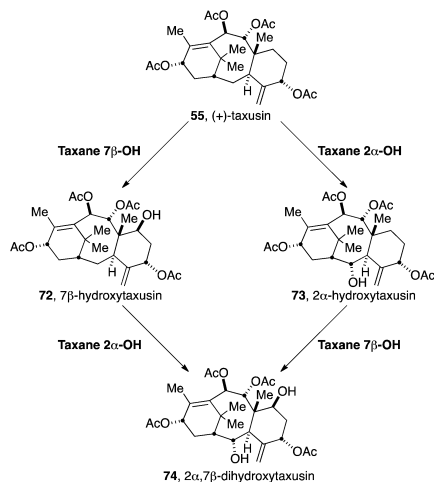
6.3 Uncharacterized hydroxylases

Oxygenation at C-9 is assumed to happen early in the biosynthetic pathway.⁴ A cDNA clone for 9 α -hydroxylase was tentatively identified using taxa-4(20),11(12)-diene-5 α -ol (**26**) as a substrate by in vivo feeding of yeast that were transformed with P450 sequences, but subsequent identification of the product has not been performed due to a lack of material, and the enzyme has not been characterized.⁸⁷ Two additional oxidation steps, at C1 and in the side-chain, remain uncharacterized.⁸⁴

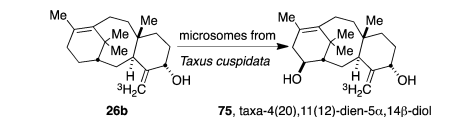
6.4 Biosynthetic conversion to the 5 α ,14 β -diol: A case of aberrant metabolism

Additional work has been done surrounding the biosynthetic conversion to 14-hydroxylated taxoids. We synthesized a large (150 mg) quantity of tritium-labeled taxa-4(20),11(12)-dien-5 α -ol^{52,71-73} (**26b**) and have used this as a substrate (~1 mg aliquots, the current maximum scale based on microsomal preps) for biosynthetic conversion to more polar products in *Taxus* microsomes. This substrate actually gives three products with a molecular mass of 304 (diol) and three products with a molecular mass of 320 (triol). We obtained 200 μ g of the major diol (a heroic, maxi-prep experiment) and have purified this substance by HPLC. Detailed ¹H NMR analysis (principally 1D TOCSY) revealed that the structure was that of a 5 α ,14 β -diol (**75**, Scheme 19).^{69,88}

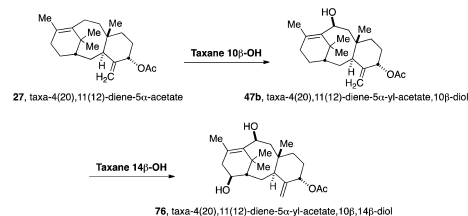
Since it is quite unlikely that such a metabolite is on the pathway to taxol, this substance presumably arose via a C-14-specific P450 hydroxylase that converts a more highly oxygenated taxoid into the C-14 β -alcohol and accepted **26b** as an adventitious substrate. Due to the low yield and difficulty in separating the other two minor diols, we are focusing on the



Scheme 18 2 α - and 7 β -hydroxylase activity.



Scheme 19 Biosynthetic formation of the 5 α , 14 β -diol (**75**).



Scheme 20 14 β -hydroxylase activity.

conversion of taxa-4(20),11(12)-dien-5 α -acetate (**27**) into the diol mono-acetates *via* the relevant recombinant P450 hydroxylases.

A clone for the 14 β -hydroxylase was discovered by *in vivo* screening of transformed yeast cells bearing candidate P450s' genes,⁷⁶ and the corresponding recombinant enzyme was characterized.^{76,88–90} Further studies determined that the 14 β -hydroxylase is able to convert taxa-4(20),11(12)-diene-5 α -yl-acetate, 10 β -diol (**47b**) to taxa-4(20),11(12)-diene-5 α -yl-acetate, 10 β ,14 β -triol, **76** (Scheme 20).

In the case of taxol, hydroxylation at the C-14 position does not occur, but the accumulation of metabolites that are hydroxylated at C-14 is quite significant. The availability of the cDNA encoding for the 14 β -hydroxylase suggests a possible strategy to suppress this gene thereby permitting redirection of the pathway flux toward taxol. Further examination of the 14 β -hydroxylase revealed that it contained several of the typical characteristics of cytochrome P450 enzymes, namely, the oxygen binding motif, a heme-binding motif with the PFG element, and a conserved cysteine at position 444. Alternately, the enzyme contained an additional number of residues at the N-terminus.⁸⁸

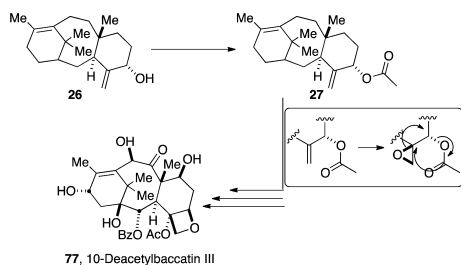
7 Studies on the formation of the oxetane ring

The biosynthetic pathway to taxol also includes five acyl-transferase-catalyzed steps. Each transacylase delivers an acyl group from acyl CoA to a pathway intermediate.^{91–93} Previous theories indicate that the ene-acetoxy functional group of taxa-4(20),11(12)-diene-5 α -yl-acetate (**26**) transforms into the 5-acetoxy-4(20)-epoxy moiety with subsequent rearrangement to the oxetane (**77**) (Scheme 21).⁹⁴

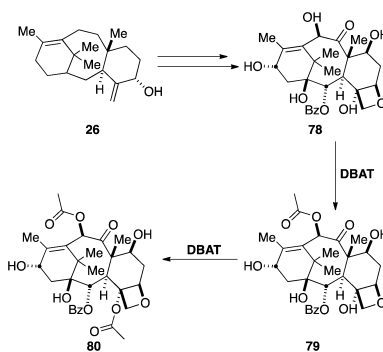
Alternatively, recent studies by Ondari and Walker now suggest another possibility. Ondari showed that when using advanced taxanes deacetylated at C4, a regioselective acetylation with a recombinantly expressed *Taxus* 10-deacetylbaaccatin 10 β -O-acetyltransferase (DBAT) catalyzes transfer to the tertiary C4 position on the oxetane ring, in this case, on 4-DAB (**79**, Scheme 22).⁹⁵ This new evidence adds another possibility to the sequence of events in the biosynthesis of taxol.

8 C13 Acylation: Final step in the biosynthesis of taxol

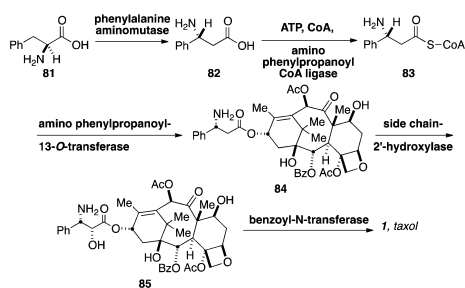
Extensive work has been done decoding the final steps towards the production of taxol, namely, the acylation at C13. Early *in*



Scheme 21 The original theory of oxetane ring formation.



Scheme 22 Acylation of C4 in advanced taxanes.



Scheme 23 C13 side-chain construction and implementation.

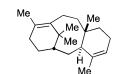
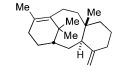
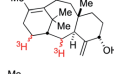
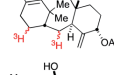
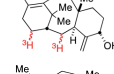
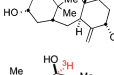
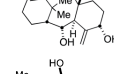
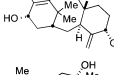
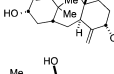
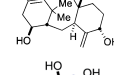
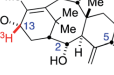
in vivo studies showed that the intact side chain⁴ was not incorporated into taxol, whereas β -phenylalanine and α -phenylalanine and phenylisoserine were incorporated. These findings suggested that β -phenylalanine is attached to baaccatin III, and that this side chain is subsequently hydroxylated and then *N*-benzoylated to complete the biosynthesis of taxol.⁹⁶ Walker and coworkers discovered a cDNA clone encoding a taxoid C13 *O*-phenylpropanoyltransferase, which yielded a recombinant enzyme that selectively catalyzed the selective 13-*O*-acylation of baaccatin III with β -phenylalanoyl CoA (**83**) as the acyl donor, forming *N*-debenzoyl-2'-deoxytaxol (**84**).^{91,92} Interestingly, 2*S*- α -phenylalanine (**81**) is converted to 3*R*- β -phenylalanine (**82**) by phenylalanine aminomutase (PAM).⁹⁷ The stereochemical mechanism of PAM actually involves the removal and interchange of the pro-3*S* hydrogen and the amino group, which subsequently rebonds at C3 with retention of configuration (Scheme 23).⁹⁷

Furthermore, the crystal structure as well as additional mechanistic insight into the phenylalanine aminomutase has been recently reported.⁹⁸

9 Conclusion

Overall, a combination of total synthesis and semi-synthesis has been used to prepare taxoids as putative substrates for

Table 1 Summary of feeding studies

Taxoid	Incorporation into Taxol in Cell Culture	Detected as a Natural Metabolite
	Yes	Yes
	?	?
	Yes	Yes
	Yes	Yes
	Yes	Yes
	Yes	?
	Tentative	?
	Yes	?
	?	?
	No	?
	Tentative	?

interrogating the substrate specificity of the cytochrome P450 enzymes involved in hydroxylations of the tricyclic hydrocarbon core of taxol. Both stable-isotope and radio-isotope labeling have been employed (feeding study results summarized in Table 1), with the former being utilized more dominantly at the present time. Furthermore a greater understanding of the biosynthetic pathway is being gained and is helping to piece together the puzzle of the biosynthesis of taxol. Although much work has yet to be complete, especially with late stage intermediates, advances in bioengineering and overexpression of recombinant enzymes are leading the way in pushing the biosynthetic pathway towards a functional synthesis of taxol.

10 Acknowledgements

The studies performed by the Williams and Croteau groups reported in this review were supported by the National Institutes of Health (Grant CA70375 to RMW and CA55254 to RBC).

11 References and notes

- 1 Paclitaxel, the generic name for Taxol®, is a registered trademark for Bristol-Myers Squibb. Due to greater familiarity with the word taxol, this will be used throughout this application and the symbol ® has been deleted for the sake of clarity and brevity.
- 2 G. Georg, S. Ali, J. Zygmunt and L. Jayasinghe, *Expert Opin. Ther. Pat.*, 1994, **4**(2), 109–120.
- 3 A. N. Boa, P. R. Jenkins and M. J. Lawrence, *Contemp. Org. Synth.*, 1994, 47–75.
- 4 H. G. Floss and U. Moeck, Biosynthesis of Taxol, in *Taxol: Science and Applications*, CRC Press: Boca Raton, 1995.
- 5 D. Guenard, F. Guerittevoegelein and P. Potier, *Acc. Chem. Res.*, 1993, **26**(4), 160–167.
- 6 D. G. I. Kingston, *Pharmacol. Ther.*, 1991, **52**(1), 1–34.
- 7 K. C. Nicolaou, W. M. Dai and R. K. Guy, *Angew. Chem., Int. Ed. Engl.*, 1994, **33**, 15–44.
- 8 J. Rohr, *Angew. Chem., Int. Ed. Engl.*, 1997, **36**, 2190–2195.
- 9 C. S. Swindell, *Org. Prep. Proced. Int.*, 1991, **23**(4), 465–543.
- 10 M. C. Wani, H. L. Taylor, M. E. Wall, P. Coggon and A. T. McPhail, *J. Am. Chem. Soc.*, 1971, **93**(9), 2325–2327.
- 11 R. A. Holton, R. R. Juo, H. B. Kim, A. D. Williams, S. Harusawa, R. E. Lowenthal and S. Yogai, *J. Am. Chem. Soc.*, 1988, **110**(19), 6558–6560.
- 12 P. A. Wender and T. P. Mucciario, *J. Am. Chem. Soc.*, 1992, **114**(14), 5878–5879.
- 13 K. C. Nicolaou, Z. Yang, J. J. Liu, H. Ueno, P. G. Nantermet, R. K. Guy, C. F. Claiborne, J. Renaud, E. A. Couladouros and K. Paulvannan, *Nature*, 1994, **367**(6464), 630–634.
- 14 K. C. Nicolaou, P. G. Nantermet, H. Ueno, R. K. Guy, E. A. Couladouros and E. J. Sorensen, *J. Am. Chem. Soc.*, 1995, **117**(2), 624–633.
- 15 K. C. Nicolaou, J. J. Liu, Z. Yang, H. Ueno, E. J. Sorensen, C. F. Claiborne, R. K. Guy, C. K. Hwang, M. Nakada and P. G. Nantermet, *J. Am. Chem. Soc.*, 1995, **117**(2), 634–644.
- 16 K. C. Nicolaou, Z. Yang, J. J. Liu, P. G. Nantermet, C. F. Claiborne, J. Renaud, R. K. Guy and K. Shibayama, *J. Am. Chem. Soc.*, 1995, **117**(2), 645–652.
- 17 K. C. Nicolaou, H. Ueno, J. J. Liu, P. G. Nantermet, Z. Yang, J. Renaud, K. Paulvannan and R. Chadha, *J. Am. Chem. Soc.*, 1995, **117**(2), 653–659.
- 18 R. A. Holton, C. Somoza, H. B. Kim, F. Liang, R. J. Biediger, P. D. Boatman, M. Shindo, C. C. Smith, S. C. Kim, H. Nadizadeh, Y. Suzuki, C. L. Tao, P. Vu, S. H. Tang, P. S. Zhang, K. K. Murthi, L. N. Gentile and J. H. Liu, *J. Am. Chem. Soc.*, 1994, **116**(4), 1597–1598.
- 19 R. A. Holton, H. B. Kim, C. Somoza, F. Liang, R. J. Biediger, P. D. Boatman, M. Shindo, C. C. Smith, S. C. Kim, H. Nadizadeh, Y. Suzuki, C. L. Tao, P. Vu, S. H. Tang, P. S. Zhang, K. K. Murthi, L. N. Gentile and J. H. Liu, *J. Am. Chem. Soc.*, 1994, **116**(4), 1599–1600.
- 20 J. J. Masters, J. T. Link, L. B. Snyder, W. B. Young and S. J. Danishefsky, *Angew. Chem., Int. Ed. Engl.*, 1995, **34**(16), 1723–1726.
- 21 P. A. Wender, N. F. Badham, S. P. Conway, P. E. Floreancig, T. E. Glass, C. Granicher, J. B. Houze, J. Janichen, D. S. Lee, D. G. Marquess, P. L. McGrane, W. Meng, T. P. Mucciario, M. Muhlebach, M. G. Natchus, H. Paulsen, D. B. Rawlins, J. Satkofsky, A. J. Shuker, J. C. Sutton, R. E. Taylor and K. Tomooka, *J. Am. Chem. Soc.*, 1997, **119**(11), 2755–2756.
- 22 P. A. Wender, N. F. Badham, S. P. Conway, P. E. Floreancig, T. E. Glass, J. B. Houze, N. E. Krauss, D. S. Lee, D. G. Marquess, P. L. McGrane, W. Meng, M. G. Natchus, A. J. Shuker, J. C. Sutton and R. E. Taylor, *J. Am. Chem. Soc.*, 1997, **119**(11), 2757–2758.
- 23 K. Morihira, R. Hara, S. Kawahara, T. Nishimori, N. Nakamura, H. Kusama and I. Kuwajima, *J. Am. Chem. Soc.*, 1998, **120**(49), 12980–12981.

- 24 L. A. Paquette, H. L. Wang, Z. Su and M. Z. Zhao, *J. Am. Chem. Soc.*, 1998, **120**(21), 5213–5225.
- 25 T. Mukaiyama, I. Shiina, H. Iwadare, M. Saitoh, T. Nishimura, N. Ohkawa, H. Sakoh, K. Nishimura, Y. Tani, M. Hasegawa, K. Yamada and K. Saitoh, *Chem.–Eur. J.*, 1999, **5**(1), 121–161.
- 26 K. H. Han, P. Fleming, K. Walker, M. Loper, W. S. Chilton, U. Mocek, M. P. Gordon and H. G. Floss, *Plant Sci.*, 1994, **95**(2), 187–196.
- 27 A. Stierle, G. Strobel and D. Stierle, *Science*, 1993, **260**(5105), 214–216.
- 28 G. Strobel, X. S. Yang, J. Sears, R. Kramer, R. S. Sidhu and W. M. Hess, *Microbiology*, 1996, **142**, 435–440.
- 29 G. A. Strobel, W. M. Hess, E. Ford, R. Sidhu and X. Yang, *J. Ind. Microbiol.*, 1996, **17**, 417–423.
- 30 G. A. Strobel, W. M. Hess, J. Y. Li, E. Ford, J. Sears, R. S. Sidhu and B. Summerell, *Aust. J. Bot.*, 1997, **45**(6), 1073–1082.
- 31 A. K. Hoffman, W. J. Waroapng, G. Strobel, D. Griffin, B. Arbogast, D. Barofsky, R. B. Boone, L. Ning, P. Zheng and L. Daley, *Spectroscopy*, 1999, **13**, 22–32.
- 32 A. Stierle, D. Stierle, G. Strobel, G. Bignami and P. Grothaus, Bioactive Metabolites of the Endophytic Fungi of Pacific Yew, *Taxus brevifolia*, in *Taxane Anticancer Agents*, American Chemical Society, 1995, pp. 82–97.
- 33 K. Shrestha, G. A. Strobel, S. P. Shrivastava and M. B. Gewali, *Planta Med.*, 2001, **67**(4), 374–6.
- 34 J. Y. Li, R. S. Sidhu, E. J. Ford, D. M. Long and G. A. Strobel, *J. Ind. Microbiol. Biotechnol.*, 1998, **20**, 259–264.
- 35 A. M. Metz, A. Haddad, J. Worapong, D. M. Long, E. J. Ford, W. M. Hess and G. A. Strobel, *Microbiology*, 2000, **146**, 2079–2089.
- 36 P. E. Fleming, A. R. Knaggs, X. G. He, U. Mocek and H. G. Floss, *J. Am. Chem. Soc.*, 1994, **116**(9), 4137–4138.
- 37 P. E. Fleming, U. Mocek and H. G. Floss, *J. Am. Chem. Soc.*, 1993, **115**(2), 805–807.
- 38 J. W. S. Harrison, R. M. and B. Lythgoe, *J. Chem. Soc. C*, 1966, 1933–1945.
- 39 F. Gueritte-Voegelein, D. Guenard and P. Potier, *J. Nat. Prod.*, 1987, **50**(1), 9–18.
- 40 B. A. Herbert, *The Biosynthesis of Secondary Metabolites*, Chapman and Hall, London, 1981.
- 41 K. Nakanishi, T. Goto, S. Ito and S. Nozoe, *Natural Products Chemistry*, Kodansha, Ltd, Tokyo, 1974, Vol. 1.
- 42 G. H. Towers, Biochemistry of the Mevalonic Acid Pathway to Terpenoids, in *Recent Advances in Phytochemistry*, ed. H. A. Stafford, Plenum Press, New York, 1990, Vol. 24.
- 43 M. Luckner, *Secondary Metabolism in Microorganisms, Plants and Animals*, Springer-Verlag, Berlin, 1990.
- 44 W. M. Eisenrich, B. P. J. Hylands, M. H. Zenk and A. Bacher, *Proc. Natl. Acad. Sci. U. S. A.*, 1996, **93**, 6431–6436.
- 45 A. E. Koepp, M. Hezari, J. Zajicek, B. S. Vogel, R. E. LaFever, N. G. Lewis and R. Croteau, *J. Biol. Chem.*, 1995, **270**(15), 8686–8690.
- 46 M. Hezari, N. G. Lewis and R. Croteau, *Arch. Biochem. Biophys.*, 1995, **322**(2), 437–444.
- 47 X. Lin, M. Hezari, A. E. Koepp, H. G. Floss and R. Croteau, *Biochemistry*, 1996, **35**(9), 2968–77.
- 48 M. R. Wildung and R. Croteau, *J. Biol. Chem.*, 1996, **271**(16), 9201–9204.
- 49 M. Hezari and R. Croteau, *Planta Med.*, 1997, **63**(4), 291–295.
- 50 D. C. Williams, B. J. Carroll, Q. Jin, C. D. Rithner, S. R. Lenger, H. G. Floss, R. M. Coates, R. M. Williams and R. Croteau, *Chem. Biol.*, 2000, **7**(12), 969–977.
- 51 S. M. Rubenstein and R. M. Williams, *J. Org. Chem.*, 1995, **60**(22), 7215–7223.
- 52 S. M. Rubenstein, Dissertation: *Elucidating the Biosynthetic Pathway to Taxol*, Colorado State University, 1996.
- 53 K. Walker and R. Croteau, *Recent Adv. Phytochem.*, 1999, **33**, 31–50.
- 54 M. Hezari, R. E. B. Ketchum, D. M. Gibson and R. Croteau, *Arch. Biochem. Biophys.*, 1997, **337**(2), 185–190.
- 55 D. C. Williams, M. R. Wildung, A. Q. W. Jin, D. Dalal, J. S. Oliver, R. M. Coates and R. Croteau, *Arch. Biochem. Biophys.*, 2000, **379**(1), 137–146.
- 56 M. Koksai, Y. Jin, R. M. Coates, R. Croteau and D. W. Christianson, *Nature*, 2011, **469**, 116–122.
- 57 Q. Jin, D. C. Williams, M. Hezari, R. Croteau and R. M. Coates, *J. Org. Chem.*, 2005, **70**(12), 4667–75.
- 58 K. E. Tyo, H. S. Alper and G. N. Stephanopoulos, *Trends Biotechnol.*, 2007, **25**(3), 132–137.
- 59 P. K. Ajikumar, K. Tyo, S. Carlsen, O. Mucha, T. H. Phon and G. Stephanopoulos, *Mol. Pharmaceutics*, 2008, **5**(2), 167–190.
- 60 P. K. Ajikumar, W. H. Xiao, K. E. J. Tyo, Y. Wang, F. Simeon, E. Leonard, O. Mucha, T. H. Phon, B. Pfeifer and G. Stephanopoulos, *Science*, 2010, **330**(6000), 70–74.
- 61 B. A. Boghigian, D. Salas, P. K. Ajikumar, G. Stephanopoulos and B. A. Pfeifer, *Appl. Microbiol. Biotechnol.*, 2012, **93**, 1651–1661.
- 62 B. A. Boghigian, J. Armando, D. Salas and B. A. Pfeifer, *Appl. Microbiol. Biotechnol.*, 2012, **93**, 2063–2073.
- 63 K. J. Shea and P. D. Davis, *Angew. Chem., Int. Ed. Engl.*, 1983, **22**, 419.
- 64 K. J. Shea and P. D. Davis, *Angew. Chem., Int. Ed. Engl.*, 1983, **22**, 546.
- 65 R. V. Bonnett and P. R. Jenkins, *J. Chem. Soc., Perkin Trans. 1*, 1989, 413.
- 66 P. A. Brown and P. R. Jenkins, *J. Chem. Soc., Perkin Trans. 1*, 1986, 1303.
- 67 P. A. Brown, P. R. Jenkins, J. Fawcett and D. R. Russell, *J. Chem. Soc., Perkin Trans. 1*, 1984, 253.
- 68 S. Jennewein, R. M. Long, R. M. Williams and R. Croteau, *Chem. Biol.*, 2004, **11**, 379–387.
- 69 A. L. Wheeler, R. M. Long, R. E. Ketchum, C. D. Rithner, R. M. Williams and R. Croteau, *Arch. Biochem. Biophys.*, 2001, **390**, 265–278.
- 70 M. Hezari and R. Croteau, *Planta Med.*, 1997, **63**(4), 291–295.
- 71 J. Hefner, S. M. Rubenstein, R. E. Ketchum, D. M. Gibson, R. M. Williams and R. Croteau, *Chem. Biol.*, 1996, **3**(6), 479–489.
- 72 S. Borman, *Chem. Eng. News*, 1996, **74**(27), 27–29.
- 73 S. M. Rubenstein, A. Vazquez, J. F. Sanz-Cervera and R. M. Williams, *J. Labelled Compd. Radiopharm.*, 2000, **43**(5), 481–491.
- 74 J. M. DeJong, Y. L. Liu, A. P. Bollon, R. M. Long, S. Jennewein, D. Williams and R. B. Croteau, *Biotechnol. Bioeng.*, 2006, **93**(2), 212–224.
- 75 D. Rontein, S. Onillon, G. Herbet, A. Lesot, D. Werck-Reichhart, C. Sallaud and A. Tissier, *J. Biol. Chem.*, 2008, **283**(10), 6067–75.
- 76 R. Croteau, R. E. Ketchum, R. M. Long, R. Kaspera and M. R. Wildung, *Phytochem. Rev.*, 2006, **5**(1), 75–97.
- 77 A. Vazquez and R. M. Williams, *J. Org. Chem.*, 2000, **65**(23), 7865–7869.
- 78 S. R. Lenger, Dissertation: *Studies on the Total Synthesis of Putative Intermediates in the Biosynthesis of Taxol*, Colorado State University, 2003.
- 79 T. Horiguchi, C. D. Rithner, R. Croteau and R. M. Williams, *J. Labelled Compd. Radiopharm.*, 2008, **51**(9–10), 325–328.
- 80 T. R. Horiguchi, C. D. R. Croteau and R. M. Williams, *J. Org. Chem.*, 2002, **67**, 4901–4903.
- 81 H. Li, T. Horiguchi, R. Croteau and R. M. Williams, *Tetrahedron*, 2008, **64**(27), 6561–6567.
- 82 T. R. Horiguchi, C. D. R. Croteau and R. M. Williams, *Tetrahedron*, 2003, **59**, 267–273.
- 83 S. Jennewein, C. D. Rithner, R. M. Williams and R. B. Croteau, *Proc. Natl. Acad. Sci. U. S. A.*, 2001, **98**(24), 13595–13600.
- 84 R. Kaspera and R. Croteau, *Phytochem. Rev.*, 2006, **5**(2), 433–444.
- 85 M. Chau and R. Croteau, *Arch. Biochem. Biophys.*, 2004, **427**(1), 48–57.
- 86 M. Chau, S. Jennewein, K. Walker and R. Croteau, *Chem. Biol.*, 2004, **11**(5), 663–672.
- 87 K. Walker, S. Fujisaki, R. Long and R. Croteau, *Proc. Natl. Acad. Sci. U. S. A.*, 2002, **99**(20), 12715–20.
- 88 S. Jennewein, C. D. Rithner, R. M. Williams and R. Croteau, *Arch. Biochem. Biophys.*, 2003, **413**(2), 262–70.
- 89 R. E. Ketchum, C. D. Rithner, D. Qiu, Y. S. Kim, R. M. Williams and R. B. Croteau, *Phytochemistry*, 2003, **62**(6), 901–909.
- 90 R. E. B. Ketchum, D. M. Gibson, R. B. Croteau and M. L. Shuler, *Biotechnol. Bioeng.*, 1999, **62**, 97–105.
- 91 K. Walker, R. Long and R. Croteau, *Proc. Natl. Acad. Sci. U. S. A.*, 2002, **99**(14), 9166–9171.
- 92 K. Walker, S. Fujisaki, R. Long and R. Croteau, *Proc. Natl. Acad. Sci. U. S. A.*, 2002, **99**(20), 12715–12720.

- 93 K. Walker and R. Croteau, *Phytochemistry*, 2001, **58**(1), 1–7.
- 94 F. Gueritte-Voegelein, D. Guenard and P. Potier, *J. Nat. Prod.*, 1987, **50**(1), 9–18; R. Kaspera, J. L. Cape, J. A. Faraldos, R. E. B. Ketchum and R. B. Croteau, *Tetrahedron Lett.*, 2010, **51**, 2017–2019.
- 95 M. E. Ondari and K. D. Walker, *J. Am. Chem. Soc.*, 2008, **130**(50), 17187–17194.
- 96 R. M. Long and R. Croteau, *Biochem. Biophys. Res. Commun.*, 2005, **338**(1), 410–417.
- 97 K. D. Walker, K. Klettke, T. Akiyama and R. Croteau, *J. Biol. Chem.*, 2004, **279**(52), 53947–53954.
- 98 L. Feng, U. Wanninayake, S. Strom, J. Geiger and K. D. Walker, *Biochemistry*, 2011, **50**(14), 2919–2930.